

1981

Digital modeling of power systems for fault transient studies

Elham Badie Makram
Iowa State University

Follow this and additional works at: <https://lib.dr.iastate.edu/rtd>



Part of the [Electrical and Electronics Commons](#), and the [Oil, Gas, and Energy Commons](#)

Recommended Citation

Makram, Elham Badie, "Digital modeling of power systems for fault transient studies " (1981). *Retrospective Theses and Dissertations*. 6830.
<https://lib.dr.iastate.edu/rtd/6830>

This Dissertation is brought to you for free and open access by the Iowa State University Capstones, Theses and Dissertations at Iowa State University Digital Repository. It has been accepted for inclusion in Retrospective Theses and Dissertations by an authorized administrator of Iowa State University Digital Repository. For more information, please contact digirep@iastate.edu.

INFORMATION TO USERS

This was produced from a copy of a document sent to us for microfilming. While the most advanced technological means to photograph and reproduce this document have been used, the quality is heavily dependent upon the quality of the material submitted.

The following explanation of techniques is provided to help you understand markings or notations which may appear on this reproduction.

1. The sign or "target" for pages apparently lacking from the document photographed is "Missing Page(s)". If it was possible to obtain the missing page(s) or section, they are spliced into the film along with adjacent pages. This may have necessitated cutting through an image and duplicating adjacent pages to assure you of complete continuity.
2. When an image on the film is obliterated with a round black mark it is an indication that the film inspector noticed either blurred copy because of movement during exposure, or duplicate copy. Unless we meant to delete copyrighted materials that should not have been filmed, you will find a good image of the page in the adjacent frame. If copyrighted materials were deleted you will find a target note listing the pages in the adjacent frame.
3. When a map, drawing or chart, etc., is part of the material being photographed the photographer has followed a definite method in "sectioning" the material. It is customary to begin filming at the upper left hand corner of a large sheet and to continue from left to right in equal sections with small overlaps. If necessary, sectioning is continued again—beginning below the first row and continuing on until complete.
4. For any illustrations that cannot be reproduced satisfactorily by xerography, photographic prints can be purchased at additional cost and tipped into your xerographic copy. Requests can be made to our Dissertations Customer Services Department.
5. Some pages in any document may have indistinct print. In all cases we have filmed the best available copy.

**University
Microfilms
International**

300 N. ZEEB RD., ANN ARBOR, MI 48106

8122539

MAKRAM, ELHAM BADIE

DIGITAL MODELING OF POWER SYSTEMS FOR FAULT TRANSIENT
STUDIES

Iowa State University

PH.D. 1981

University
Microfilms
International

300 N. Zeeb Road, Ann Arbor, MI 48106

PLEASE NOTE:

In all cases this material has been filmed in the best possible way from the available copy.
Problems encountered with this document have been identified here with a check mark ✓.

1. Glossy photographs or pages _____
2. Colored illustrations, paper or print _____
3. Photographs with dark background _____
4. Illustrations are poor copy _____
5. Pages with black marks, not original copy _____
6. Print shows through as there is text on both sides of page _____
7. Indistinct, broken or small print on several pages _____
8. Print exceeds margin requirements _____
9. Tightly bound copy with print lost in spine _____
10. Computer printout pages with indistinct print ✓ _____
11. Page(s) _____ lacking when material received, and not available from school or author.
12. Page(s) _____ seem to be missing in numbering only as text follows.
13. Two pages numbered _____. Text follows.
14. Curling and wrinkled pages _____
15. Other _____

University
Microfilms
International

Digital modeling of power systems
for fault transient studies

by

Elham Badie Makram

A Dissertation Submitted to the
Graduate Faculty in Partial Fulfillment of
The Requirements for the Degree of
DOCTOR OF PHILOSOPHY

Major: Electrical Engineering

Approved:

Signature was redacted for privacy.

In Charge of Major Work

Signature was redacted for privacy.

For the Major Department

Signature was redacted for privacy.

For the Graduate College

Iowa State University
Ames, Iowa

1981

TABLE OF CONTENTS

	Page
LIST OF SYMBOLS	iv
I. INTRODUCTION	1
A. Background and Objectives	1
B. Scope of the Work	4
II. LITERATURE REVIEW	6
A. Transmission Line Model	6
1. Time-domain methods	9
2. Frequency domain methods	13
B. Synchronous Generator Model	15
III. TRANSIENT AND STEADY-STATE ANALYSIS OF TRANSMISSION LINES	19
A. Formulation of Three-Phase Transmission Line Equations	19
1. Voltage equations	19
2. Current equations	21
B. Calculation of the Line Parameters	25
C. Transmission Line Losses	30
IV. GENERAL EQUATIONS AND SOLUTION FOR FAULTED POWER TRANSMISSION SYSTEMS	37
V. BOUNDARY CONDITIONS AND SIMULATION OF FAULTED POWER SYSTEMS	50
A. The General Power System Simulation	50
1. Load, generator, and transformer simulations	50
2. Fault simulation	51
B. Formulations of Boundary-Condition Equations	52
1. Steady-state solution	52
2. Transient solution	54

	Page
C. Voltage at Fault Location for Different Types of Faults	57
1. Three-phase to ground fault	57
2. Single line to ground fault	59
3. Line to line fault	61
4. Double line to ground fault	62
D. Fault Transient Waveforms	64
VI. SYNCHRONOUS MACHINE EQUATIONS IN FREQUENCY DOMAIN	82
A. Machine Equations in the Direct-Quadrature Components	85
B. Transformations Between Different Sets of Components	92
C. Voltage Equations at the Sending-End Bus	96
VII. INTERCONNECTION OF SYNCHRONOUS MACHINES AND TRANSMISSION LINES IN FAULTED POWER SYSTEMS	103
A. Formulation of the Transmission Line Equations in the Shifted-Frequency Domain	103
B. Fault Transient Waveforms for Three-Phase Fault	113
VIII. METHOD OF COMPUTATION	116
IX. COMPARISONS AND CONCLUSIONS	131
X. REFERENCES	164
XI. ACKNOWLEDGMENTS	167
XII. APPENDIX A: NUMERICAL EXAMPLE	168
XIII. APPENDIX B: FAULT TRANSIENT PROGRAM	174

LIST OF SYMBOLS

L_{ii}	Self series inductance of the transmission line per unit length
L_{ij}	Mutual inductance of the transmission line per unit length
C_{ii}	Self shunt capacitance of the transmission line per unit length
C_{ij}	Capacitance between conductors per unit length
G_{ii}	Self shunt conductance of the transmission line per unit length
G_{ij}	Shunt conductance between conductors per unit length
R	Resistance of the transmission line per unit length
R_f	Fault resistance
L_f	Fault inductance
R_{tr}	Series resistance of the transformer
L_{tr}	Series inductance of the transformer
R_ℓ	Load resistance
L_ℓ	Load inductance
r_a	Stator resistance
r_F	Field resistance
r_D, r_Q	Resistances of the damper windings
L_i	Self inductance of the generator windings
M_i	Mutual inductance between the stator windings and the rotor windings

v_i	Voltage in time-domain of phase i
i_i	Current in time-domain of phase i
V_i	Voltage in s-domain of phase i
I_i	Current in s-domain of phase i
α	Attenuation constant
β	Phase constant
γ	Propagation constant
ℓ	Total length of the transmission line
t	Time
ϕ	Phase angle
ω	Angular frequency
x_i	Distance measured from the sending-end or the receiving-end of the line
\underline{Q}	Current transformation matrix
\underline{S}	Voltage transformation matrix
\underline{T}_i	Transformation matrix
\underline{U}	Identity matrix
s1	Sending-end bus
s2	Receiving-end bus
r	Fault location
λ	Flux linkage
δ	Rotor angle
E	Generator EMF in steady-state condition
\underline{P}	Park transformation

A_{012}	Fortescue transformation (sequence components transformation)
s	Complex number in frequency domain
s'	Complex number in shifted frequency domain
ω_o	Synchronous speed of the generator
r_i	Radius of conductor i
ρ	Earth resistivity
f	Frequency in Hz.
a, b, c	Stator terminals of the machine
F, D, Q	Rotor terminals of the machine
\bar{v}	Phasor
\underline{v}	Matrix
$\underline{V}_{abc}, \underline{I}_{abc}$	Direct phase voltages and currents (a-b-c)
$\underline{V}_{0dq}, \underline{I}_{0dq}$	Voltages and currents in direct and quadrature axis (0-d-q)
$\underline{V}_{0fb}, \underline{I}_{0fb}$	Voltages and currents in forward and backward components (0-f-b)
$\underline{V}_{012}, \underline{I}_{012}$	Voltages and currents in sequence components (0-1-2)

I. INTRODUCTION

A. Background and Objectives

An abrupt change in boundary conditions, such as the actuation of a switch or the inception of a fault, will induce transients in an electrical power system. Although a power system is in a steady state most of the time, it must be designed to withstand worst possible stresses to which it may be subjected. These extreme stresses usually occur during transients. Consequently, power system design is determined by transient conditions, rather than by steady state behavior. The size of transmission line towers, the clearances for transmission line conductors, insulation of windings in power apparatus, rating of circuit breakers, loading capability of equipment--all of these specifications are dictated by considerations of power system transients.

The solution of the system equations depends upon the model of each part in the system. Thus a transmission line may be treated as a short bus section, as an infinitely long line, or as a distortionless line, depending upon the specific transient phenomenon being investigated. Similarly, a transformer may be represented by an inductance, by a network of capacitances, or by a combination of the two. Conceptually, one could imagine a mathematical model for a component which represents it correctly under all circumstances. However, even if such models existed, they would be cumbersome and inefficient simulation programs.

The model of the transmission line is the most important element in the analysis of fault induced transients on a power system. The

transmission line has four distributed parameters: a series resistance (R), a shunt conductance (G), a series inductance (L), and a shunt capacitance (C) per unit length. The analysis of transients may involve differential equations. These equations are always solved under conditions where simplifying assumptions are made. Typical assumptions are lumped parameters, frequency independent parameters, or completely transposed line. However, these assumptions should only be used for restricted conditions for which they are valid. Also a great advantage using distributed parameters is that, once a general solution is found, a fault occurring anywhere on the line can be simulated. In a lumped parameter model, the only available line locations are the discrete points of the interconnected sections.

Transformers or rotating machines are typically represented by an inductance, sometimes with capacitance at its terminals. Such representations may be adequate if the fault location is remote from the terminals. When the fault location is close to the source, this representation is questionable. In such cases, a more accurate machine model is needed. Therefore, representing the transmission line without unreasonable assumptions and with a more accurate machine model would improve the accuracy of the current and voltage waveforms that would be deduced from a simulation.

Transients due to fault inception on a power system may produce overvoltages, overcurrents, and abnormal waveforms.

Overvoltages:

A fault gives rise to induced voltages on the unfaulted phases, and often the switching surges produced by the fault are causes of significant overvoltages. The design and insulation coordination of power apparatus and systems are determined by overvoltages. The system insulation level must be sufficiently high to assure reliability, but at the same time there are strong economic reasons for keeping it as low as possible. As a result of these opposing factors, a much greater emphasis is being placed on predicted system overvoltages at the planning stage, in order that steps may be taken to reduce their severity and to minimize the system insulation level.

Overcurrents:

Overcurrents result from system faults and their study helps determine the interrupting duty on circuit breakers and the mechanical and thermal stresses within machines, transformers, and buses. Unbalanced fault simulation is often required for determining the currents in machines. An accurate representation of the machines during fault transient is required for the boundary condition.

Abnormal waveforms:

The waveforms of power system voltages and currents during the first few cycles following the fault occurrence are of considerable importance. For example, the response of a protective relay to the fault generated transient waveforms is of great concern in determining its reliability for a given application. Certain control equipment,

such as the automatic control system of HVDC systems is sensitive to the waveforms and harmonic content.

Simulation of all these system conditions requires an accurate representation of power systems during the transient period.

B. Scope of the Work

The main objective of this work is to develop an accurate digital simulation of a typical power system during the fault transient period. The work contains the following parts:

1. Modeling of the transmission line.
2. Solution of the transmission line equation. This procedure is general and can be used to find the transient and steady-state solutions for the transmission line equations without imposing unrealistic simplifying assumptions.
3. Modeling the fault.
4. Developing a method that makes the machine and transmission line equations mutually compatible. This method is based on finding a transformation matrix that transforms the synchronous machine equations from the 0-d-q components to the 0-1-2 components in frequency domain to account correctly for the variation of the machine parameters.
5. Formulation of the transmission line equations with the machine equations. The machine equations are based on the simple machine model and the full machine model.

6. Development of a FORTRAN computer program for simulation. This program allows for frequency dependent parameters and untransposition of the transmission line along with the simple or full generator model. The program is used to obtain the three-phase voltage and current waveforms at the fault location and at the sending end.
7. Conclusions based on the comparison of the different cases. Such comparisons illustrate the effects of the different assumptions and when they can be applied without jeopardizing the solution. The effects of the following factors on the fault transient waveforms are examined:
 - skin effect
 - load level
 - fault location
 - type of fault
 - generator size
 - fault impedance.

II. LITERATURE REVIEW

A. Transmission Line Model

Transient phenomena in power systems have been studied by many authors. In 1855, William Thomson investigated the theory of transients on long cables by assuming the magnetic effect to be negligibly small. He considered only the resistance R and the capacitance C per unit length and derived the well-known diffusion equation for which J. B. J. Fourier (1822) had given solutions. In 1857, Kirchhoff, who formulated the two well-known electric circuit laws, had extended the long-line theory to include the effect of self-induction and also at that time deduced the finite velocity of propagation of electromagnetic waves. Heaviside also examined the induction-effect in 1881 and established what is now known as the traveling-wave solution. In 1886, he introduced for the first time "leakance" (also known as shunt conductance) as the fourth parameter into the transmission line equations and later formulated the conditions necessary for a "distortionless line." Heaviside had used the word "impedance" for the first time in 1884, and "reactance," which he introduced from France in 1893. Since Heaviside, the general transmission line model includes four distributed line parameters; namely, series resistance R , series inductance L , shunt capacitance C , and shunt conductance G per unit length. In power transmission lines, the shunt conductance G is very small compared to the other three parameters and is usually neglected.

Methods of transmission line simulation for transient analysis have been introduced by many authors and they can be classified into three

main categories: miniature power system simulation, analog and hybrid computer simulation, and digital computer simulation.

Miniature power system simulation:

These simulators are commonly known as Transient Network Analyzers (TNAs) or Power Simulators. Electromagnetic transients have been studied with transient network analyzers since the late 1930s. Inductors wound on magnetic cores with specially selected characteristics were used to represent transmission line sections, transformers, source impedances, etc. The generators were represented by ideal voltage sources behind appropriate reactances and were operated at the nominal power frequency. This leads to simulation of transient phenomena in real time, which often is a valuable asset. There are many problems which require that the simulation be in real time. The advantage to consider is the fact that in a real time simulation, the actual generation and display of the transient is also in real time, which is generally quite short, of the order of a few milliseconds. Thus, whenever a particular study requires a large number of repetitive runs, the actual run time on a network simulator for the entire set of studies is quite short. Another advantage of the physical model is that there are no computationally unstable solutions in a physical miniature model system. This problem is known to occur occasionally in computer simulations, especially with studies involving long run times. There are certain aspects of miniature model simulations which often present problems. Analog simulators are relatively inflexible. Setting up for a study on the simulator is a time consuming process. Also, the size of the

system that can be simulated for a study is limited by the available equipment. Simulators capable of representing a system of reasonable size are fairly large installations. In addition to the problems associated with the size and inflexibility, there are certain technical limitations to all physical simulations such as the finite length representation of transmission lines. In spite of these disadvantages, the TNA technique was the dominant tool in transient analysis for many years.

Analog and hybrid computer simulation:

Analog and hybrid computers have been used for some specific transient simulation studies such as practical industry problems. The major advantage of analog computer simulation is that it does simultaneous integration of all the differential equations in a problem. On a digital computer, the differential equations must be processed sequentially (in a computational sense, and not necessarily in a structural sense). Even so, the analog computer simulations are rarely as fast as the network simulators. Recently, some very high speed analog simulations have been attempted, but they are not general purpose analog computer systems, rather they tend to be special hardwired simulation tools. The problem set-up time with analog and hybrid computers tends to be high. Also, algebraic equations, requiring loops without time lags, cannot be solved easily on analog computers.

Digital computer simulation:

For many years, digital computer methods have been employed for the calculation of transient phenomena on power system networks caused by

switching operations. The computational techniques used may be broadly classified into time-domain methods and frequency-domain methods.

1. Time-domain methods

a. Basic methods and transient programs Historically, digital computer programs for power transients began with techniques for studying wave propagation phenomena on transmission lines. The wave propagation problem was basically solved by two techniques known as the Bewelys lattice diagram [1,2] and Bergeron's graphical method [3].

The Bewelys Lattice diagram method uses reflection coefficients calculated for wave incident upon a discontinuity. Assuming a constant reflection coefficient, the incoming wave is broken into a reflected and a transmitted component. By keeping track of both components as they travel along the line, the voltage vs. time at any bus may be obtained. As the complexity of power systems grew, it was necessary to adapt the lattice method for solutions on digital computers using numerical techniques. The lattice method was implemented by, amongst others, Barthold and Carter [4], and McElroy and Porter [5].

The Bergeron method is based on forward and backward traveling waves, but solved graphically. This method uses linear relationships between voltage and current. The Bergeron method was more suitable for computer programs as it considers the terminal constraints of the line. Many authors [6,7] have adopted this technique for transmission line problems, but assumed the line to be lossless. Both methods provided efficient pictorial techniques for the bookkeeping. In spite

of the approximations involved in both methods (lossless lines with constant parameters), the solutions obtained illustrated the main structure of the phenomena.

Consequently, Dommel [8], after approximating the derivative by first order backward difference, devised a constant resistance ($\sqrt{L/C}$) and a current source equivalent circuit for the transmission line at each end. Such equivalent circuits were decoupled. He also used the past history of the traveling wave to compute the values of voltage and current at each end. The program was essentially based on Bergeron's method, but used numerical techniques instead of graphical techniques. This program is known as the Electromagnetic Transient Program (EMTP), originally developed by Dommel [8] and nurtured at the Bonneville Power Administration by Meyer and Liu [9].

Some other programs have also been in use for solving power system transient problems. The program METAP [10] uses a constant lumped parameter model for the transmission line, and similar models for the different equipment in the network. The connections between different equipment in the network are handled by connection equations satisfying Kirchhoff's circuit laws. Another such program is TRANSO [11], which uses Bergeron's method to simulate transmission line transients. Each lumped component is approximated by a stub transmission line of appropriate length and characteristic impedance. Both of these programs have been (and are being) used to solve practical electric utility problems.

There are a few programs with a more general applicability, which have seen some use in power system applications. The program ECAP [12] is used fairly wide as a circuit analysis tool. In many universities and research organizations, it is used for solving electronic circuit problems of small to moderate size. Although it could be used for power system transient analysis, many of its features--including its input and output facilities--are not convenient for practical power system use. Although the digital approach has not supplanted the traditional method of using miniature network models, it certainly has the capability to solve transient problems efficiently and economically. Many more options can now be examined because of the ready availability of the computer program than would have been possible just a few years ago. Certainly the trend seems to be towards an increasing role for digital simulation techniques in transient analysis.

b. Approximating line losses Most of the transient programs are only efficient for distortionless or lossless lines. Yet propagation on overhead transmission lines is far from distortionless and approximations for line losses had to be found. Such approximations considered the line losses to be represented by a constant resistor at each end of the line [13]. Some other researchers propose to divide the line into two sections and include a resistance at both terminals and between the two sections [14]. With these approximations, the main line equations or section equations were solved as lossless lines. Most

of these programs were originally written for single-phase networks, and then extended to three-phase configurations. In the case of a single line above earth, the effect of line losses is to attenuate and retard a voltage wave traveling along the line. In more complicated three-phase systems, mutual coupling exists between phases and second order changes of voltage in each phase are functions of the voltages in other phases. Losses in such cases cannot be represented by simply attenuating and retarding the voltages in each phase.

Matrix theory provided an approximate solution to the problem by representing the line by a number of modes of propagation, the voltages of which travel independently of one another and free of mutual effects. This approach is described by Wedepohl [15] and assumes that the line parameters are frequency independent. Also it is assumed that the line has symmetric configuration.

c. Frequency dependence of line parameters Attempts have been made to approximate the frequency dependence of the line parameters. Methods have therefore been developed for modifying Bergeron's method to include the effect of frequency dependent parameters. Dommel and Meyer [14] suggested that more past history points of the traveling wave be weighted with an exponentially decaying weighting function. Mathematically, this is done with a convolution integral. This procedure produced an approximation for an attenuation and a distortion of the pulse as it travels from one end of the line to the other.

Carroll and Nozari [16] suggested a method to obtain the characteristic impedance and propagation coefficient of a single phase line in

the frequency domain. Then applying the inverse Fourier integral, they obtained a time function for the characteristic impedance and the propagation constant to be used in a convolution integral with Bergeron's method. The method was extended to include the three-phase transmission line problem, but with equal mutual coupling between phases. In this method, the boundary conditions are assumed to be known at the line terminals.

As a summary, most transient analysis time domain computer programs are based on Bergeron's method. The problem was solved first for single phase and lossless lines. Modifications have been made to approximate losses and frequency dependent parameters. However, the time domain solution does not allow a direct method to account for the actual variation of the line parameters with frequency. The three-phase transmission line is assumed to have equal mutual coupling between phases. The difficulty in handling the boundary condition restricts the technique to special problems. For example, Carroll and Nozari [16] applied the technique to study a fault on an open end transmission line and a surge voltage traveling on a HVDC transmission line. Also, the time domain solution requires large amounts of computer storage and computation time. Theoretically, time varying parameters can be handled by the time domain solution.

2. Frequency domain methods

For any power transmission line, only the shunt capacitance is constant, whereas the resistance and the inductance are functions of the frequency. The transmission line equations with frequency dependent

parameters are still linear, which means that superposition technique still applies. Laplace and Fourier transformations therefore provide a rigorous solution to the problem. Conceptually, the time varying voltages and currents are transformed into the frequency domain to display their frequency spectrum. Then for any frequency, the appropriate line parameters are used and the response can be found. Finally, all such incremental responses are added by means of inverse Fourier or Laplace transformations back to the time domain, giving the total response.

This idea of frequency-domain solution was applied to transient problems in power systems in the mid 1970s. Jones and Aggarwal [17] developed a digital simulation of a transmission line in the complex frequency domain. In this method, the transmission line was considered ideally transposed with frequency dependent parameters. The faulted transmission line was treated as a network of cascaded sections. Each section was represented by a two-port transfer matrix. For example, a transfer matrix represented the line section up to the point of fault, another transfer matrix represented the fault discontinuity, and a third transfer matrix represented the line section between the fault and the receiving end busbars. The multiplication of these matrices gave the relationships between the currents and the voltages at either end of the line in the frequency domain. The inverse Fourier transform was used to determine the corresponding time variation of the voltage and current of interest.

Trizezenberg [18] developed a technique for simulating the transmission line based on the finite Fourier transform. In this technique, a transformation of the spatial independent variable x (distance along the line) is used. The final step of this technique uses state variable methods and four transfer functions to approximate the relations between the currents and voltages at both ends of the line. The four transfer functions were characterized by eleven poles in the complex frequency domain. This technique is similar to cascaded π or T sections of the transmission line. This technique was applied to special cases because of the difficulty in obtaining the boundary conditions at the fault location or at the sending end of the line. Also, this technique assumed the line parameters to be constant and independent of frequency.

Although the frequency domain method offers a solution for the frequency dependence of the line parameters, there is a difficulty in handling the time varying parameters. In this technique, it has been assumed that the line has equal mutual coupling between phases. Also it has been common to assume zero fault resistance at the fault location and a transmission line connected to an infinite bus. Some of these assumptions are invalid for certain studies.

B. Synchronous Generator Model

In order to make any review of the literature pertaining to synchronous machines sensible, it is necessary to make some preliminary comments about the machine per se. A three-phase synchronous machine has three stator coils that are as physically alike as is feasible within the limits of manufacturing practice. These coils are oriented at 120° to one

another in space and are usually designated as a, b, c . The machine also has a rotor that contains two shorted coils (damper windings) and one coil excited from a DC voltage source (field winding). The self inductances of the stator coils and the mutual inductances between the stator and rotor coils are all functions of the angular displacement of the rotor. The coil currents and the angular position of the rotor are the dependent variables in the machine differential equations.

The machine equations are easy to formulate in these terms (this formulation is said to be based on $a-b-c$ coordinates), but the coefficients are functions of angular displacement, and the equations per se are mathematically refractory. As a consequence, a variety of transformations have been developed to produce a more tractable set of equations. The most important of these is the Park transformation [19] in which the coordinates are designated $(0-d-q)$. This transformation produces a set of equations with constant coefficients. A second transformation called the $(0-1-2)$ transformation due to Fortescue [20] is also available to simplify the analysis of unbalanced three-phase circuits. This transformation does not pertain to the machine per se, but it can be used in conjunction with the $(0-d-q)$ transformation to solve machine problems.

Generally, the Park transform cannot be used in fault studies without going back to the $(a-b-c)$ components. With the advent of modern computers, numerical methods have been used for solving nonlinear differential equations. In such cases, the direct three-phase $(a-b-c)$ nonlinear differential equations could be used for the study of

synchronous machine performance during fault transients. Subramaniam and Malik [21] devised a fourth order Runge-Kutta method to solve non-linear machine equations in the (a-b-c) components. This method requires considerable computational effort and its accuracy depends on the step size. The difficulty in handling boundary conditions restricts the method to the solution of special problems. Such special problems are fault transient analysis of unloaded machines or machine connected to an infinite bus (constant voltage with zero impedance).

As indicated in the last section (A), the frequency domain solution has been used to account correctly for the distributed nature and the frequency variation of the line parameters. Therefore, it is desirable to simulate the synchronous machines in the frequency domain. The works of Ku [19] and Adkins [22] are typical and pertinent examples. Both used the Park transform in describing the transient behavior of the synchronous machine. Ku analyzed a mechanically unloaded synchronous machine transient due to a fault. Adkins described the transient behavior of a synchronous machine connected to an infinite bus by assuming constant rotor speed and equal mutual coupling between the rotor and the stator. He indicated that the assumption of constant speed gives acceptable accuracy during the first few cycles following the fault, and the rotor swing may be safely ignored.

As a summary, most of transient analysis of synchronous machines assumed known boundary conditions at the machine terminals. For example, a synchronous machine connected to an infinite bus or unloaded machine were common assumptions. The analysis of a fault transient on a

transmission line necessarily requires recognition of the fact that the line is connected to a machine. Subsequent reference is made to a "simple" machine model. Basically, this consists of representing the machine by a Thevenin's equivalent which establishes sending-end boundary conditions. While this is mathematically convenient, it cannot be rigorously justified in transient analysis; the line equations are formulated in (a-b-c) coordinates, and the machine can only be represented by a Thevenin equivalent in (0-d-q) coordinates.

One of the most important elements in this thesis is the development of a set of transformations that make it possible to couple the machine equations with the line equations. The only ad hoc assumption that must then be invoked is based upon Adkins' [22] assurance that the rotor swing during the first few cycles is negligibly small.

III. TRANSIENT AND STEADY-STATE ANALYSIS OF TRANSMISSION LINES

The transmission line possesses a certain inductance, capacitance, and resistance, so that these quantities are truly distributed over tens or hundreds of miles. The main purpose of analysis is to determine the magnitude of current and voltage at any point on the transmission line, and to transfer the greatest amount of usable power to the load. The analysis is general for short, medium, and long transmission lines.

A. Formulation of Three-Phase Transmission Line Equations

1. Voltage equations

Figure 3.1 represents a section of a three-phase transmission line with length Δx . The ground return of an overhead conductor is called Carson's line [23] which is a single conductor dd' with length Δx and parallel to the ground.

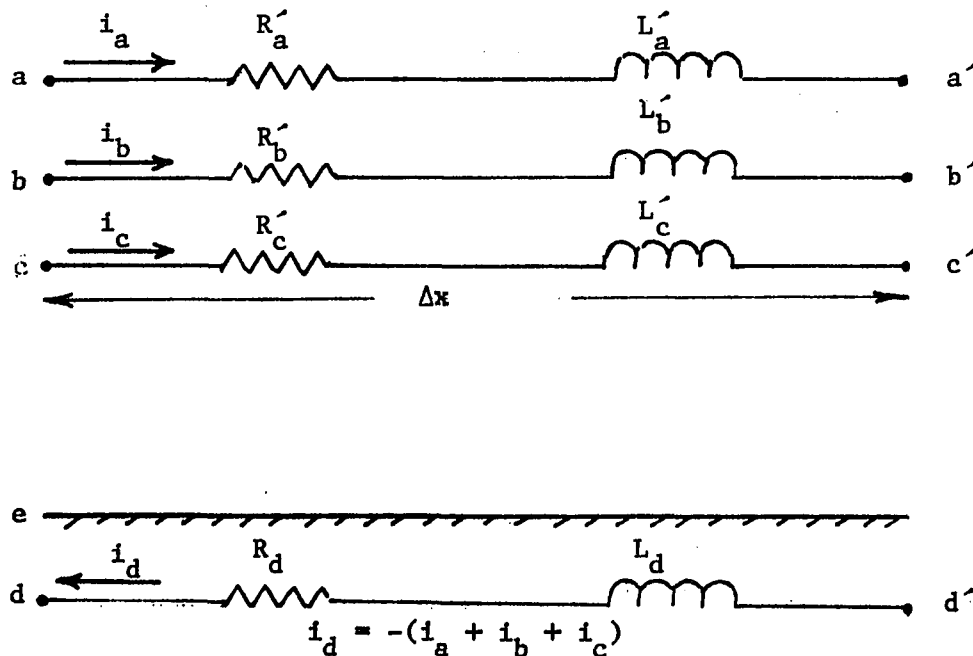


Figure 3.1. A section of a three-phase transmission line with ground return

The voltage equations of the three-phase transmission line are:

$$-\frac{\partial}{\partial x} v'_a(x,t) = R'_a i_a(x,t) + L'_{aa} \frac{\partial}{\partial t} i_a(x,t) + L'_{ab} \frac{\partial}{\partial t} i_b(x,t) \\ + L'_{ac} \frac{\partial}{\partial t} i_c(x,t) + L'_{ad} \frac{\partial}{\partial t} i_d(x,t)$$

$$-\frac{\partial}{\partial x} v'_b(x,t) = L'_{ba} \frac{\partial}{\partial t} i_a(x,t) + R'_b i_b(x,t) + L'_{bb} \frac{\partial}{\partial t} i_b(x,t) \\ + L'_{bc} \frac{\partial}{\partial t} i_c(x,t) + L'_{bd} \frac{\partial}{\partial t} i_d(x,t)$$

$$-\frac{\partial}{\partial x} v'_c(x,t) = L'_{ca} \frac{\partial}{\partial t} i_a(x,t) + L'_{cb} \frac{\partial}{\partial t} i_b(x,t) + R'_c i_c(x,t) \\ + L'_{cc} \frac{\partial}{\partial t} i_c(x,t) + L'_{cd} \frac{\partial}{\partial t} i_d(x,t)$$

$$-\frac{\partial}{\partial x} v'_d(x,t) = L'_{da} \frac{\partial}{\partial t} i_a(x,t) + L'_{db} \frac{\partial}{\partial t} i_b(x,t) + L'_{dc} \frac{\partial}{\partial t} i_c(x,t) \\ + R'_d i_d(x,t) + L'_{dd} \frac{\partial}{\partial t} i_d(x,t)$$

The above equation can be written in a matrix form as

$$-\frac{\partial}{\partial x} \begin{bmatrix} v'_a(x,t) \\ v'_b(x,t) \\ v'_c(x,t) \\ \vdots \\ v'_d(x,t) \end{bmatrix} = \begin{bmatrix} R'_a & & & & \\ & R'_b & & & \\ & & R'_c & & \\ \vdots & & & \ddots & \\ 0 & & & & R'_d \end{bmatrix} \begin{bmatrix} i_a(x,t) \\ i_b(x,t) \\ i_c(x,t) \\ \vdots \\ i_d(x,t) \end{bmatrix} \\ + \begin{bmatrix} L'_{aa} & L'_{ab} & L'_{ac} & & L'_{ad} \\ L'_{ba} & L'_{bb} & L'_{bc} & & L'_{bd} \\ L'_{ca} & L'_{cb} & L'_{cc} & & L'_{cd} \\ \vdots & \vdots & \vdots & \ddots & \vdots \\ L'_{da} & L'_{db} & L'_{dc} & & L'_{dd} \end{bmatrix} \frac{\partial}{\partial t} \begin{bmatrix} i_a(x,t) \\ i_b(x,t) \\ i_c(x,t) \\ \vdots \\ i_d(x,t) \end{bmatrix} \quad (3.1)$$

or

$$-\frac{\partial}{\partial x} \underline{v}_{abcd}(x,t) = \underline{R}_{abcd} \cdot \underline{i}_{abcd}(x,t) + \underline{L}_{abcd} \frac{\partial}{\partial t} \underline{i}_{abcd}(x,t).$$

Since $v_d(x,t) = 0$, then equation (3.1) is reduced as

$$-\frac{\partial}{\partial t} \begin{bmatrix} v_a(x,t) \\ v_b(x,t) \\ v_c(x,t) \end{bmatrix} = \begin{bmatrix} R_a & & \\ & R_b & \\ & & R_c \end{bmatrix} \begin{bmatrix} i_a(x,t) \\ i_b(x,t) \\ i_c(x,t) \end{bmatrix} + \begin{bmatrix} L_{aa} & L_{ab} & L_{ac} \\ L_{ba} & L_{bb} & L_{bc} \\ L_{ca} & L_{cb} & L_{cc} \end{bmatrix} \frac{\partial}{\partial t} \begin{bmatrix} i_a(x,t) \\ i_b(x,t) \\ i_c(x,t) \end{bmatrix}$$

or

$$-\frac{\partial}{\partial t} \underline{v}_{abc}(x,t) = \underline{R}_{abc} \underline{i}_{abc}(x,t) + \underline{L}_{abc} \frac{\partial}{\partial t} \underline{i}_{abc}(x,t)$$

By dropping the abc

$$-\frac{\partial}{\partial x} \underline{v}(x,t) = \underline{R} \underline{i}(x,t) + \underline{L} \frac{\partial}{\partial t} \underline{i}(x,t) \quad (3.2)$$

In many physical transmission lines, wires are added above the phase wires to "shield" the line against direct lightning strokes. These ground wires have an effect on the line impedance. The same previous steps can be followed in obtaining the voltage equation in case of lines with one or more ground wires, and the same final result as equation (3.2) can be obtained.

2. Current equations

The nodal analysis can be applied to find the current at each phase as

$$\begin{aligned}
 -\frac{\partial}{\partial x} i_a &= C_{ag} \frac{\partial}{\partial t} v_a(x,t) + G_a v_a(x,t) + C_{ab} \frac{\partial}{\partial t} [v_a(x,t) - v_b(x,t)] \\
 &\quad + C_{ac} \frac{\partial}{\partial t} [v_a(x,t) - v_c(x,t)]
 \end{aligned}$$

$$\begin{aligned}
 -\frac{\partial}{\partial x} i_b &= C_{ba} \frac{\partial}{\partial t} [v_b(x,t) - v_a(x,t)] + C_{bg} \frac{\partial}{\partial t} v_b(x,t) + G_b v_b(x,t) \\
 &\quad + C_{bc} \frac{\partial}{\partial t} [v_b(x,t) - v_c(x,t)]
 \end{aligned}$$

$$\begin{aligned}
 -\frac{\partial}{\partial x} i_c &= C_{ca} \frac{\partial}{\partial t} [v_c(x,t) - v_a(x,t)] + C_{cb} \frac{\partial}{\partial t} [v_c(x,t) - v_b(x,t)] \\
 &\quad + C_{cg} \frac{\partial}{\partial t} v_c(x,t) + G_c v_c(x,t)
 \end{aligned}$$

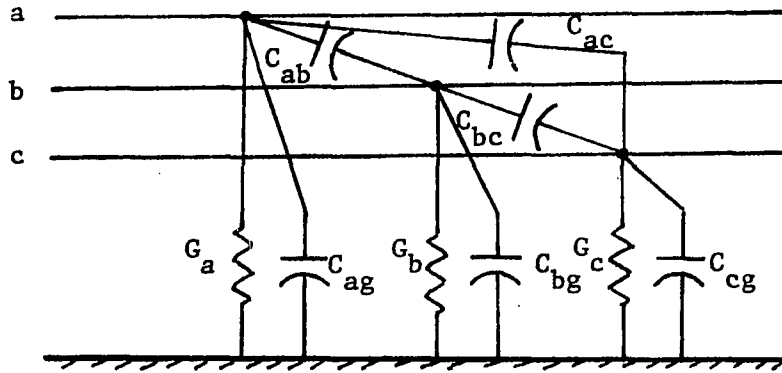


Figure 3.2. Capacitances and conductances in three-phase transmission line

The above equations can be written in a matrix form as

$$\begin{aligned}
-\frac{\partial}{\partial x} \begin{bmatrix} i_a(x,t) \\ i_b(x,t) \\ i_c(x,t) \end{bmatrix} &= \begin{bmatrix} G_a & & \\ & G_b & \\ & & G_c \end{bmatrix} \begin{bmatrix} v_a(x,t) \\ v_b(x,t) \\ v_c(x,t) \end{bmatrix} \\
&+ \begin{bmatrix} (C_{ag} + C_{ab} + C_{ac}) & -C_{ab} & -C_{ac} \\ -C_{ba} & (C_{bg} + C_{ba} + C_{bc}) & -C_{bc} \\ -C_{ca} & -C_{cb} & (C_{cg} + C_{cb} + C_{ca}) \end{bmatrix} \frac{\partial}{\partial t} \begin{bmatrix} v_a(x,t) \\ v_b(x,t) \\ v_c(x,t) \end{bmatrix}
\end{aligned}$$

or

$$-\frac{\partial}{\partial x} \underline{i}_{abc}(x,t) = \underline{G}_{abc} \cdot \underline{v}_{abc}(x,t) + \underline{C}_{abc} \cdot \frac{\partial}{\partial t} \underline{v}_{abc}(x,t).$$

By dropping the abc in the above equation as

$$-\frac{\partial}{\partial x} \underline{i}(x,t) = \underline{G} \cdot \underline{v}(x,t) + \underline{C} \cdot \frac{\partial}{\partial t} \underline{v}(x,t) \quad (3.3)$$

By differentiating equations (3.2) and (3.3) with respect to x, and substituting the values of $\frac{\partial}{\partial x} \underline{i}$ and $\frac{\partial}{\partial x} \underline{v}$ the results are

$$\begin{aligned}
-\frac{\partial^2}{\partial x^2} \underline{v}(x,t) &= \underline{R} \frac{\partial}{\partial x} \underline{i}(x,t) + \underline{L} \frac{\partial}{\partial t} \frac{\partial}{\partial x} \underline{i}(x,t) \\
&= \underline{R} [-\underline{G} \underline{v}(x,t) - \underline{C} \frac{\partial}{\partial t} \underline{v}(x,t)] \\
&\quad + \underline{L} \frac{\partial}{\partial t} [-\underline{G} \underline{v}(x,t) - \underline{C} \frac{\partial}{\partial t} \underline{v}(x,t)]
\end{aligned}$$

$$\begin{aligned}
-\frac{\partial^2}{\partial x^2} \underline{v}(x,t) &= -\underline{R} \underline{G} \underline{v}(x,t) - \underline{R} \underline{C} \frac{\partial}{\partial t} \underline{v}(x,t) \\
&\quad - \underline{L} \underline{G} \frac{\partial}{\partial t} \underline{v}(x,t) - \underline{L} \underline{C} \frac{\partial^2}{\partial t^2} \underline{v}(x,t)
\end{aligned}$$

or

$$\begin{aligned} \frac{\partial^2}{\partial x^2} v(x,t) &= R G v(x,t) + R C \frac{\partial}{\partial t} v(x,t) \\ &+ L G \frac{\partial}{\partial t} v(x,t) + L C \frac{\partial^2}{\partial x^2} v(x,t) \end{aligned}$$

In any power transmission line, the value of G is insignificant ($10^{-6} - 10^{-8}$), so it can be neglected and the above equations can be written as

$$\frac{\partial^2}{\partial x^2} v(x,t) = R C \frac{\partial}{\partial t} v(x,t) + L C \frac{\partial^2}{\partial x^2} v(x,t) \quad (3.4)$$

Also,

$$\begin{aligned} - \frac{\partial^2}{\partial x^2} i(x,t) &= G \frac{\partial}{\partial x} v(x,t) + C \frac{\partial}{\partial t} \frac{\partial}{\partial x} v(x,t) \\ &= G [-R i(x,t) - L \frac{\partial}{\partial t} i(x,t)] \\ &+ C [-R \frac{\partial}{\partial t} i(x,t) - L \frac{\partial^2}{\partial t^2} i(x,t)] \end{aligned}$$

or

$$\begin{aligned} \frac{\partial^2}{\partial x^2} i(x,t) &= G R i(x,t) + C R \frac{\partial}{\partial t} i(x,t) \\ &+ G L \frac{\partial}{\partial t} i(x,t) + C L \frac{\partial^2}{\partial t^2} i(x,t) \end{aligned}$$

By ignoring the parameter G

$$\frac{\partial^2}{\partial x^2} i(x,t) = C R \frac{\partial}{\partial t} i(x,t) + C L \frac{\partial^2}{\partial t^2} i(x,t) \quad (3.5)$$

Equations (3.4) and (3.5) represent the partial differential equations of any three-phase transmission line where

\underline{L} is a (3 x 3) inductance matrix in Henry per unit distance.

\underline{C} is a (3 x 3) capacitance matrix in Farad per unit distance.

\underline{R} is a (3 x 3) resistance matrix in Ohm per unit distance.

\underline{G} is a (3 x 3) conductance matrix in Siemens per unit distance.

B. Calculation of the Line Parameters

A transmission line is characterized by four distributed line parameters, namely, R, L, C, and G per unit length. Usually G has a very small value (10^{-6} - 10^{-8}) and it is neglected. The inductance matrix \underline{L} in equations (3.4) and (3.5) can be obtained by using the equations in reference [23] for any configuration of the line. The general expressions of the series impedance of the transmission line with ground wire are

$$Z_{ii} = (R_i + R_d) + j (2\pi f) k \ln \frac{D_e}{D_{si}} \text{ ohm/unit length} \quad (3.6)$$

$$Z_{ij} = R_d + j (2\pi f) k \ln \frac{D_e}{D_{ij}} \text{ ohm/unit length} \quad (3.7)$$

where

Z_{ii} = self impedance of conductor i in ohm/unit length and the diagonal terms of the impedance matrix.

Z_{ij} = off diagonal terms of the impedance matrix in ohm/unit length.

R_i = series line resistance in ohm/unit length

D_{si} = self geometric mean radius of conductor i in ft. and for cylindrical conductor $D_s = .779 r$ ft.

D_{ij} = distance between conductor i and conductor j in ft.

f = frequency in Hz.

k = constant which is chosen according to the user's units and its values in reference [23].

R_d = earth resistance = $1.588 \times 10^{-3} f$ Ohm/mi.
 $= 9.869 \times 10^{-4} f$ Ohm/km.

D_e is a function derived in reference [23] and it is equal to
 $2160 \sqrt{\frac{\rho}{f}}$ ft.

ρ = Earth resistivity

Equations (3.6) and (3.7) show that the impedance of the line is a function of frequency. The numerical example in Appendix A is taken to find the impedance matrix as in equations (3.6) and (3.7) at different frequencies by using the computer. The results are shown in Figures 3.3 and 3.4. Figure 3.3 shows that the real part of the elements (1,1) and (1,2) of the impedance matrix increases rapidly with frequency. Figure 4.4 shows that the imaginary part of the elements (1,1) and (1,2) decrease with frequency, but the variation after 400 Hz. is insignificant.

Calculation of the admittance matrix of the transmission line is also discussed in reference [23]. The capacitance of any three-phase transmission line with ground wires can be calculated by using the equation $\underline{V} = \underline{P} \underline{q}$ where

\underline{P} = Potential coefficient matrix in Farad^{-1} unit length

\underline{q} = Charge matrix in Coulomb per unit length

\underline{V} = Voltage to neutral matrix

By using the subscript abc to denote the phase conductors, and the subscript n to denote the ground wire, the voltage equations in matrix form are:

$$\begin{bmatrix} V_{abc} \\ \vdots \\ V_n \end{bmatrix} = \begin{bmatrix} P_1 & P_2 \\ \vdots & \vdots \\ P_3 & P_4 \end{bmatrix} \begin{bmatrix} q_{abc} \\ \vdots \\ q_n \end{bmatrix} \quad (3.8)$$

By knowing $V_n = 0$, equation (3.8) can be reduced to three equations to present the three-phase voltage by eliminating the fourth row and column.

The result is

$$\begin{aligned} \underline{V}_{abc} &= (\underline{P}_1 - \underline{P}_2 \underline{P}_4^{-1} \underline{P}_3) \underline{q}_{abc} \\ &= \underline{P}_{abc} \underline{q}_{abc} \end{aligned}$$

where $\underline{P}_{abc} = \underline{P}_1 - \underline{P}_2 \underline{P}_4^{-1} \underline{P}_3$

By dropping the subscript abc, then

$$\underline{V} = \underline{P} \underline{q} \quad (3.9)$$

\underline{P} is a (3×3) matrix and it is equal to the inverse of the capacitance matrix. The elements of \underline{P} are

$$P_{ii} = \frac{1}{2\pi\epsilon} \ln \left(\frac{H_i}{r_i} \right) = 11.185 \ln \left(\frac{H_i}{r_i} \right) \text{ MF}^{-1} \cdot \text{mi} \quad (3.10)$$

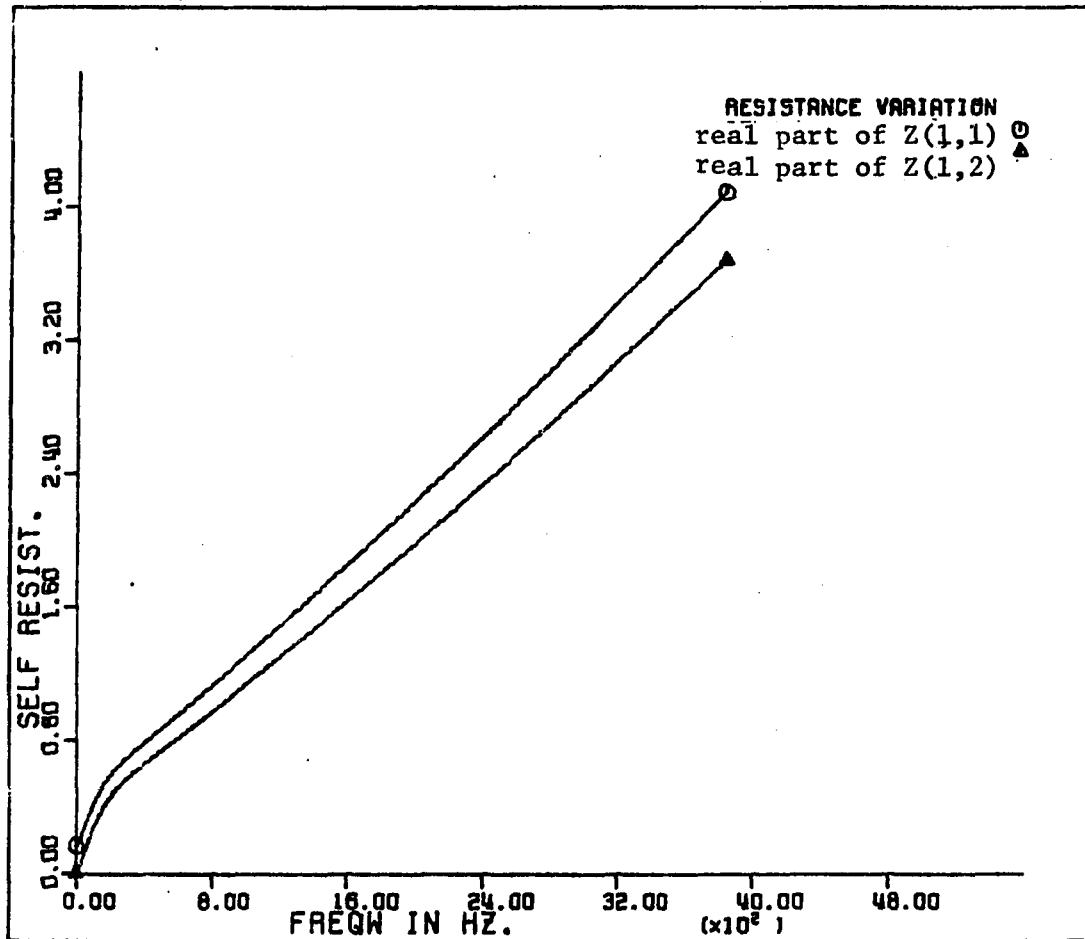


Figure 3.3. Resistance variation with frequency

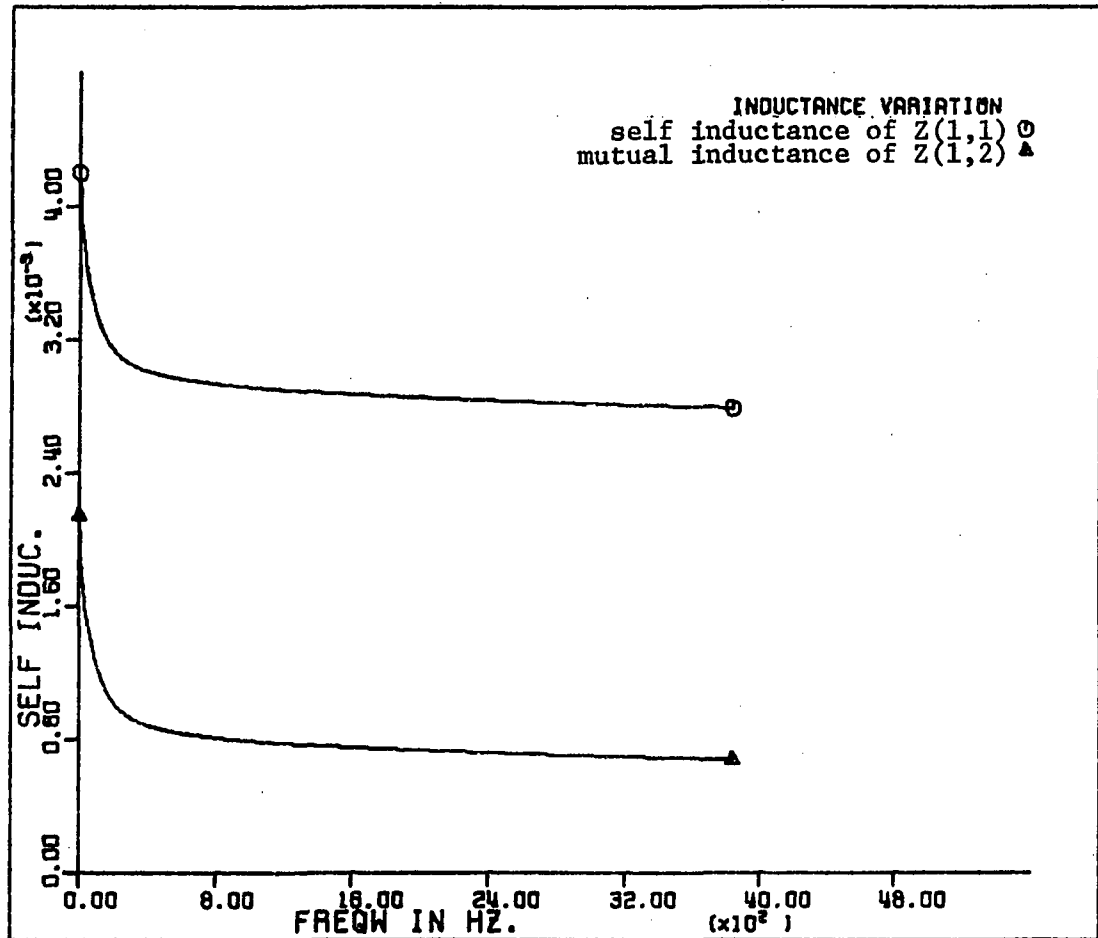


Figure 3.4. Inductance variation with frequency

$$P_{ij} = \frac{1}{2\pi\epsilon} \ln \left(\frac{H_{ij}}{D_{ij}} \right) = 11.185 \ln \left(\frac{H_{ij}}{D_{ij}} \right) \text{ MF}^{-1} \cdot \text{mi} \quad (3.11)$$

where

H_{ij} = GMD between conductors and their images

D_{ij} = GMD between conductors

and

r_i = radius of the conductor

By finding the \underline{P} matrix, then the capacitance matrix can be obtained from $\underline{C} = \underline{P}^{-1}$.

The admittance matrix of the transmission line $\underline{Y} = j\omega\underline{C}$ and it is (3×3) matrix for three-phase line. The computer program in Appendix B is used to find the admittance matrix from the line configuration. The calculations of impedance and admittance matrices are based on distributed line parameters.

C. Transmission Line Losses

Any practical transmission line cannot be lossless and completely transposed, and will usually be terminated at both ends as shown in figure 3.5. Most of the existing fault transient programs neglect the transmission line losses to simplify the solution of the line equations.

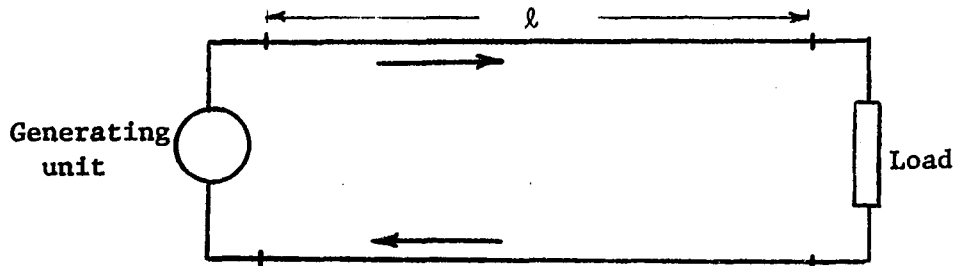


Figure 3.5. Practical transmission system

Some of these programs have been modified to include the transmission line resistance in their line model by different ways [24]. The analyses of lossless lines have been discussed in many references as [25,26], which are based on Bewley Lattice diagram.

A sudden occurrence of a fault on a power transmission line causes a propagation of traveling waves toward both ends of the transmission line. When the traveling waves reach the ends of the transmission line, they are reflected back to the faulted point. The line resistance and the other losses tend to attenuate and distort the waveforms of voltage and current. Therefore, the waveforms of the lossless line cannot produce correct estimates of the magnitude of voltages and currents.

In the transmission of power, there are many other losses which can be studied. The high electric field intensity surrounding high-voltage power lines accounts for an additional energy loss in the transmission line. The high voltage gradient at the surface of a wire sometimes accelerates electrons in the air sufficiently to ionize air molecules by collision. If the voltage gradient at the wire exceeds a certain critical value, the process of ionization becomes cumulative and results in appreciable loss of energy. The ionization is characterized by a faint glow surrounding the wire and is called corona. The critical voltage depends on wire size, spacing, and on atmospheric conditions. Corona is most likely to occur when the diameter of the conductor is small compared to the distance between wires. High voltage, small wires, and close spacing contribute to a high voltage gradient which may introduce corona. Damp weather increases the loss from corona, and a

rough or dirty surface on a conductor increases the probability of the occurrence of corona. Empirical methods for the calculation of corona loss are available in many references [27] and it is usually small.

Another loss occurring on transmission lines is caused by the leakage of current at the insulators which support the lines at the towers. Since leakage at insulators of overhead lines is negligible and corona loss is usually small, also the conductance between conductors of overhead lines is assumed to be zero.

In a transmission line there is a nonuniformity of current distribution in addition to that caused by skin effect. In a two-wire line, slightly fewer lines of flux link the elements nearest each other on opposite sides of the line than link the elements farther apart. Therefore, elements in the near sides have lower inductance than elements on the far sides. The result is a higher current density in the element of adjacent conductors nearest each other than in the elements farther apart. The effective resistance is increased by the nonuniformity of current distribution. The phenomenon is known as proximity effect. The increase in resistance depends on the frequency, distance between conductors, conductor size, and permeability. Proximity effect is present for three-phase as well as single-phase circuits. Even at high frequencies, if the ratio of spacing between wires to the radius of the wires of a two-wire line is greater than 15 to 1, the increase of resistance due to proximity effect is only 1% as discussed in reference [28]. Usually the proximity effect is not introducing error in determining the resistance and it is neglected.

Skin effect phenomenon:

A uniform distribution of current throughout the cross section of a conductor exists only for direct current. As the frequency of alternating current increases, the nonuniformity of distribution becomes more pronounced. An increase in frequency causes more current to be concentrated near the surface of the conductor and less in the interior. This phenomenon is called skin effect.

Skin effect resistance ratio:

The internal impedance of a conductor is composed of resistance and inductive reactance. The real part of the complex impedance is the effective resistance. The method of calculating the effective resistance of the line is discussed in many references [23,28] as

$$R = \frac{\rho' m}{\pi} \frac{\text{ber}(mr) \cdot \text{bei}'(mr) - \text{bei}(mr) \cdot \text{ber}'(mr)}{(\text{bei}'(mr))^2 + (\text{ber}'(mr))^2} \quad \text{Ohm/unit length}$$

The d-c resistance R_o for a round conductor is

$$R_o = \rho' / A = \rho' / \pi r^2$$

The ratio of effective resistance to d-c resistance is

$$R/R_o = \alpha_R = \frac{mr}{2} \frac{\text{ber}(mr) \cdot \text{bei}'(mr) - \text{bei}(mr) \cdot \text{ber}'(mr)}{(\text{bei}'(mr))^2 + (\text{ber}'(mr))^2} \quad (3.12)$$

$$mr = r \sqrt{\frac{2\pi f \mu}{\rho'}} = .0636 \sqrt{\frac{\mu_{rf}}{R_o}}$$

where

R_o = d-c resistance in ohm/unit length

r = radius of the conductor

μ_r = relative permeability of the wire

The functions ber , bei are complex functions, and ber' , bei' are their derivatives as

$$\text{ber}(mr) = 1 - \frac{(mr)^4}{2^2 \cdot 4^2} + \frac{(mr)^8}{2^2 \cdot 4^2 \cdot 6^2 \cdot 8^2} + \dots$$

$$\text{bei}(mr) = \frac{(mr)^2}{2^2} - \frac{(mr)^6}{2^2 \cdot 4^2 \cdot 6^2} + \dots$$

$$\text{ber}'(mr) = \frac{d}{d(mr)} \text{ber}(mr) = \frac{1}{m} \frac{d}{dr} \text{ber}(mr)$$

$$\text{bei}'(mr) = \frac{d}{d(mr)} \text{bei}(mr) = \frac{1}{m} \frac{d}{dr} \text{bei}(mr)$$

The variation of α_R with the frequency is plotted in reference [23]. This variation cannot be neglected particularly in large conductors because of the skin effect.

Skin-effect inductance ratio:

The imaginary component of the internal impedance of a conductor is the inductive reactance due to internal flux linkages. The expression for internal inductive reactance is in reference [22] as

$$\omega L_i = \frac{\rho' m}{2\pi r} \frac{\text{bei}(mr) \cdot \text{bei}'(mr) + \text{ber}(mr) \cdot \text{ber}'(mr)}{(\text{bei}(mr))^2 + (\text{ber}'(mr))^2} \text{ ohm/unit length}$$

If L_{i0} is the internal inductance at frequencies so low as is equal to $\frac{\mu}{8\pi}$, then the ratio of internal inductance of a wire at any frequency to internal inductance is

$$\frac{L_i}{L_{i0}} = \alpha_L = \frac{4}{\pi r} \left[\frac{\text{bei}(\pi r) \cdot \text{bei}'(\pi r) + \text{ber}(\pi r) \cdot \text{ber}'(\pi r)}{(\text{bei}'(\pi r))^2 + (\text{ber}'(\pi r))^2} \right] \quad (3.13)$$

That ratio approaches unity as the frequency approaches zero. As the frequency increases, the ratio becomes smaller, for skin effect causes the current to crowd toward the surface of the wire and thereby reduces the number of internal flux linkages. Tabulated values of skin effect inductance ratio are available in many references [28]. Therefore, the self and mutual inductances can be obtained by taking the skin effect into consideration as

$$L_s = K \left[\ln \left(\frac{2 D_{ij} e^{\alpha L}}{D_{si}} \right) - 1 \right] \quad \text{Henry/unit length} \quad (3.14)$$

$$L_m = K \left[\ln \left(\frac{2 D_{ij} e^{\alpha L}}{\text{GMD}} \right) - 1 \right] \quad \text{Henry/unit length} \quad (3.15)$$

where

L_s = self inductance

L_m = mutual inductance

D_{ij} = distance between conductor i and j

GMD = geometric mean distance

K = constant depends on the units used

D_{si} = self geometric mean distance of conductor i

The skin effect inductance ratio is less important than the skin effect resistance ratio in the total impedance of the line.

The calculation of the impedance matrix of a three-phase transmission line is obtained by using two methods. The first method is based on Carson's line by using equations (3.6) and (3.7) and the second method uses equations (3.12), (3.14), and (3.15) which are derived from Maxwell's equations. The waveforms of voltage and current were obtained by using both methods.

IV. GENERAL EQUATIONS AND SOLUTION FOR FAULTED POWER TRANSMISSION SYSTEMS

As previously discussed, the line is untransposed with frequency dependent parameters. Based on this model, the solution of voltage and current can be obtained by solving the partial differential equations of the transmission line, i.e., equations (3.2) and (3.3).

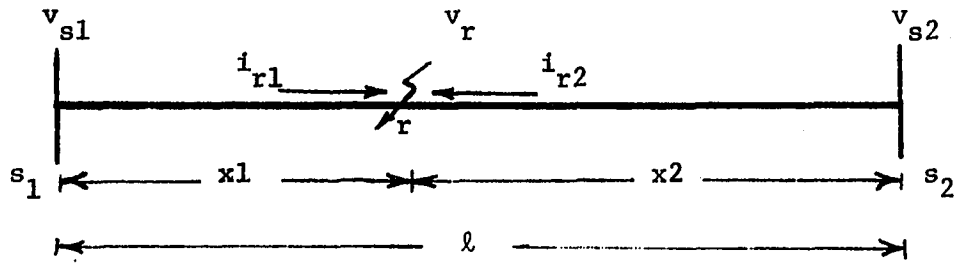


Figure 4.1. Single line diagram of faulted transmission systems

Figure 4.1 defines the voltages at the sending end, receiving end, and the fault location. These are designated v_{s1} , v_{s2} , and v_r respectively. The fault is located at distance x_1 from the sending end, and at distance x_2 from the receiving end. Therefore, the total length of the line l is equal to $(x_1 + x_2)$.

By applying Laplace transform with zero initial conditions to equations (3.2) and (3.3), the following are obtained:

$$\begin{aligned}
 -\frac{d}{dx} \underline{V}(x,s) &= \underline{R} \underline{I}(x,s) + s\underline{L} \underline{I}(x,s) \\
 &= \underline{Z}(s) \underline{I}(x,s)
 \end{aligned}
 \tag{4.1}$$

$$\begin{aligned}
-\frac{d}{dx} \underline{I}(x,s) &= s \underline{C} \underline{V}(x,s) \\
&= \underline{Y}(s) \underline{V}(x,s)
\end{aligned} \tag{4.2}$$

where

$$\underline{Z}(s) = \underline{R} + s \underline{L}$$

$$\underline{Y}(s) = s \underline{C}$$

$$s = a + j\omega$$

The second derivatives of equations (4.1) and (4.2) are

$$\begin{aligned}
\frac{d^2}{dx^2} \underline{V}(x,s) &= -\underline{Z}(s) \frac{d}{dx} \underline{I}(x,s) \\
&= \underline{Z}(s) \underline{Y}(s) \underline{V}(x,s) \\
&= \underline{A} \underline{V}(x,s)
\end{aligned} \tag{4.3}$$

and

$$\begin{aligned}
\frac{d^2}{dx^2} \underline{I}(x,s) &= -\underline{Y}(s) \frac{d}{dx} \underline{V}(x,s) \\
&= \underline{Y}(s) \underline{Z}(s) \underline{I}(x,s) \\
&= \underline{A}^t \underline{I}(x,s)
\end{aligned} \tag{4.4}$$

where

$$\underline{A} = \underline{Z}(s) \underline{Y}(s)$$

$$\underline{A}^t = \underline{Y}(s) \underline{Z}(s)$$

Since $\underline{Z}(s)$ and $\underline{Y}(s)$ are symmetrical matrices, then \underline{A} will be a symmetrical matrix if and only if \underline{Z} and \underline{Y} commute.

Equations (4.3) and (4.4) are coupled. They can be decoupled by using a modal-transformation [15]. In the case of an untransposed line,

the eigenvalues and eigenvectors vary with frequency, and the modal transformation matrix has to be calculated at each frequency.

The matrix solution is based on a linear transformation of voltage and current, so the second-order differential relationships will involve diagonal matrices only. Mutual effects can be eliminated by using the following method.

If \underline{S} is the voltage-transformation matrix, and \underline{Q} is the current-transformation matrix, then the modal voltage and the modal current can be defined as

$$\underline{V}^+ = \underline{S}^{-1} \underline{V} \quad (4.5)$$

$$\underline{I}^+ = \underline{Q}^{-1} \underline{I} \quad (4.6)$$

As \underline{S} and \underline{Q} matrices are neither orthogonal nor unitary, then neither $\underline{S} \underline{S}^t$ nor $\underline{Q} \underline{Q}^t$ is diagonal. But, since \underline{S} and \underline{Q} are mutually orthogonal, then the products

$$\underline{Q}^t \underline{S} = \underline{S}^t \underline{Q} = \underline{D} \quad (4.7)$$

are diagonal. The transformed impedance and admittance matrices are also diagonal, i.e.,

$$\underline{S}^{-1} \underline{Z} \underline{Q} = \underline{D}_Z \quad (4.8)$$

and

$$\underline{Q}^{-1} \underline{Y} \underline{S} = \underline{D}_Y \quad (4.9)$$

The product of the transformed impedance and admittance matrices commute. This product is the propagation matrix $\underline{\Gamma}^2$, i.e., $\underline{D}_Z \underline{D}_Y = \underline{D}_Y \underline{D}_Z = \underline{\Gamma}^2$.

If \underline{S} is chosen as the matrix of the eigenvectors of matrix \underline{A} , and \underline{Q} is the matrix of the eigenvectors of matrix \underline{A}^t , then the matrix product $\underline{Q}^t \underline{S}$ can be chosen as a diagonal matrix \underline{D} or as an identity matrix [24], or

$$\underline{Q} = [\underline{S}^{-1}]^t \quad (4.10)$$

By diagonalizing the matrices \underline{A} and \underline{A}^t in equations (4.3), (4.4) and transforming the phase voltage and current into the modal voltage and current, the following relations are obtained:

$$\frac{d^2}{dx^2} \underline{V}^+(x,s) = \underline{S}^{-1} \underline{A} \underline{S} \underline{V}^+(x,s) \quad (4.11)$$

and

$$\frac{d^2}{dx^2} \underline{I}^+(x,s) = \underline{Q}^{-1} \underline{A}^t \underline{Q} \underline{I}^+(x,s) \quad (4.12)$$

The products of $\underline{S}^{-1} \underline{A} \underline{S}$ and $\underline{Q}^{-1} \underline{A}^t \underline{Q}$ are diagonal matrices where the diagonal elements are the eigenvalues. These eigenvalues are complex and vary with frequency, i.e.,

$$\gamma_{i,i} = \alpha_{i,i} + j \beta_{i,i} \quad , \quad i=1,2,3$$

where

$$\gamma_{i,i} = \text{propagation constant}$$

$$\alpha_{i,i} = \text{attenuation constant in nepers per unit length}$$

$$\beta_{i,i} = \text{phase constant in radians per unit length}$$

Figures 4.2 and 4.3 show the variation of $\alpha_{i,i}$ and $\beta_{i,i}$ with frequency.

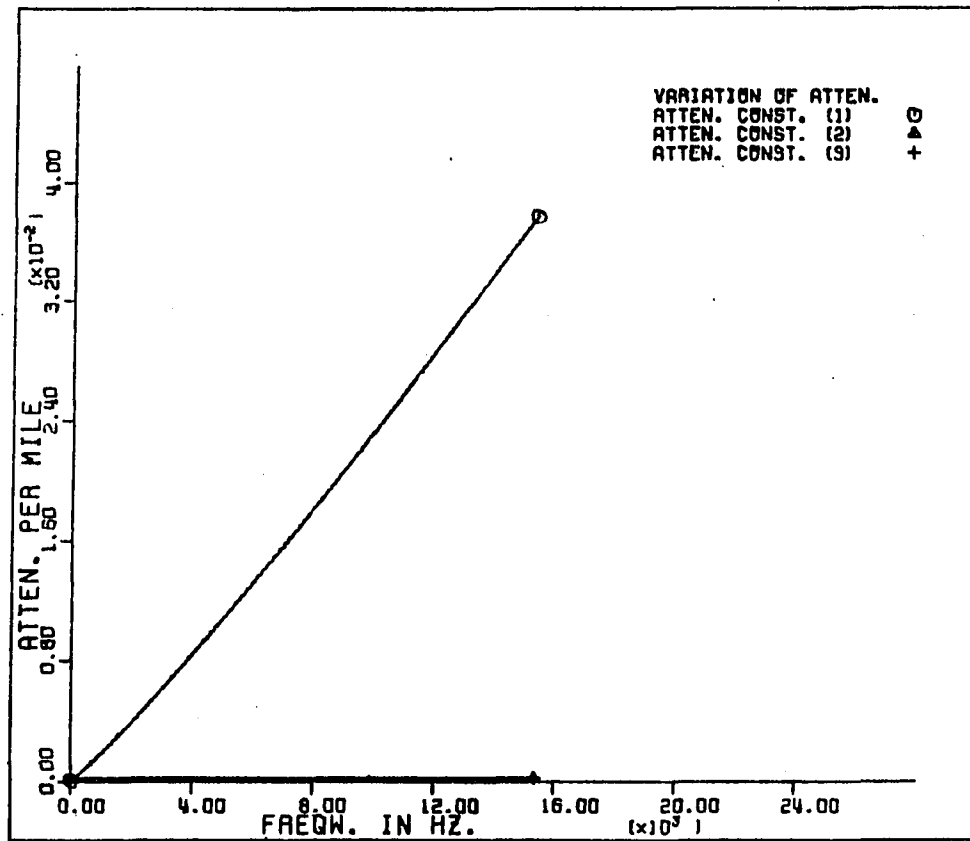


Figure 4.2. Variation of attenuation constant in nepers/unit length

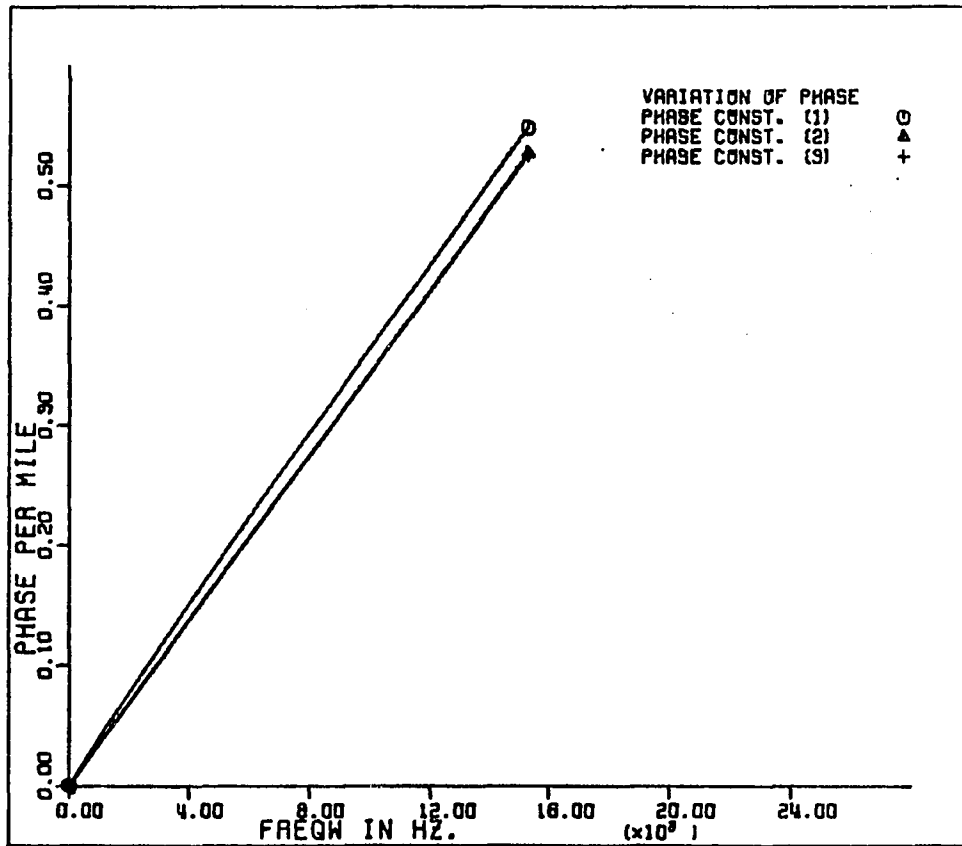


Figure 4.3. Variation of phase constant in radians/unit length

Equations (4.11) and (4.12) can be written as

$$\frac{d^2}{dx^2} \underline{V}^+(x,s) = \underline{D}_z \underline{D}_y \underline{V}^+(x,s) = \underline{\Gamma}^2 \underline{V}^+(x,s) \quad (4.13)$$

$$\frac{d^2}{dx^2} \underline{I}^+(x,s) = \underline{D}_y \underline{D}_z \underline{I}^+(x,s) = \underline{\Gamma}^2 \underline{I}^+(x,s) \quad (4.14)$$

Equations (4.13) and (4.14) are fully decoupled and the solution of these equations can be obtained as

$$\underline{V}^+(x,s) = \underline{A1} \exp(-\underline{\Gamma} x) + \underline{B1} \exp(\underline{\Gamma} x) \quad (4.15)$$

$$\underline{I}^+(x,s) = \underline{C1} \exp(-\underline{\Gamma} x) + \underline{D1} \exp(\underline{\Gamma} x) \quad (4.16)$$

Where $\underline{A1}$, $\underline{B1}$, $\underline{C1}$, and $\underline{D1}$ are determined by the boundary conditions.

Refer to Figure 4.1, at $x = 0$

$$\underline{V}^+ = \underline{V}_r \text{ and } \underline{I}^+ = \underline{I}^+ , \text{ consequently}$$

$$\underline{V}_r^+ = \underline{A1} + \underline{B1} \quad (4.17)$$

$$\underline{I}_{r1}^+ = \underline{C1} + \underline{D1} \quad (4.18)$$

Also at $x = x1$

$$\underline{V}^+ = \underline{V}_{s1}^+ \text{ and } \underline{I}^+ = \underline{I}_{s1}^+ , \text{ then}$$

$$\underline{V}_{s1}^+ = \underline{A1} \exp(-\underline{\Gamma} x1) + \underline{B1} \exp(\underline{\Gamma} x1) \quad (4.19)$$

$$\underline{I}_{s1}^+ = \underline{C1} \exp(-\underline{\Gamma} x1) + \underline{D1} \exp(\underline{\Gamma} x1) \quad (4.20)$$

By differentiating equations (4.15) and (4.16) with respect to x ,

$$\begin{aligned}
\frac{d}{dx} \underline{V}^+(x,s) &= -\underline{\Gamma} \underline{A1} \exp(-\underline{\Gamma} x) + \underline{\Gamma} \underline{B1} \exp(\underline{\Gamma} x) \\
&= -\underline{D}_z \underline{I}^+(x,s)
\end{aligned} \tag{4.21}$$

and

$$\begin{aligned}
\frac{d}{dx} \underline{I}^+(x,s) &= -\underline{\Gamma} \underline{C1} \exp(-\underline{\Gamma} x) + \underline{\Gamma} \underline{D1} \exp(\underline{\Gamma} x) \\
&= -\underline{D}_y \underline{V}^+(x,s)
\end{aligned} \tag{4.22}$$

At $X=0$, equations (4.21) and (4.22) became

$$\begin{aligned}
\frac{d}{dx} \underline{V}_{-r}^+ &= -\underline{\Gamma} \underline{A1} + \underline{\Gamma} \underline{B1} = \underline{\Gamma} (-\underline{A1} + \underline{B1}) \\
&= -\underline{D}_z \underline{I}_{-r1}^+
\end{aligned} \tag{4.23}$$

and

$$\begin{aligned}
\frac{d}{dx} \underline{I}_{-r1}^+ &= -\underline{\Gamma} \underline{C1} + \underline{\Gamma} \underline{D1} = \underline{\Gamma} (-\underline{C1} + \underline{D1}) \\
&= -\underline{D}_y \underline{V}_{-r}^+
\end{aligned} \tag{4.24}$$

Equations (4.23) and (4.24) become

$$\underline{I}_{-r1}^+ = \underline{D}_z^{-1} \underline{\Gamma} (\underline{A1} - \underline{B1}) \tag{4.25}$$

$$\underline{V}_{-r}^+ = \underline{D}_y^{-1} \underline{\Gamma} (\underline{C1} - \underline{D1}) \tag{4.26}$$

Finally, equations (4.19), (4.20), (4.25), and (4.26) can be combined to obtain $\underline{A1}$, $\underline{B1}$, $\underline{C1}$ and $\underline{D1}$ as

$$\underline{A1} = \frac{1}{2} [\underline{\Gamma}^{-1} \underline{D}_z \underline{I}_{-r1}^+ + \underline{V}_{-r}^+] \tag{4.27}$$

$$\underline{B}_1 = \frac{1}{2} [\underline{V}_r^+ - \underline{\Gamma}^{-1} \underline{D}_z \underline{I}_{r1}^+] \quad (4.28)$$

$$\underline{C}_1 = \frac{1}{2} [\underline{\Gamma}^{-1} \underline{D}_y \underline{V}_r^+ + \underline{I}_{r1}^+] \quad (4.29)$$

and

$$\underline{D}_1 = \frac{1}{2} [\underline{I}_{r1}^+ - \underline{\Gamma}^{-1} \underline{D}_y \underline{V}_r^+] \quad (4.30)$$

By substituting \underline{A}_1 , \underline{B}_1 , \underline{C}_1 , and \underline{D}_1 in equations (4.26) through (4.30) the voltage and current equations at the sending end become

$$\begin{aligned} \underline{V}_{s1}^+ &= \frac{1}{2} [\underline{\Gamma}^{-1} \underline{D}_z \underline{I}_{r1}^+ + \underline{V}_r^+] \exp(-\underline{\Gamma} x_1) + \\ &\quad \frac{1}{2} [-\underline{\Gamma}^{-1} \underline{D}_z \underline{I}_{r1}^+ + \underline{V}_r^+] \exp(\underline{\Gamma} x_1) \\ &= \frac{1}{2} \underline{\Gamma}^{-1} \underline{D}_z [\exp(-\underline{\Gamma} x_1) - \exp(\underline{\Gamma} x_1)] \underline{I}_{r1}^+ + \\ &\quad \frac{1}{2} [\exp(-\underline{\Gamma} x_1) + \exp(\underline{\Gamma} x_1)] \underline{V}_r^+ \end{aligned}$$

or

$$\underline{V}_{s1}^+ = \underline{D}_{c1} \underline{V}_r^+ + \underline{\Gamma}^{-1} \underline{D}_z \underline{D}_{s1} \underline{I}_{r1}^+ \quad (4.31)$$

where

$$\underline{D}_{c1} = \cosh (\gamma_{i,i} x_1) = \frac{1}{2} [\exp(-\gamma_{i,i} x_1) + \exp(\gamma_{i,i} x_1)]$$

i,i

$$\underline{D}_{s1} = \sinh (\gamma_{i,i} x_1) = \frac{1}{2} [\exp(-\gamma_{i,i} x_1) - \exp(\gamma_{i,i} x_1)]$$

i,i

Both \underline{D}_{c1} , \underline{D}_{s1} are diagonal matrices.

Also,

$$\begin{aligned}
\underline{I}_{s1}^+ &= \frac{1}{2} [\underline{\Gamma}^{-1} \underline{D}_y \underline{V}_r^+ + \underline{I}_{r1}^+] \exp(-\underline{\Gamma} x1) \\
&\quad + \frac{1}{2} [-\underline{\Gamma}^{-1} \underline{D}_y \underline{V}_r^+ + \underline{I}_{r1}^+] \exp(\underline{\Gamma} x1) \\
&= \frac{1}{2} [\exp(-\underline{\Gamma} x1) + \exp(\underline{\Gamma} x1)] \underline{I}_{r1}^+ \\
&\quad + \frac{1}{2} \underline{\Gamma}^{-1} \underline{D}_y [\exp(-\underline{\Gamma} x1) - \exp(\underline{\Gamma} x1)] \underline{V}_r^+
\end{aligned}$$

or

$$\underline{I}_{s1}^+ = \underline{D}_{c1} \underline{I}_{r1}^+ + \underline{\Gamma}^{-1} \underline{D}_y \underline{D}_{s1} \underline{V}_r^+ \quad (4.32)$$

Since $\underline{\Gamma}$, \underline{D}_z , and \underline{D}_y in equations (4.31) and (4.32) are diagonal matrices, then

$$\underline{\Gamma}^{-1} \underline{D}_y = \underline{D}_y \underline{\Gamma}^{-1}$$

and

$$\begin{aligned}
(\underline{\Gamma}^{-1} \underline{D}_z) (\underline{D}_y \underline{\Gamma}^{-1}) &= (\underline{\Gamma}^{-1} \underline{S}^{-1} \underline{Z} \underline{Q}) (\underline{Q}^{-1} \underline{Y} \underline{S} \underline{\Gamma}^{-1}) \\
&= \underline{\Gamma}^{-1} (\underline{S}^{-1} \underline{Z} \underline{Y} \underline{S}) \underline{\Gamma}^{-1} \\
&= \underline{\Gamma}^{-1} (\underline{S}^{-1} \underline{A} \underline{S}) \underline{\Gamma}^{-1} \\
&= \underline{\Gamma}^{-1} \underline{\Gamma}^2 \underline{\Gamma}^{-1} \\
&= \underline{U} \text{ (identity matrix)}
\end{aligned}$$

So, if $\underline{\Gamma}^{-1} \underline{D}_z = \underline{Z}_o^+$, then $\underline{D}_y \underline{\Gamma}^{-1} = (\underline{Z}_o^+)^{-1}$

Equations (4.31) and (4.32) become

$$\underline{V}_{s1}^+ = \underline{D}_{c1} \underline{V}_r^+ + \underline{Z}_o^+ \underline{D}_{s1} \underline{I}_{r1}^+ \quad (4.33)$$

$$\underline{I}_{s1}^+ = \underline{D}_{s1} \underline{I}_{r1}^+ + (\underline{Z}_o^+)^{-1} \underline{D}_{s1} \underline{V}_r^+$$

Equations (4.5) and (4.6) are used to transfer the modal variables back to the phase variables. The sequence of transformations begins with

$$\underline{V}_{s1} = \underline{S} \underline{D}_{c1} \underline{S}^{-1} \underline{V}_r + \underline{S} \underline{Z}_o^+ \underline{D}_{s1} \underline{Q}^{-1} \underline{I}_{r1}$$

$$\text{but } \underline{S} \underline{Z}_o^+ = \underline{S} \underline{\Gamma}^{-1} \underline{S}^{-1} \underline{Z} \underline{Q}$$

$$= \underline{S} (\underline{S}^{-1} \underline{Z} \underline{Q}) \underline{\Gamma}^{-1}$$

$$= \underline{Z} \underline{Q} \underline{\Gamma}^{-1}$$

or

$$\underline{S} \underline{Z}_o^+ = \underline{S} (\underline{S}^{-1} \underline{Z} \underline{Q}) \underline{\Gamma}^{-1}$$

$$= (\underline{S} \underline{\Gamma}^{-1} \underline{S}^{-1} \underline{Z}) \underline{Q}$$

$$= \underline{Z}_o \underline{Q}$$

$$\text{where } \underline{Z}_o = \underline{S} \underline{\Gamma}^{-1} \underline{S}^{-1} \underline{Z}$$

then,

$$\underline{V}_{s1} = (\underline{S} \underline{D}_{c1} \underline{S}^{-1}) \underline{V}_r + (\underline{Z}_o \underline{Q} \underline{D}_{s1} \underline{Q}^{-1}) \underline{I}_{r1} \quad (4.35)$$

and

$$\underline{I}_{s1} = \underline{Q} \underline{D}_{c1} \underline{Q}^{-1} \underline{I}_{r1} + \underline{Q} (\underline{Z}_o^+)^{-1} \underline{D}_{s1} \underline{S}^{-1} \underline{V}_r$$

Since \underline{Z}_o^+ and \underline{D}_{s1} are diagonal matrices, then

$$(\underline{Z}_o^+)^{-1} \underline{D}_{s1} = \underline{D}_{s1} (\underline{Z}_o^+)^{-1}$$

and

$$\begin{aligned}
(\underline{z}_o^+)^{-1} \underline{s}^{-1} &= (\underline{\Gamma}^{-1} \underline{s}^{-1} \underline{z} \underline{Q})^{-1} \underline{s}^{-1} \\
&= (\underline{s} \underline{\Gamma}^{-1} \underline{s}^{-1} \underline{z} \underline{Q})^{-1} \\
&= \underline{Q}^{-1} (\underline{s} \underline{\Gamma}^{-1} \underline{s}^{-1} \underline{z})^{-1} \\
&= \underline{Q}^{-1} \underline{z}_o^{-1}
\end{aligned}$$

Then,

$$\underline{I}_{s1} = (\underline{Q} \underline{D}_{c1} \underline{Q}^{-1}) \underline{I}_{r1} + (\underline{Q} \underline{D}_{s1} \underline{Q}^{-1} \underline{z}_o^{-1}) \underline{V}_r \quad (4.36)$$

Equations (4.35) and (4.36) are used to find the phase voltage and current at the sending-end in the s-domain.

The receiving-end equations are based on the boundary conditions at the fault location and at the receiving-end.

From Figure 4.1, at $x = 0$

$$\underline{V} = \underline{V}_r, \quad \underline{I} = \underline{I}_{r2}$$

and at $x = x_2$

$$\underline{V} = \underline{V}_{s2}, \quad \underline{I} = \underline{I}_{s2}$$

The same procedure used to derive (4.35) and (4.36) produces the receiving-end equations

$$\underline{V}_{s2} = (\underline{s} \underline{D}_{c2} \underline{s}^{-1}) \underline{V}_r + (\underline{z}_o \underline{Q} \underline{D}_{s2} \underline{Q}^{-1}) \underline{I}_{r2} \quad (4.37)$$

$$\underline{I}_{s2} = (\underline{Q} \underline{D}_{c2} \underline{Q}^{-1}) \underline{I}_{r2} + (\underline{Q} \underline{D}_{s2} \underline{Q}^{-1} \underline{z}_o^{-1}) \underline{V}_r \quad (4.38)$$

where

$$D_{c2_{i,i}} = \cosh (\gamma_{i,i} x_2)$$

$$D_{s2_{i,i}} = \sinh (\gamma_{i,i} x_2)$$

The sending-end voltages and currents or the receiving-end voltages and currents can be obtained by using the above equations if \underline{V}_r , \underline{I}_{r1} , and \underline{I}_{r2} are known or if the boundary condition at the fault location is specified. This boundary condition depends on the type of fault. There are four types of faults: three-phase fault, single-line-to-ground fault, line-to-line fault, and double-line-to-ground fault. Methods of finding the boundary condition at the fault location for each type of fault will be discussed in the next chapter.

V. BOUNDARY CONDITIONS AND SIMULATION OF FAULTED POWER SYSTEMS

In order to apply the equations developed in the previous chapter, it is necessary to develop a general technique for modeling a fault, and to specify the boundary conditions at the ends of the line. Once these factors have been dealt with, simulation of the line transients is largely a matter of developing a computer program and applying it. A general fault model is developed in this chapter, boundary conditions are specified at the terminals, and the fault transients on a hypothetical transmission line are simulated.

A. The General Power System Simulation

A power system consists of three primary components: The generating system, the transmission line, and the load. Chapter III was concerned with modeling the transmission line in detail. For the purposes of fault transient analysis, all that really needs to be done with either the generator or the load is to characterize them sufficiently well to impose realistic boundary conditions upon the line differential equations. In this chapter, conventional models for each are used. It is also necessary to simulate a line fault. Simulations for the load, the transformer, the generator, and the fault are described in the next two subsections.

1. Load, generator, and transformer simulations

The load is connected at the receiving-end of the line. This load is represented by a constant impedance (R_l, L_l).

The transformer and the generator are connected to the sending end. The transformer is represented by a series impedance (R_{tr} , L_{tr}). The synchronous generator is represented by the Thevenin equivalent (constant voltage behind a transient impedance). One of the most important conclusions of this thesis is that this generator model is inaccurate in transient analysis particularly when the fault is near the generator. This model is in fact widely used, and is only involved here for comparative purposes. The next two chapters develop a more accurate technique for dealing with the generator, and subsequent work compares the results obtained by two processes.

2. Fault simulation

Fault initiation is simulated in the following manner:

- a. The voltage v_x at the fault location is calculated just prior to the instant of fault inception.
- b. Define a fault voltage (v_f)

$$v_f = -u(t) v_x$$

where the fault is stipulated to occur at time $t = 0$.

- c. The fault per se is simulated as a resistance in series with an inductance.
- d. Construct the circuit shown in Figure 5.1 at the fault location.

For $t < 0$, $i_f = 0$. For $t \geq 0$, the state of the line can be deduced by using superposition, i.e., two separate calculations (steady-state and transient) are performed. The steady-state and transient solutions

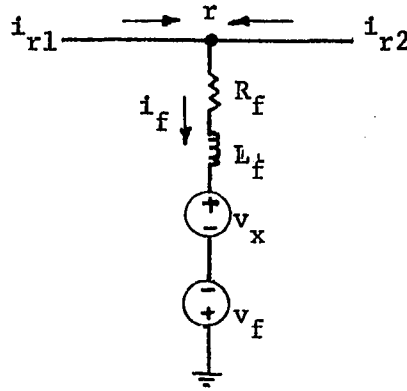


Figure 5.1. Fault simulation

are discussed in the next section. The superposition of the steady-state response and the transient response gives the total response.

B. Formulations of Boundary-Condition Equations

1. Steady-state solution

The voltage and current equations at any distance x from the receiving end are similar to equations (4.35) and (4.36). These equations are:

$$\underline{V}_{-x} = \underline{S} \underline{D}_{-cx} \underline{S}^{-1} \underline{V}_{-s2} + \underline{Z}_0 \underline{Q} \underline{D}_{-sx} \underline{Q}^{-1} \underline{I}_{-s2} \quad (5.1)$$

$$\underline{I}_{-x} = \underline{Q} \underline{D}_{-cx} \underline{Q}^{-1} \underline{I}_{-s2} + \underline{Q} \underline{D}_{-sx} \underline{Q}^{-1} \underline{Z}_0^{-1} \underline{V}_{-s2} \quad (5.2)$$

where:

\underline{S} and \underline{Q} were defined in Chapter IV

$$\underline{D}_{-cx} = \cosh (\gamma_{i,i} x)$$

i,i

$$\underline{D}_{-sx} = \sinh (\gamma_{i,i} x)$$

i,i

\underline{V}_{s2} and \underline{I}_{s2} are the prefault voltages and currents at the receiving end bus.

\underline{V}_x and \underline{I}_x are the prefault voltages and currents at distance x measured from the receiving end bus as shown in Figure 5.2.

$$\underline{Z}_o = \underline{S} \underline{\Gamma}^{-1} \underline{S}^{-1} \underline{Z}$$

$$\underline{\Gamma}^2 = \underline{S}^{-1} \underline{A} \underline{S} = \underline{Q}^{-1} \underline{A}^t \underline{Q}$$

$$\underline{A} = \underline{Z} \underline{Y}$$

$$\underline{Z} = \underline{R} + j\omega \underline{L}$$

$$\underline{Y} = j\omega \underline{C}$$

$$\omega = 120\pi$$

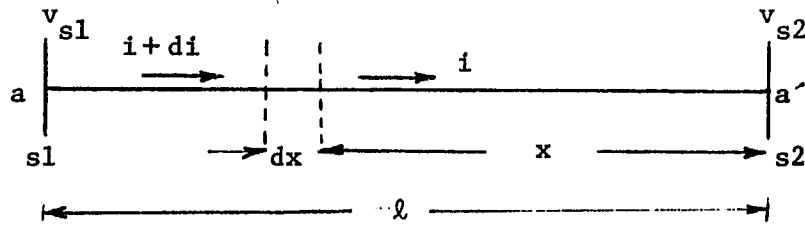


Figure 5.2. A schematic diagram for a transmission line of phase a

For subsequent work it is useful to specialize (5.1) and (5.2) to pertain to the sending end. The result is

$$\underline{V}_{s1} = \underline{S} \underline{D}_{cl} \underline{S}^{-1} \underline{V}_{s2} + \underline{Z}_o \underline{Q} \underline{D}_{sl} \underline{Q}^{-1} \underline{I}_{s2} \quad (5.3)$$

$$\underline{I}_{s1} = \underline{Q} \underline{D}_{cl} \underline{Q}^{-1} \underline{I}_{s2} + \underline{Q} \underline{D}_{sl} \underline{Q}^{-1} \underline{Z}_o^{-1} \underline{V}_{s2} \quad (5.4)$$

where

$$D_{c\ell} = \cosh (\gamma_{i,i} \ell)$$

$$D_{s\ell} = \sinh (\gamma_{i,i} \ell)$$

The line parameters and the line configuration are known, the computer program in Appendix B can be used to find the prefault voltages and currents at any location on the line at 60 Hz.

2. Transient solution

Transient analysis is based upon the circuit shown in Figure 5.3. This circuit is derived by using the fault simulation in Figure 5.1 with the steady-state voltage, v_x , properly removed. The voltage at the fault location is

$$\underline{V}_r(s) = \underline{R}_f \underline{I}_f(s) + s \underline{L}_f \underline{I}_f(s) + \underline{V}_f(s)$$

or

$$\underline{V}_r = \underline{Z}_f \underline{I}_f + \underline{V}_f \quad (5.5)$$

where:

R_f = fault resistance

\underline{L}_f = fault inductance

$\underline{Z}_f = \underline{R}_f + s \underline{L}_f$ which is a (3x3) diagonal matrix

\underline{V}_f = superimposed voltage with all other sources properly removed

\underline{I}_f = fault current which is equal to $(\underline{I}_{r1} + \underline{I}_{r2})$

From Figure 5.3, the sending end equation with the source voltage removed is

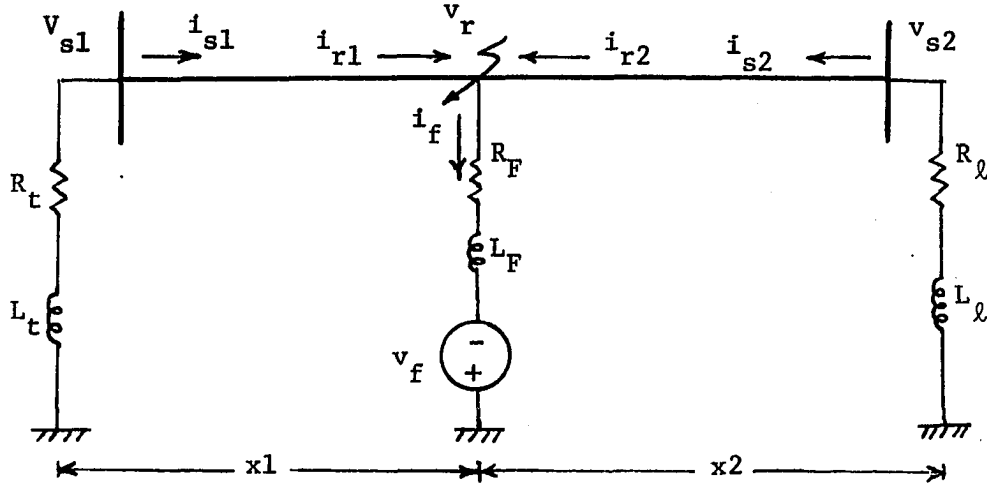


Figure 5.3. Simulation of a faulted power system with only super-imposed voltage and all other voltage sources properly removed

$$\underline{V}_{-s1}(s) = -(\underline{R}_{-r} + s \underline{L}_{-t}) \underline{I}_{-s1}(s)$$

or

$$\underline{V}_{-s1} = -\underline{Z}_{-t} \underline{I}_{-s1} \quad (5.6)$$

where:

\underline{R}_{-t} = total resistance of the generator and transformer

\underline{L}_{-t} = total inductance of the generator and transformer

$\underline{Z}_{-t} = \underline{R}_{-t} + s \underline{L}_{-t}$ which is a (3x3) diagonal matrix

Similarly, the receiving end equation is

$$\underline{V}_{-s2}(s) = -(\underline{R}_{-l} + s \underline{L}_{-l}) \underline{I}_{-s2}(s)$$

or

$$\underline{V}_{-s2} = -\underline{Z}_{-l} \underline{I}_{-s2} \quad (5.7)$$

\underline{R}_ℓ = load resistance matrix

\underline{L}_ℓ = load inductance matrix

$\underline{Z}_\ell = \underline{R}_\ell + s \underline{L}_\ell$ which is a (3×3) diagonal matrix

Using equations (4.35), (4.36), and (5.6) to eliminate \underline{V}_{s1} and \underline{I}_{s1} produces

$$\begin{aligned}\underline{V}_{s1} &= (\underline{S} \underline{D}_{c1} \underline{S}^{-1}) \underline{V}_r + (\underline{Z}_o \underline{Q} \underline{D}_{s1} \underline{Q}^{-1}) \underline{I}_{r1} \\ &= -\underline{Z}_t [(\underline{Q} \underline{D}_{c1} \underline{Q}^{-1}) \underline{I}_{r1} + (\underline{Q} \underline{D}_{s1} \underline{Q}^{-1} \underline{Z}_o^{-1}) \underline{V}_r]\end{aligned}$$

Thus, by rearrangement,

$$\begin{aligned}[\underline{S} \underline{D}_{c1} \underline{S}^{-1} + \underline{Z}_t \underline{Q} \underline{D}_{s1} \underline{Q}^{-1} \underline{Z}_o^{-1}] \underline{V}_r = \\ - [\underline{Z}_o \underline{Q} \underline{D}_{s1} \underline{Q}^{-1} + \underline{Z}_t \underline{Q} \underline{D}_{c1} \underline{Q}^{-1}] \underline{I}_{r1}\end{aligned}$$

or

$$\underline{T}_1 \underline{V}_r = -\underline{T}_2 \underline{I}_{r1} \quad (5.8)$$

where:

$$\underline{T}_1 = \underline{S} \underline{D}_{c1} \underline{S}^{-1} + \underline{Z}_t \underline{Q} \underline{D}_{s1} \underline{Q}^{-1} \underline{Z}_o^{-1}$$

and

$$\underline{T}_2 = \underline{Z}_o \underline{Q} \underline{D}_{s1} \underline{Q}^{-1} + \underline{Z}_t \underline{Q} \underline{D}_{c1} \underline{Q}^{-1}$$

Also, by using equations (4.37), (4.38), and (5.7) to eliminate \underline{V}_{s2} and \underline{I}_{s2} , we find

$$\begin{aligned}\underline{V}_{s2} &= (\underline{S} \underline{D}_{c2} \underline{S}^{-1}) \underline{V}_r + (\underline{Z}_o \underline{Q} \underline{D}_{s2} \underline{Q}^{-1}) \underline{I}_{r2} \\ &= -\underline{Z}_\ell [(\underline{Q} \underline{D}_{c2} \underline{Q}^{-1}) \underline{I}_{r2} + (\underline{Q} \underline{D}_{s2} \underline{Q}^{-1} \underline{Z}_o^{-1}) \underline{V}_r]\end{aligned}$$

This can be rewritten in the compact form

$$\underline{T}_3 \underline{V}_r = -\underline{T}_4 \underline{I}_{r2} \quad (5.9)$$

where:

$$\underline{T}_3 = \underline{S} \underline{D}_{c2} \underline{S}^{-1} + \underline{Z}_\ell \underline{Q} \underline{D}_{s2} \underline{Q}^{-1} \underline{Z}_o^{-1}$$

and

$$\underline{T}_4 = \underline{Z}_o \underline{Q} \underline{D}_{s2} \underline{Q}^{-1} + \underline{Z}_\ell \underline{Q} \underline{D}_{c2} \underline{Q}^{-1}$$

Equations (5.8) and (5.9) can now be condensed into the form

$$\underline{I}_{r1} = -\underline{T}_3^{-1} \underline{T}_1 \underline{V}_r \quad (5.10)$$

$$\underline{I}_{r2} = -\underline{T}_4^{-1} \underline{T}_2 \underline{V}_r \quad (5.11)$$

The voltage \underline{V}_r at the fault location depends on the type of fault. Methods of finding \underline{V}_r for each type of fault are discussed in the next section.

C. Voltage at Fault Location for Different Types of Faults

The four possible types of faults are designated by

1. Three phase to ground fault (3LG)
2. Single line to ground fault (SLG)
3. Line to line fault (LL)
4. Double line to ground fault (2LG)

1. Three-phase to ground fault

For a three-phase fault, the voltage at fault location in the s-domain is

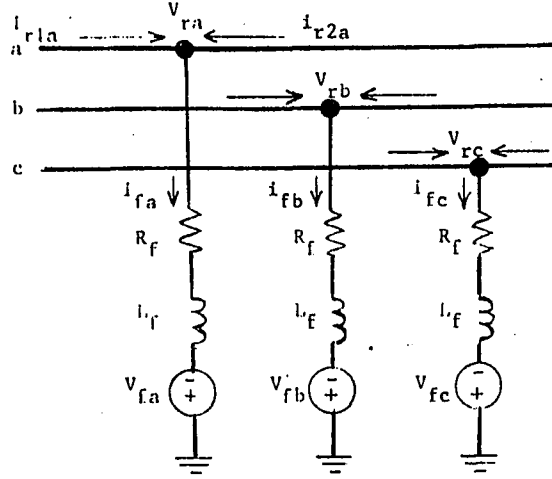


Figure 5.4. Three-phase to ground fault

$$\underline{V}_r = \underline{Z}_f \underline{I}_f + \underline{V}_f$$

$$\text{and } \underline{I}_f = \underline{I}_{r1} + \underline{I}_{r2}$$

therefore:

$$\underline{V}_r = \underline{Z}_f (\underline{I}_{r1} + \underline{I}_{r2}) + \underline{V}_f \quad (5.12)$$

By substituting \underline{I}_{r1} and \underline{I}_{r2} in equations (5.10) and (5.11) into equation (5.12) we obtain

$$\underline{V}_r = \underline{Z}_f (-\underline{T}_2^{-1} \underline{T}_1 - \underline{T}_4^{-1} \underline{T}_3) \underline{V}_r + \underline{V}_f$$

then,

$$\underline{V}_f = [\underline{U} + \underline{Z}_f \underline{T}] \underline{V}_r$$

or

$$\underline{V}_r = [\underline{U} + \underline{Z}_f \underline{T}]^{-1} \underline{V}_f \quad (5.13)$$

where \underline{U} is an identity matrix and

$$\underline{T} = \underline{T}_2^{-1} \underline{T}_1 + \underline{T}_4^{-1} \underline{T}_3$$

2. Single line to ground fault

By assuming the fault on phase a, then the boundary conditions in the s-domain are

$$I_{fa} = I_{r1a} + I_{r2a}$$

$$I_{fb} = 0$$

$$I_{fc} = 0$$

Depending on the above boundary condition, the fault current is

$$\begin{aligned} \underline{I}_f &= [I_{fa} \quad 0 \quad 0]^t \\ &= \underline{I}_{r1} + \underline{I}_{r2} \end{aligned} \quad (5.14)$$

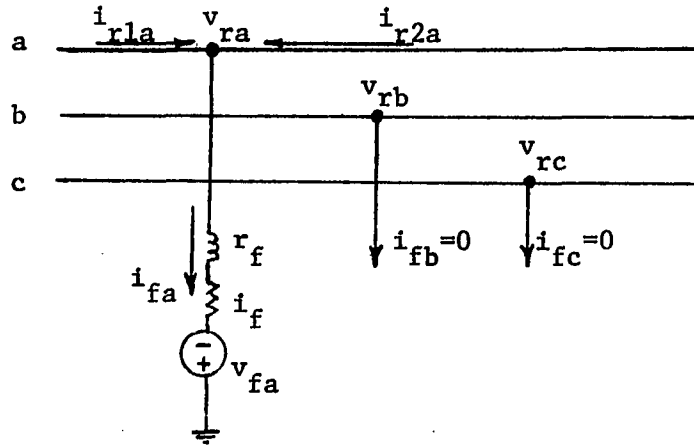


Figure 5.5. Single line to ground fault (a)

By substituting \underline{I}_{r1} and \underline{I}_{r2} from equations (5.10) and (5.11) into equation (5.14) as

$$\begin{aligned} \underline{I}_f &= -[\underline{T}_2^{-1} \quad \underline{T}_1 + \underline{T}_4^{-1} \quad \underline{T}_3] \underline{V}_r \\ &= -\underline{T} \underline{V}_r \end{aligned}$$

then

$$\underline{V}_r = -\underline{T}^{-1} \underline{I}_f = -\underline{H} \underline{I}_f \quad (5.15)$$

where $\underline{H} = \underline{T}^{-1}$

Equation (5.15) can be written in a matrix form as

$$\begin{bmatrix} V_{ra} \\ V_{rb} \\ V_{rc} \end{bmatrix} = - \begin{bmatrix} H_{11} & H_{12} & H_{13} \\ H_{21} & H_{22} & H_{23} \\ H_{31} & H_{32} & H_{33} \end{bmatrix} \begin{bmatrix} I_{fa} \\ 0 \\ 0 \end{bmatrix} \quad (5.16)$$

or

$$V_{ra} = -H_{11} I_{fa}$$

$$V_{rb} = -H_{21} I_{fa}$$

$$V_{rc} = -H_{31} I_{fa}$$

then

$$\underline{V}_r = -[H_{11} \quad H_{21} \quad H_{31}]^t I_{fa} \quad (5.17)$$

I_{fa} can be obtained from the voltage at fault location of phase (a) as shown in Figure 5.5

$$V_{ra} = V_{fa} + Z_f I_{fa}$$

$$= -H_{11} I_{fa}$$

$$I_{fa} = \frac{-V_{fa}}{H_{11} + Z_f} \quad (5.18)$$

By finding I_{fa} from equation (5.18), then \underline{V}_r can be obtained by applying equation (5.16).

3. Line to line fault

By assuming the fault occurs on phases b and c, then the boundary conditions in the s-domain are

$$I_{fa} = 0$$

$$I_{fb} = -I_{fc}$$

$$= I_{r1b} + I_{r2b}$$

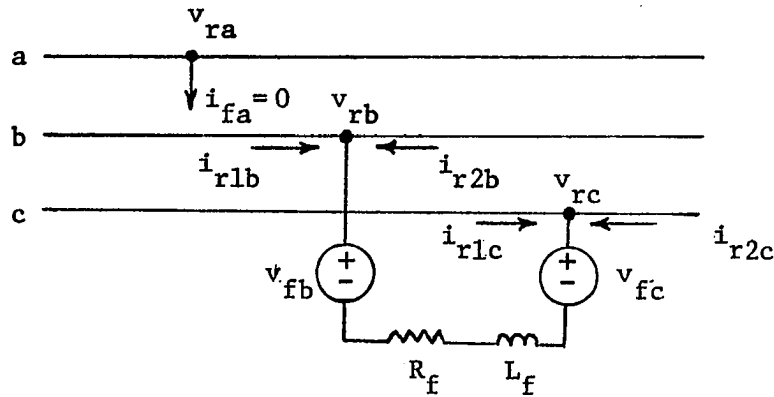


Figure 5.6. Line to line fault (b-c)

Depending on the above boundary condition, the fault current is

$$\begin{aligned} \underline{I}_f &= [0 \quad I_{fb} \quad -I_{fb}]^t \\ &= \underline{I}_{r1} + \underline{I}_{r2} \end{aligned} \tag{5.19}$$

By applying equation (5.15) to obtain \underline{V}_r as

$$\begin{bmatrix} V_{ra} \\ V_{rb} \\ V_{rc} \end{bmatrix} = - \begin{bmatrix} H_{11} & H_{12} & H_{13} \\ H_{21} & H_{22} & H_{23} \\ H_{31} & H_{32} & H_{33} \end{bmatrix} \begin{bmatrix} 0 \\ I_{fb} \\ -I_{fb} \end{bmatrix} \quad (5.20)$$

$$V_{ra} = (H_{13} - H_{12}) I_{fb}$$

$$V_{rb} = (H_{23} - H_{22}) I_{fb}$$

$$V_{rc} = (H_{33} - H_{32}) I_{fb}$$

then,

$$V_{rb} - V_{rc} = (H_{23} - H_{22} - H_{33} + H_{32}) I_{fb} \quad (5.21)$$

From Figure 5.6:

$$V_{rb} - V_{rc} = V_{fb} - V_{fc} + Z_f I_{fb} \quad (5.22)$$

From equations (5.21) and (5.22), I_{fb} can be obtained as

$$I_{fb} = \frac{V_{fb} - V_{fc}}{(H_{23} - H_{22} - H_{33} + H_{32} - Z_f)} \quad (5.23)$$

By finding I_{fb} from equation (5.23), then \underline{V}_r can be obtained by applying equation (5.20).

4. Double line to ground fault

When the fault occurs on phases b and c, then

$$I_{fa} = 0$$

or

$$I_f = [0 \quad I_{fb} \quad I_{fc}]^t \quad (5.24)$$

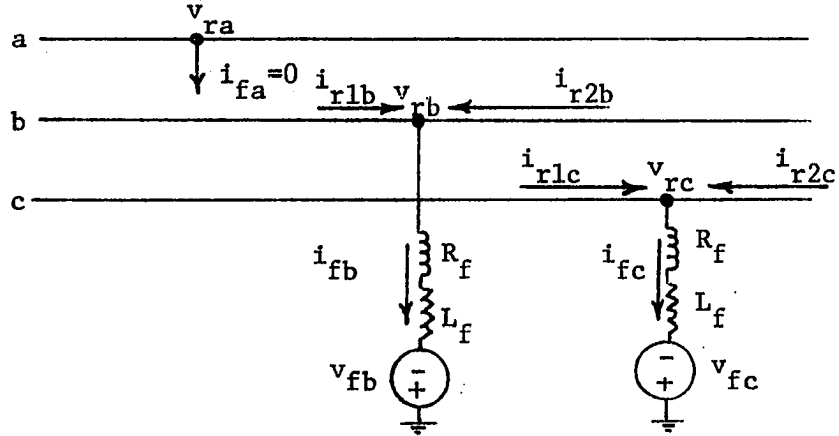


Figure 5.7. Double line to ground fault (b-c)

By applying equation (5.15) to obtain \underline{V}_r as

$$\begin{bmatrix} V_{ra} \\ V_{rb} \\ V_{rc} \end{bmatrix} = - \begin{bmatrix} H_{11} & H_{12} & H_{13} \\ H_{21} & H_{22} & H_{23} \\ H_{31} & H_{32} & H_{33} \end{bmatrix} \begin{bmatrix} 0 \\ I_{fb} \\ I_{fc} \end{bmatrix} \quad (5.25)$$

V_{rb} and V_{rc} can also be obtained from Figure 5.7 as

$$V_{rb} = Z_f I_{fb} + V_{fb} \quad (5.26)$$

$$V_{rc} = Z_f I_{fc} + V_{fc} \quad (5.27)$$

From equations (5.25), (5.26), and (5.27), then

$$Z_f I_{fb} + V_{fb} = -(H_{22} I_{fb} + H_{23} I_{fc}) \quad (5.28)$$

$$Z_f I_{fc} + V_{fc} = -(H_{32} I_{fb} + H_{33} I_{fc}) \quad (5.29)$$

By solving equations (5.28) and (5.29) to obtain I_{fb} and I_{fc} as

$$I_{fb} = \frac{-1}{H_{32}} [(Z_f + H_{33}) I_{fc} + V_{fc}] \quad (5.30)$$

$$I_{fc} = \frac{-1}{H_{23}} [(Z_f + H_{22}) I_{fb} + V_{fb}] \quad (5.31)$$

Elimination of I_{fc} produces

$$I_{fb} = \frac{-1}{H_{32}} \{ (Z_f + H_{33}) \left[\frac{-1}{H_{23}} (Z_f + H_{22}) I_{fb} - \frac{1}{H_{23}} V_{fb} \right] + V_{fc} \}$$

or

$$I_{fb} = \frac{-(Z_{ft} V_{fb} + V_{fc})}{Z_{ft} (Z_f + H_{22}) + H_{32}} \quad (5.32)$$

where

$$Z_{ft} = \frac{-1}{H_{23}} (Z_f + H_{33})$$

From equation (5.31) and (5.32), I_{fc} can be obtained. Once I_{fb} and I_{fc} are obtained, then V_r can be obtained from equation (5.25).

Methods for finding V_r for each type of fault are written as sub-routines in the main program in Appendix B.

D. Fault Transient Waveforms

The currents at the fault location (I_{r1} , I_{r2}) are obtained by applying equations (5.10) and (5.11). The voltage and current at the sending end can also be obtained from equations (4.35) and (4.36). This process for transforming the transient solution from the s-domain into the time domain is discussed in Chapter VIII. The total solutions of voltages and currents at the fault location and at the sending end are

obtained by adding the transient solution to the steady-state solution in the time domain.

Appendix B consists of a computer program for numerical analysis of the various boundary value problems posed thus far. The program is general, and can be used for any line length, configuration, or fault type. Appendix A describes a hypothetical power system to be used for program testing and determining the relative importance of the various parameters that are or may be important in fault transient analysis. Figure 5.8 to 5.11 show some of the results obtained by simulation of the system described in Appendix A. In particular, Figures a and b in 5.8 to 5.11 show current and voltage waveforms at the sending end that ensue from a fault at the middle of the line.

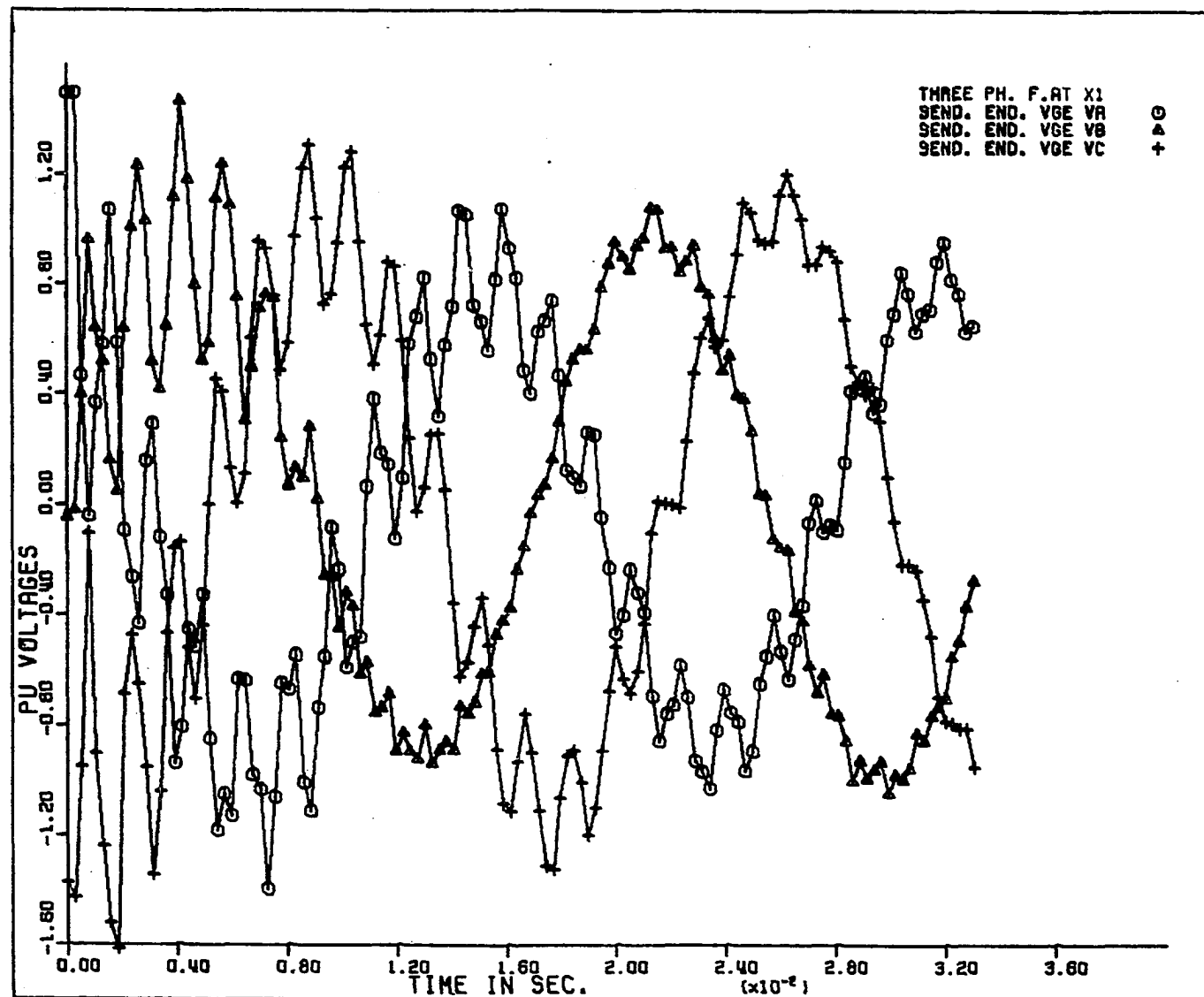


Figure 5.8a. Sending-end voltages for three-phase-to-ground fault

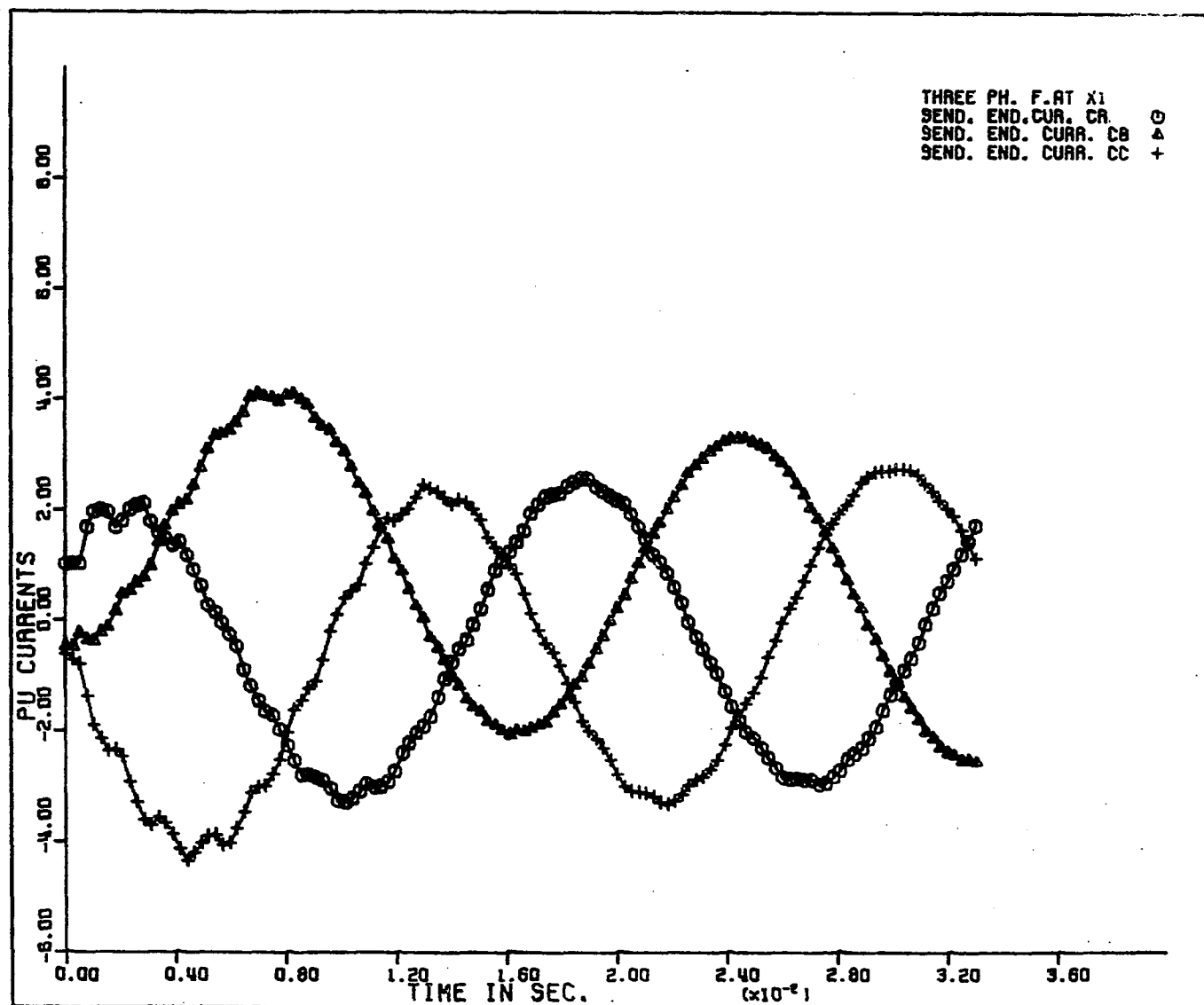


Figure 5.8b. Sending-end currents for three-phase-to-ground fault

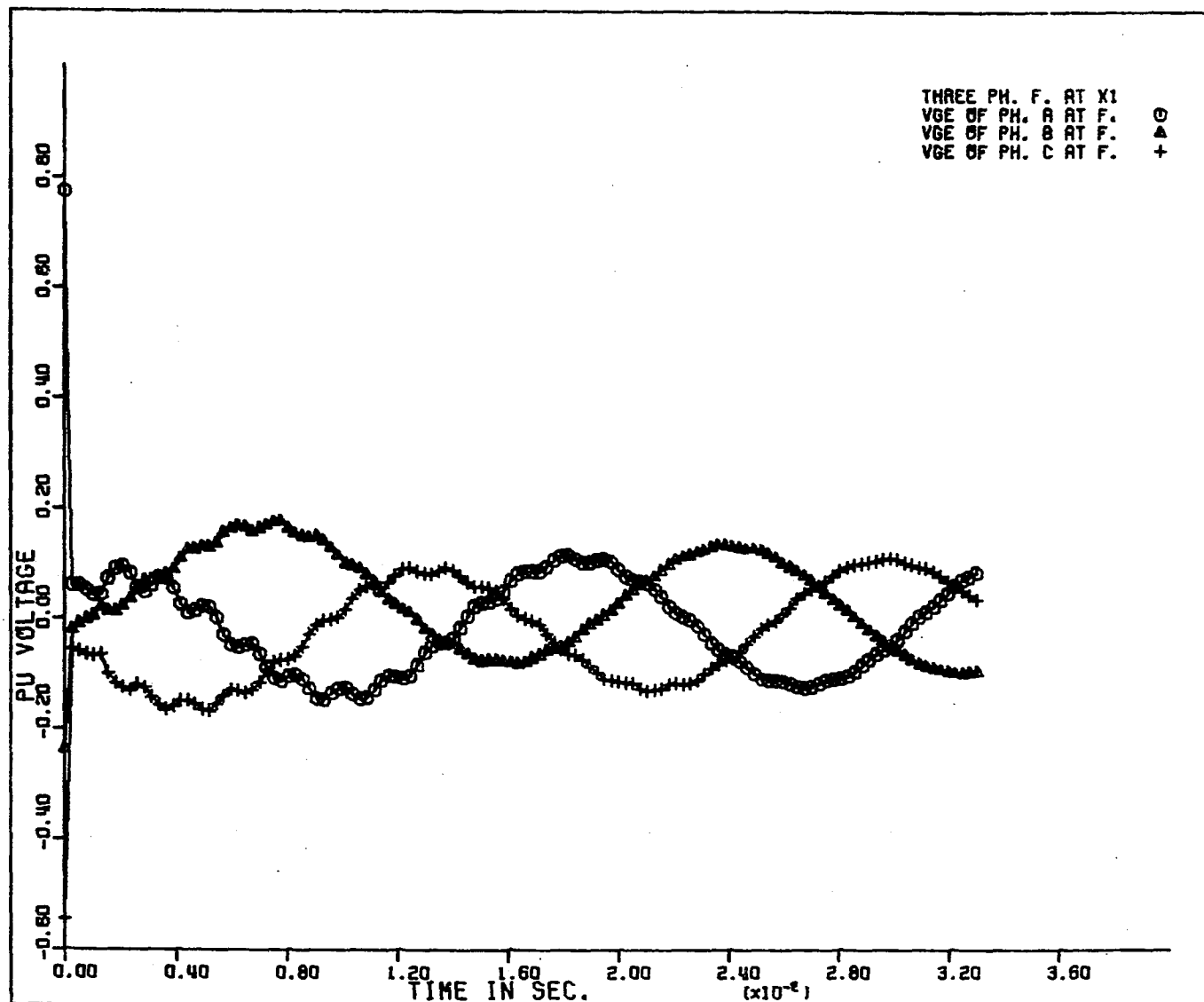


Figure 5.8c. Voltages at the fault location for three-phase-to-ground fault

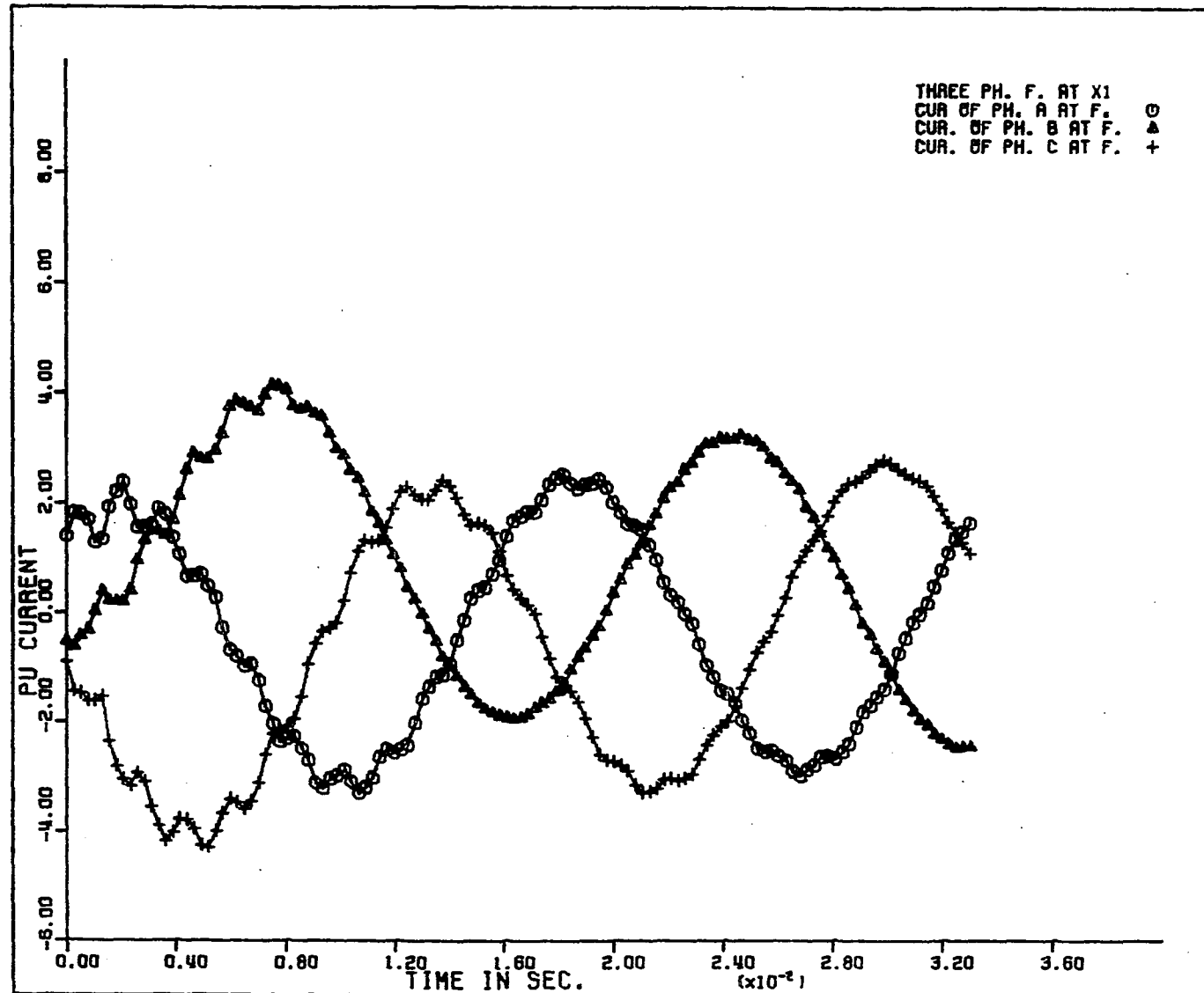


Figure 5.8d. Currents i_{r1} at the fault location for three-phase-to-ground fault

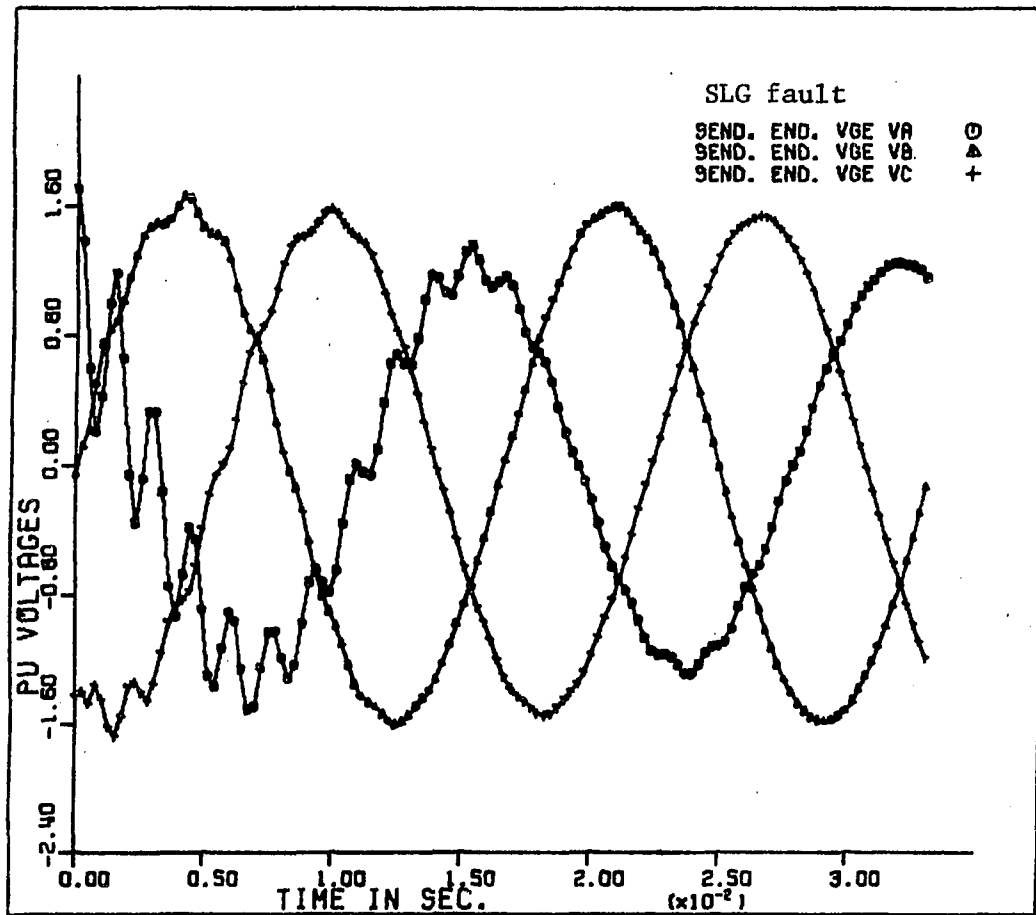


Figure 5.9a. Sending-end voltages for single-line-to-ground fault on phase a

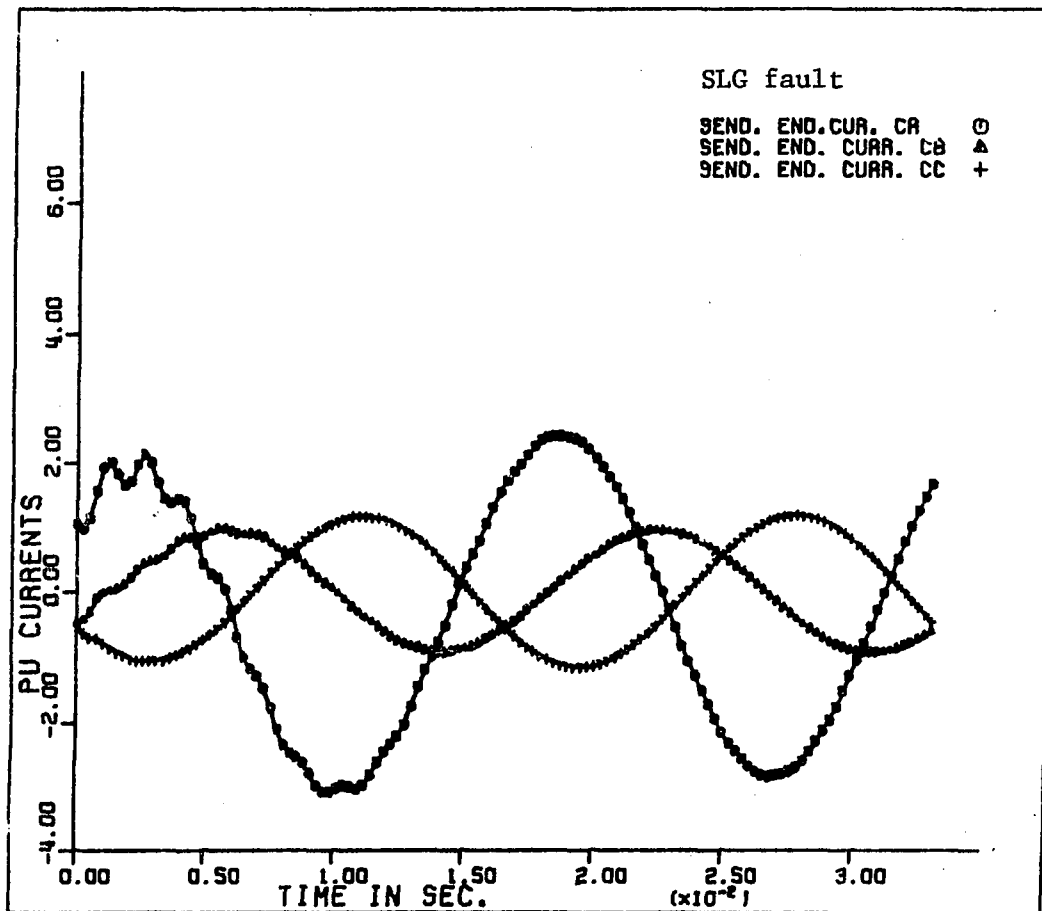


Figure 5.9b. Sending-end currents for single-line-to-ground fault on phase a

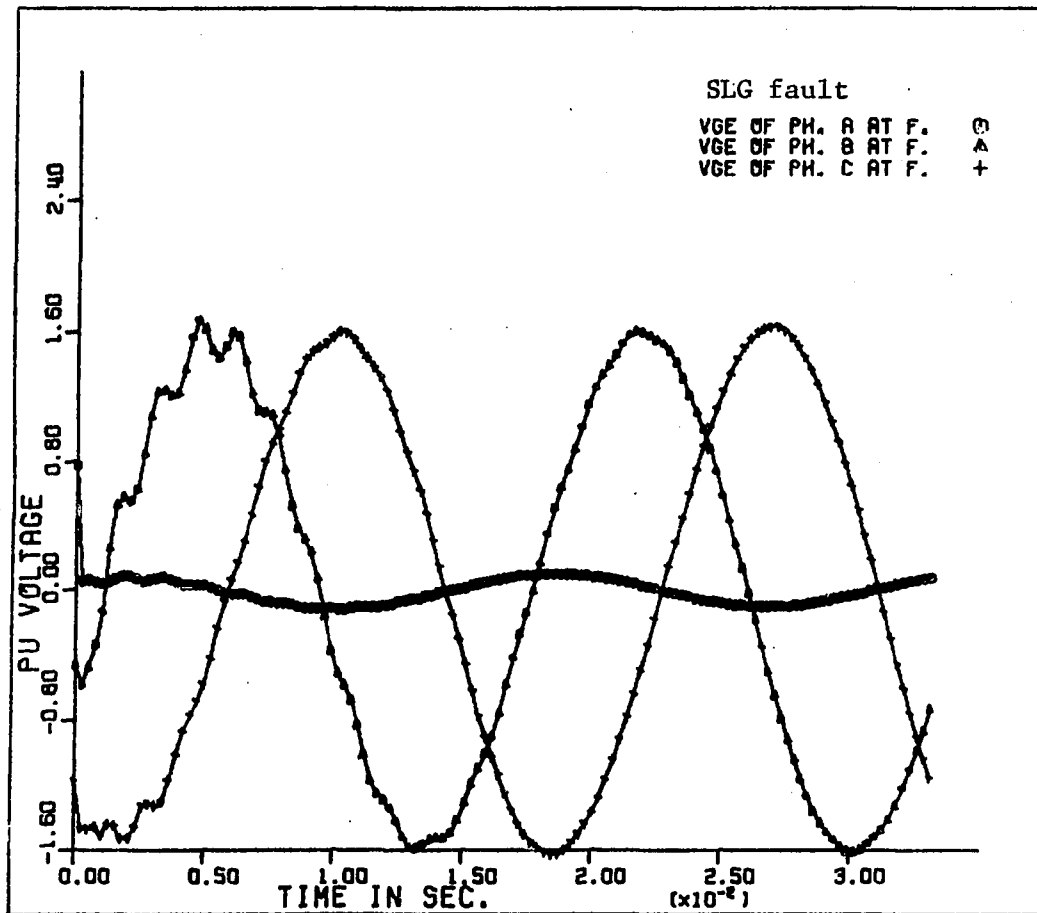


Figure 5.9c. Voltages at the fault location for single-line to-ground fault on phase a

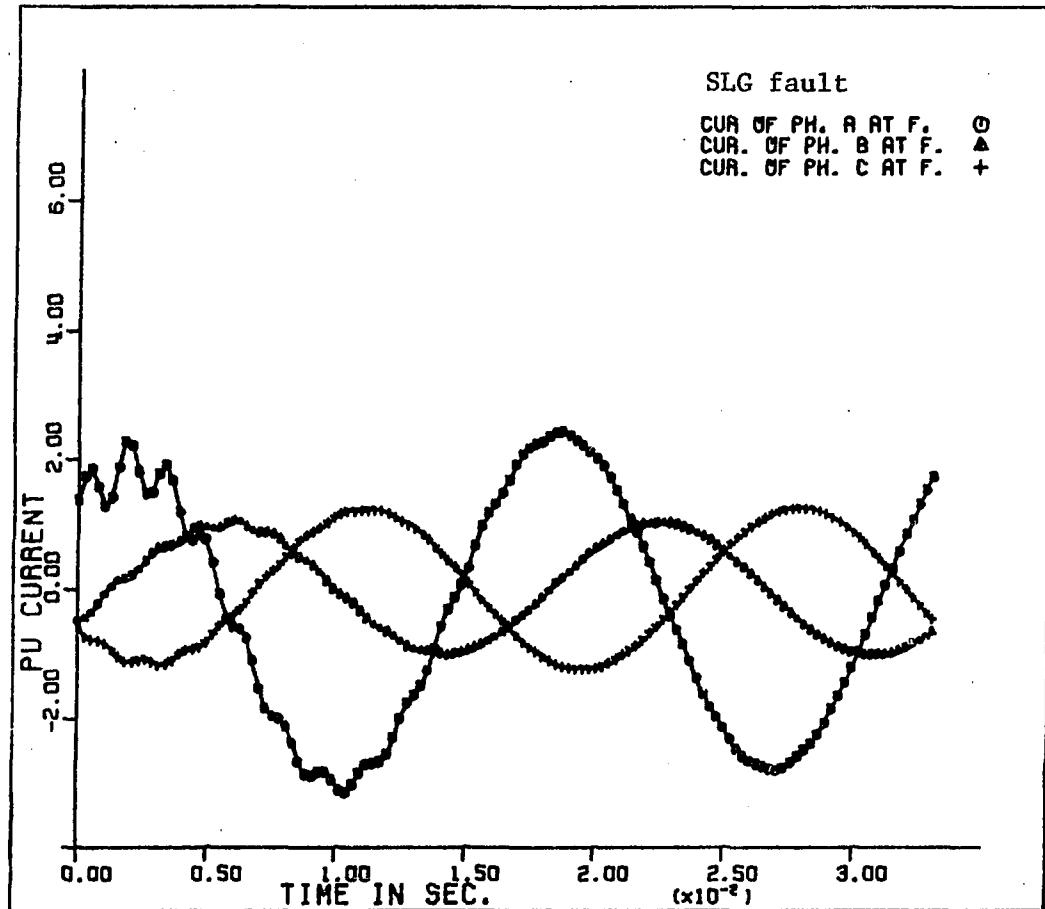


Figure 5.9d. Currents i_{r1} at the fault location for single-line-to-ground fault on phase a

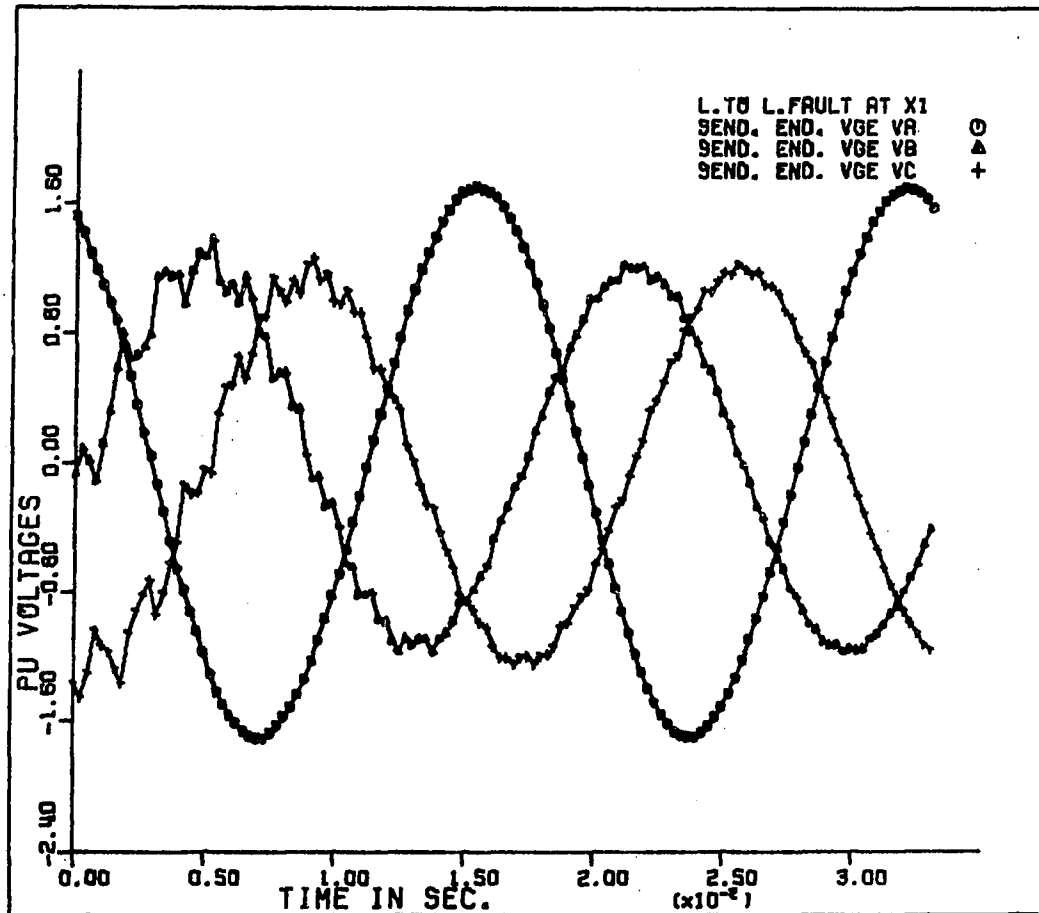


Figure 5.10a. Sending-end voltages for line-to-line fault on phases b and c

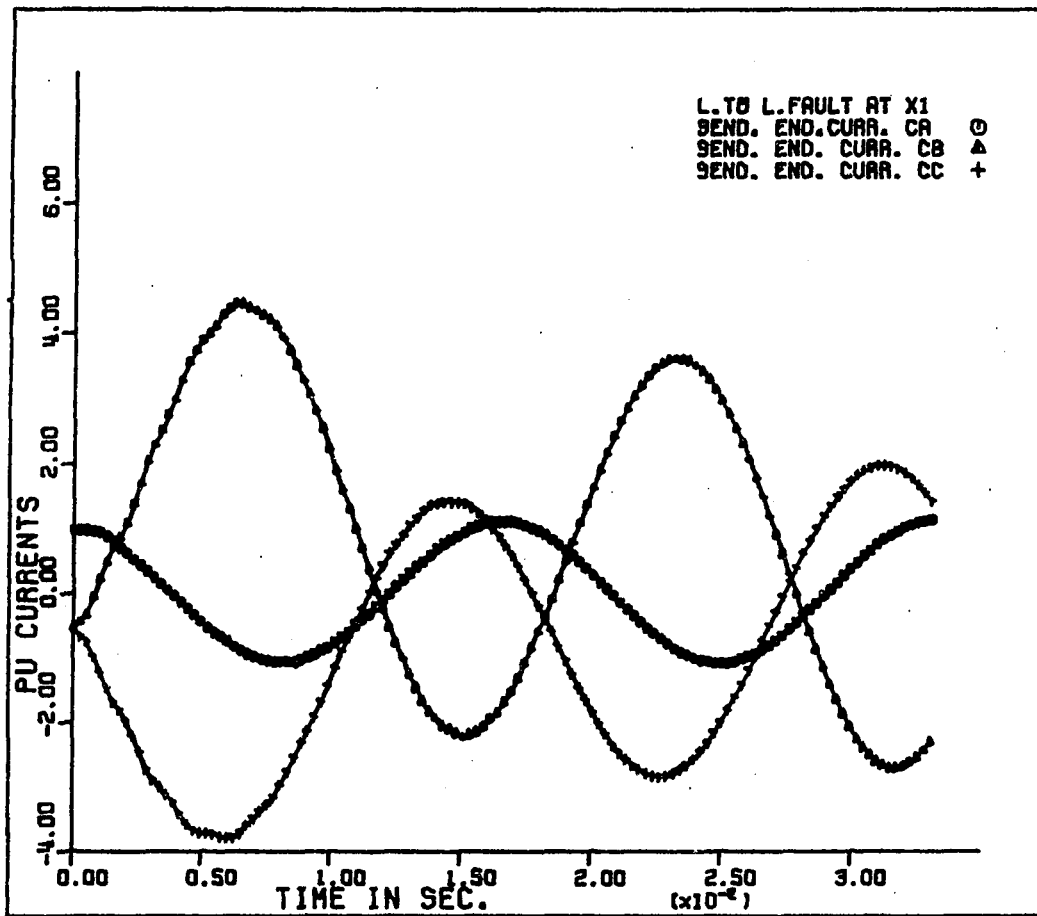


Figure 5.10b. Sending-end currents for line-to-line fault on phases b and c

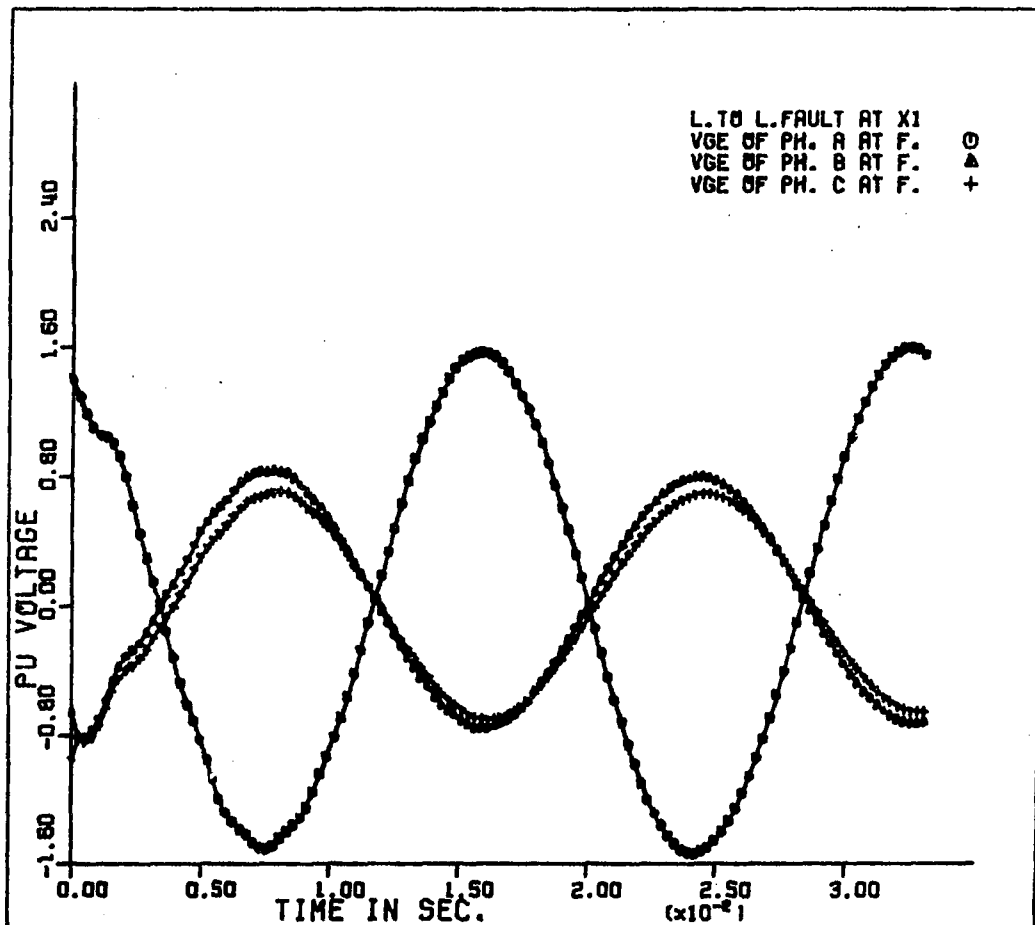


Figure 5.10c. Voltages at the fault location for line-to-line fault on phases b and c

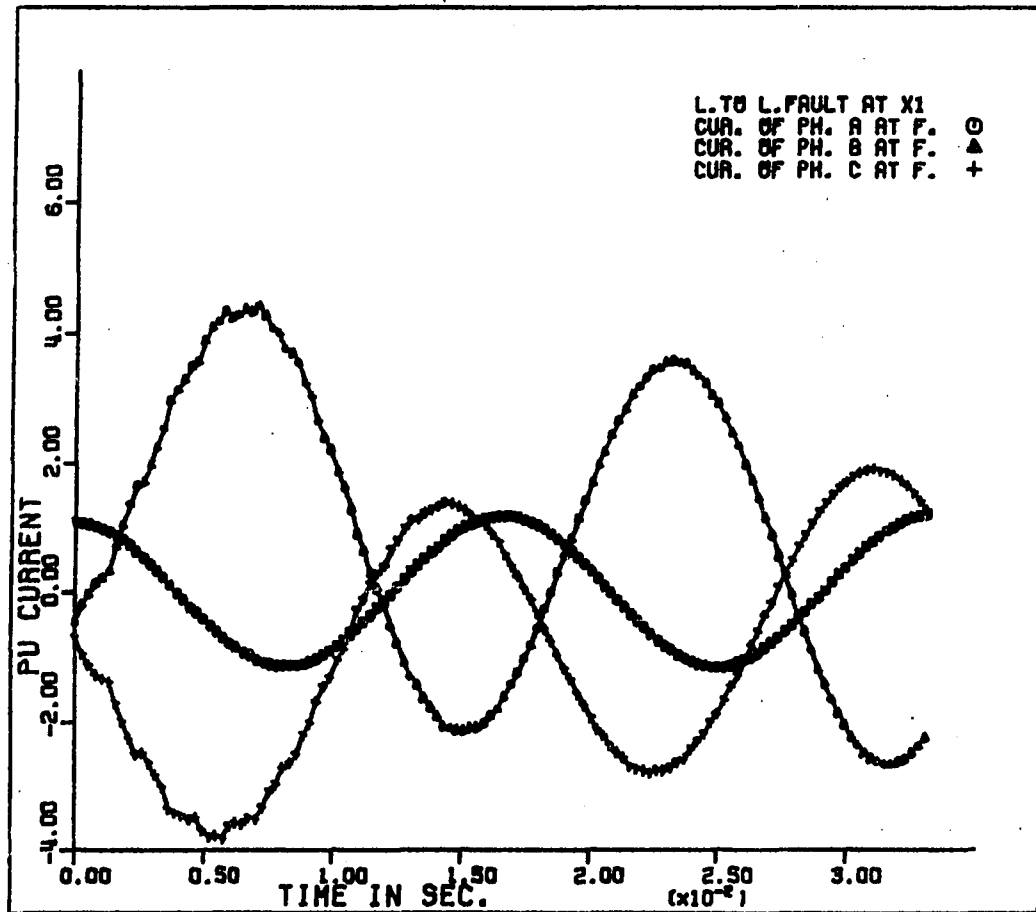


Figure 5.10d. Currents \underline{i}_{r1} at the fault location for line-to-line fault on phases b and c

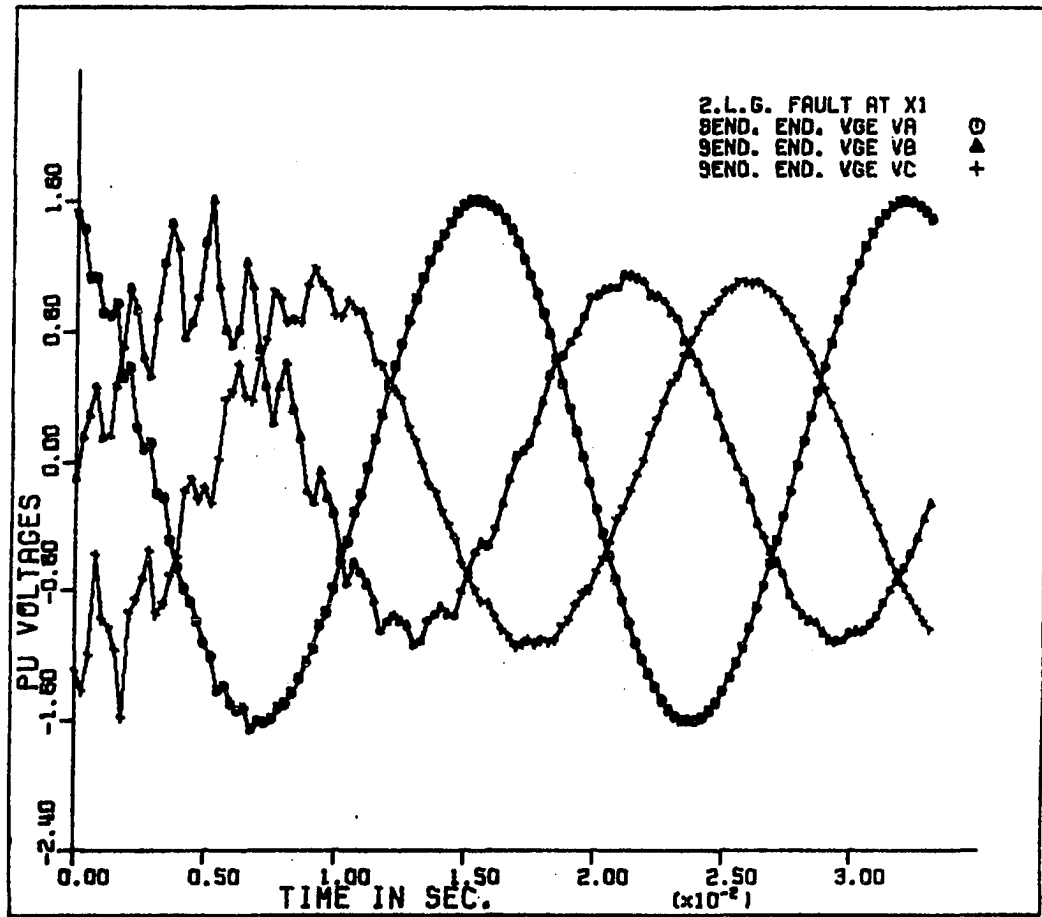


Figure 5.11a. Sending-end voltages for double-line-to-ground fault on phases b and c

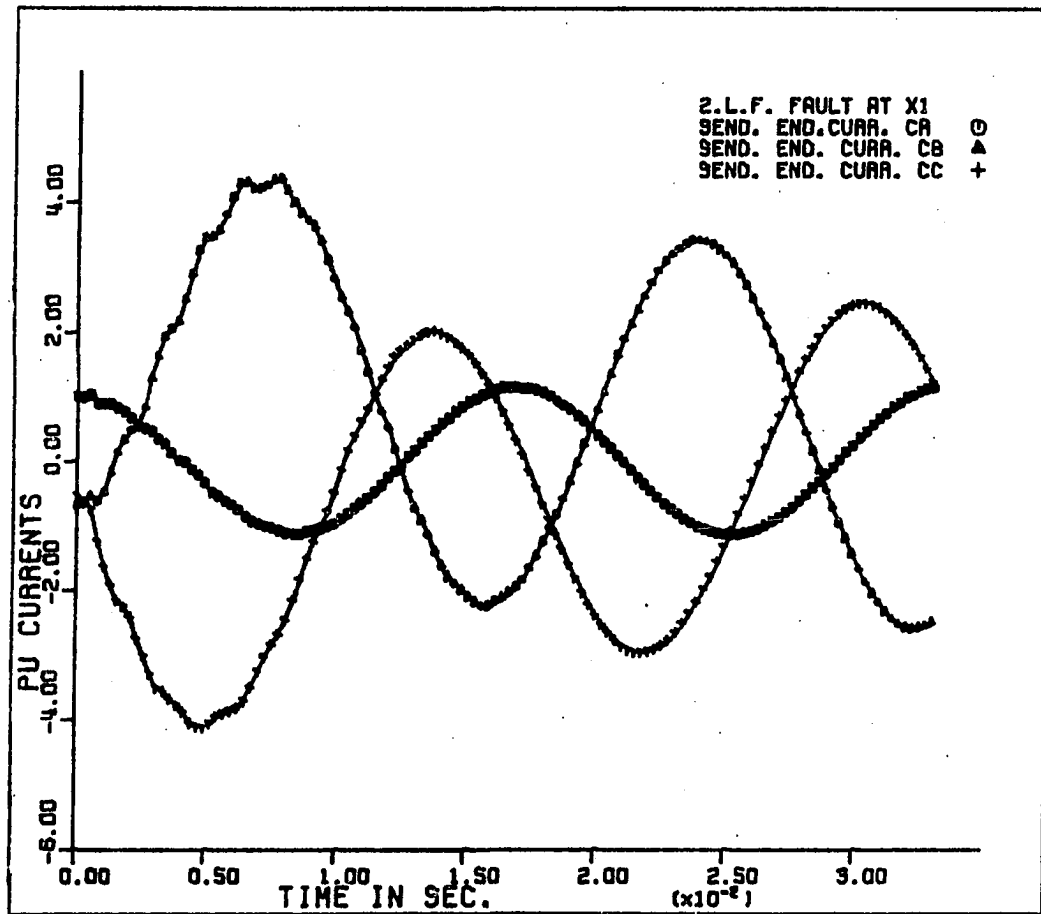


Figure 5.11b. Sending-end currents i_{s1} for double-line-to-ground fault on phases b and c

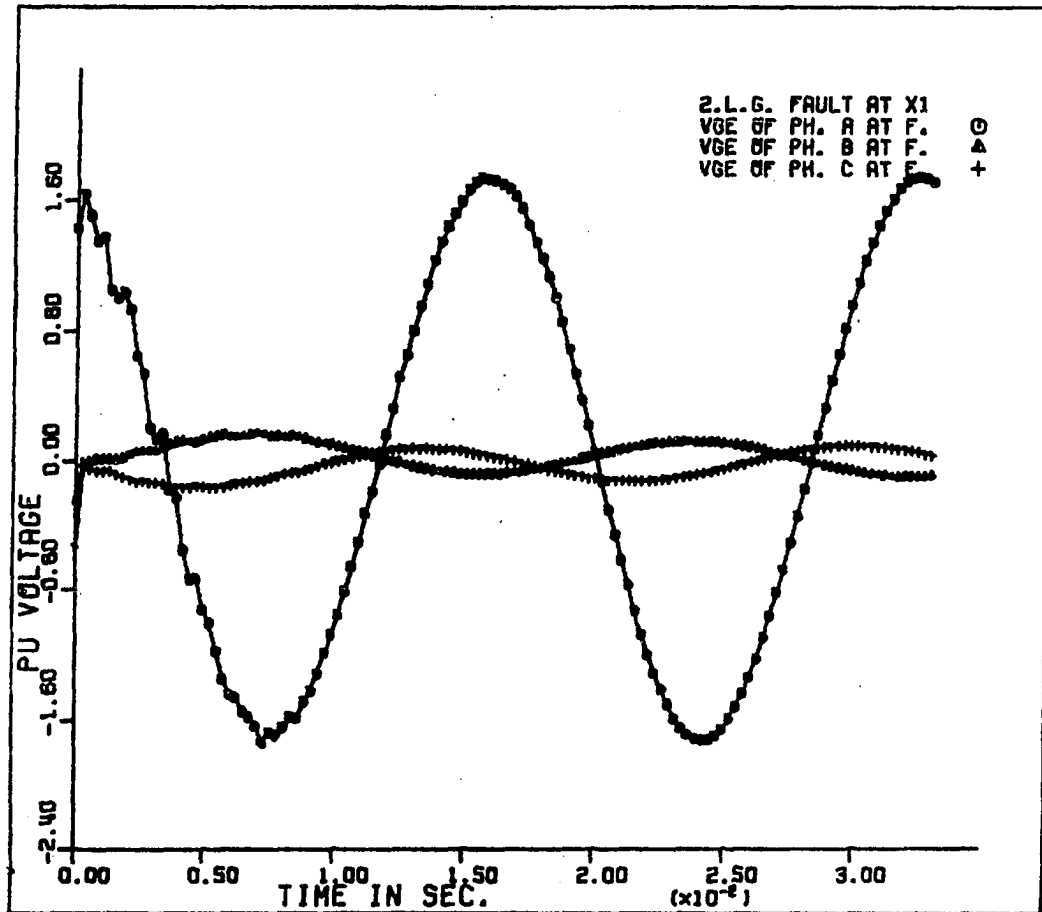


Figure 5.11c. Voltages at the fault location of double-line-to-ground fault on phases b and c

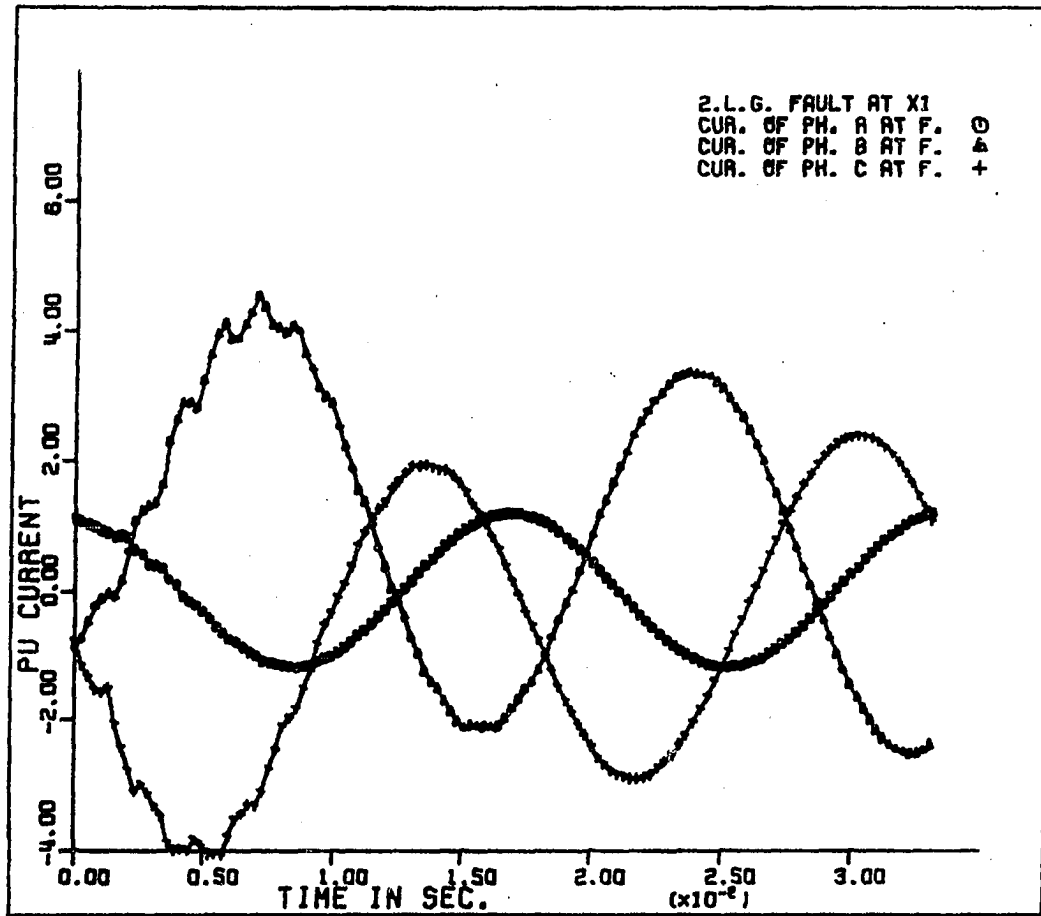


Figure 5.11d. Currents i_{r1} at the fault location for double-line-to-ground fault on phases b and c

VI. SYNCHRONOUS MACHINE EQUATIONS IN FREQUENCY DOMAIN

In the previous chapter, the generator and transformer were represented by a constant source behind a transient impedance. This representation is so commonly used in transient analysis that it can be considered to be classical or standard. It is also subject to criticism; the very fact that a distinction must be made between "transient" inductance and steady-state inductance is tacit recognition that the generator is an inherently nonlinear circuit element which can only be represented by a Thevenin equivalent under rather special conditions.

This research suggests that the errors introduced into transient analysis by use of the classical model are negligible when the fault is remote from the generator. When the fault is near the generator, these errors are significant.

This section develops a sequence of transformations that make it possible to couple the generator equations with the line equations in the frequency domain. This eliminates the errors that arise when the fault is near the generator.

Reference [29] described the full-machine model in the time domain. The model is shown in Figure 6.1 where: aa' , bb' , and cc' are the three-phase stator windings, FF' is the field winding, and DD' and QQ' are the damper windings.

The flux linkage equations in matrix form are

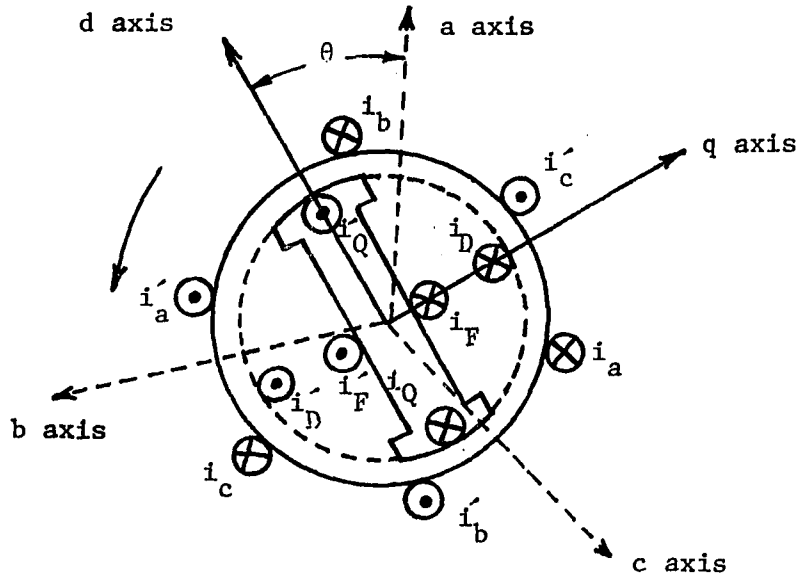


Figure 6.1. Full model of synchronous machine

$$\begin{bmatrix} \lambda_a \\ \lambda_b \\ \lambda_c \\ \lambda_F \\ \lambda_D \\ \lambda_Q \end{bmatrix} = \begin{bmatrix} L_{aa} & L_{ab} & L_{ac} & L_{aF} & L_{aD} & L_{aQ} \\ L_{ba} & L_{bb} & L_{bc} & L_{bF} & L_{bD} & L_{bQ} \\ L_{ca} & L_{cb} & L_{cc} & L_{cF} & L_{cD} & L_{cQ} \\ L_{Fa} & L_{Fb} & L_{Fc} & L_{FF} & L_{FD} & L_{FQ} \\ L_{Da} & L_{Db} & L_{Dc} & L_{DF} & L_{DD} & L_{DQ} \\ L_{Qa} & L_{Qb} & L_{Qc} & L_{QF} & L_{QD} & L_{QQ} \end{bmatrix} \begin{bmatrix} i_a \\ i_b \\ i_c \\ i_F \\ i_D \\ i_Q \end{bmatrix}$$

or

$$\begin{bmatrix} \lambda_{abc} \\ \lambda_{FCQ} \end{bmatrix} = \begin{bmatrix} L_{SS} & L_{SR} \\ L_{RS} & L_{RR} \end{bmatrix} \begin{bmatrix} i_{abc} \\ i_{FDQ} \end{bmatrix} \quad (6.1)$$

where

 L_{SS} = stator-stator inductances L_{SR} and L_{RS} = stator-rotor inductances

L_{RR} = rotor-rotor inductances

The elements in the inductance matrix in equation (6.1) are identified in reference [29] as

Stator self-inductances:

$$L_{aa} = L_s + L_m \cos 2\theta \quad H$$

$$L_{bb} = L_s + L_m \cos 2(\theta - 2\pi/3) \quad H$$

$$L_{cc} = L_s + L_m \cos 2(\theta + 2\pi/3) \quad H$$

where L_s and L_m are constants

Rotor self-inductances:

$$L_{FF} = L_F \quad H, \quad L_{DD} = L_D \quad H, \quad \text{and} \quad L_{QQ} = L_Q \quad H$$

Stator mutual-inductances:

$$L_{ab} = L_{ba} = -M_s - L_m \cos 2(\theta + \pi/6) \quad H$$

$$L_{bc} = L_{cb} = -M_s - L_m \cos 2(\theta - \pi/2) \quad H$$

$$L_{ca} = L_{ac} = -M_s - L_m \cos 2(\theta + 5\pi/6) \quad H$$

Rotor mutual-inductances:

$$L_{FD} = L_{DF} = M_R \quad H$$

$$L_{FD} = L_{QF} = 0$$

$$L_{DQ} = L_{QD} = 0$$

Mutual inductances between the stator and the rotor

$$L_{aF} = L_{Fa} = M_F \cos \theta \quad H$$

$$L_{bF} = L_{Fc} = M_F \cos \left(\theta - \frac{2\pi}{3} \right) \quad H$$

$$L_{cF} = L_{Fc} = M_F \cos \left(\theta + \frac{2\pi}{3} \right) \quad H$$

$$L_{aD} = L_{Da} = M_D \cos \theta \quad H$$

$$L_{bD} = L_{Db} = M_D \cos \left(\theta - \frac{2\pi}{3} \right) \quad H$$

$$L_{cD} = L_{Dc} = M_D \cos \left(\theta + \frac{2\pi}{3} \right) \quad H$$

$$L_{aQ} = L_{Qa} = M_Q \sin \theta \quad H$$

$$L_{bQ} = L_{Qb} = M_Q \sin \left(\theta - \frac{2\pi}{3} \right) \quad H$$

$$L_{cQ} = L_{Qc} = M_Q \sin \left(\theta + \frac{2\pi}{3} \right) \quad H$$

A. Machine Equations in the Direct-Quadrature Components

The synchronous machine equations can be transformed into the (0-d-q) components by using the modified Park's transformation [29].

The Park's transformation consists of the set of equations:

$$\underline{i}_{0dq} \triangleq \underline{P} \underline{i}_{abc}$$

$$\underline{v}_{0dq} \triangleq \underline{P} \underline{v}_{abc}$$

$$\underline{\lambda}_{0dq} \triangleq \underline{P} \underline{\lambda}_{abc}$$

$$\text{where } \underline{P} \triangleq \sqrt{\frac{2}{3}} \begin{bmatrix} 1/\sqrt{2} & 1/\sqrt{2} & 1/\sqrt{2} \\ \cos \theta & \cos \left(\theta - \frac{2\pi}{3} \right) & \cos \left(\theta + \frac{2\pi}{3} \right) \\ \sin \theta & \sin \left(\theta - \frac{2\pi}{3} \right) & \sin \left(\theta + \frac{2\pi}{3} \right) \end{bmatrix}$$

The following method is used to transform the machine equations in the s-domain. Applying Park's transformation to the (a-b-c) partition, equation (6.1) produces

$$\begin{bmatrix} P & 0 \\ - & - \\ 0 & U \end{bmatrix} \begin{bmatrix} \lambda_{abc} \\ - \\ \lambda_{FDQ} \end{bmatrix} = \begin{bmatrix} P & 0 \\ - & - \\ 0 & U \end{bmatrix} \begin{bmatrix} L_{SS} & L_{SR} \\ - & - \\ L_{RS} & L_{RR} \end{bmatrix} \begin{bmatrix} P & 0 \\ - & - \\ 0 & U \end{bmatrix} \begin{bmatrix} P^{-1} & 0 \\ - & - \\ 0 & U \end{bmatrix} \begin{bmatrix} i_{abc} \\ - \\ i_{FDQ} \end{bmatrix} \quad (6.2)$$

The final result of the matrix multiplications in equation (6.2) is

$$\begin{bmatrix} \lambda_{0dq} \\ - \\ \lambda_{FDQ} \end{bmatrix} = \begin{bmatrix} L_{0dq} & M_{FDQ} \\ - & - \\ M_{FDQ}^t & L_{FDQ} \end{bmatrix} \begin{bmatrix} i_{0dq} \\ - \\ i_{FDQ} \end{bmatrix}$$

or

$$\begin{bmatrix} \lambda_0 \\ \lambda_d \\ \lambda_q \\ - \\ \lambda_F \\ \lambda_D \\ \lambda_Q \end{bmatrix} = \begin{bmatrix} L_0 & 0 & 0 & 0 & 0 & 0 \\ 0 & L_d & 0 & KM_F & KM_D & 0 \\ 0 & 0 & L_q & 0 & 0 & KM_Q \\ - & - & - & - & - & - \\ 0 & KM_F & 0 & L_F & M_R & 0 \\ 0 & KM_D & 0 & M_R & L_D & 0 \\ 0 & 0 & KM_Q & 0 & 0 & L_Q \end{bmatrix} \begin{bmatrix} i_0 \\ i_d \\ i_q \\ - \\ i_F \\ i_D \\ i_Q \end{bmatrix}, \quad K = \sqrt{\frac{3}{2}} \quad (6.3)$$

L_0 , L_d , and L_q are defined as

$$L_0 = L_s - 2M_s \quad H$$

$$L_d = L_s + M_s + \frac{3}{2} L_m \quad H$$

$$L_q = L_s + M_s - \frac{3}{2} L_m \quad H$$

The voltage equations:

From the equivalent circuit of a synchronous generator in Figure 6.2, the voltage equations in the (a-b-c) components are:

$$\underline{v} = -\underline{r} \underline{i} - \underline{\dot{\lambda}} \quad (6.4)$$

and

$$\underline{\dot{\lambda}} = \underline{L} \underline{\dot{i}} + \underline{\dot{L}} \underline{i}$$

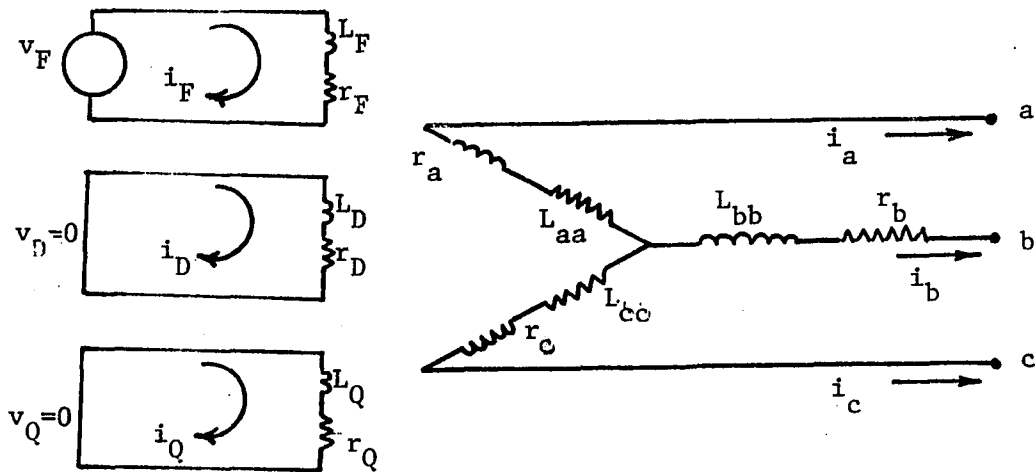


Figure 6.2. Equivalent circuit of a synchronous generator

Equation (6.4) in a matrix form is

$$\begin{bmatrix} v_a \\ v_b \\ v_c \\ -v_F \\ 0 \\ 0 \end{bmatrix} = \begin{bmatrix} r_a & & & & & \\ & r_b & & & & \\ & & r_c & & & \\ & & & r_F & & \\ & & & & r_D & \\ & & & & & r_Q \end{bmatrix} \begin{bmatrix} i_a \\ i_b \\ i_c \\ i_F \\ i_D \\ i_Q \end{bmatrix} - \begin{bmatrix} \dot{\lambda}_a \\ \dot{\lambda}_b \\ \dot{\lambda}_c \\ \dot{\lambda}_F \\ \dot{\lambda}_D \\ \dot{\lambda}_Q \end{bmatrix}$$

or in a compact form as

$$\begin{bmatrix} v_{abc} \\ \hline v_{FDQ} \end{bmatrix} = - \begin{bmatrix} R_{abc} & 0 \\ \hline 0 & R_{FDQ} \end{bmatrix} \begin{bmatrix} i_{abc} \\ \hline i_{FDQ} \end{bmatrix} + \begin{bmatrix} \dot{\lambda}_{abc} \\ \hline \dot{\lambda}_{FDQ} \end{bmatrix} \quad (6.5)$$

Applying Park's transformation to the equations in (6.5), the final results in the (0-d-q) components are

$$\begin{bmatrix} v_{0dq} \\ \hline v_{FDQ} \end{bmatrix} = - \begin{bmatrix} R_{abc} & 0 \\ \hline 0 & R_{FDQ} \end{bmatrix} \begin{bmatrix} i_{0dq} \\ \hline i_{FDQ} \end{bmatrix} - \begin{bmatrix} \dot{\lambda}_{0dq} \\ \hline \dot{\lambda}_{FDQ} \end{bmatrix} + \begin{bmatrix} F \\ \hline 0 \end{bmatrix} \quad (6.6)$$

where $\underline{F} = \underline{P} \underline{P}^{-1} \dot{\lambda}_{0dq}$

$$= \begin{bmatrix} 0 \\ -\omega_o \lambda_q \\ \omega_o \lambda_d \end{bmatrix}$$

From equation (6.6) the voltage equations are

$$\begin{aligned} v_0 &= -\dot{\lambda}_0 - r_a i_0 \\ v_d &= -\dot{\lambda}_d - \omega_o \lambda_q - r_a i_d \\ v_q &= -\dot{\lambda}_q + \omega_o \lambda_d - r_a i_q \\ -v_F &= -\dot{\lambda}_F - r_F i_F \\ 0 &= -\dot{\lambda}_D - r_D i_D \\ 0 &= -\dot{\lambda}_Q - r_Q i_Q \end{aligned}$$

Substituting λ_0 , λ_d , and λ_q in the above equations, they become

$$v_0 = -(r_a i_0 + L_0 \dot{i}_0)$$

$$v_d = -(r_a i_d + \omega_o L_q i_q + \omega_o K M_Q i_Q + L_d \dot{i}_d + K M_F \dot{i}_F + K M_D \dot{i}_D)$$

$$v_q = -(r_a i_q - \omega_o L_d i_d - \omega_o K M_F i_F - \omega_o K M_D i_D + L_q \dot{i}_q + K M_Q \dot{i}_Q)$$

$$v_F = r_F i_F + K M_F \dot{i}_d + L_F \dot{i}_F + M_R \dot{i}_D$$

$$0 = -(r_D i_D + K M_D \dot{i}_D + M_R \dot{i}_F + L_D \dot{i}_D)$$

$$0 = -(r_Q i_Q + K M_Q \dot{i}_Q + L_Q \dot{i}_Q)$$

The speed of the synchronous machine is assumed to be constant in the first few cycles after fault inception. This assumption enables the machine equations to be transformed to the s-domain. Applying Laplace transform to the above equations with zero initial condition produces

$$V_0(s) = -(r_a + s L_0) I_0(s)$$

$$V_d(s) = -[(r_a + s L_d) I_d(s) + \omega_o L_q I_q(s) + s K M_F I_F(s) + s K M_D I_D(s) + \omega_o K M_Q I_Q(s)]$$

$$V_q(s) = \omega_o L_d I_d(s) - (r_a + s L_q) I_q(s) + \omega_o K M_F I_F(s) + \omega_o K M_D I_D(s) - s K M_Q I_Q(s)$$

$$V_F(s) = s K M_F I_d(s) + (r_F + s L_F) I_F(s) + s M_R I_D(s)$$

$$0 = -[s K M_D I_d(s) + s M_R I_F(s) + (r_D + s L_D) I_D(s)]$$

$$0 = -[s K M_Q I_q(s) + (r_Q + s L_Q) I_Q(s)]$$

Preceding equations can be written in the matrix form

$$\begin{bmatrix} V_0(s) \\ v_d(s) \\ v_q(s) \\ \hline V_F(s) \\ V_D(s) \\ V_Q(s) \end{bmatrix} = \begin{bmatrix} -(r_a + sL_a) & 0 & 0 & | & 0 & 0 & 0 \\ 0 & -(r_a + sL_d) & -\omega_o L_q & | & -sKM_F & -sKM_D & -\omega_o KM_Q \\ 0 & \omega_o L_d & -(r_a + sL_q) & | & \omega_o KM_F & \omega_o KM_D & -sKM_Q \\ \hline 0 & sKM_F & 0 & | & (r_F + sL_F) & sM_R & 0 \\ 0 & -sKM_D & 0 & | & -sM_R & -(r_D + sL_D) & 0 \\ 0 & 0 & -sKM_Q & | & 0 & 0 & -(r_Q + sL_Q) \end{bmatrix} \times \begin{bmatrix} I_0(s) \\ I_d(s) \\ I_q(s) \\ \hline I_F(s) \\ I_D(s) \\ I_Q(s) \end{bmatrix} \quad (6.7)$$

or

$$\begin{bmatrix} V_{0dq}(s) \\ \hline V_{FDQ}(s) \end{bmatrix} = \begin{bmatrix} Z_{11} & | & Z_{12} \\ \hline Z_{21} & | & Z_{22} \end{bmatrix} \begin{bmatrix} I_{0dq}(s) \\ \hline I_{FDQ}(s) \end{bmatrix}$$

where

$$Z_{11} = \begin{bmatrix} -(r_a + sL_0) & 0 & 0 \\ 0 & -(r_a + sL_d) & -\omega_o L_q \\ 0 & \omega_o L_d & -(r_a + sL_q) \end{bmatrix} \quad (6.8)$$

$$\underline{Z}_{12} = \begin{bmatrix} 0 & 0 & 0 \\ -s K M_F & -s K M_D & -\omega_o K M_Q \\ \omega_o K M_F & \omega_o K M_D & -s K M_Q \end{bmatrix} \quad (6.9)$$

$$\underline{Z}_{21} = \begin{bmatrix} 0 & s K M_F & 0 \\ 0 & -s K M_D & 0 \\ 0 & 0 & -s K M_Q \end{bmatrix} \quad (6.10)$$

$$\underline{Z}_{22} = \begin{bmatrix} (r_F + s L_F) & s M_R & 0 \\ -s M_R & -(r_D + s L_D) & 0 \\ 0 & 0 & -(r_Q + s L_Q) \end{bmatrix} \quad (6.11)$$

Elimination of rotor variables:

Since V_F is constant (dc source), then the superimposed value of the field voltage V_F' is zero and the rotor variables can be eliminated. The superimposed voltages $V_0'(s)$, $V_d'(s)$, and $V_q'(s)$ can be obtained by applying Kron reduction to the matrix partition.

$$\begin{bmatrix} V_{0dq}'(s) \\ \text{---} \\ 0 \end{bmatrix} = \begin{bmatrix} Z_{11} & | & Z_{12} \\ \text{---} & + & \text{---} \\ Z_{21} & | & Z_{22} \end{bmatrix} \begin{bmatrix} I_{0dq}'(s) \\ \text{---} \\ I_{FDQ}'(s) \end{bmatrix} \quad (6.12)$$

Then,

$$\begin{aligned} V_{0dq}'(s) &= [Z_{11} - Z_{12} Z_{22}^{-1} Z_{21}] I_{0dq}'(s) \\ &= Z_{0dq}'(s) I_{0dq}'(s) \end{aligned} \quad (6.13)$$

where:

$$Z_{0dq}(s) = Z_{11} - Z_{12} Z_{22}^{-1} Z_{21}$$

B. Transformations Between Different Sets of Components

As shown in the block diagram in Figure 6.3, the (0-d-q) components are related to the (a-b-c) components. Similarly, the (0-f-b) components are related to the (0-d-q) components. The (0-f-b) components are found to be very useful in the interconnection of the rotating part and stationary part in the power systems.

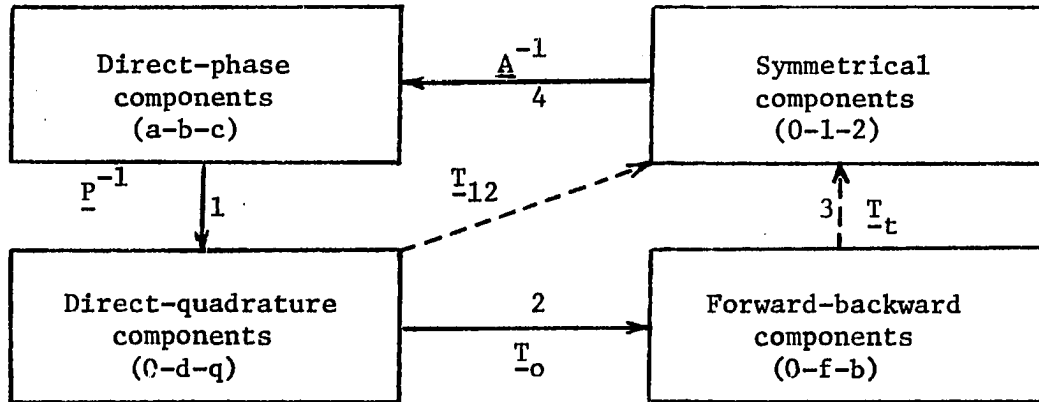


Figure 6.3. Block diagram of different transformation matrices

The transformation between the (0-d-q) components and the (0-f-b) components is defined as

$$i_d \triangleq i_f + i_b$$

$$ji_q \triangleq -i_f + i_b$$

(when the q-axis lags the d-axis as Figure 6.4).

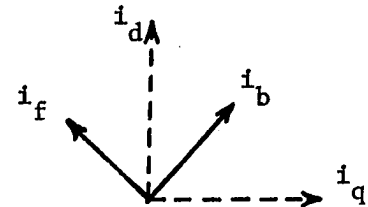


Figure 6.4. Forward-backward components

$$\begin{aligned}
i_f &= (i_d - j i_q)/2 \\
i_b &= (i_d + j i_q)/2
\end{aligned}
\tag{6.14}$$

By using the same transformation for voltages, the instantaneous power is

$$\begin{aligned}
v_d i_d + v_q i_q &= (v_f + v_b)(i_f + i_b) + j(v_f - v_b)j(i_f - i_b) \\
&= v_f i_f + v_b i_b + v_b i_f + v_f i_b - (v_f i_f + v_b i_b - v_f i_b) \\
&= 2(v_f i_b + v_b i_f)
\end{aligned}
\tag{6.15}$$

In order to make the transformation power invariant (the instantaneous power in terms of both sets of components does not involve a factor 2) it is evident that the factor 1/2 in equation (6.15) should be distributed between the two sets of equations. Thus the transformation matrix that transforms voltage or current from (d-q) axis to (f-b) components is

$$\begin{matrix} & \begin{matrix} 0 & f & b \end{matrix} \\ \begin{matrix} 0 \\ \underline{T}_o \\ q \end{matrix} & \begin{bmatrix} 1 & 0 & 0 \\ 0 & 1/\sqrt{2} & 1/\sqrt{2} \\ 0 & j/\sqrt{2} & -j/\sqrt{2} \end{bmatrix} \end{matrix}
\tag{6.16}$$

The inverse of the matrix \underline{T}_o is

$$\begin{matrix} & \begin{matrix} 0 & d & q \end{matrix} \\ \begin{matrix} 0 \\ \underline{T}_o^{-1} \\ f \\ b \end{matrix} & \begin{bmatrix} 1 & 0 & 0 \\ 0 & 1/\sqrt{2} & -j/\sqrt{2} \\ 0 & 1/\sqrt{2} & j/\sqrt{2} \end{bmatrix} \end{matrix}$$

where $\underline{T}_0^{-1} = [\underline{T}_0^*]^t$, so \underline{T}_0 is a power invariant transformation matrix.

Another transformation matrix (\underline{A}_{012}) is defined in many references [23] to transform the (a-b-c) to the (0-1-2) components.

$$\underline{A}_{012} = \frac{1}{h} \begin{bmatrix} 1 & 1 & 1 \\ 1 & a^2 & a \\ 1 & a & a^2 \end{bmatrix} \quad (6.17)$$

where $h=1$ for the Fortescue transformation

$h = \sqrt{3}$ for the power transformation

and "a" is an operator which is equal to $1/\underline{120}^\circ$

when $h = \sqrt{3}$, $\underline{A}_{012}^{-1} = [\underline{A}_{012}^*]^t$ or

$$\underline{A}_{012}^{-1} = \frac{1}{\sqrt{3}} \begin{bmatrix} 1 & 1 & 1 \\ 1 & a & a^2 \\ 1 & a^2 & a \end{bmatrix}$$

The modified Park's transformation matrix is also a power invariant transformation matrix because

$$\underline{P}^{-1} = \sqrt{\frac{2}{3}} \begin{bmatrix} 1/\sqrt{2} & \cos \theta & \sin \theta \\ 1/\sqrt{2} & \cos (\theta - 120) & \sin (\theta - 120) \\ 1/\sqrt{2} & \cos (\theta + 120) & \sin (\theta + 120) \end{bmatrix} \quad (6.18)$$

$$= \underline{P}^t \quad (\text{orthogonal matrix})$$

Since all the tranformation matrices are power invariant, then any impedance matrix can be transformed from any component system to any

other system. For example, if \underline{Z}_{old} represents the impedance matrix in the old system and \underline{Z}_{new} represents the impedance matrix in the new system, then

$$\underline{Z}_{new} = \underline{T}^{*t} \underline{Z}_{old} \underline{T} \quad (6.19)$$

where \underline{T} can be any power-invariant-transformation matrix.

In order to synthesize the previous developments into a useful process, it is necessary to find a matrix that transforms from the (0-f-b) components to the (0-1-2) components. As in the block diagram in Figure 6.3, the relations between the (0-d-q) components and the (0-f-b) components can be obtained by the transformation matrix \underline{T}_o . Then, the relation between the (0-f-b) components and the (0-1-2) component can be obtained by the following methods.

$$\begin{aligned} \underline{v}_{0fb} &= \underline{T}_o^{-1} \underline{v}_{0dq} \\ &= \underline{T}_o^{-1} \underline{P} \underline{v}_{abc} \\ &= (\underline{T}_o^{-1} \underline{P} \underline{A}_{012}) \underline{v}_{012} \\ &= \underline{T}_{2p} \underline{v}_{012} \end{aligned}$$

where

$$\underline{T}_{2p} = \underline{T}_o^{-1} \underline{P} \underline{A}_{012}$$

or

$$\begin{aligned}
T_{2p} &= \begin{bmatrix} 1 & 0 & 0 \\ 0 & 1/\sqrt{2} & -j/\sqrt{2} \\ 0 & 1/\sqrt{2} & j/\sqrt{2} \end{bmatrix} \cdot \sqrt{\frac{2}{3}} \begin{bmatrix} 1/\sqrt{2} & 1/\sqrt{2} & 1/\sqrt{2} \\ \cos \theta & \cos(\theta - \frac{2\pi}{3}) & \cos(\theta + \frac{2\pi}{3}) \\ \sin \theta & \sin(\theta - \frac{2\pi}{3}) & \sin(\theta + \frac{2\pi}{3}) \end{bmatrix} \times \\
&\quad \frac{1}{\sqrt{3}} \begin{bmatrix} 1 & 1 & 1 \\ 1 & a^2 & a \\ 1 & a & a^2 \end{bmatrix} \\
&= f \begin{bmatrix} 0 & 1 & 2 \\ 1 & 0 & 0 \\ 0 & -j\theta_e & 0 \\ 0 & 0 & j\theta_e \end{bmatrix} \quad (6.20)
\end{aligned}$$

where

$$\theta = \omega_o t + \delta + \pi/2, \quad \omega_o = 377 \text{ rad/sec} \quad (6.21)$$

The method of finding the angle δ will be discussed in the next section.

T_{2p} is also a power invariant matrix because $[T_{2p}]^{-1} = [T_{2p}^*]^t$. The matrix in equation (6.20) is a very simple transformation matrix, since it is equal to its own transpose and it has only diagonal elements.

C. Voltage Equations at the Sending-End Bus

From equation (6.20), the superimposed voltages in the (0-f-b) components are

$$\begin{aligned}
v_f' &= v_1' e^{-j\theta} \\
&= v_1' e^{-j\omega_o t} \cdot e^{-j\delta'} \quad (6.22)
\end{aligned}$$

and

$$v_b' = v_2' e^{j\omega_o t} e^{j\delta'} \quad (6.23)$$

where $\delta' = \delta + \pi/2$

Equations (6.22) and (6.23) are in the time-domain. They can be transformed into s-domain by means $f(t) \exp(j\omega_o t) \Leftrightarrow F(s - j\omega_o)$, then

$$\begin{aligned} V_f'(s) &= V_1'(s + j\omega_o) \exp(-j\delta') \\ V_b'(s) &= V_2'(s - j\omega_o) \exp(j\delta') \end{aligned} \quad (6.24)$$

Similarly,

$$\begin{aligned} I_f'(s) &= I_1'(s + j\omega_o) \exp(-j\delta') \\ I_b'(s) &= I_2'(s - j\omega_o) \exp(j\delta') \end{aligned} \quad (6.25)$$

Since the zero sequence of voltage and current do not change from one set of components to another, equations (6.24) and (6.25) can be written in a matrix form as

$$\begin{bmatrix} V_0'(s) \\ V_f'(s) \\ V_b'(s) \end{bmatrix} = \begin{bmatrix} 1 & 0 & 0 \\ 0 & -j\delta' \\ 0 & 0 & j\delta' \\ & e & e \end{bmatrix} \begin{bmatrix} V_0'(s) \\ V_1'(s + j\omega_o) \\ V_2'(s - j\omega_o) \end{bmatrix}$$

or

$$\underline{V}_{0fb}'(s) = \underline{T}_t \underline{V}_{012}'(s') \quad (6.26)$$

and

$$\underline{I}_{0fb}'(s) = \underline{T}_t \underline{I}_{012}'(s') \quad (6.27)$$

If $\underline{Z}_{0dq}(s)$ in equation (6.13) represents the impedance matrix in the old system and $\underline{Z}_{0fb}(s)$ represents the impedance matrix in the new system,

then similar to equation (6.19) $Z_{0fb}(s)$ can be obtained as

$$Z_{0fb}(s) = \underline{T}_o^{*t} Z_{0dq}(s) \underline{T}_o \quad (6.28)$$

\underline{T}_o^{*t} denotes the conjugate transpose of \underline{T}_o . Similarly,

$$Z_{012}(s) = \underline{T}_t^{*t} Z_{0fb}(s) \underline{T}_t \quad (6.29)$$

By substituting $Z_{0fb}(s)$ in (6.28) into (6.29), the result is

$$\begin{aligned} Z_{012}(s) &= \underline{T}_t^{*t} \underline{T}_o^{*t} Z_{0dq}(s) \underline{T}_o \underline{T}_t \\ &= (\underline{T}_o^* \underline{T}_t^*)^t Z_{0dq}(s) (\underline{T}_o \underline{T}_t) \\ &= \underline{T}_{12}^{*t} \cdot Z_{0dq}(s) \cdot \underline{T}_{12} \end{aligned} \quad (6.30)$$

where

$$\begin{aligned} \underline{T}_{12} &= \underline{T}_o \underline{T}_t \\ &= \begin{bmatrix} 1 & 0 & 0 \\ 0 & 1/\sqrt{2} & 1/\sqrt{2} \\ 0 & j/\sqrt{2} & -j/\sqrt{2} \end{bmatrix} \begin{bmatrix} 1 & 0 & 0 \\ 0 & \exp(-j\delta') & 0 \\ 0 & 0 & \exp(j\delta') \end{bmatrix} \\ &= \frac{1}{\sqrt{2}} \begin{bmatrix} \sqrt{2} & 0 & 0 \\ 0 & \exp(-j\delta') & \exp(j\delta') \\ 0 & j \exp(-j\delta') & -j \exp(j\delta') \end{bmatrix} \end{aligned} \quad (6.31)$$

The above transformation matrices are used to find the superimposed generator terminal voltages (\underline{v}_g') in the sequence components as follows.

As equation (6.13)

$$\begin{aligned}
\bar{V}'_{g0dq}(s) &= \bar{Z}_{0dq}(s) \cdot \bar{I}'_{g0dq}(s) \\
\bar{T}_o \bar{V}'_{g0fb}(s) &= \bar{Z}_{0dq}(s) \cdot \bar{T}_o \cdot \bar{I}'_{g0fb}(s) \\
\bar{T}_o \cdot \bar{T}_t \cdot \bar{V}'_{g012}(s') &= \bar{Z}_{0dq}(s) \cdot \bar{T}_o \cdot \bar{T}_t \cdot \bar{I}'_{g012}(s') \\
\bar{V}'_{g012}(s') &= \bar{T}_{12}^{-1} \cdot \bar{Z}_{0dq}(s) \cdot \bar{T}_{12} \cdot \bar{I}'_{g012}(s') \\
&= \bar{T}_{12}^{*t} \cdot \bar{Z}_{0dq}(s) \cdot \bar{T}_{12} \cdot \bar{I}'_{g012}(s') \\
&= \bar{Z}_{g012}(s) \cdot \bar{I}'_{g012}(s') \tag{6.32}
\end{aligned}$$

where

$$\begin{aligned}
\bar{Z}_{g012}(s) &= \bar{T}_{12}^{*t} \cdot \bar{Z}_{0dq}(s) \cdot \bar{T}_{12} \\
\bar{V}'_{g012}(s') &= \begin{bmatrix} V'_0(s) \\ V'_1(s + j\omega_o) \\ V'_2(s - j\omega_o) \end{bmatrix} \quad \text{and} \quad \bar{I}'_{g012}(s') = \begin{bmatrix} I'_0(s) \\ I'_1(s + j\omega_o) \\ I'_2(s - j\omega_o) \end{bmatrix}
\end{aligned}$$

(s') representing the shifted s -domain, (i.e.,) no shifting in zero sequence, shifting the positive sequence by ($j\omega_o$), and shifting the negative sequence by ($-j\omega_o$).

If v_g represents the generator terminal voltage and v_{s1} represents the sending end voltage, then the sending end voltage equation from the generator side can be obtained.

As shown in Figure 6.5, the sending-end voltage in the shifted s -domain can be written as

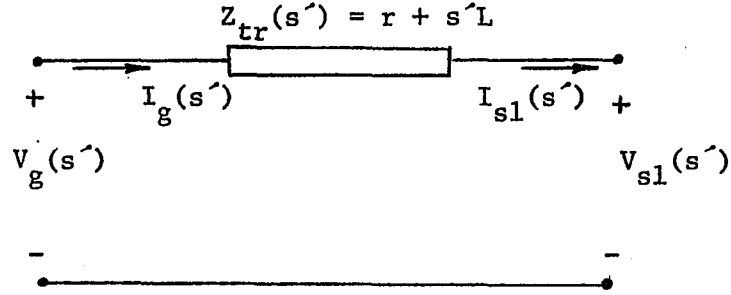


Figure 6.5. Equivalent circuit of the transformer in the shifted s-domain

$$\underline{V}'_{sl_{012}}(s') = \underline{V}'_{g_{012}}(s') - \underline{Z}_{tr}(s') \cdot \underline{I}'_{sl}(s') \quad (6.33)$$

where \underline{Z}_{tr} is the impedance matrix of the transformer in the shifted s-domain which is written as

$$\underline{Z}_{tr}(s') = \begin{bmatrix} \underline{Z}_{tr0}(s) & 0 & 0 \\ 0 & \underline{Z}_{tr1}(s + j\omega_o) & 0 \\ 0 & 0 & \underline{Z}_{tr2}(s - j\omega_o) \end{bmatrix}$$

Equations (6.32) and (6.33) are combined as

$$\underline{V}'_{sl_{012}}(s') = \underline{Z}_{g_{012}}(s) \cdot \underline{I}'_{g_{012}}(s') - \underline{Z}_{tr}(s') \cdot \underline{I}'_{sl_{012}}(s')$$

but $\underline{I}'_{g_{012}}(s') = \underline{I}'_{sl_{012}}(s')$, then

$$\begin{aligned} \underline{V}'_{sl_{012}}(s') &= (\underline{Z}_{g_{012}}(s) - \underline{Z}_{tr}(s')) \underline{I}'_{sl_{012}}(s') \\ &= \underline{Z}_{gt} \cdot \underline{I}'_{sl_{012}}(s') \end{aligned} \quad (6.34)$$

where $\underline{Z}_{gt} = \underline{Z}_{g_{012}}(s) - \underline{Z}_{tr}(s')$

Equation (6.34) is used to find the sending-end voltage from the generator and the transformer side in sequence components and in shifted s-domain. With the above method, the machine equations (having time varying parameters) can be combined with the transmission line equations (having frequency varying parameters) in frequency domain.

Rotor angle of synchronous machine:

The main field-winding flux is along the direction of the direct axis as shown in Figure 6.1. This flux produces an EMF that lags by 90° . Therefore, the machine EMF (\bar{E}) is primarily along the rotor q axis. In steady-state analysis, the phasor \bar{E} leads the general terminal voltage \bar{v}_t . The angle between \bar{E} and \bar{v}_t is the machine torque angle δ . At zero time, the phasor \bar{v}_t is located at the axis of phase a (reference axis) as shown in Figure 6.6. The q axis is located at an angle δ , and the d axis is located at $\theta = \delta + \pi/2$. At $t > 0$, the reference axis is located at an angle $\omega_0 t$ with respect to the axis of phase a. The d axis of the rotor is therefore located at $\theta = \omega_0 t + \delta + \pi/2$ where ω_0 is the rated (synchronous) angular frequency in rad./s and δ is the synchronous torque angle in electrical radians. The angle δ can be obtained from the steady-state condition. The boundary conditions are the terminal voltage v_t , the terminal current i_t , and the angle ϕ between v_t and i_t .

From the phasor diagram in Figure 6.6

$$E_{qa} \triangleq \bar{v}_t + (r_a + j X_q) \bar{i}_t \quad (6.35)$$

where r_a = stator resistance and \bar{i}_t = sending-end current \bar{i}_s .

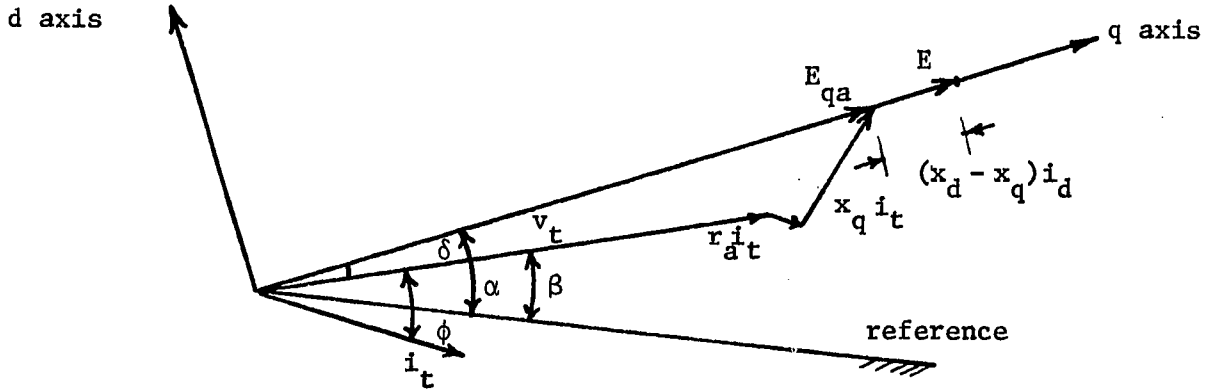


Figure 6.6. Phasor diagram of the synchronous machine

The terminal machine voltage is

$$\bar{v}_t = \bar{v}_s + (r_{tr} + j X_{tr}) \bar{i}_s \quad (6.36)$$

From (6.35) and (6.36)

$$\begin{aligned} \bar{E}_{qa} &= \bar{v}_s + (r_{tr} + j X_{tr}) \bar{i}_s + (r_a + j X_q) \bar{i}_s \\ &= \bar{v}_s + (r_{tot} + j X_{tot}) \bar{i}_s \end{aligned} \quad (6.37)$$

where

$$r_{tot} = r_a + r_{tr}$$

$$X_{tot} = X_q + X_{tr}$$

Therefore δ is the angle of \bar{E}_{qa} .

By knowing the rotor angle δ , then the transformation matrix T_{12} in equation (6.31) can be obtained.

VII. INTERCONNECTION OF SYNCHRONOUS MACHINES AND TRANSMISSION LINES IN FAULTED POWER SYSTEMS

In order to make the line equations compatible with the machine equations, the line equations must be formulated in sequence components and in shifted s-domain (s').

A. Formulation of the Transmission Line Equations in the Shifted-Frequency Domain

Equations (4.3) and 4.4) are transformed into sequence components by using the transformation matrix \underline{A}_{012} in equation (6.17).

$$\begin{aligned} -\frac{d}{dx} \underline{V}_{012}(x,s) &= \underline{A}_{012}^{-1} \underline{Z}(s) \underline{A}_{012} \underline{I}_{012}(x,s) \\ &= \underline{Z}_{012} \underline{I}_{012}(x,s) \end{aligned} \quad (7.1)$$

Similarly,

$$-\frac{d}{dx} \underline{I}_{012}(x,s) = \underline{Y}_{012} \underline{V}_{012}(x,s) \quad (7.2)$$

where

$$\begin{aligned} \underline{Z}_{012} &= \underline{A}_{012}^{-1} \underline{Z}(s) \underline{A}_{012} \\ \underline{Y}_{012} &= \underline{A}_{012}^{-1} \underline{Y}(s) \underline{A}_{012} \end{aligned}$$

The second derivatives of equations (7.1) and (7.2) are

$$\begin{aligned} \frac{d^2}{dx^2} \underline{V}_{012}(x,s) &= \underline{Z}_{012} \underline{Y}_{012} \underline{V}_{012}(x,s) \\ &= \underline{A} \underline{V}_{012}(x,s) \end{aligned}$$

and

$$\begin{aligned}
\frac{d^2}{dx^2} \underline{I}_{012}(x,s) &= \underline{Y}_{012} \underline{Z}_{012}(x,s) \\
&= \underline{A}^t \underline{I}_{012}(x,s)
\end{aligned} \tag{7.4}$$

where

$$\underline{A} = \underline{Z}_{012} \underline{Y}_{012}$$

$$\underline{A}^t = \underline{Y}_{012} \underline{Z}_{012}$$

The same method that was used in Chapter IV is used in this chapter to solve equations (7.3) and (7.4). $\underline{I}_{012}(x,s)$ and $\underline{V}_{012}(x,s)$ are written as \underline{I} and \underline{V} to simplify the notation. Equations (7.3) and (7.4) are decoupled by using the modal transformation introduced in Chapter IV. The following relations are obtained:

$$\frac{d^2}{dx^2} \underline{V}^+ = (\underline{S}^{-1} \underline{A} \underline{S}) \underline{V}^+ \tag{7.5}$$

Similarly,

$$\frac{d^2}{dx^2} \underline{I}^+ = (\underline{Q}^{-1} \underline{A}^t \underline{Q}) \underline{I}^+ \tag{7.6}$$

where:

\underline{S} is the eigenvector matrix of \underline{A}

\underline{Q} is the eigenvector matrix of \underline{A}^t

\underline{V}^+ and \underline{I}^+ are the modal voltages and currents in sequence components.

$(\underline{S}^{-1} \underline{A} \underline{S})$ and $(\underline{Q}^{-1} \underline{A}^t \underline{Q})$ are diagonal matrices where the diagonal elements are the eigenvalues of \underline{A} or \underline{A}^t .

Therefore,

$$\underline{\hat{S}}^{-1} \underline{\hat{A}} \underline{\hat{S}} = \underline{\hat{Q}}^{-1} \underline{\hat{A}}^t \underline{\hat{Q}} = \underline{\hat{\Gamma}}^2$$

Equations (7.1) and (7.2) can also be decoupled as

$$\frac{d}{dx} \underline{\hat{V}}^+ = -\underline{\hat{S}}^{-1} \underline{Z}_{012} \underline{\hat{Q}} \underline{\hat{I}}^+ = -\underline{\hat{D}}_z \underline{\hat{I}}^+ \quad (7.7)$$

$$\frac{d}{dx} \underline{\hat{I}}^+ = -\underline{\hat{Q}}^{-1} \underline{Y}_{012} \underline{\hat{S}} \underline{\hat{V}}^+ = -\underline{\hat{D}}_y \underline{\hat{V}}^+ \quad (7.8)$$

Solutions of (7.5) and (7.6) are known as

$$\underline{\hat{V}}^+ = \underline{\hat{A}}_1 \exp(-\underline{\hat{\Gamma}} x) + \underline{\hat{B}}_1 \exp(\underline{\hat{\Gamma}} x) \quad (7.9)$$

$$\underline{\hat{I}}^+ = \underline{\hat{C}}_1 \exp(-\underline{\hat{\Gamma}} x) + \underline{\hat{D}}_1 \exp(\underline{\hat{\Gamma}} x) \quad (7.10)$$

$\underline{\hat{A}}_1$, $\underline{\hat{B}}_1$, $\underline{\hat{C}}_1$, and $\underline{\hat{D}}_1$ are obtained from the boundary conditions as specified in Chapter IV.

$$\underline{\hat{A}}_1 = \frac{1}{2} [\underline{\hat{\Gamma}}^{-1} \underline{\hat{D}}_z \underline{\hat{I}}_{r1}^+ + \underline{\hat{V}}_r^+]$$

$$\underline{\hat{B}}_1 = \frac{1}{2} [\underline{\hat{V}}_r^+ - \underline{\hat{\Gamma}}^{-1} \underline{\hat{D}}_z \underline{\hat{I}}_{r1}^+]$$

$$\underline{\hat{C}}_1 = \frac{1}{2} [\underline{\hat{\Gamma}}^{-1} \underline{\hat{D}}_y \underline{\hat{V}}_r^+ + \underline{\hat{I}}_{r1}^+]$$

$$\underline{\hat{D}}_1 = \frac{1}{2} [\underline{\hat{I}}_{r1}^+ - \underline{\hat{\Gamma}}^{-1} \underline{\hat{D}}_y \underline{\hat{V}}_r^+]$$

Substituting $\underline{\hat{A}}_1$, $\underline{\hat{B}}_1$, $\underline{\hat{C}}_1$, and $\underline{\hat{D}}_1$ into equations (7.9) and (7.10) produces the sending end equations

$$\underline{\hat{V}}_{s1}^+ = \underline{\hat{D}}_{c1} \underline{\hat{V}}_r^+ + \underline{\hat{D}}_{s1} \underline{\hat{Z}}_o^+ \underline{\hat{I}}_{r1}^+ \quad (7.11)$$

$$\hat{\Gamma}_{s1}^+ = \hat{D}_{c1} \hat{\Gamma}_{r1} + (\hat{Z}_o^+)^{-1} \hat{D}_{s1} \hat{V}_r^+ \quad (7.12)$$

where

$$\hat{D}_{c1} = \cosh (\hat{\gamma}_{i,i} x_1)$$

$$\hat{D}_{s1} = \sinh (\hat{\gamma}_{i,i} x_1)$$

$$\hat{Z}_o^+ = \hat{\Gamma}^{-1} \hat{D}_z$$

Note that $\hat{\Gamma}$, \hat{Z}_o^+ , \hat{D}_{c1} , and \hat{D}_{s1} are diagonal matrices.

The primes in the above equation are used to indicate that all the parameters and variables are in sequence components (0-1-2). Equations (7.11) and (7.12) are obtained in the shifted s-domain (s') by the following procedure:

- No shift in zero sequence components
- The positive sequence component is shifted by $j\omega_o$
- The negative sequence component is shifted by $-j\omega_o$

So, equations (7.11) and (7.12) become

$$\hat{V}_{s1}^+(s') = \hat{D}_{cs1} \hat{V}_r^+(s') + \hat{D}_{ss1} \hat{Z}_{os}^+ \hat{\Gamma}_{r1}^+(s') \quad (7.13)$$

$$\hat{\Gamma}_{s1}^+(s') = \hat{D}_{cs1} \hat{\Gamma}_{r1}^+(s') + (\hat{Z}_{os}^+)^{-1} \hat{D}_{ss1} \hat{V}_r^+(s') \quad (7.14)$$

The modal variables are transformed back to the phase variables as in Chapter IV. Equations (7.13) and (7.14) become

$$\begin{aligned} \hat{V}_{s1}(s') &= (\hat{S} \hat{D}_{cs1} \hat{S}^{-1}) \hat{V}_r(s') \\ &+ (\hat{Z}_{os} \hat{Q} \hat{D}_{ss1} \hat{Q}^{-1}) \hat{\Gamma}_{r1}(s') \end{aligned} \quad (7.15)$$

$$\begin{aligned} \hat{I}_{s1}(s') &= (\hat{Q} \hat{D}_{cs1} \hat{Q}^{-1}) \hat{I}_{r1}(s') \\ &+ (\hat{Q} \hat{D}_{ss1} \hat{Q}^{-1} \hat{Z}_{os}^{-1}) \hat{V}_{-r}(s) \end{aligned} \quad (7.16)$$

The sending end voltage from the generator side was obtained in Chapter VI, thus equations (6.35), (7.15), and (7.16) can be combined.

The result is

$$\begin{aligned} (\hat{S} \hat{D}_{cs1} \hat{S}^{-1}) \hat{V}_{-r}(s') &+ (\hat{Z}_{os} \hat{Q} \hat{D}_{ss1} \hat{Q}^{-1}) \hat{I}_{r1}(s') = \\ Z_{gt} [(\hat{Q} \hat{D}_{cs1} \hat{Q}^{-1}) \hat{I}_{r1}(s') &+ (\hat{Q} \hat{D}_{ss1} \hat{Q}^{-1} \hat{Z}_{os}^{-1}) \hat{V}_{-r}(s')] \end{aligned}$$

Then,

$$\hat{T}_{-1} \hat{V}_{-r}(s') = -\hat{T}_{-2} \hat{I}_{r1}(s')$$

or

$$\hat{I}_{r1}(s') = -\hat{T}_{-2}^{-1} \hat{T}_{-1} \hat{V}_{-r}(s') \quad (7.17)$$

where:

$$\hat{T}_{-1} = \hat{S} \hat{D}_{cs1} \hat{S}^{-1} - Z_{gt} \hat{Q} \hat{D}_{ss1} \hat{Q}^{-1} \hat{Z}_{os}^{-1}$$

and

$$\hat{T}_{-2} = \hat{Z}_{os} \hat{Q} \hat{D}_{ss1} \hat{Q}^{-1} - \hat{Z}_{gt} \hat{Q} \hat{D}_{cs1} \hat{Q}^{-1}$$

The receiving-end equations in the s-domain are

$$\begin{aligned} \hat{V}_{s2}(s') &= (\hat{S} \hat{D}_{cs2} \hat{S}^{-1}) \hat{V}_{-r}(s') \\ &+ (\hat{Z}_{os} \hat{Q} \hat{D}_{ss2} \hat{Q}^{-1}) \hat{I}_{r2}(s') \end{aligned} \quad (7.18)$$

$$\begin{aligned}\hat{I}_{s2}(s') &= (\hat{Q} \hat{D}_{cs2} \hat{Q}^{-1}) \hat{I}_{r2}(s') \\ &+ (\hat{Q} \hat{D}_{ss2} \hat{Q}^{-1} \hat{Z}_{os}^{-1}) \hat{V}_r(s')\end{aligned}\quad (7.19)$$

The receiving-end voltage equation from the load side in the s' -domain is

$$\hat{V}_{s2}(s') = -\hat{Z}_{\ell s} \hat{I}_{s2}(s') \quad (7.20)$$

where $\hat{Z}_{\ell s} = R_{\ell} + s' L_{\ell}$ and it is a (3×3) diagonal matrix. Similarly, equations (7.18), (7.19), and (7.20) can be combined and they become:

$$\begin{aligned}\hat{V}_{s2}(s') &= (\hat{S} \hat{D}_{cs2} \hat{S}^{-1}) \hat{V}_r(s') + (\hat{Z}_{os} \hat{Q} \hat{D}_{ss2} \hat{Q}^{-1}) \hat{I}_{r2}(s') \\ &= -\hat{Z}_{\ell s} [(\hat{Q} \hat{D}_{cs2} \hat{Q}^{-1}) \hat{I}_{r2}(s') + (\hat{Q} \hat{D}_{ss2} \hat{Q}^{-1} \hat{Z}_{os}^{-1}) \hat{V}_r(s')]\end{aligned}\quad (7.21)$$

Equation (7.21) is rewritten in a compact form as

$$\hat{T}_3 \hat{V}_r(s') = -\hat{T}_4 \hat{I}_{r2}(s')$$

or

$$\hat{I}_{r2}(s') = -\hat{T}_4^{-1} \hat{T}_3 \hat{V}_r(s') \quad (7.22)$$

where

$$\hat{T}_3 = \hat{S} \hat{D}_{cs2} \hat{S}^{-1} + \hat{Z}_{\ell s} \hat{Q} \hat{D}_{ss2} \hat{Q}^{-1} \hat{Z}_{os}^{-1}$$

and

$$\hat{T}_4 = \hat{Z}_{os} \hat{Q} \hat{D}_{ss2} \hat{Q}^{-1} + \hat{Z}_{\ell s} \hat{Q} \hat{D}_{cs2} \hat{Q}^{-1}$$

The voltage equations at the fault location (V_r) are obtained for all types of faults in Chapter V. In order to use these, they must be

transformed into sequence components and s -domain in the same manner as the other equations derived in this chapter. To clarify the above procedure, a three-phase fault is taken as an example. As discussed in Chapter V, the voltage at the fault location in s-domain is given by

$$\underline{V}_r(s) = \underline{Z}_f \underline{I}_f(s) + \underline{V}_f(s)$$

Applying the transformations

$$\hat{\underline{V}}_r(s) = \underline{A}_{012}^{-1} \underline{V}_r(s)$$

$$\hat{\underline{I}}_{r1}(s) = \underline{A}_{012}^{-1} \underline{I}_{r1}(s)$$

$$\hat{\underline{I}}_{r2}(s) = \underline{A}_{012}^{-1} \underline{I}_{r2}(s)$$

$$\hat{\underline{Z}}_f = \underline{A}_{012}^{-1} \underline{Z}_f \underline{A}_{012}$$

to the preceding equation produces

$$\hat{\underline{V}}_r(s) = \hat{\underline{Z}}_f \hat{\underline{I}}_f(s) + \hat{\underline{V}}_f(s) \quad (7.23)$$

In equation (7.23), the positive sequence is shifted by $j\omega_0$ and the negative sequence is shifted by $-j\omega_0$. Then equation (7.23) can be written as

$$\hat{\underline{V}}_r(s') = \hat{\underline{Z}}_{fs} \hat{\underline{I}}_f(s') + \hat{\underline{V}}_f(s')$$

and

$$\hat{\underline{I}}_f(s') = \hat{\underline{I}}_{r1}(s') + \hat{\underline{I}}_{r2}(s')$$

If the prefault voltage is assumed as a cosine function, then prefault voltage at the fault location is

$$\underline{v}_f = \underline{v}_M \cos(\omega_o t + \phi + \alpha_i) \quad , \quad i=0,120,240 \quad (7.24)$$

Equation (7.24) is transformed in the (0-1-2) components, and the result is written in a matrix form as

$$\begin{bmatrix} v_{f0} \\ v_{f1} \\ v_{f2} \end{bmatrix} = \frac{1}{3} v_M \begin{bmatrix} 1 & 1 & 1 \\ 1 & a & a^2 \\ 1 & a^2 & a \end{bmatrix} \begin{bmatrix} \cos(\omega_o t + \phi + 0) \\ \cos(\omega t) + \phi - 120) \\ \cos(\omega t + \phi + 120) \end{bmatrix} \quad (7.25)$$

But,

$$\begin{aligned} \cos(\omega_o t + \phi + \alpha_i) &= \frac{1}{2} [\exp(j\omega_o t) \exp j(\phi + \alpha_i) \\ &\quad + \exp(-j\omega_o t) \exp -j(\phi + \alpha_i)] \end{aligned} \quad (7.26)$$

Equations (7.25) and (7.26) are combined and the result is

$$v_{f0} = 0 \quad (7.27)$$

$$\begin{aligned} v_{f1} &= \frac{v_M}{6} [(e^{j\omega_o t} e^{j\phi} + e^{-j\omega_o t} e^{-j\phi}) \\ &\quad + e^{j120} (e^{j\omega_o t} e^{j\phi} e^{-j120} + e^{-j\omega_o t} e^{-j\phi} e^{j120}) \\ &\quad + e^{j240} (e^{j\omega_o t} e^{j\phi} e^{j120} + e^{-j\omega_o t} e^{-j\phi} e^{-j120})] \\ &= \frac{v_M}{2} [e^{j\omega_o t} e^{j\phi}] \end{aligned} \quad (7.28)$$

Similarly,

$$v_{f2} = \frac{v_M}{2} [e^{-j\omega_o t} e^{-j\phi}] \quad (7.29)$$

Equations (7.27), (7.28), and (7.29) are written in a matrix form as

$$\begin{bmatrix} v_{f0} \\ v_{f1} \\ v_{f2} \end{bmatrix} = \frac{v_M}{2} \begin{bmatrix} 0 & & \\ e^{-j\omega_o t} & e^{j\phi} & \\ & e^{-j\omega_o t} & e^{j\phi} \end{bmatrix} \quad (7.30)$$

By taking Laplace transform of equation (7.30), then the result is

$$\underline{\hat{v}}_f(s) = \begin{bmatrix} V_{f0}(s) \\ V_{f1}(s) \\ V_{f2}(s) \end{bmatrix} = \frac{v_M}{2} \begin{bmatrix} 0 & & \\ 1/(s - j\omega_o) & e^{j\phi} & \\ 1/(s + j\omega_o) & e^{-j\phi} & \end{bmatrix} \quad (7.31)$$

In order to find equation (7.31) in the s' -domain, the positive sequence is shifted by $j\omega_o$ and the negative sequence is shifted by $-j\omega_o$. Thus equation (7.31) in the shifted s -domain (s') is

$$\underline{\hat{v}}_f(s') = \frac{v_M}{2s'} \begin{bmatrix} 0 \\ e^{j\phi} \\ e^{-j\phi} \end{bmatrix} \quad (7.32)$$

Once $\underline{\hat{v}}_f(s')$ is obtained, then the voltage at the fault location can be obtained from equation (7.23) as follows

$$\underline{\hat{v}}_r(s') = \underline{\hat{z}}_{fs} [\underline{\hat{I}}_{r1}(s') + \underline{\hat{I}}_{r2}(s')] + \underline{\hat{v}}_f(s') \quad (7.33)$$

Equations (7.17) and (7.22) can be used to eliminate $\underline{\hat{I}}_{r1}(s')$ and $\underline{\hat{I}}_{r2}(s')$ to produce

$$\underline{\hat{V}}_r(s') = \underline{\hat{Z}}_{fs} [-\underline{\hat{T}}_2^{-1} \underline{\hat{T}}_1 - \underline{\hat{T}}_4^{-1} \underline{\hat{T}}_3] \underline{\hat{V}}_r(s') + \underline{\hat{V}}_f(s')$$

$$\begin{aligned} \underline{\hat{V}}_f(s') &= [\underline{U} + \underline{\hat{Z}}_{fs} (\underline{\hat{T}}_2^{-1} \underline{\hat{T}}_1 + \underline{\hat{T}}_4^{-1} \underline{\hat{T}}_3)] \underline{\hat{V}}_r(s') \\ &= [\underline{U} + \underline{\hat{Z}}_{fs} \underline{\hat{T}}] \underline{\hat{V}}_r(s') \end{aligned}$$

or

$$\underline{\hat{V}}_r(s') = [\underline{U} + \underline{\hat{Z}}_{fs} \underline{\hat{T}}]^{-1} \underline{\hat{V}}_f(s') \quad (7.34)$$

where

$$\underline{\hat{T}} = \underline{\hat{T}}_2^{-1} \underline{\hat{T}}_1 + \underline{\hat{T}}_4^{-1} \underline{\hat{T}}_3$$

after $\underline{\hat{V}}_r(s')$ is obtained, then $\underline{\hat{I}}_{r1}(s')$ and $\underline{\hat{I}}_{r2}(s')$ are obtained from equations (7.17) and (7.22). Consequently, the sending-end voltages and currents can be obtained from equations (7.15) and (7.16) in the s' -domain. The above equations give the transient solution of the voltages and currents in the (0-1-2) components.

The total solution for voltages and currents can be obtained by the following steps:

- The shifting in the frequency domain must be changed back. The positive sequence component is shifted by $-j\omega_0$ and the negative sequence component is shifted by $j\omega_0$ for both voltage and current components.
- The voltages and currents at the fault location and at the sending-end are transformed from (0-1-2) components to (a-b-c) components by using the transformation matrix A_{012} .
- The above voltages and currents are transformed into time domain by using the fast-Fourier transform (FFT).

Therefore, the total solution for voltages and currents can be obtained by adding the steady-state solution to the transient solution at the point of interest.

B. Fault Transient Waveforms for Three-Phase Fault

The method of finding time variation of voltages or currents of interest is described in Chapter VIII. The example in Appendix A is used to test the proposed solution. The computer program in Appendix B is modified that can handle the system equations with the full machine model. The waveforms of the three-phase sending-end voltages and currents are obtained for three-phase fault at the middle of the line. These waveforms are shown in Figures (7.1a) and (7.1b).

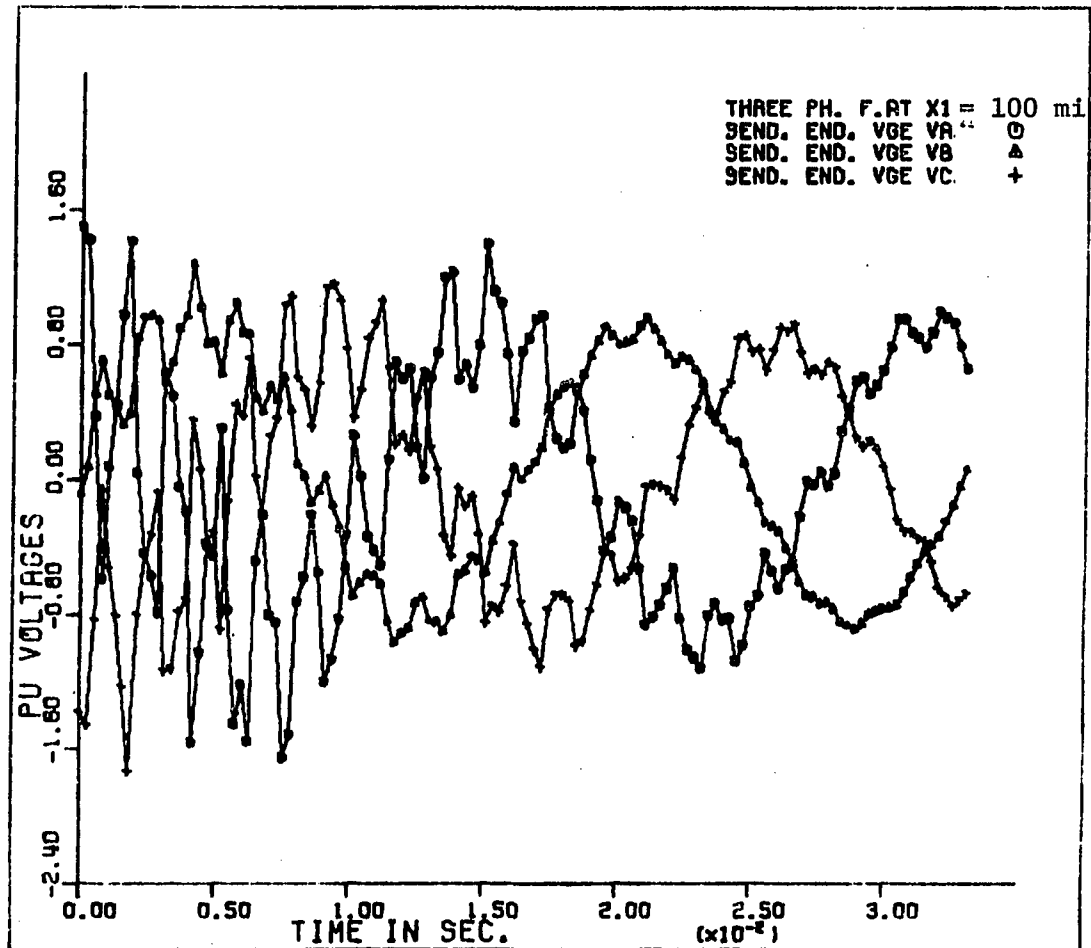


Figure 7.1a. Sending-end voltage for three-phase fault

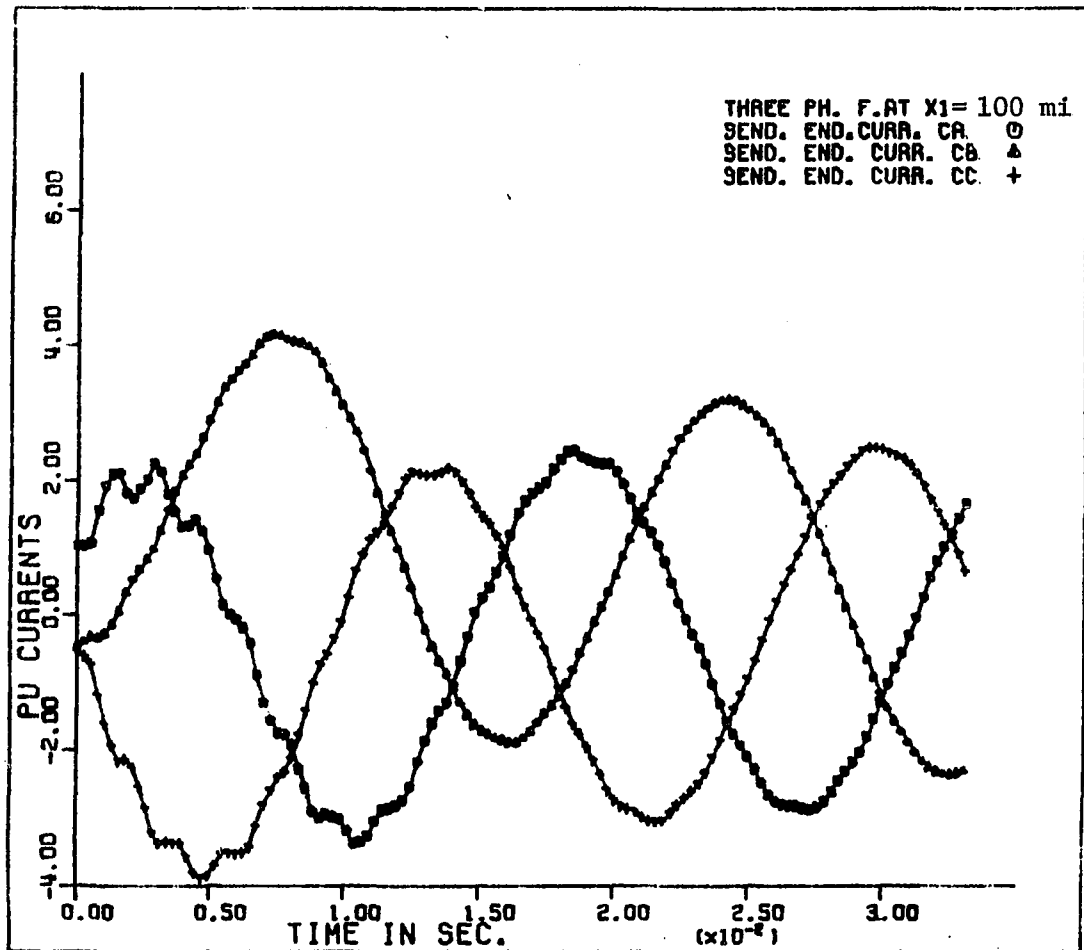


Figure 7.1b. Sending-end current for three-phase fault

VIII. METHOD OF COMPUTATION

Appendix B consists of the FORTRAN program used to obtain numerical solutions of the faulted power system equations. In this program, well-established library subroutines have been utilized. These subroutines, called LEQT1C and EIGCC, are said to be "zero-error" programs. The first inverts any $n \times n$ complex matrix and the latter computes the eigenvalues and the real eigenvectors matrix of a complex $n \times n$ matrix. Such subroutines have an error indication (IER) which will terminate the program if a singularity is indicated in the LEQT1C subroutine or if the EIGCC subroutine fails to find the eigenvectors of the matrix. A well-known fast Fourier transform subroutine (FFT) is also used which is based on decimation in time techniques [30].

Transform method of solution:

Time domain solutions are obtained from frequency domain equations by the inverse Laplace transform integral

$$f(t) = \frac{1}{2\pi j} \int_{a-j\infty}^{a+j\infty} F(s) \exp(st) ds \quad (8.1)$$

Since the system is stable, all poles are located in the left half plane in the complex frequency domain. Also, since the solution includes a 60 Hz component, there will be at least one complex conjugate pair along the imaginary axis. Therefore, the path of integration has to be displaced from the imaginary axis by a so-called convergence factor (a). The inverse Laplace transform [31] has precisely the desired effect of shifting the line of integration. This may be seen by making the

substitution

$$s = a + j\omega \quad (8.2)$$

in the inverse Laplace transform of equation (8.1) which then becomes

$$f(t) = \frac{1}{2\pi} \int_{-\infty}^{\infty} F(a + j\omega) \exp(at) \exp(j\omega t) d\omega \quad (8.3)$$

where $t \geq 0$

and $f(t) = 0$ for $t < 0$.

The integral in equation (8.3) cannot be evaluated analytically and it is necessary to evaluate it by numerical methods. In order to carry out the numerical integration, it is necessary to truncate the finite range of the integral to some finite value, say $(-\Omega, \Omega)$. This introduces a truncation error which, being multiplied by $\exp(at)$, increases rapidly with (at) . This sets an upper bound to the choice of (a) . The best value to use is discussed later.

To examine the nature of the truncation error, the value of $f(t)$ with the integration range truncated is given as

$$f(t) = \frac{\exp(at)}{2\pi} \int_{-\Omega}^{\Omega} F(a + j\omega) \exp(j\omega t) d\omega$$

or

$$f(t) = \frac{\exp(at)}{2\pi} \int_{-\infty}^{\infty} F(a + j\omega) \phi(j\omega) \exp(j\omega t) d\omega$$

where

$$\phi(j\omega) = \begin{array}{ll} 1 & , \quad |\omega| \leq \Omega \\ 0 & , \quad |\omega| > \Omega \end{array}$$

The complete Fourier transform of $\phi(j\omega)$ is given in reference [32] as

$$\phi(t) = \frac{1}{2\pi} \int_{-\Omega}^{\Omega} \exp(j\omega t) d\omega = \frac{\sin(\Omega t)}{\pi t} \quad (8.4)$$

One interpretation of this truncation is that the function $f(t)$ is scanned by the passage of the Dirichlet Kernel $\sin(\Omega\tau/\pi\tau)$ over it [33]. The periodic nature of this function gives rise to Gibb's oscillations [34].

Since the period of oscillations of $\phi(t)$ is $2\pi/\Omega$, as shown in Figure 8.1, a better representation of $f(t)$, say $f_{\sigma}(t)$, is achieved by averaging over this period in the following way.

$$f_{\sigma}(t) = \left[\frac{\Omega}{2\pi} \int_{t-\pi/\Omega}^{t+\pi/\Omega} f(\tau) d\tau \right] \quad (8.5)$$

$$= \exp(at) \frac{\Omega}{(2\pi)^2} \int_{-\Omega}^{\Omega} F(a+j\omega) d\omega \int_{t-\pi/\Omega}^{t+\pi/\Omega} \exp(j\omega\tau) d\tau \quad (8.6)$$

Evaluation of the inner integral (as in reference [34]) gives

$$f_{\sigma}(t) = \frac{\exp(at)}{2\pi} \int_{-\Omega}^{\Omega} F(a+j\omega) \sigma(\omega) \exp(j\omega t) d\omega \quad (8.7)$$

where

$$\sigma(\omega) = \frac{\sin(\pi\omega/\Omega)}{(\pi\omega/\Omega)} \quad (8.8)$$

The function $\sigma(\omega)$ is called the sigma factor [32-34]. Since the function $f_{\sigma}(t)$ is a real function, it implies that:

$$F(a+j\omega) = F^*(a-j\omega) \quad (8.9)$$

Therefore

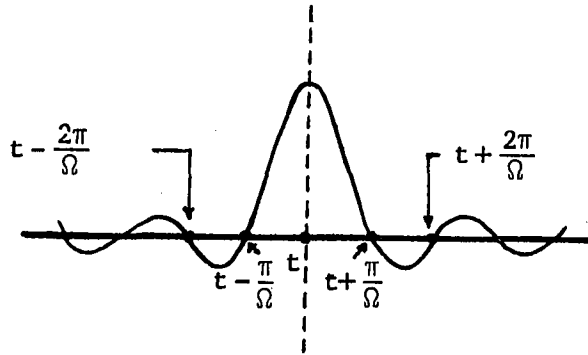


Figure 8.1. The Dirichlet Kernel $\frac{\sin(\Omega t)}{\Omega t}$

$$f_{\sigma}(t) = \frac{\exp(at)}{\pi} \operatorname{Real} \left\{ \int_0^{\Omega} F(a + j\omega) \sigma(\omega) \exp(j\omega t) d\omega \right\} \quad (8.10)$$

The sigma factor:

The sigma factor, as explained above, is a mathematical device which is often used in conjunction with the numerical inversion of the Laplace (or Fourier) transform. Its purpose is to suppress the Gibb's oscillations, which sometimes appear in the computed time function.

To illustrate the problem involved, consider the Laplace transform of a unit step function. The Fourier integral for the step function $-\pi/2$ for $t < 0$, $\pi/2$ for $t > 0$, may be represented by the integral

$$\int_0^{\infty} \frac{\sin(\omega t)}{\omega} d\omega \quad [32]$$

On truncating the range of integration (say Ω) the sine integral is obtained, i.e.,

$$\int_0^{\Omega} \frac{\sin \omega t}{\omega} d\omega = Si(\Omega t) \quad (8.11)$$

where $\Omega = N \cdot \Delta\omega$ and $\Delta\omega$ is chosen as 7.5π

$$N = 2^M$$

This function is shown in Figure 8.2. with and without the sigma factor. In curve 2, the Gibb's oscillations are apparent and sustained. On introducing the sigma factor and carrying out the integration process numerically, curve 1 in Figure 8.2 was obtained. Clearly the Gibb's oscillations are virtually eliminated by the use of the sigma factor.

Numerical integration:

The numerical evaluation of the integral of equation (8.10) is based on discrete samples of $F(a+j\omega)$ taken at points lying along the path of integration. Let these samples be taken at $j \frac{\Delta\omega}{2}$, $j \frac{3\Delta\omega}{2}$, etc. as indicated in Figure 8.3. Application of the midpoint rule of numerical integration then gives the following expression for the value of $f_{\sigma}(t)$ at a selected time instant t_k

$$f_{\sigma}(t_k) = \frac{\exp(at)}{\pi} \text{Real} \sum_{i=1}^N \left\{ F(a + j \frac{2i-1}{2} \Delta\omega) \sigma \left(\frac{2i-1}{2} \Delta\omega \right) \times \exp \left[(j \frac{2i-1}{2} \Delta\omega) \Delta t \cdot k \right] \right\} \Delta\omega \quad (8.12)$$

where

$$\Omega = N \Delta\omega$$

$$\sigma \left[\left(\frac{2i-1}{2} \right) \Delta\omega \right] = \frac{\sin \left(\left(\frac{2i-1}{2} \right) \pi/N \right)}{\left(\frac{2i-1}{2} \right) \pi/N}$$

Proceeding with equation (8.12)

$$f_{\sigma}(t_k) = \frac{\exp(at)}{\pi} \text{Real} \left\{ \left(\sum_{i=1}^N F_i(\omega) e^{j(i\Delta\omega \cdot \Delta t \cdot k)} \right) e^{-j \frac{\Delta\omega}{2} \cdot \Delta t \cdot k} \right\} \quad (8.13)$$

$$\Delta\omega = 7.5\pi$$

$$M = 9, \quad N = \frac{9}{2} = 512$$

$$\Omega = 512 * 7.5\pi$$

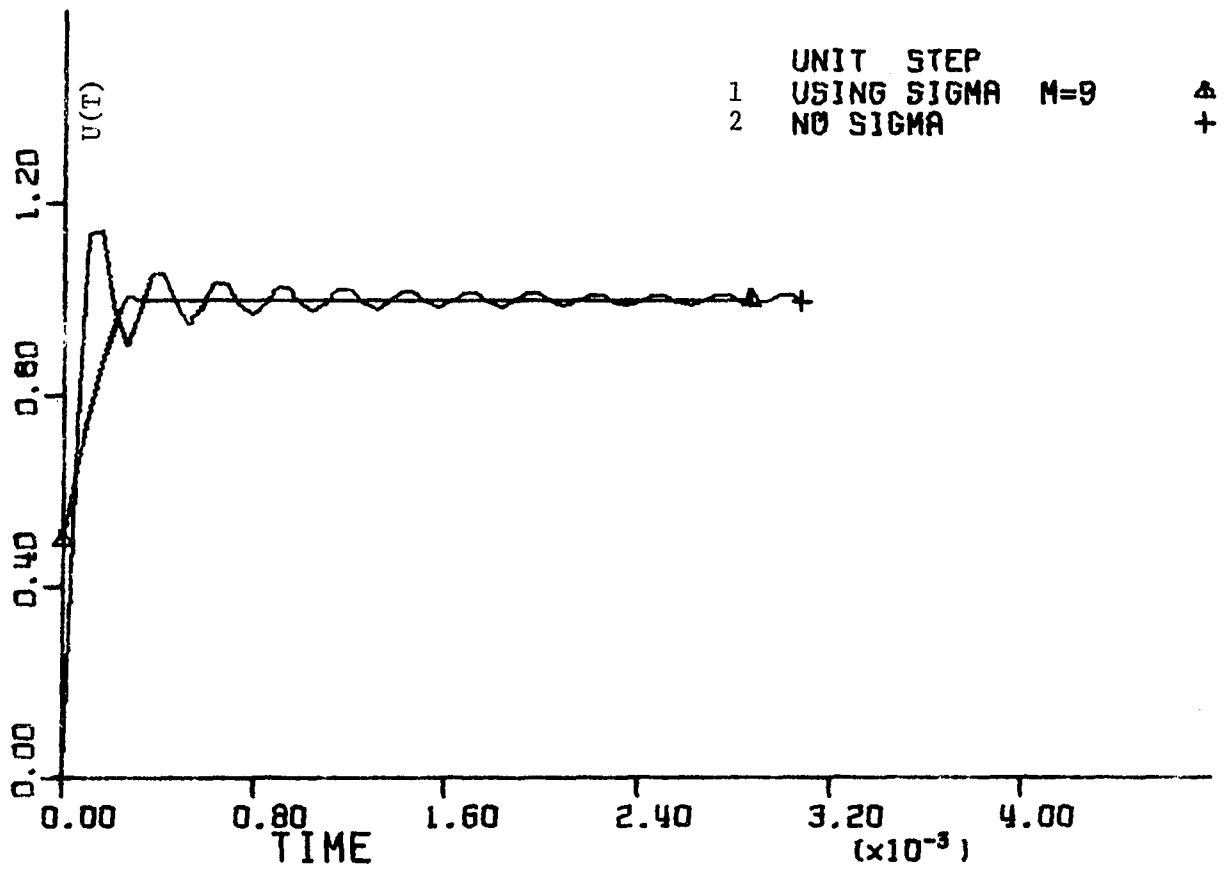


Figure 8.2. Effect of sigma factor

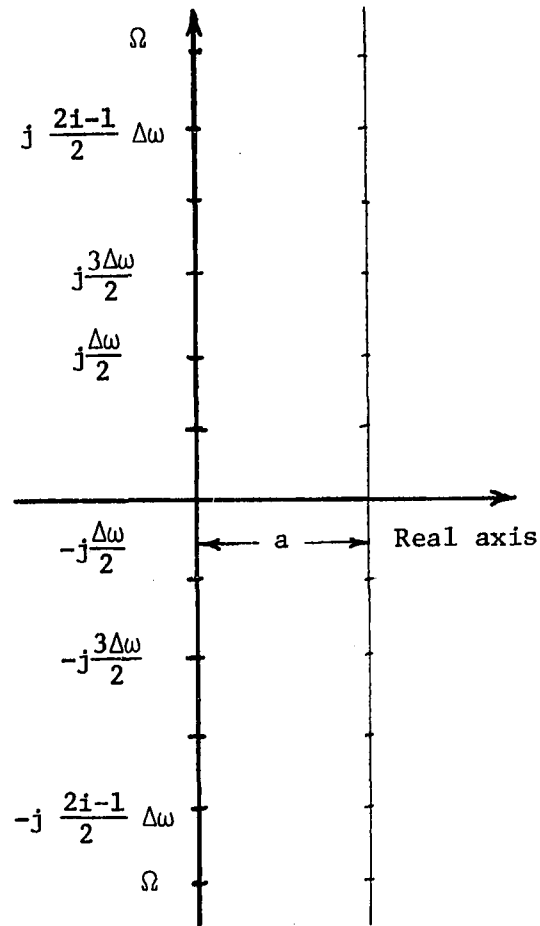


Figure 8.3. Frequency domain

and

$$F_i(\omega) = F\left(a + j \frac{2i-1}{2} \Delta\omega\right) \sigma\left(\frac{2i-1}{2} \Delta\omega\right) \Delta\omega$$

Since N discrete samples in the frequency domain result in N discrete values in the time domain,

$$\Delta t = \frac{2\pi}{\Omega} = \frac{2\pi}{\Delta\omega \cdot N}$$

and equation (8.13) becomes

$$f_{\sigma}(t_k) = \frac{e^{at}}{\pi} \text{Real} \left\{ \left[\sum_{i=1}^N F_i(\omega) \exp \left(\frac{j2\pi i k}{N} \right) \right] \exp \left(-j \frac{\Delta\omega}{2} \Delta t k \right) \right\} \quad (8.14)$$

$$= \frac{e^{at}}{\pi} \text{Real} \left\{ F(k) \exp \left(\frac{-\Delta\omega}{2} \Delta t k \right) \right\} \quad (8.15)$$

where $F(k)$ is obtained by FFT algorithm [31].

The special form of equations (8.14) and (8.15) allows the use of FFT algorithm which is well-known to be computationally efficient. This is because the FFT algorithm requires only $N \log_2 N$ units of computation [31] compared with N^2 units in the case of the direct method. Computational requirements are thus reduced by a factor of approximately $N/\log_2 N$, e.g., 102.4 for $N = 1024$. In short, a very substantial reduction is obtained.

Numerical integration parameters:

As indicated in the last section, it is necessary to assign values to the convergence factor (a), the step size ($\Delta\omega$) and the range (Ω). These parameters are not only interrelated in a complex way but their choice depends on the time over which the solution is required.

Choice of Ω :

If Ω is chosen too small, it may limit the rate of rise and some high frequency components may not appear in the solution. This is illustrated in Figure 8.4 by applying the technique to a unit step function with two different values of Ω . It is clear that using a higher value of Ω results in elimination in the rise time. The value used based on the mathematical experimentation is:

$$\Omega = N \cdot \Delta\omega = 24,127.43 \text{ rad/sec. for } M=10, \Delta\omega = 7.5\pi.$$

However, the above value of Ω was increased by a factor of 2, 4, and 8 and it did not give any significant change in the final results. Therefore, the choice of Ω could be the above value multiplied by 2^i , and $i=0,1,2,\dots$ etc., depending on the case under study to include the highest frequency that may be in the solution.

Choice of ($\Delta\omega$)

The step size should not be too large or too small for an accurate solution. The following choices have shown (Figure 8.5) to be accurate

$$\Delta\omega = 7.5 \pi \text{ or } 15 \pi$$

Choice of (a)

The parameter (a) plays an important role in numerical integration. As previously mentioned, truncation in the frequency domain introduces errors. Such errors may increase rapidly if (a) is not precisely chosen. To find the best value, different numerical values were assigned to (a). The value that gave the best results was equal to the step size ($\Delta\omega$). An illustration of such choice is shown in Figure 8.6 for two values of (a).

Finally, the following parameters were tested on sinusoidal and cosinusoidal waveforms (Figures 8.7 and 8.8):

$$\Delta\omega = 7.5 \pi$$

$$a = \Delta\omega$$

$$\Omega = 2^{\frac{10}{10}} \times 7.5 \pi = 24,127.43 \text{ rad/sec.}$$

In summary, as a result of extensive mathematical experimentation, the parameters that have been chosen gave eminently satisfactory results for the severe cases that were tested. The cosinusoidal, sinusoidal, and unit step function have poles on the imaginary axis. However, the solution is accurate and stable. This validates the technique for any other functions that have their poles on the imaginary axis or in the left half plane. As a conclusion, the technique implemented in this work is numerically stable and accurate. Furthermore, the inversion process includes a FFT program which has been proven to be computationally efficient.

$$\begin{aligned}\Omega &= N \cdot \Delta\omega \\ &= 2^M (7.5 \pi)\end{aligned}$$

- 1 M = 6
- 2 M = 9

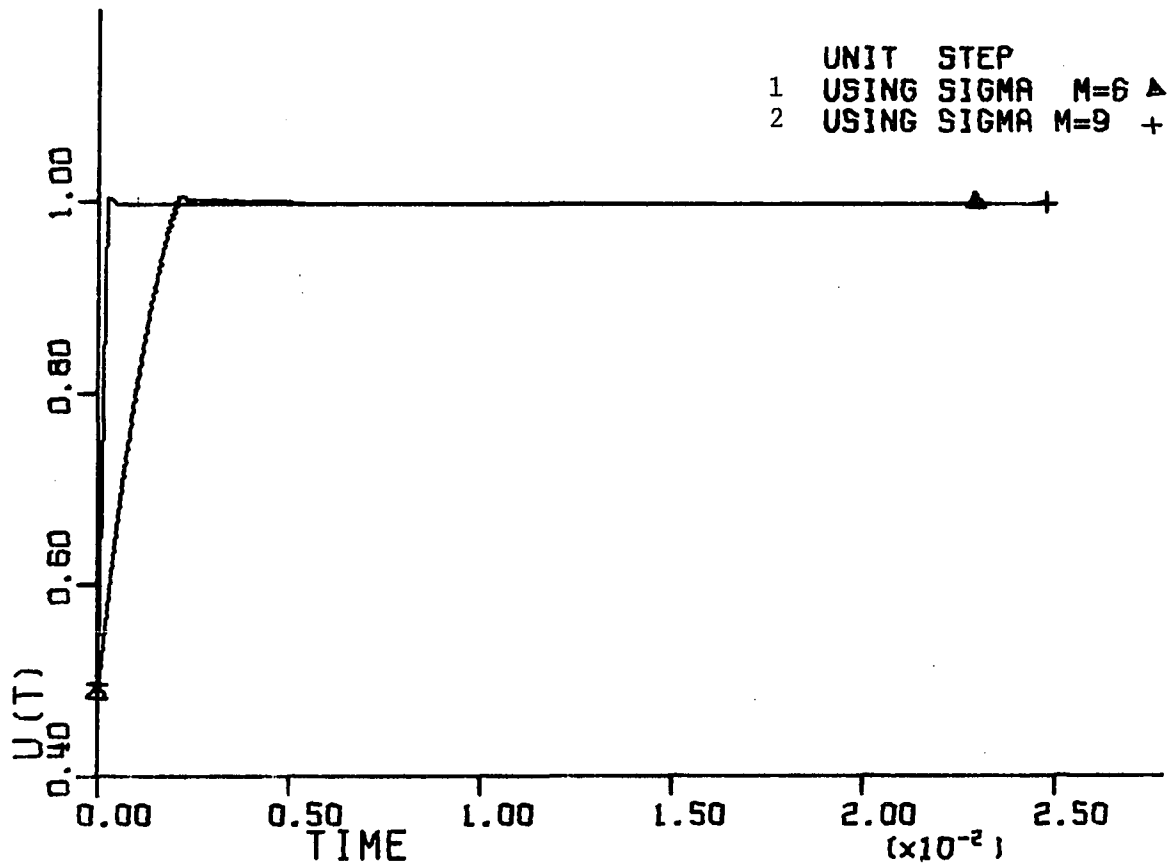


Figure 8.4. Effect of Ω

$$\Omega = N \cdot \Delta\omega = \frac{9}{2} \cdot \Delta\omega$$

$$1 \quad \Delta\omega = \frac{60}{16} \pi = 3.75 \pi$$

$$2 \quad \Delta\omega = \frac{60}{8} \pi = 7.5 \pi$$

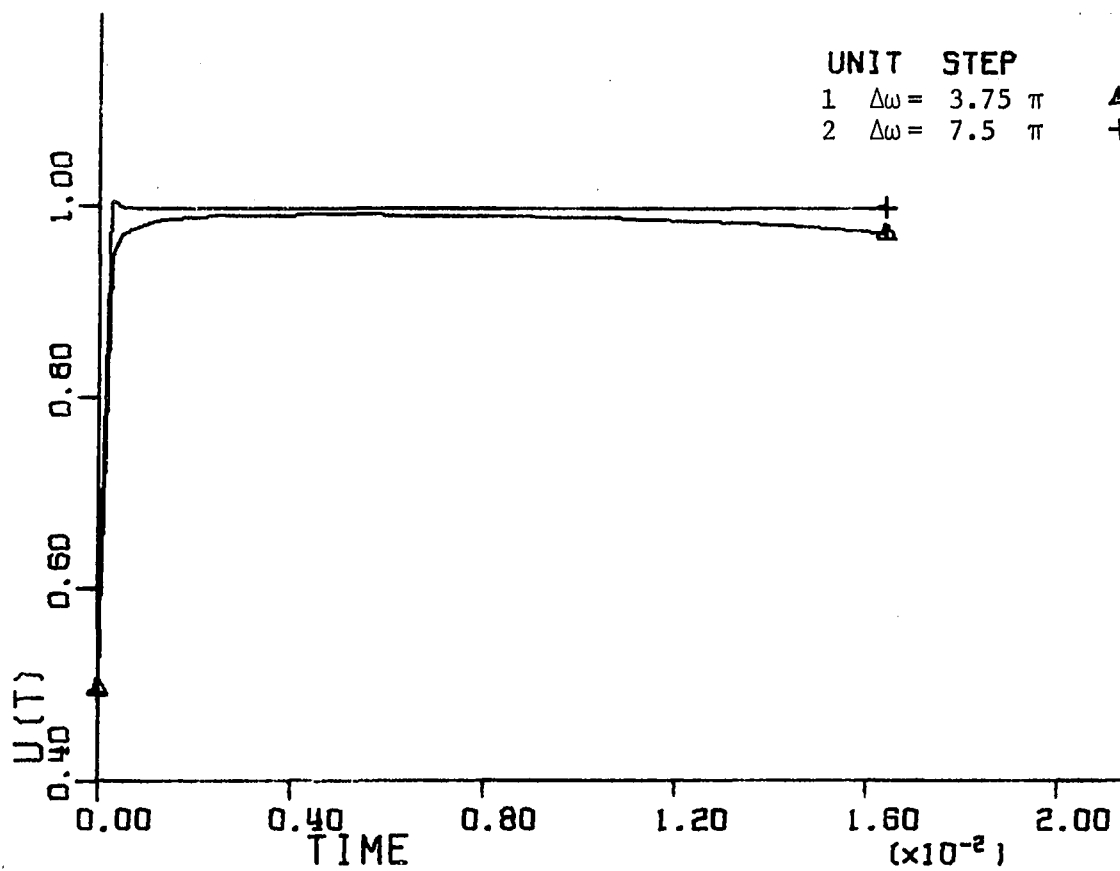


Figure 8.5. Effect of $\Delta\omega$

$$\Omega = N \cdot \Delta\omega, \quad N = 2^{10}, \quad \Delta\omega = 7.5 \pi$$

1 $a = \Delta\omega = 23.562$

2 $a = \frac{1}{2} \Delta\omega = 11.781$

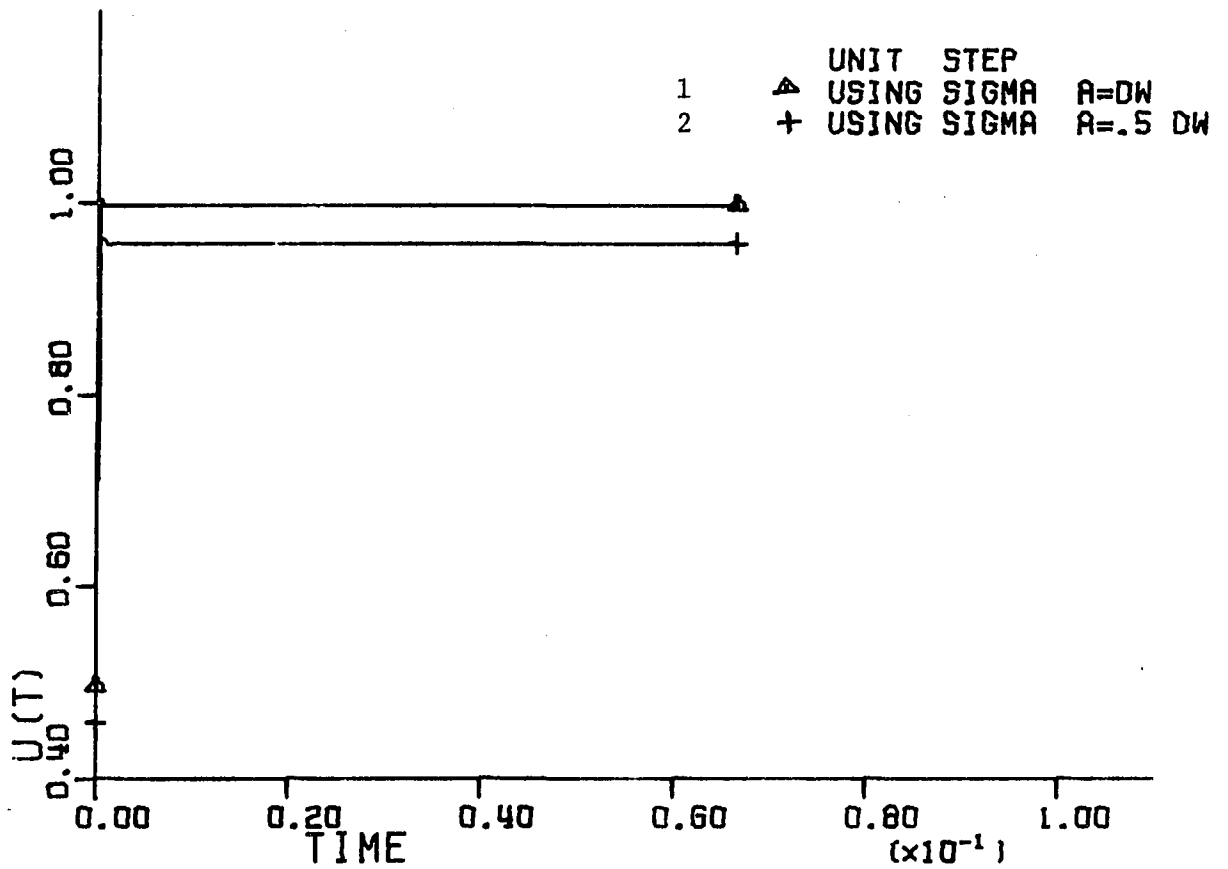


Figure 8.6. Choice of the parameter (a)

$$\Omega = 2^M \cdot \Delta\omega$$

$$\Delta\omega = 7.5 \pi, M = 10, a = \Delta\omega$$

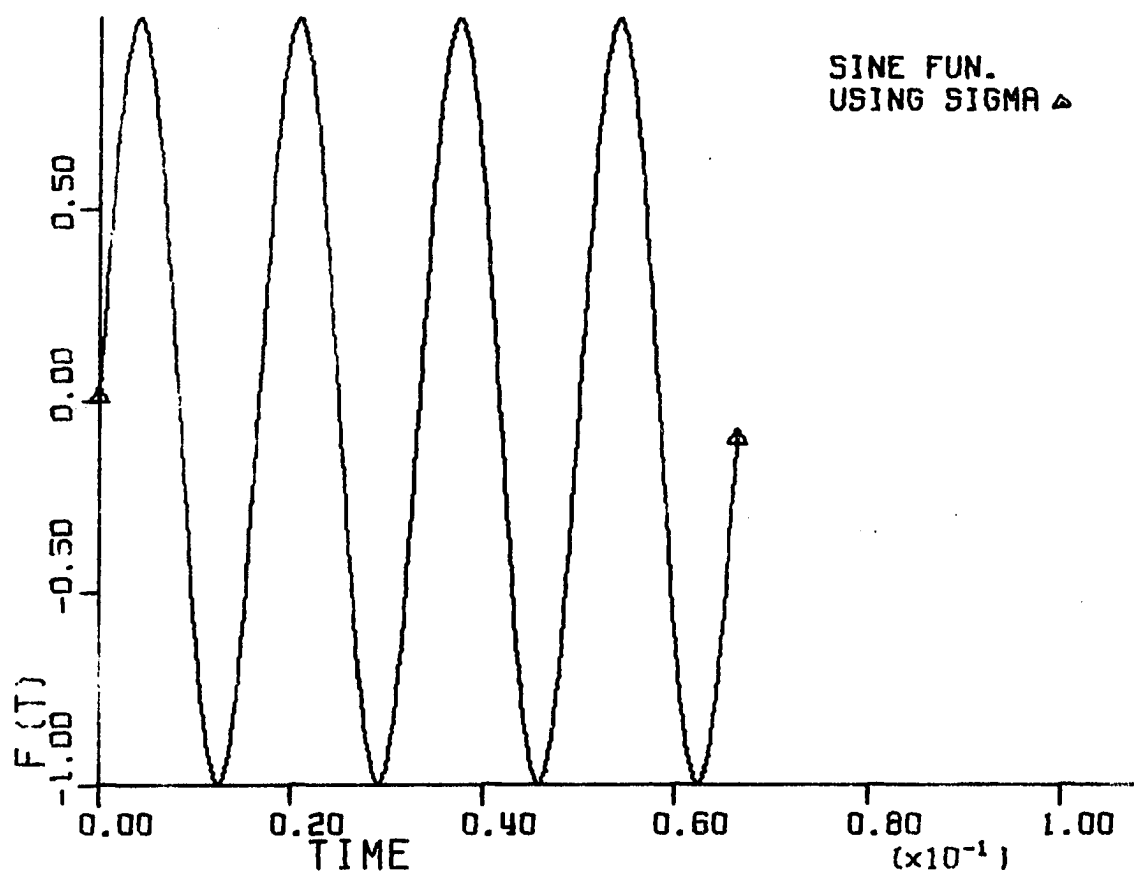


Figure 8.7. Sinusoidal function with sigma factor

$$\Omega = 2^M \cdot \Delta\omega$$

$$\Delta\omega = 7.5 \pi, \quad M = 10, \quad a = \Delta\omega$$

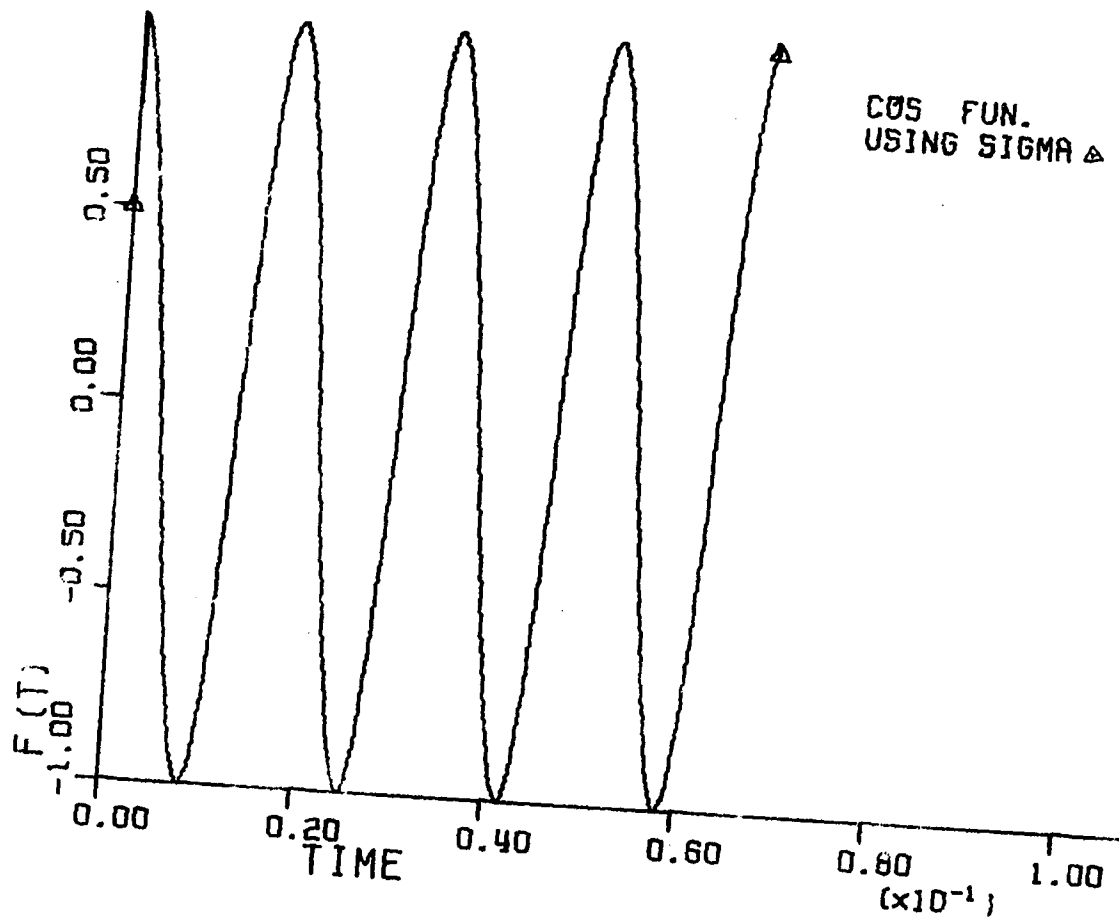


Figure 8.8. Cosine function with sigma factor

IX. COMPARISONS AND CONCLUSIONS

In almost any simulation study, there comes a point where mathematical expediency prevails over physical reality. In the specific case of transmission line transient simulations, previous investigators have found it expedient to ignore asymmetric magnetic coupling between the lines (untransposed lines), and/or frequency variation of line parameters. Expediency is also dictated to some degree by mathematical strategy; when frequency dependent line parameters are included, it is necessary to use frequency domain analysis. In such cases, expediency has made it convenient to represent the generator by a Thevenin equivalent with constant inductance. This thesis has developed a simulation method that transcends these particular limitations. One of the important consequences of this work is that it makes it possible to do comparative studies that show the consequences of including or neglecting a particular factor. Subsequent sections in this chapter compare the consequences of:

- assuming that the lines are ideally transposed
- neglecting the variation of line parameters with frequency
- modeling the generator as a Thevenin equivalent
- neglecting the fault impedance
- neglecting the skin effect
- assuming lossless line.

Effect of transposition:

The magnitudes of the fault-induced voltages depend on the values of the mutual terms of the line surge impedance matrix, and this in turn

depends on the spacings and configuration of the conductors of the line. Equal spacing or equal mutual couplings between the conductors is equivalent to assuming transposition of the three phases of the line. With the line untransposed, the mutual terms of the surge impedance matrix will not, of course, all be equal. As a result, the voltage induced in a particular phase will depend on its position on the tower relative to the phase or phases energized. The effect of transposition on the sending-end voltage waveforms can be shown in Figure 9.1 and 9.2 for a single line and double line to ground faults at the middle of the line. The occurrence of such faults gives an increase in the peak value of voltage (25% - 35%) on the unfaulted phase or phases. This increase in voltage cannot be shown in case of transposed line due to the assumption of equal coupling between phases. The effect of transposition in the faulted phase can also be shown in Figure 9.3. This figure shows the frequency spectra of the transient sending-end voltage for single line to ground fault at the middle of the line. The effect of transposition in the case of three-phase fault at the middle of the line can also be shown in Figure 9.4.

These comparisons show that the unequal mutual coupling (untransposed line) could be very important in certain studies such as the design and insulation coordination of power apparatus and systems to avoid underestimation of overvoltages.

Effect of generator model:

Comparisons are made between the simple machine model and the full machine model for three-phase fault at different locations. The

waveforms of voltage and current show that the difference between these two models is insignificant when the fault was located at the receiving-end of the line (load side). Figures 9.5a and 9.5b show the difference in the sending-end voltage and current waveforms of phase a due to three-phase fault at the middle of the line. The difference in the peak values of the sending-end voltage varies between 10% to 25%. This difference increases to 30% to 40% when the fault was located at the sending-end as shown in Figure 9.6a and 9.6b. The effect of the machine model on the frequency spectra of the transient sending-end voltage for three-phase fault at the middle of the line is also shown in Figure 9.7.

These results indicate that the high frequency component, in case of full machine model, has a higher initial value and a higher rate of decay compared to those obtained using the simple machine model. Moreover, the frequency of the traveling wave is more than 10% lower (Figure 9.7). Such information is needed for setting traveling wave relays and a more than 10% error in this frequency will cause more than 10% overreach in the traveling wave relays operation. Therefore, it is necessary to represent the generator by its full model, particularly when the fault close to the source produces realistic current and voltage waveforms and to assure the reliability of a system for a given application.

Effect of fault impedance:

Most fault transient programs assume solid connection between the fault and the earth. This assumption may introduce an error due to the fact that at the fault location there is a resistance (arc resistance and line resistance) and an inductance (line inductance). Figure 9.8

shows the difference between the sending-end voltage waveforms due to three-phase fault at the middle of the line with zero fault impedance and with a fault impedance ($R_f = 10 \text{ ohm}$, $L_f = .1 \text{ mH}$). It is clear that the traveling wave components become progressively more damped when the fault impedance is included (due to the fault resistance). The fault impedance not only affects the magnitude of voltage but also affects the frequency of the traveling wave as shown in Figure 9.9.

These results indicate that the assumption of zero fault impedance overestimates the magnitude of voltage and underestimates the magnitude of current. At the same time, the frequency of the traveling wave is about 10% lower. Such information is needed for accurate design of insulation, circuit breakers, and relays.

Effect of line resistance:

Many utilities still use the lossless line model for transient studies. Figures 9.10a and 9.10b contrast the case where losses are neglected with the case where they are included for three-phase fault. These comparisons show that in case of lossy line model, the high frequency components are highly attenuated due to the damping effect of the line resistance. Therefore, the difference between the two waveforms (Figure 9.10a) started with 10% to 40% in the first half cycle and then increased to 80% to 95% in the second half cycle. The lossless line model gives incorrect results in the transient solution as shown in Figure 9.11.

Based on these results, the lossless line model greatly overestimates the voltage and it cannot be used in insulation design for

economic reasons. It also might introduce misleading results in voltages and currents with consequent effects on system reliability.

Effect of frequency variation of line parameters:

Most methods that use time-domain solutions are based on the assumption of frequency independent line parameters. Figure 9.12 shows the waveforms of the sending-end voltage of phase a in cases of frequency-dependent and independent line parameters. The variation of these parameters with frequency increases the damping effect on the high frequency components. Therefore, neglecting such variation would underestimate the rate of decay of the high frequency components. Consequently, this assumption leads to higher insulation levels due to the overestimation of the high frequency components of voltage.

Skin effect:

The results showed that the skin effect is insignificant in transient analysis as shown in Figure 9.13. However, the skin effect may be considered for larger line conductors.

Other results and waveforms were obtained for different studies such as: effect of fault location, effect of load, effect of generator size, and effect of type of fault.

Effect of fault location:

Figures 9.14a and 9.14b show the effect of fault location on transient waveforms for three-phase faults at 100 miles and 50 miles from the sending-end bus. The magnitude of voltage decreases and the magnitude of current increases as the distance between the fault location and the

sending-end bus is decreased. Table 1 shows the effect of fault location on the magnitude of sending-end voltage (phase a) at the dominant frequency for three-phase fault at different locations.

Taken together, Figures 9.14 and Table 1 show a trend in the relationships between the distance from the generator to the fault, and the amplitudes of the high frequency components in the voltage and current waveforms. In order to interpret this, it is necessary to recall that the resistance per unit length increases rapidly with frequency (see Figure 3.3) and to note that the nearer the fault, the higher the dominant frequency is. The net result is that even though the distance is halved (100 miles to 50 miles) the dominant frequency component is attenuated by a factor of about 4.

Table 1. Effect of fault location

Fault location measured from the sending-end	Magnitude of sending-end voltage at 60 Hz	Dominant frequency	Magnitude of sending-end voltage at dominant frequency
150 miles	1.23 pu	450 Hz	.2117 pu
100 miles	1.07 pu	630 Hz	.1909 pu
50 miles	.7887 pu	1080 Hz	.0471 pu
25 miles	.5547 pu	1605 Hz	.02648 pu

Effect of load:

Figures 9.15a and 9.15b contrast the case where the system was under heavy load and the case where the system was under light load for

three-phase fault. These figures show that the pattern of voltage and current waveforms were not significantly affected by load condition, but the magnitudes were different.

Effect of generator size:

As a larger generator has a smaller inductance, using the simple machine model concept, the reflection coefficient of the incident wave will be higher. Consequently, when a 615 MVA generator was used, the high frequency components of the current waveform were higher than the corresponding waveform for a 160 MVA generator. The traveling wave components of current propagated into the source do not cause significant voltage drop if the source impedance is small (for large generator size). These results are depicted in Figure 9.16a and 9.16b.

The same argument applies when a full generator model was used, but the difference between the waveforms was greater. In general, the larger generator has smaller values of the inductance matrix. This in turn affects the magnitudes of dominant frequency as well as the rate of decay. The results obtained by using the full machine model are shown in Figures 9.17a and 9.17b.

Effect of type of fault:

The results show that the high frequency components of voltage and current vary according to the type of fault. Some of these results are shown in Table 2. The waveforms shown in Figure 9.18 were used to compare line to line fault with double line to ground fault on phases b and c at the middle of the line. The waveform due to double line to ground

fault has higher high frequency components than the waveform due to line to line fault. In general, any fault to ground involves two modes: the earth mode and the faulted phase mode.

Table 2. Comparison between 3LG fault and sLG fault at the middle of the line

Type of fault	Dominant frequency	S.E. voltage of phase a at this frequency
Three-phase fault (3LG)	630 Hz	.1909 pu
Single line to ground fault on phase a (sLG)	645 Hz	.08173 pu

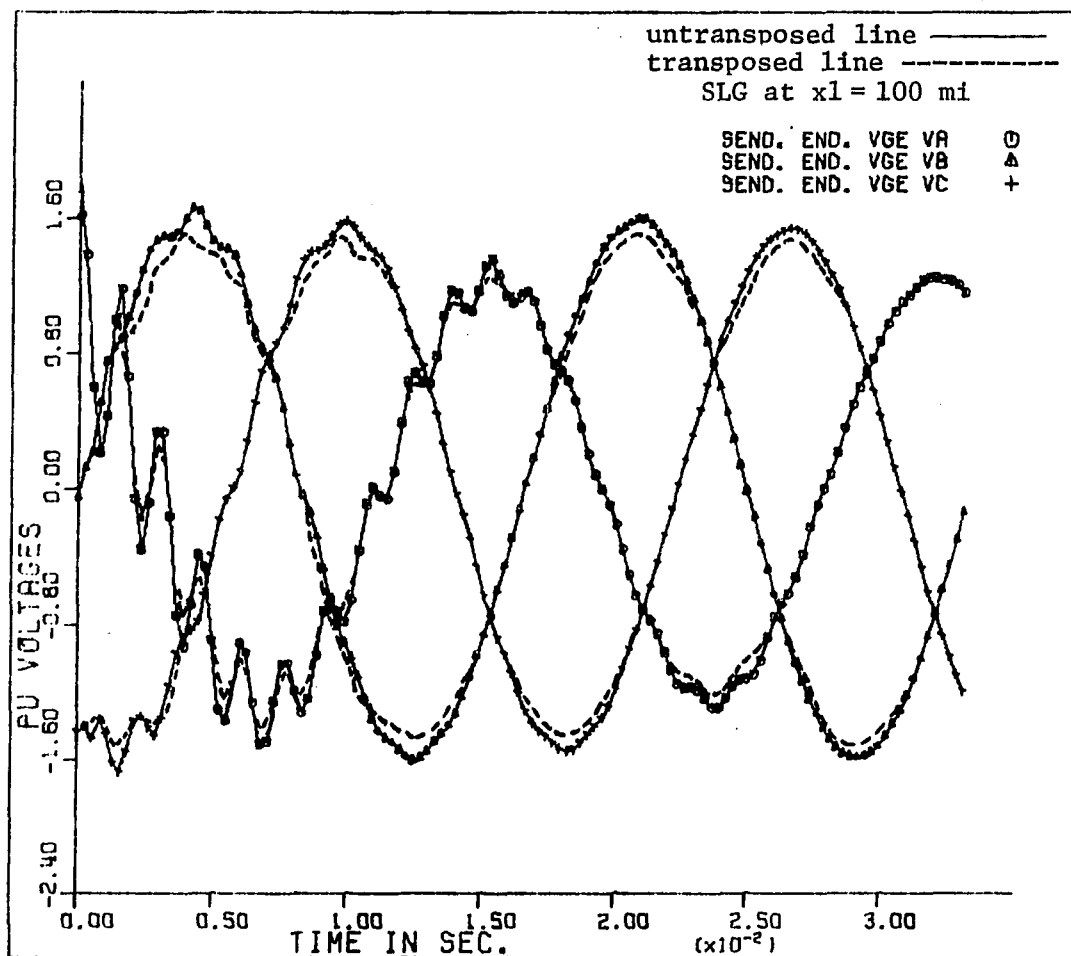


Figure 9.1. Effect of transposition on S.E. voltage for SLG fault (a)

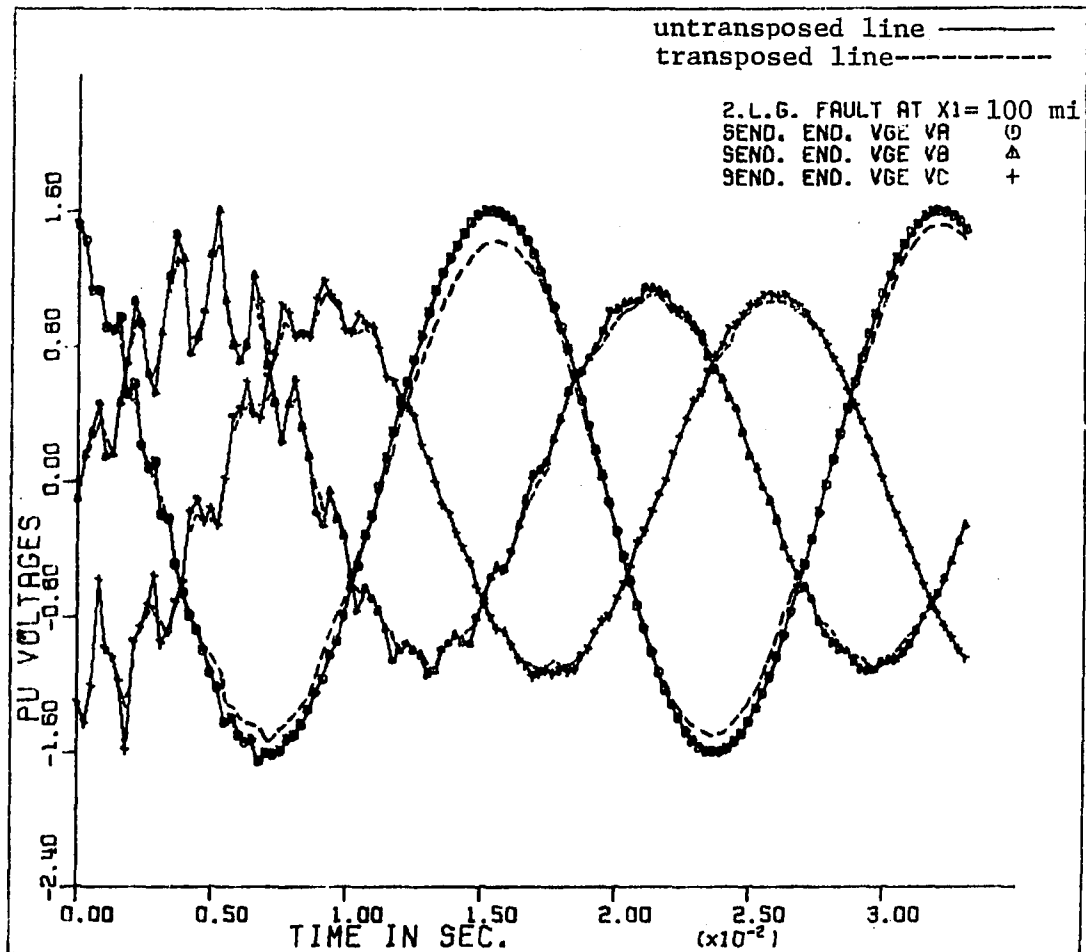


Figure 9.2. Effect of transposition on S.E. voltage for eLG fault (b-c)

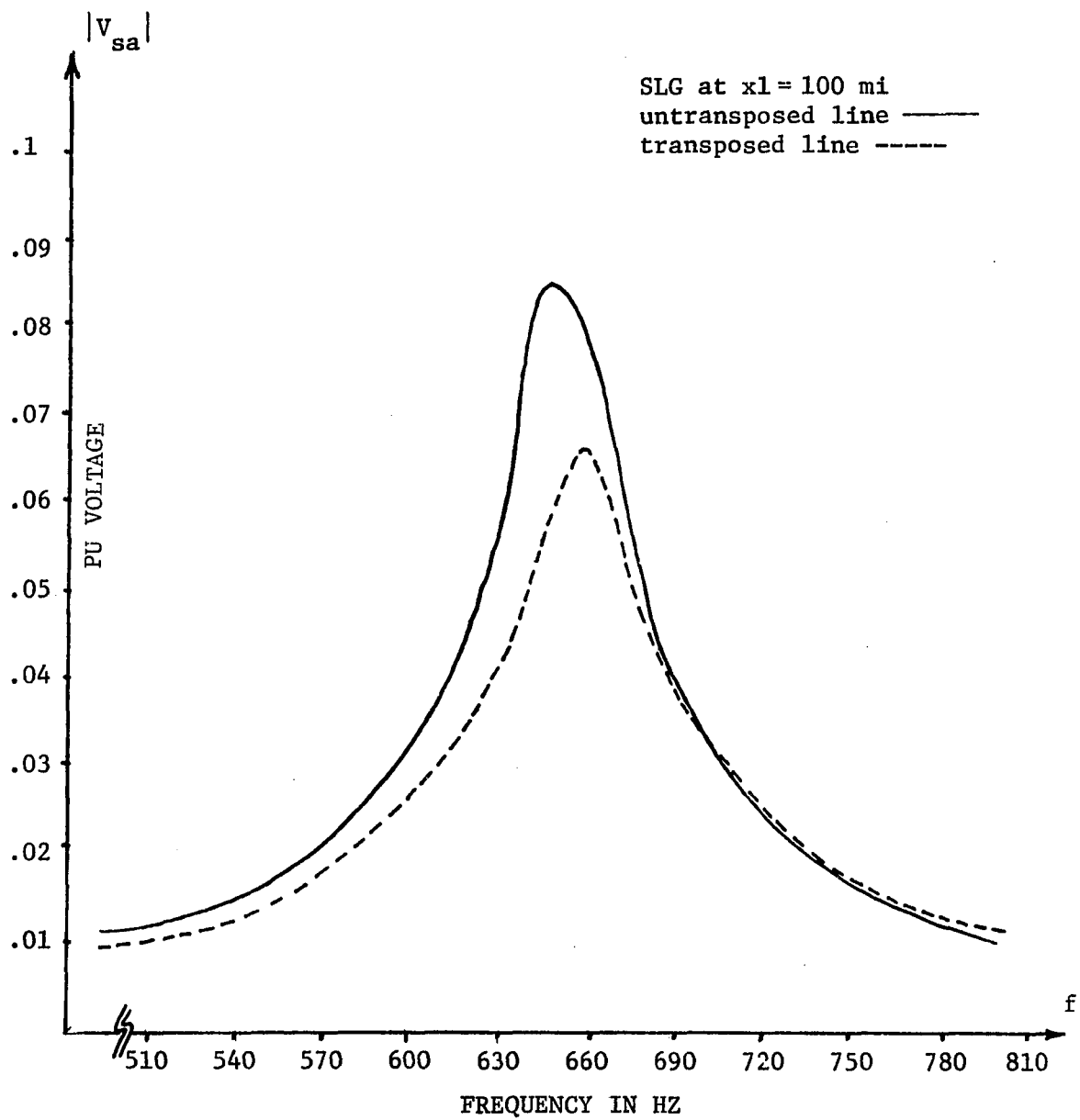


Figure 9.3. Effect of transposition on the frequency spectra for SLG fault (a)

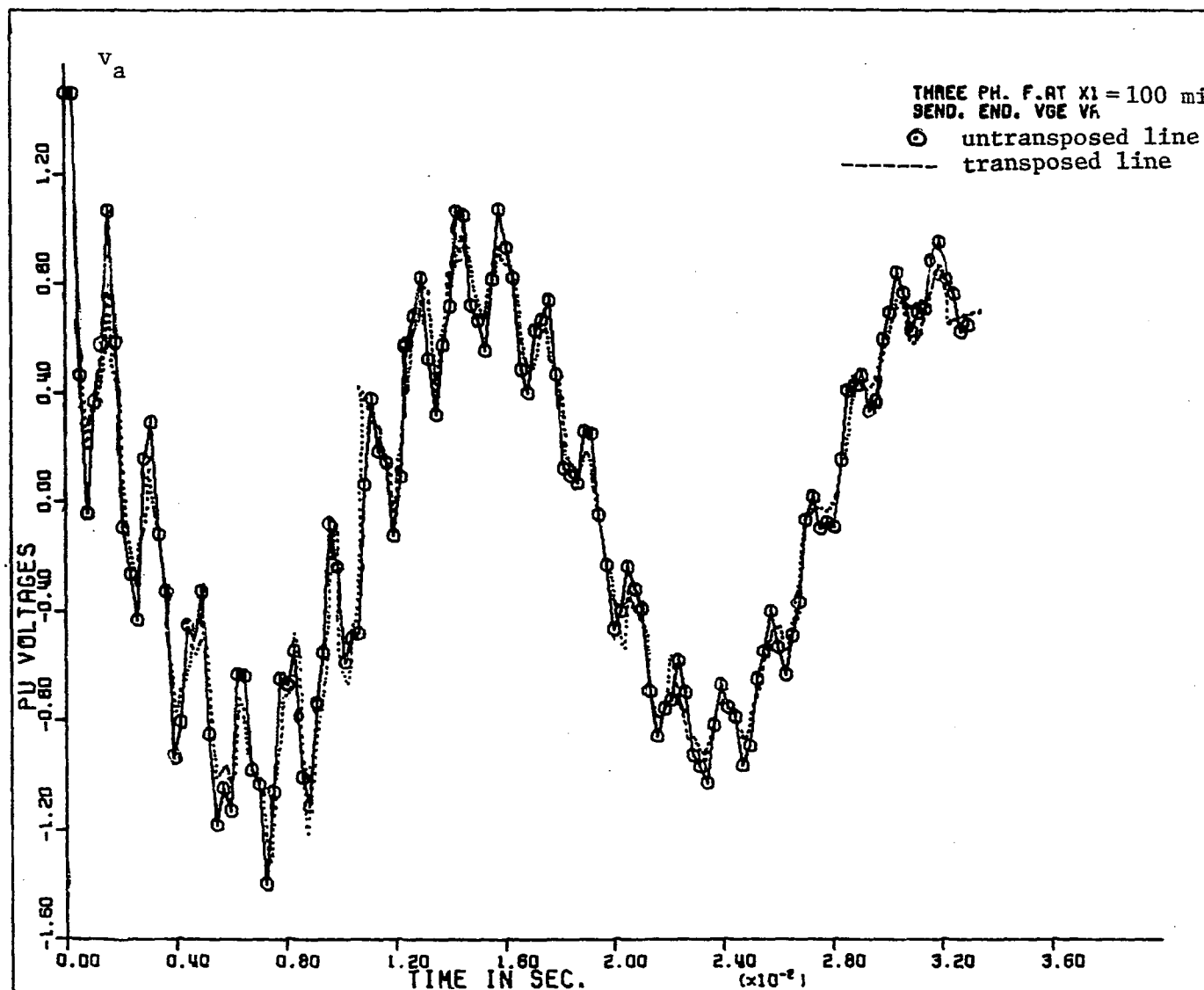


Figure 9.4. Effect of transposition on S.E. voltage for 3LG fault

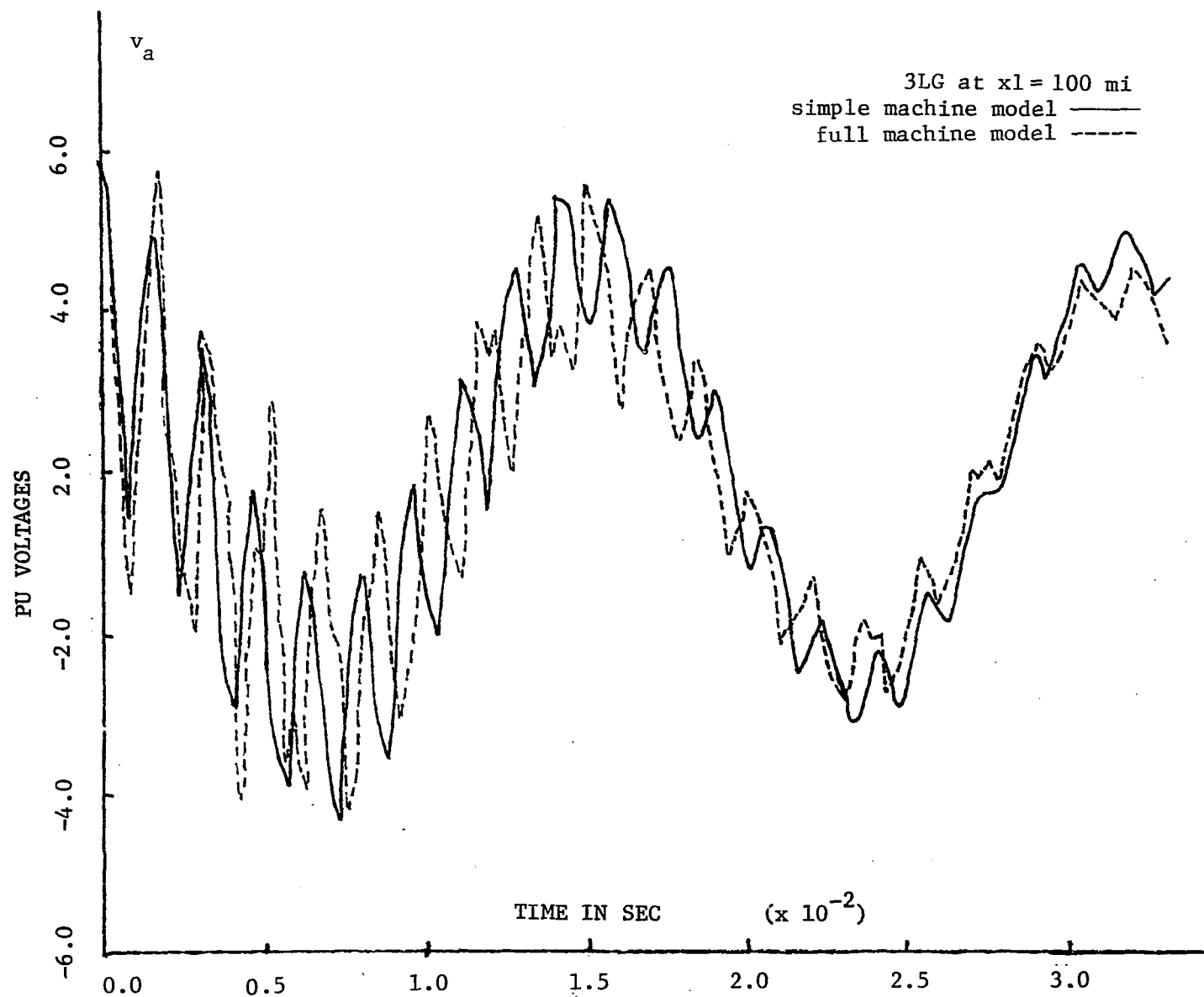


Figure 9.5a. Effect of generator model on S.E. voltage for 3LG fault

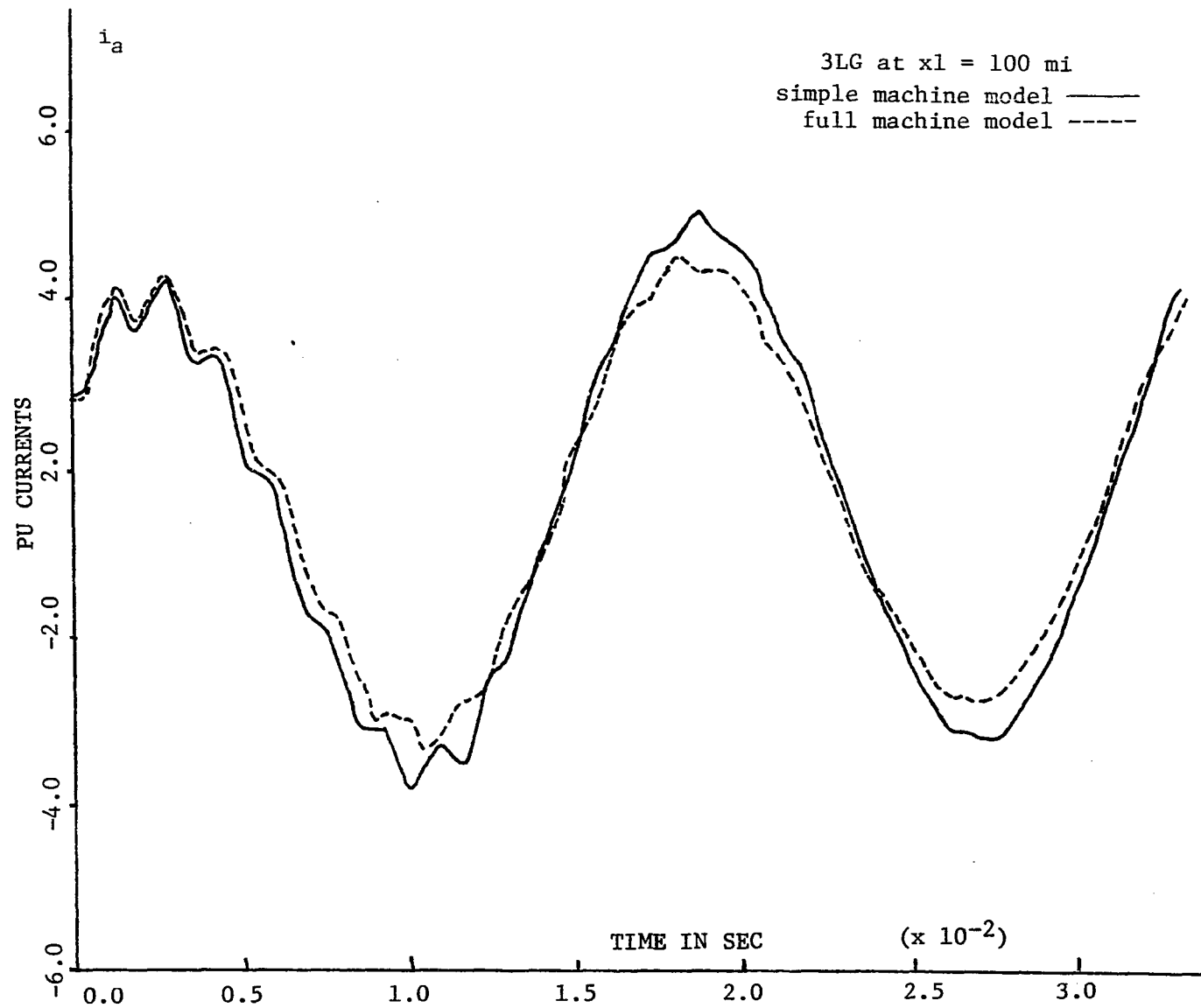


Figure 9.5b. Effect of generator model on S.E. current for 3LG fault

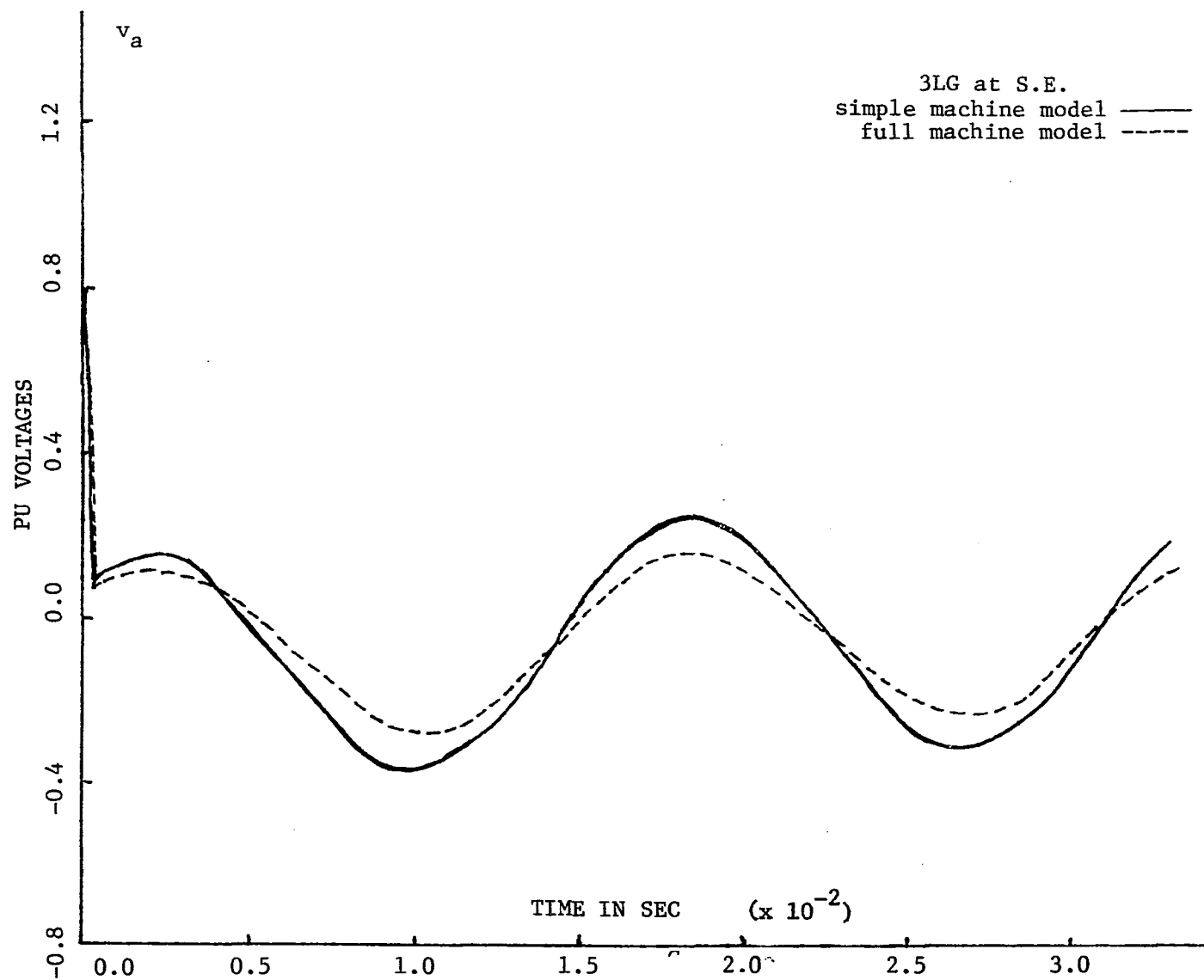


Figure 9.6a. Effect of generator model on S.E. voltage for 3LG fault

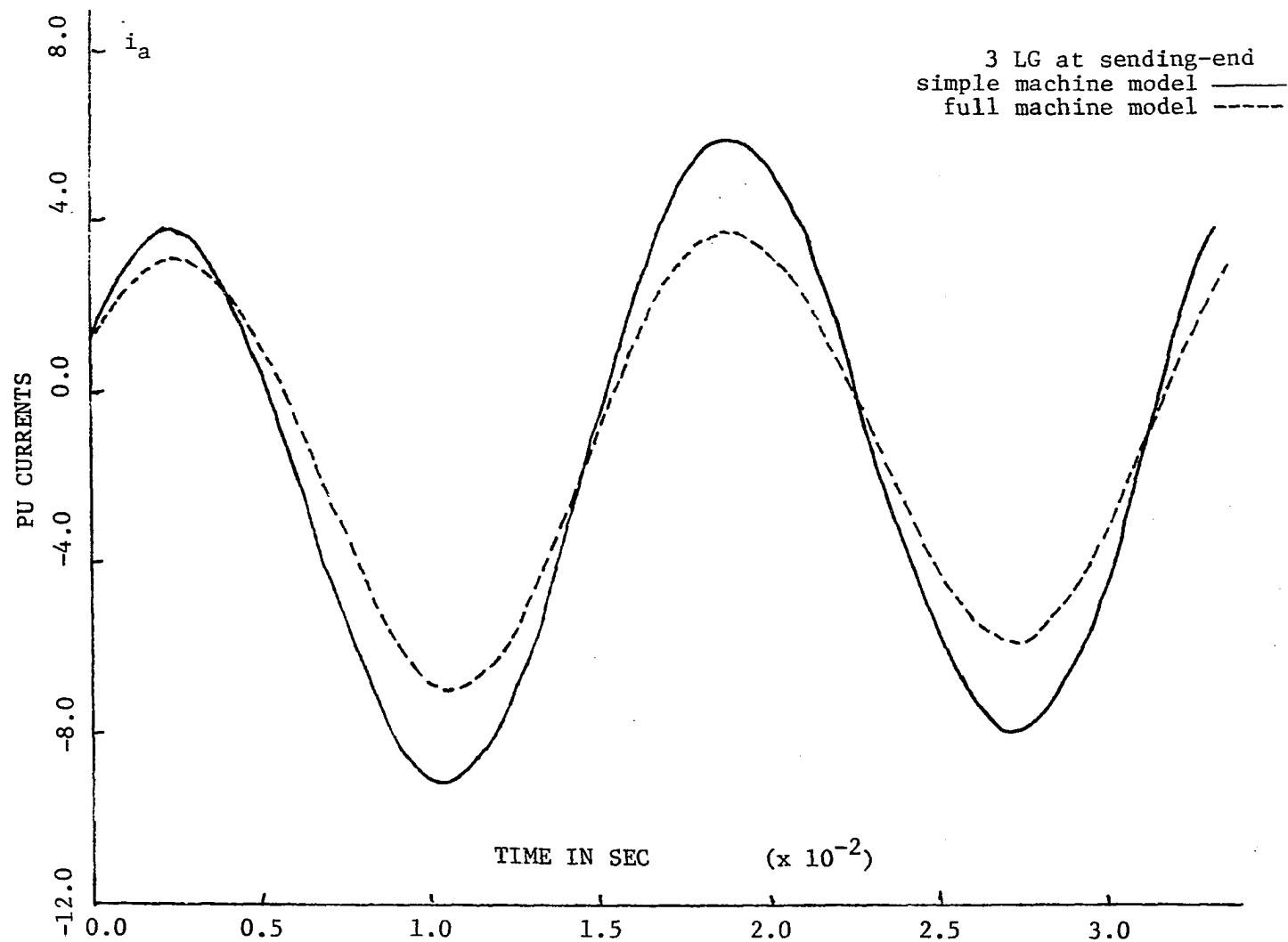


Figure 9.6b. Effect of generator model on S.E. current for 3LG fault

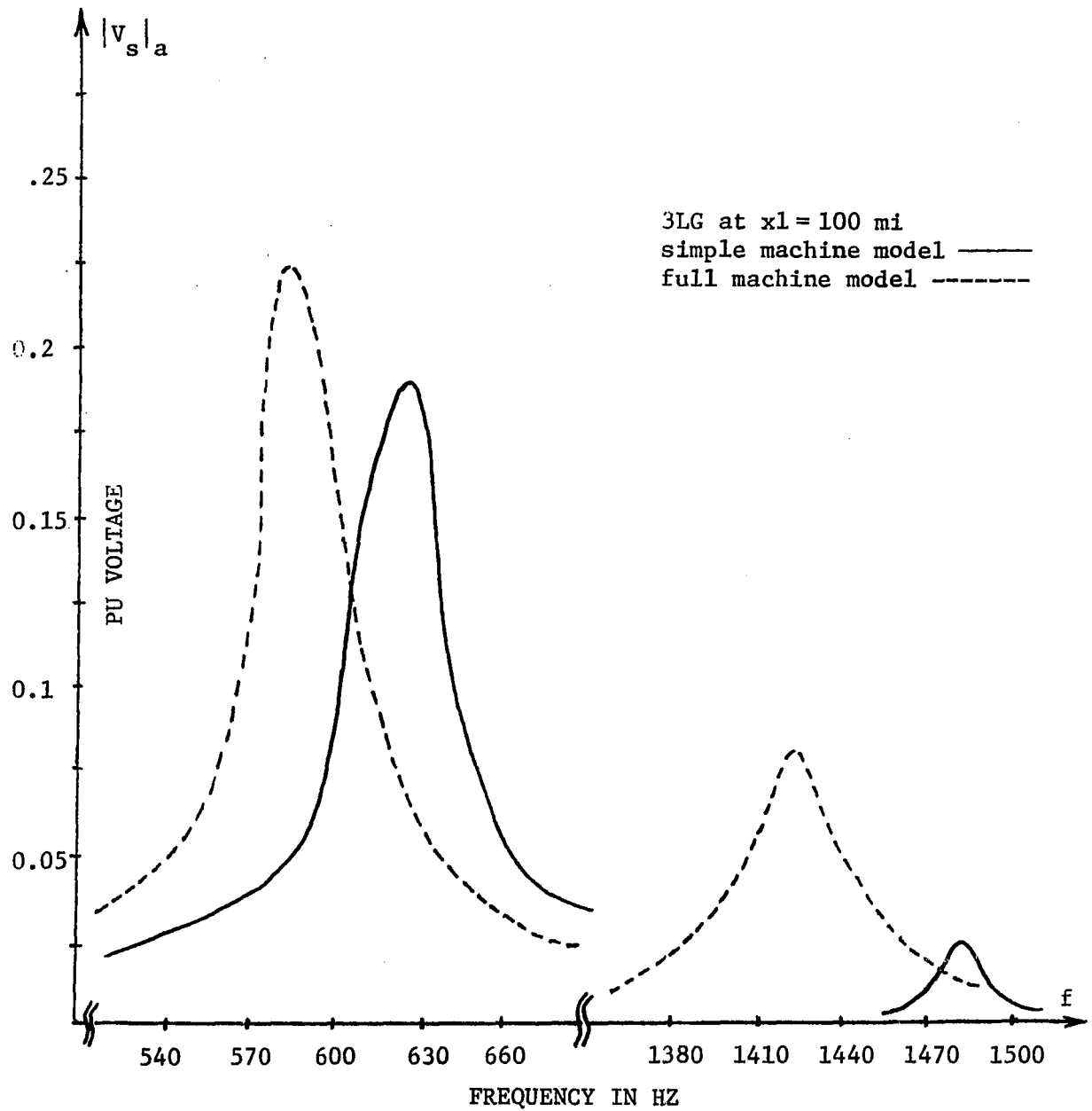


Figure 9.7. Effect of generator model on frequency spectra of S.E. voltage for 3LG fault

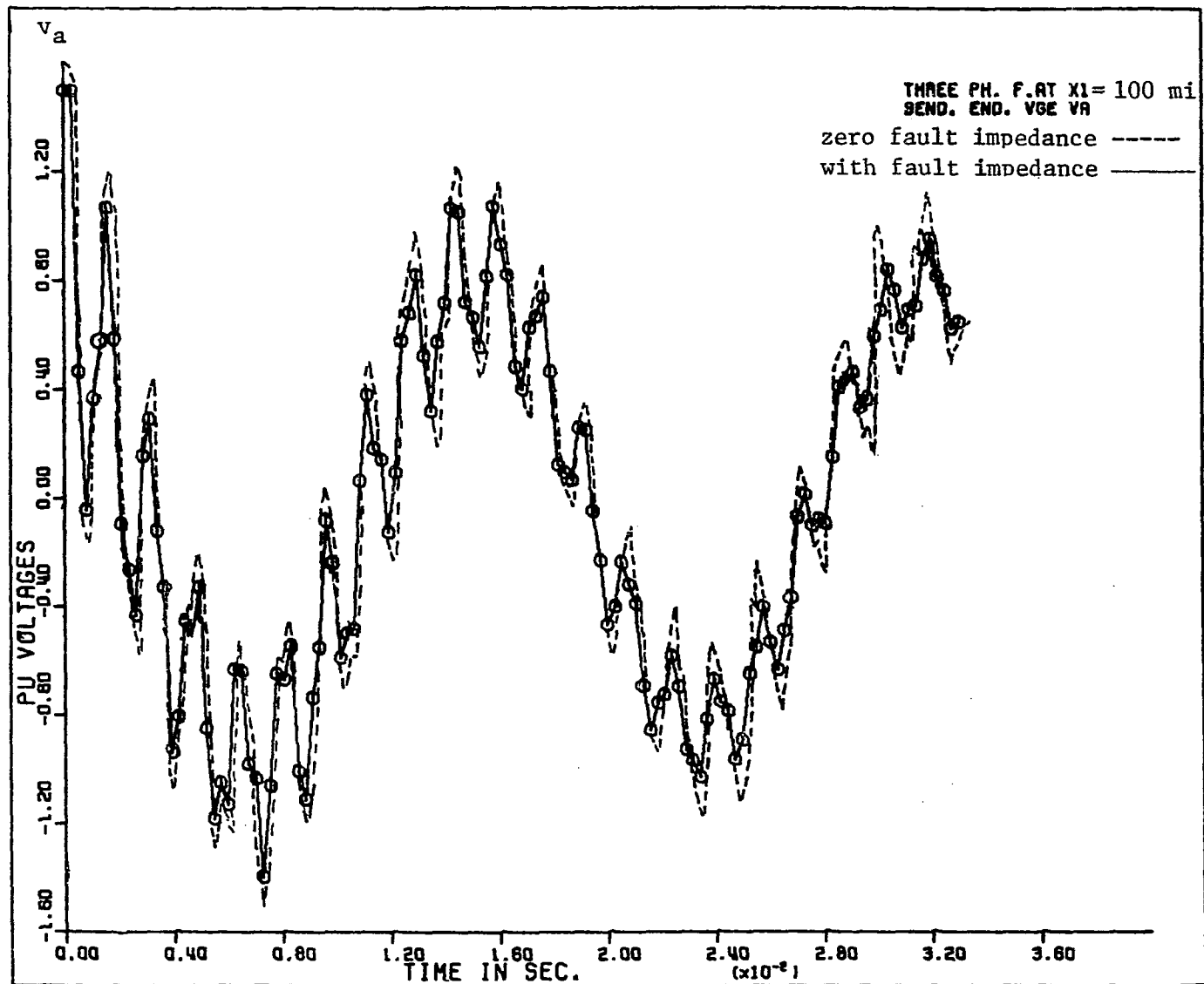


Figure 9.8. Effect of fault impedance on S.E. voltage for 3LG fault

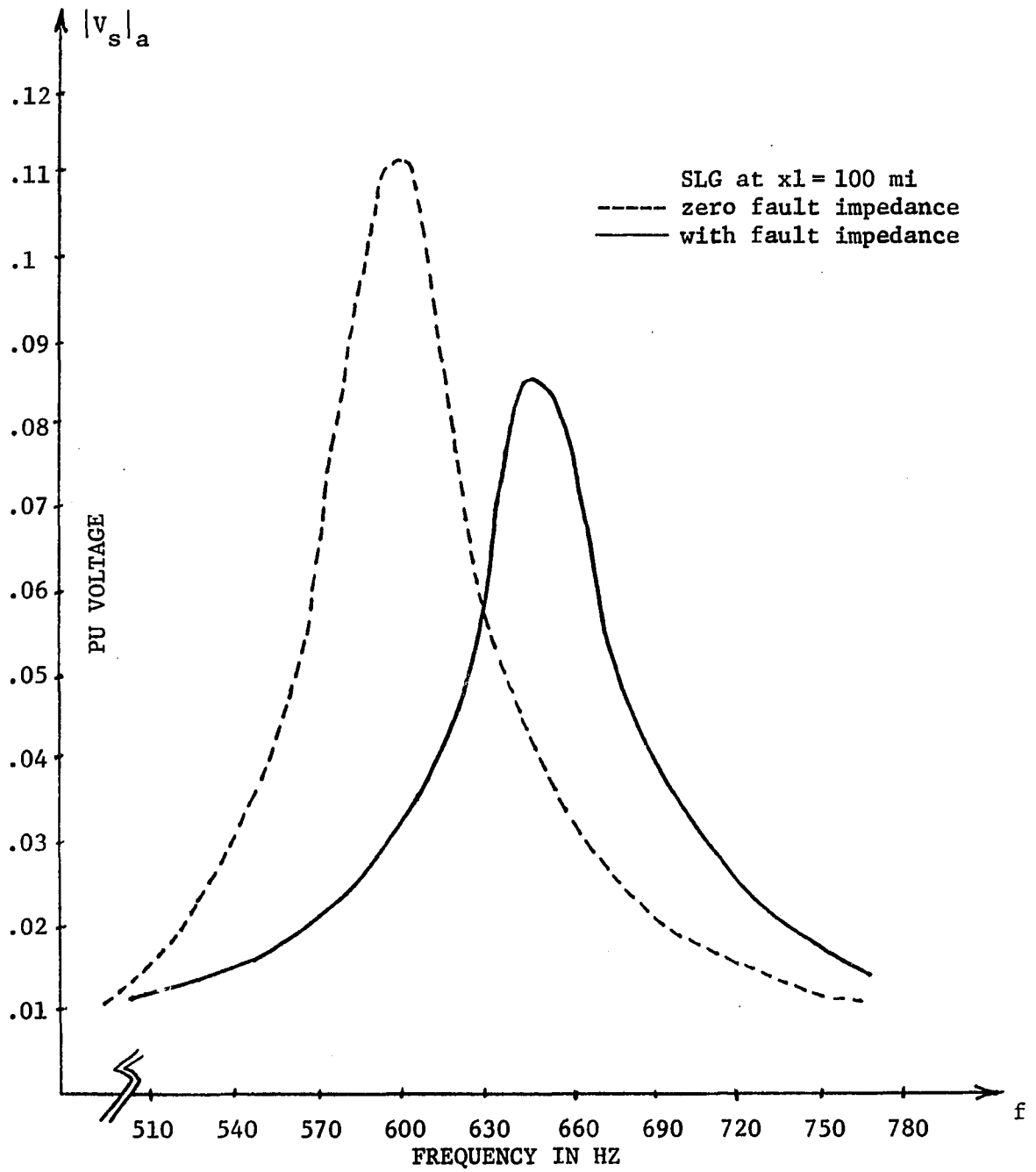


Figure 9.9. Effect of fault impedance on frequency spectra of S.E. voltage for SLG fault

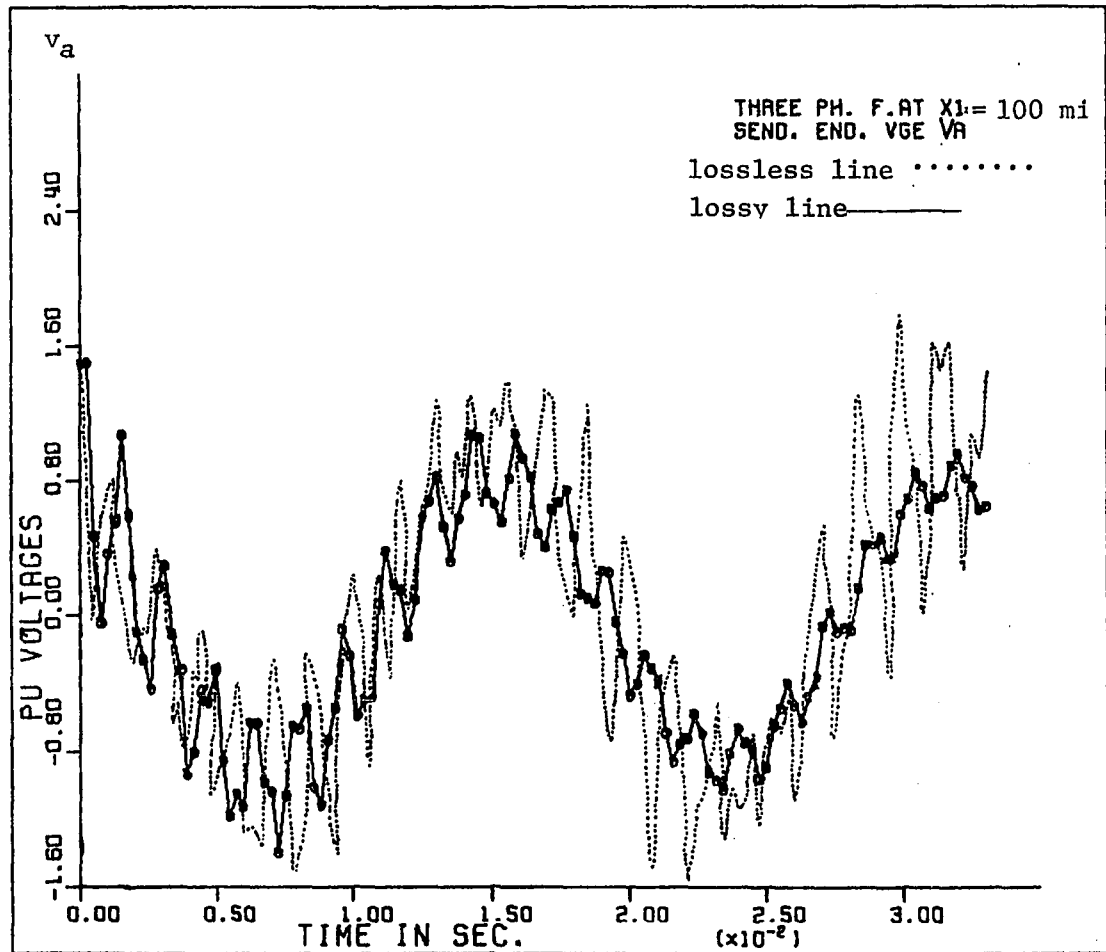


Figure 9.10a. Effect of the line losses on S.E. voltage for 3LG fault

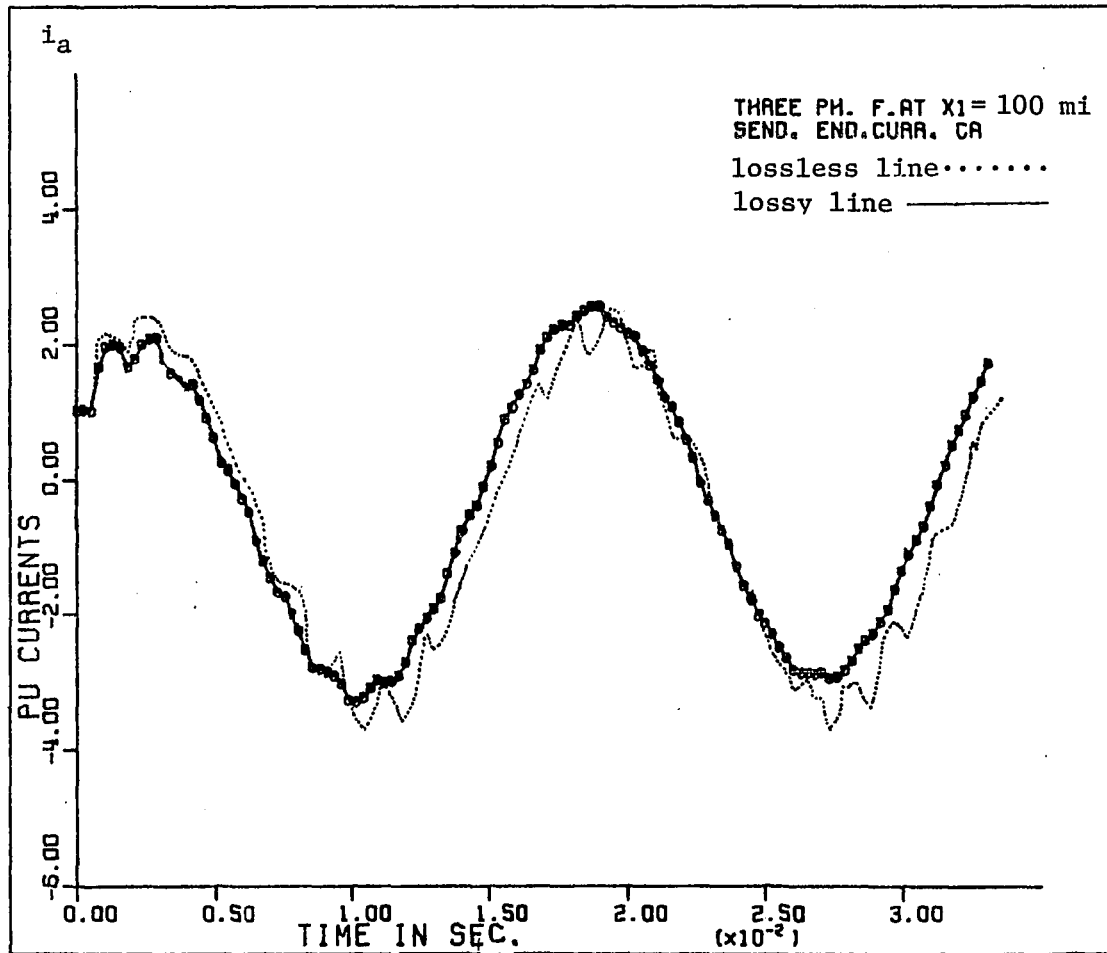


Figure 9.10b. Effect of the line losses on S.E. current for 3LG fault

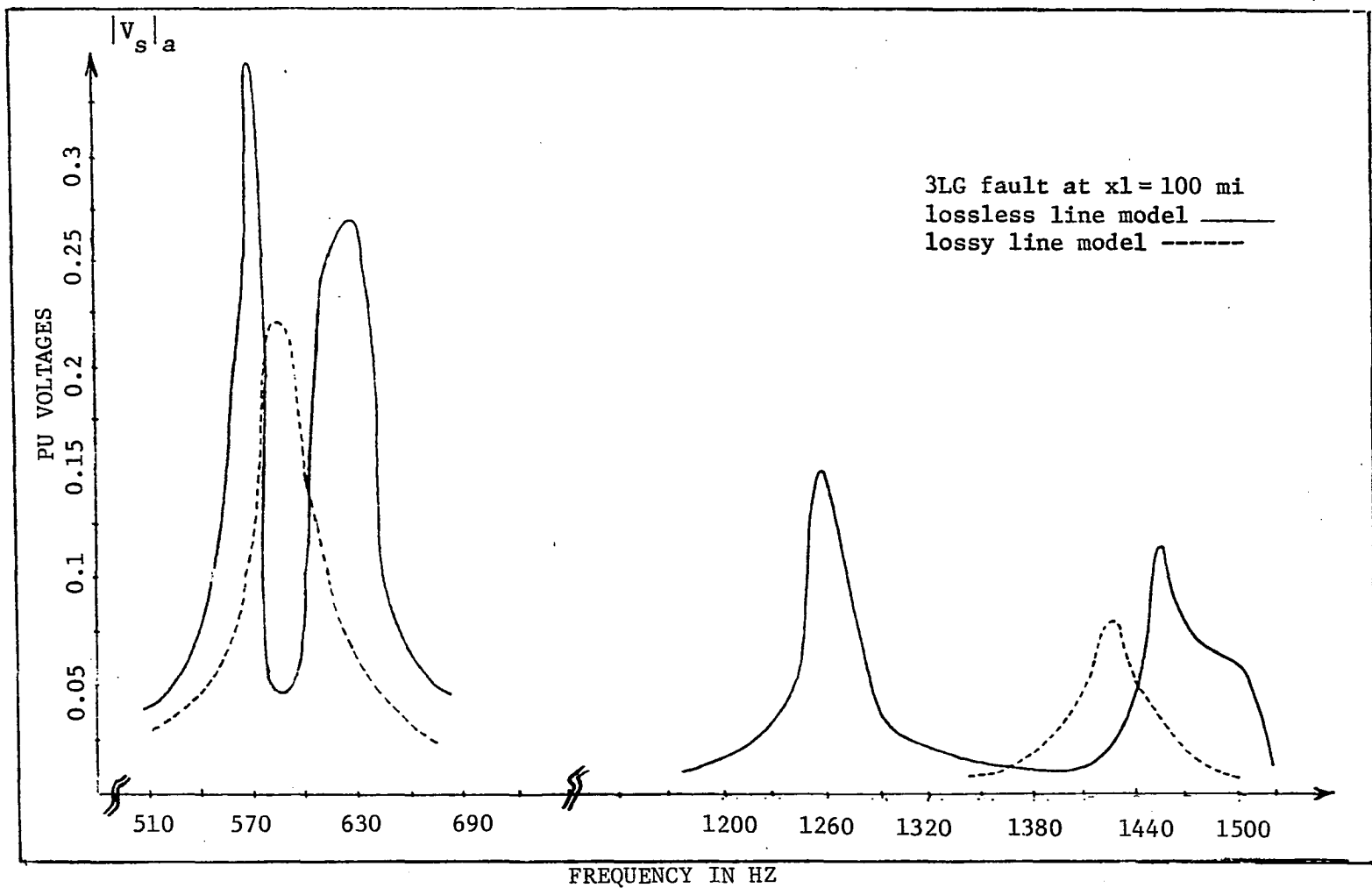


Figure 9.11. Frequency spectra of the transient S.E. voltage for both models

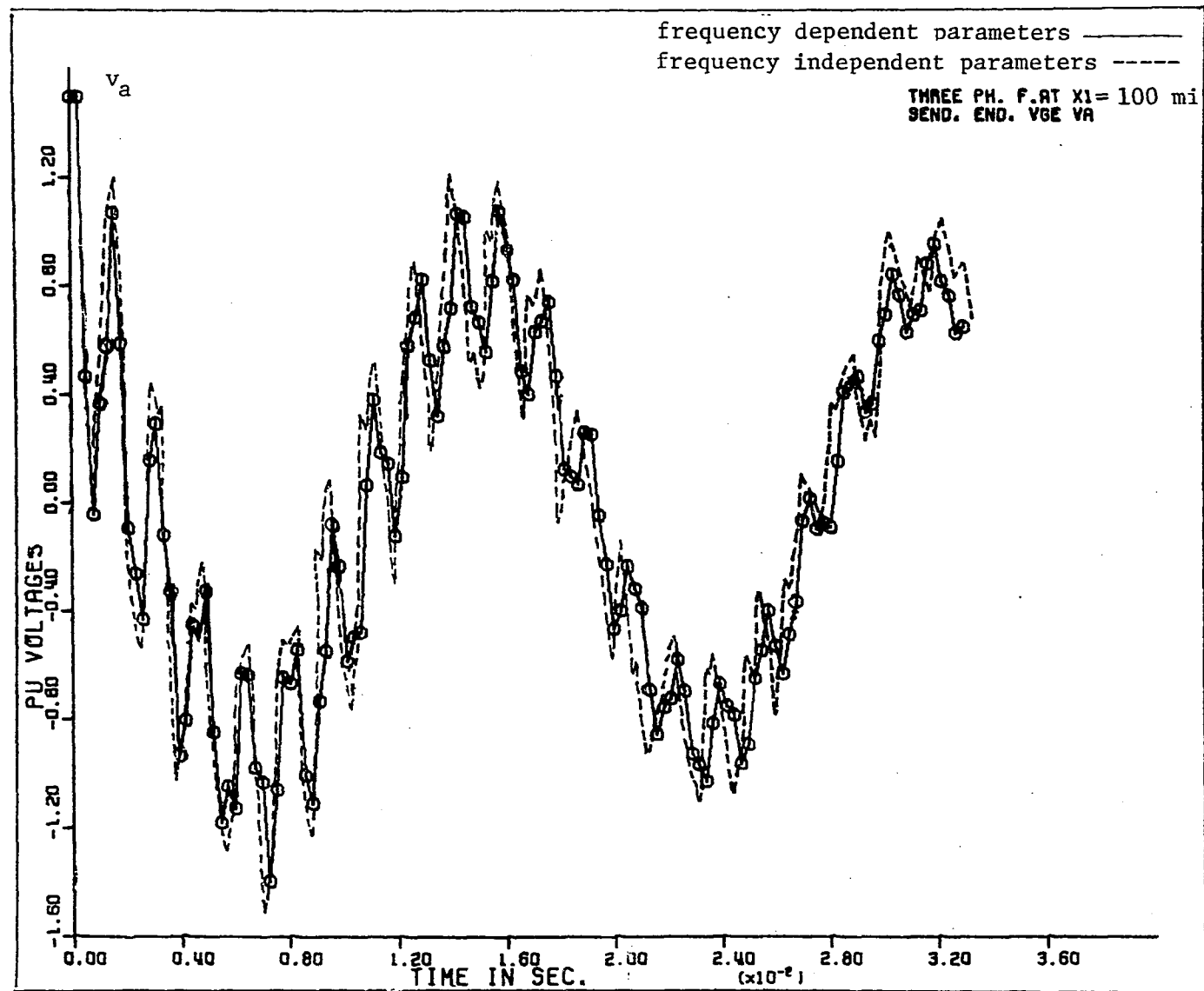


Figure 9.12. Effect of frequency variation of line parameters on S.E. voltage for 3LG fault

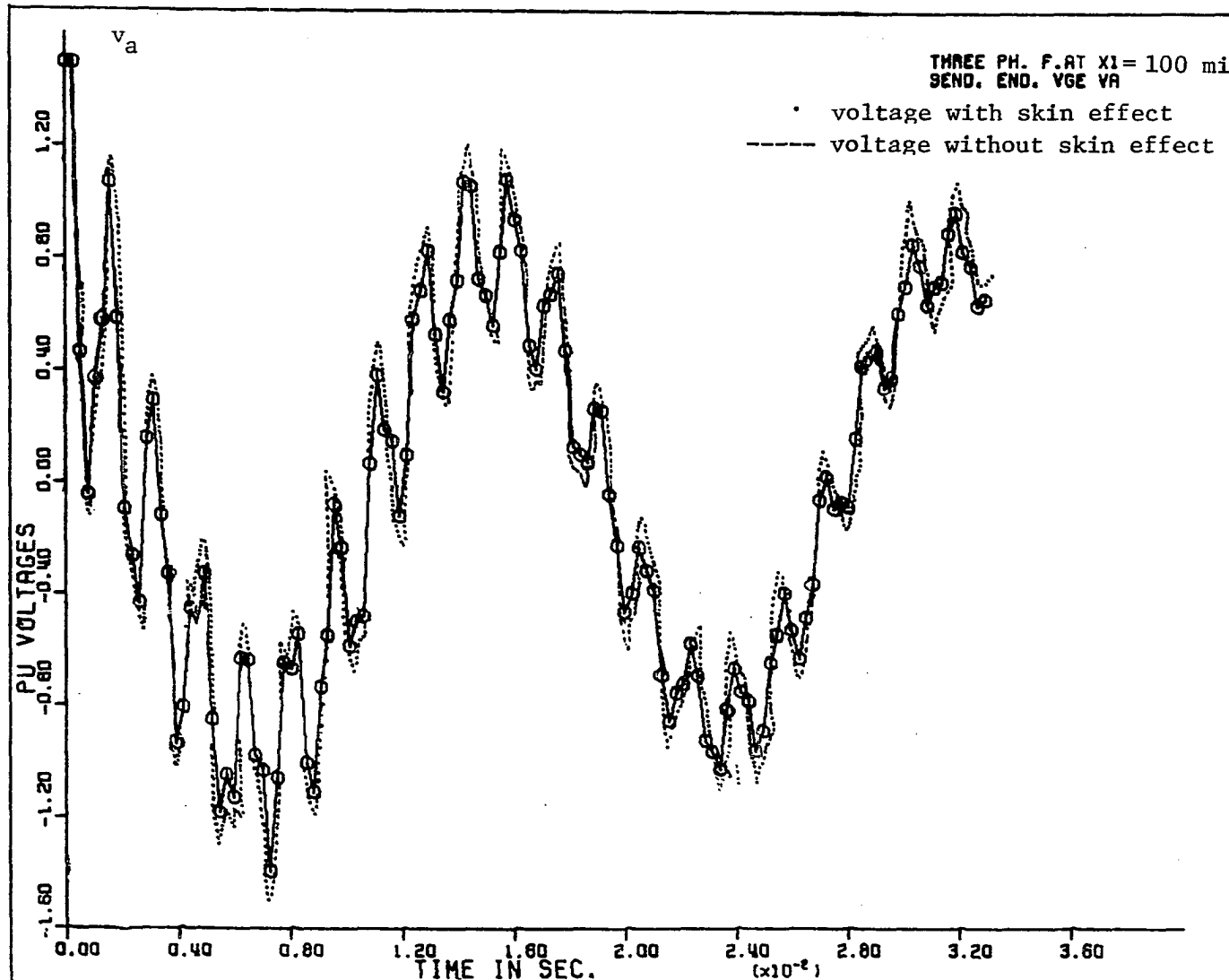


Figure 9.13. Skin effect on S.E. voltage for 3LG fault

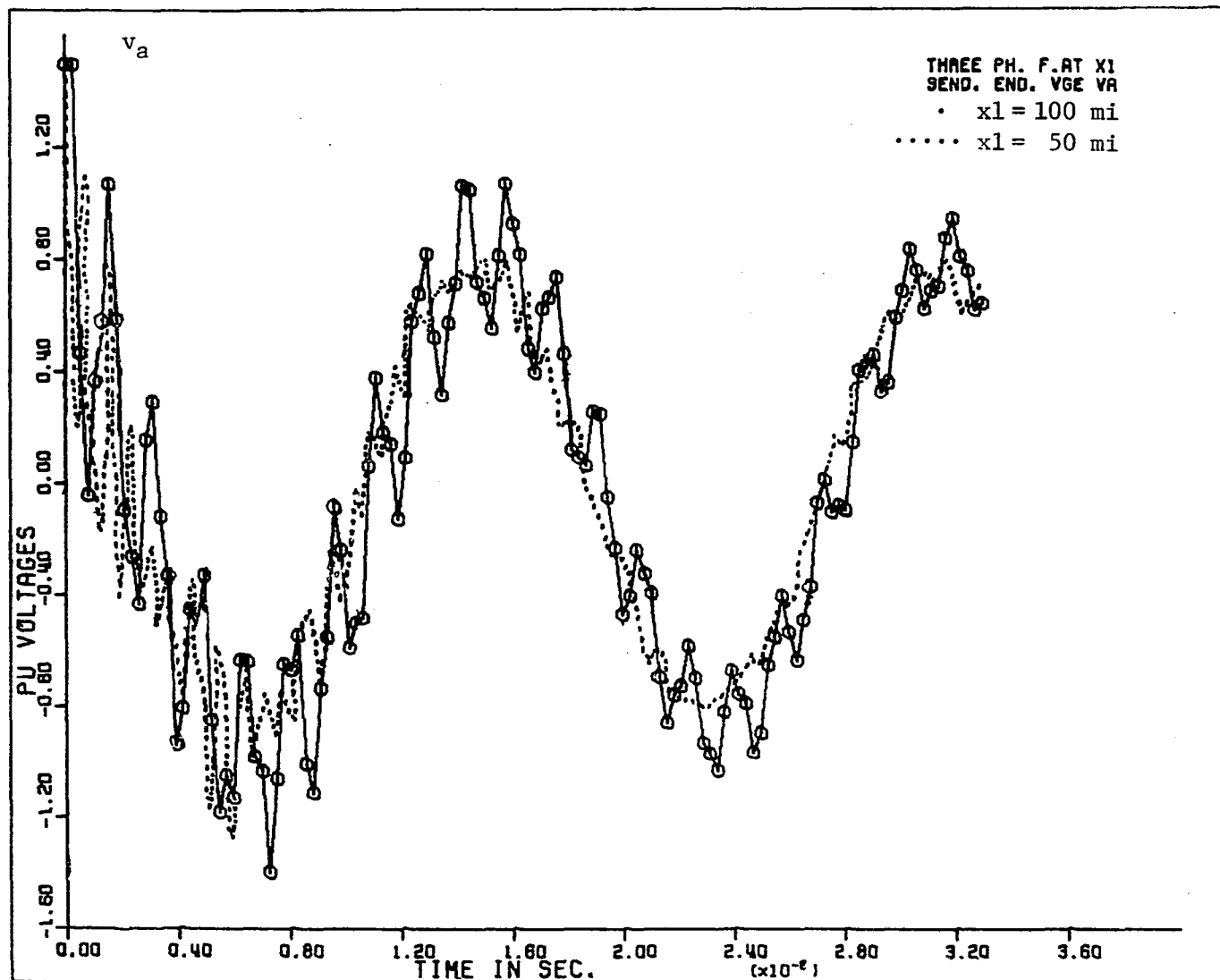


Figure 9.14a. Effect of fault location on S.E. voltage for 3LG fault

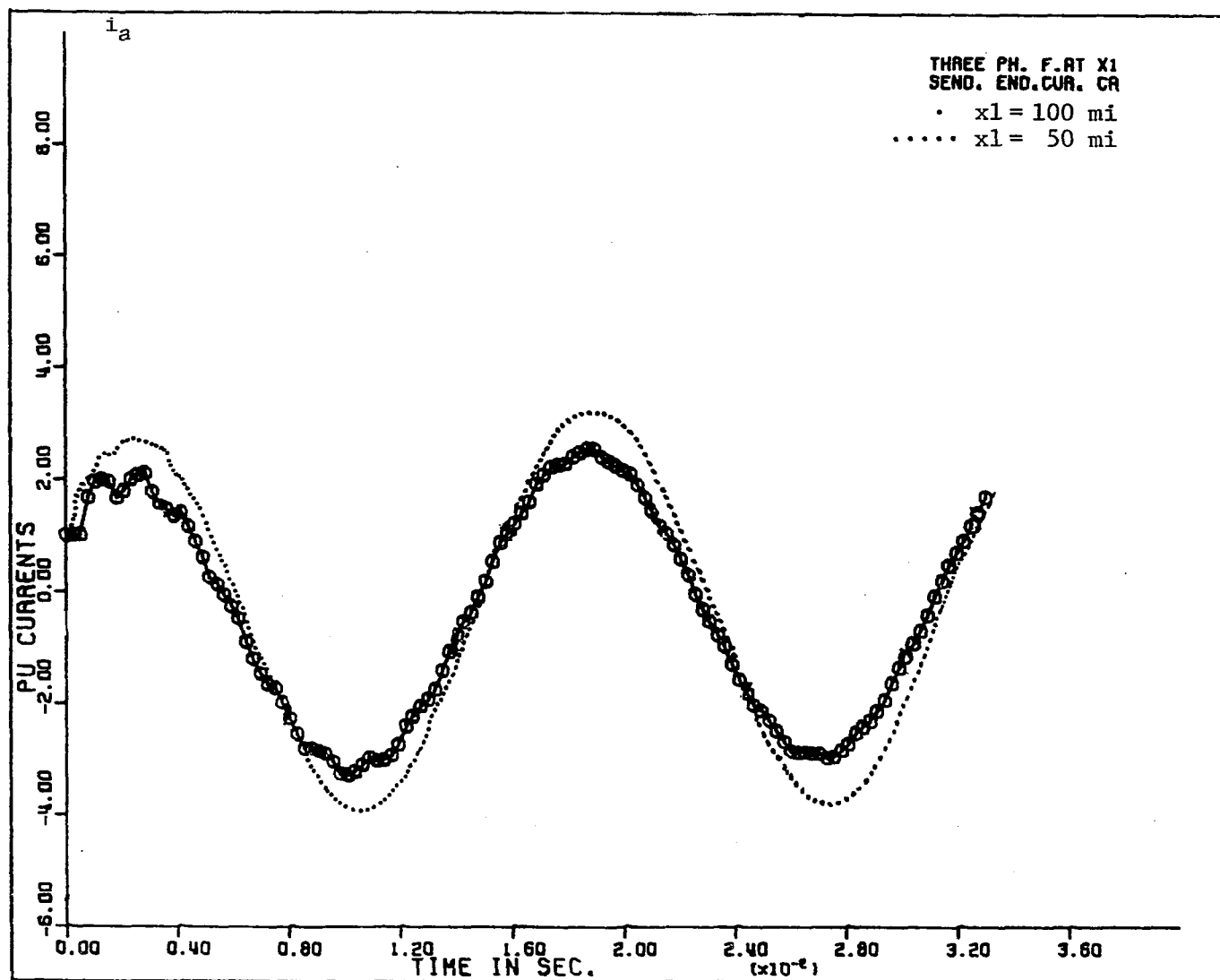


Figure 9.14b. Effect of fault location on S.E. current for 3LG fault

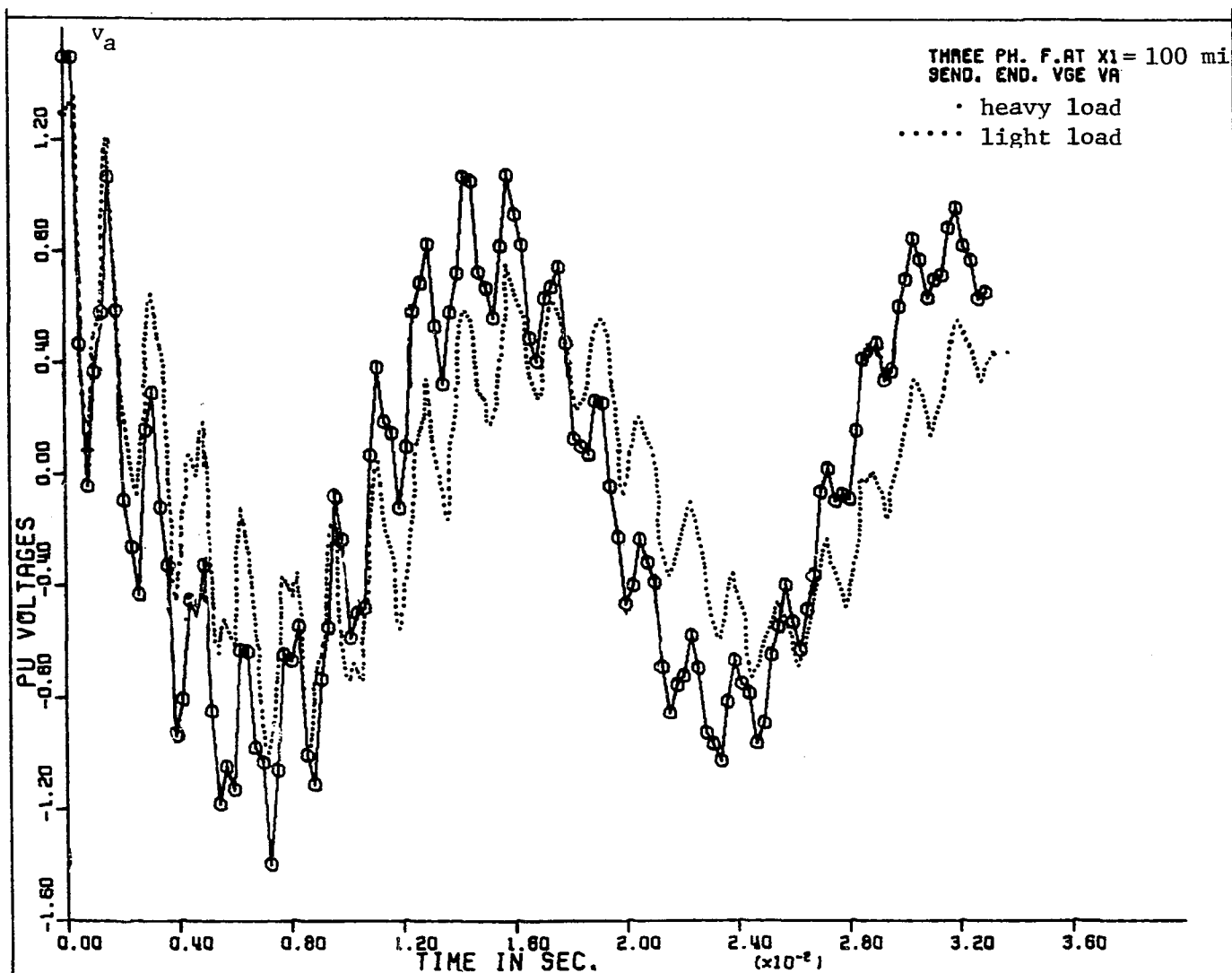


Figure 9.15a. Effect of load on S.E. voltage for 3LG fault

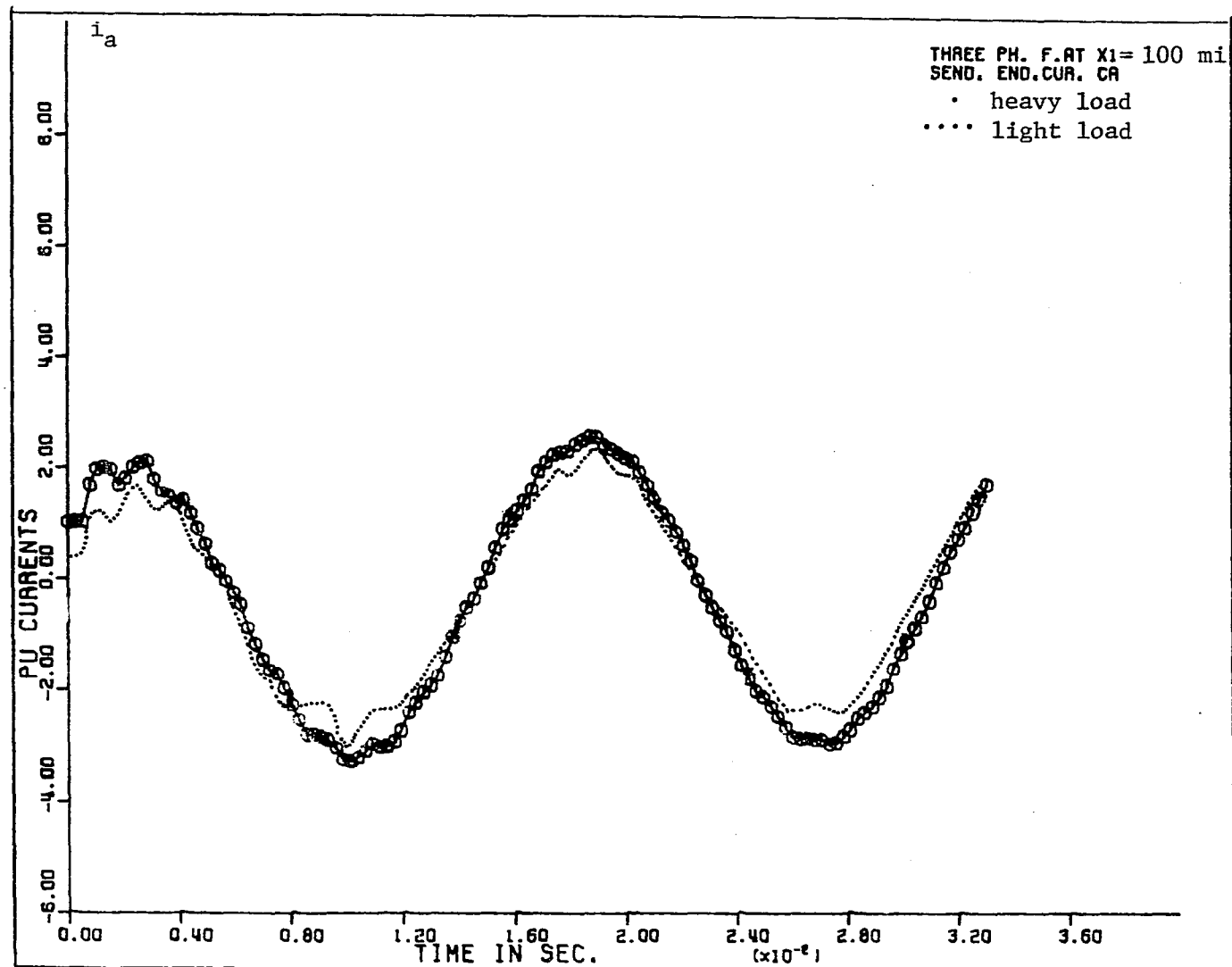


Figure 9.15b. Effect of load on S.E. current for 3LG fault

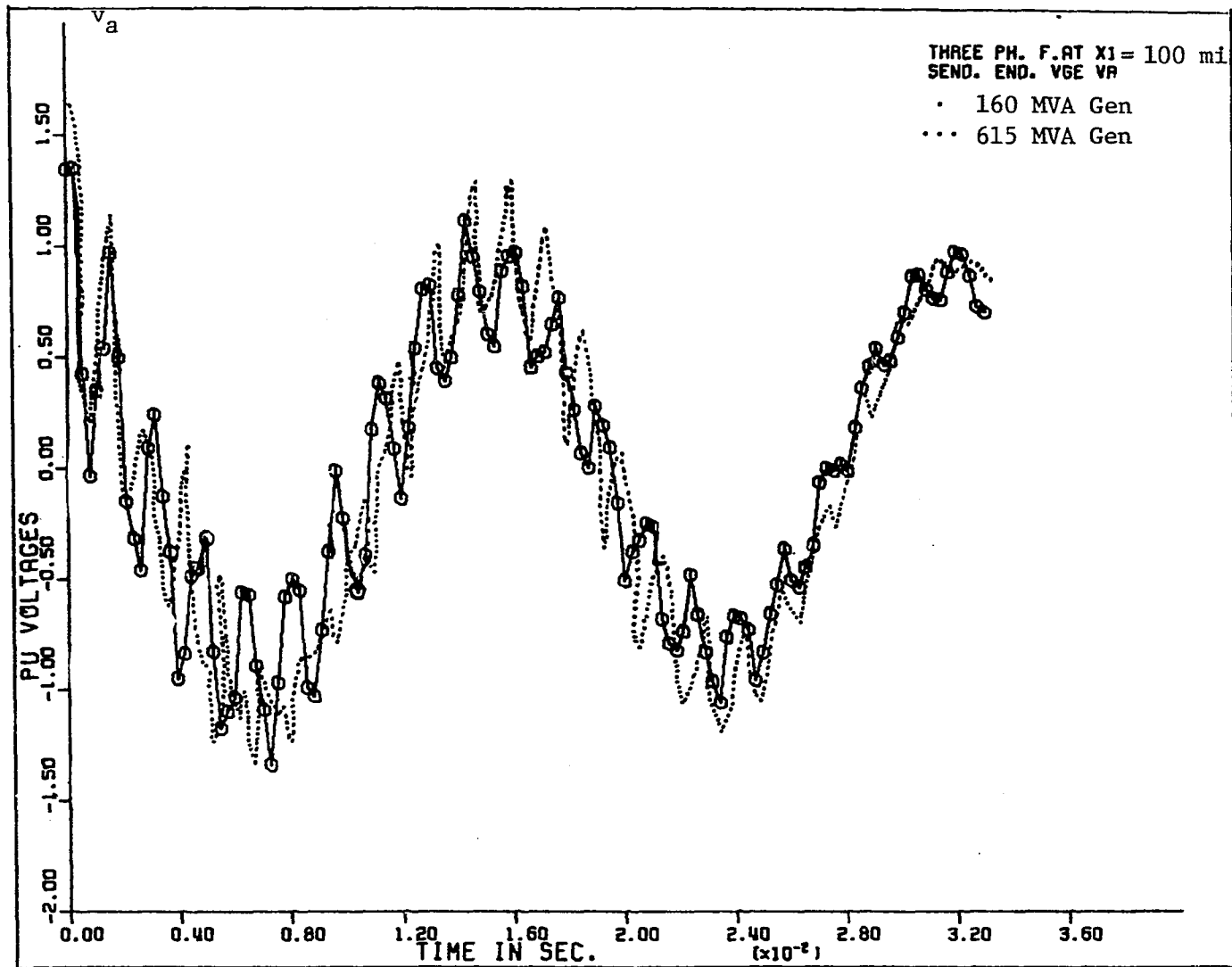


Figure 9.16a. Effect of generator size on S.E. voltage for 3LG fault (simple machine models)

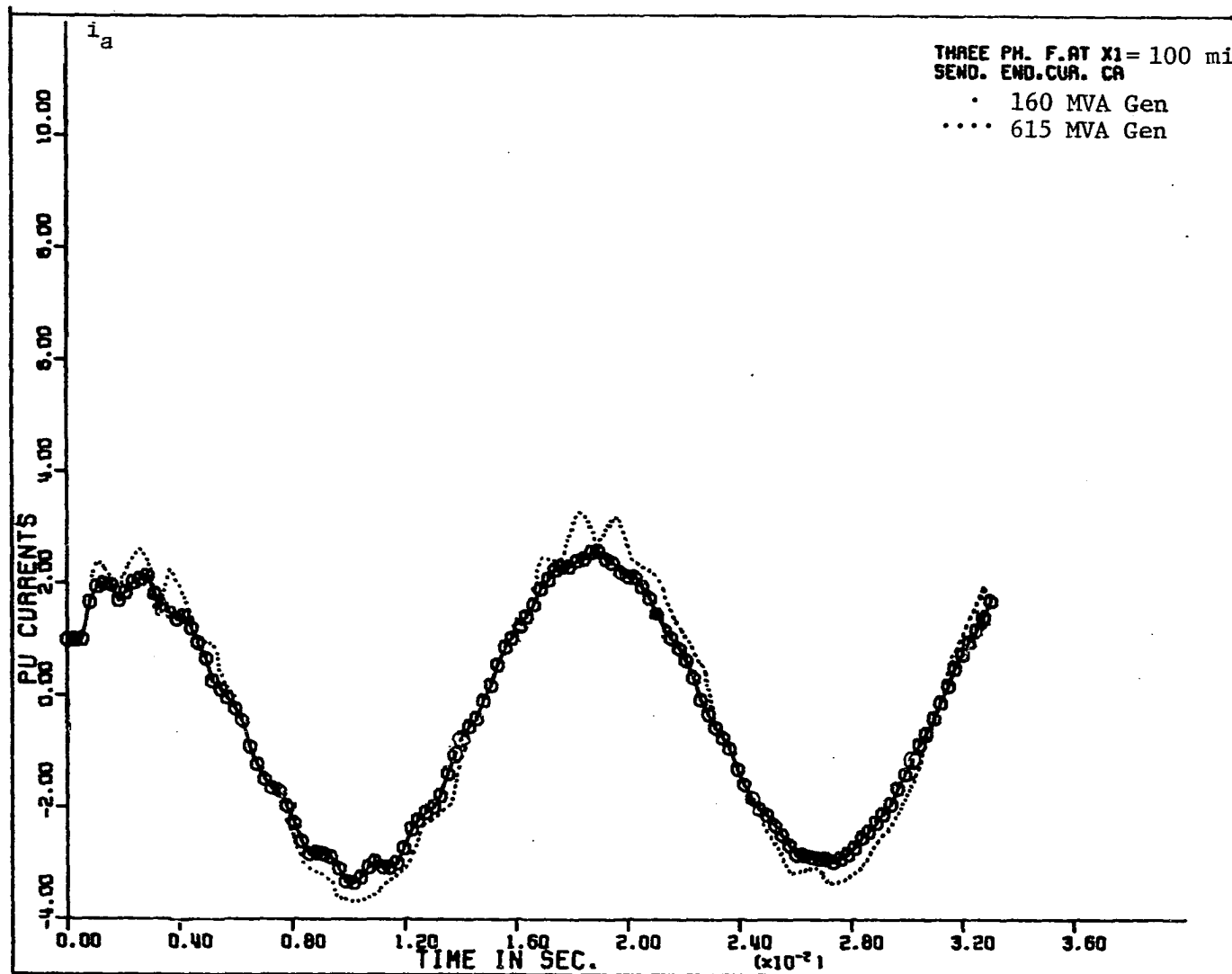


Figure 9.16b. Effect of generator size on S.E. current for 3LG fault (simple machine model)

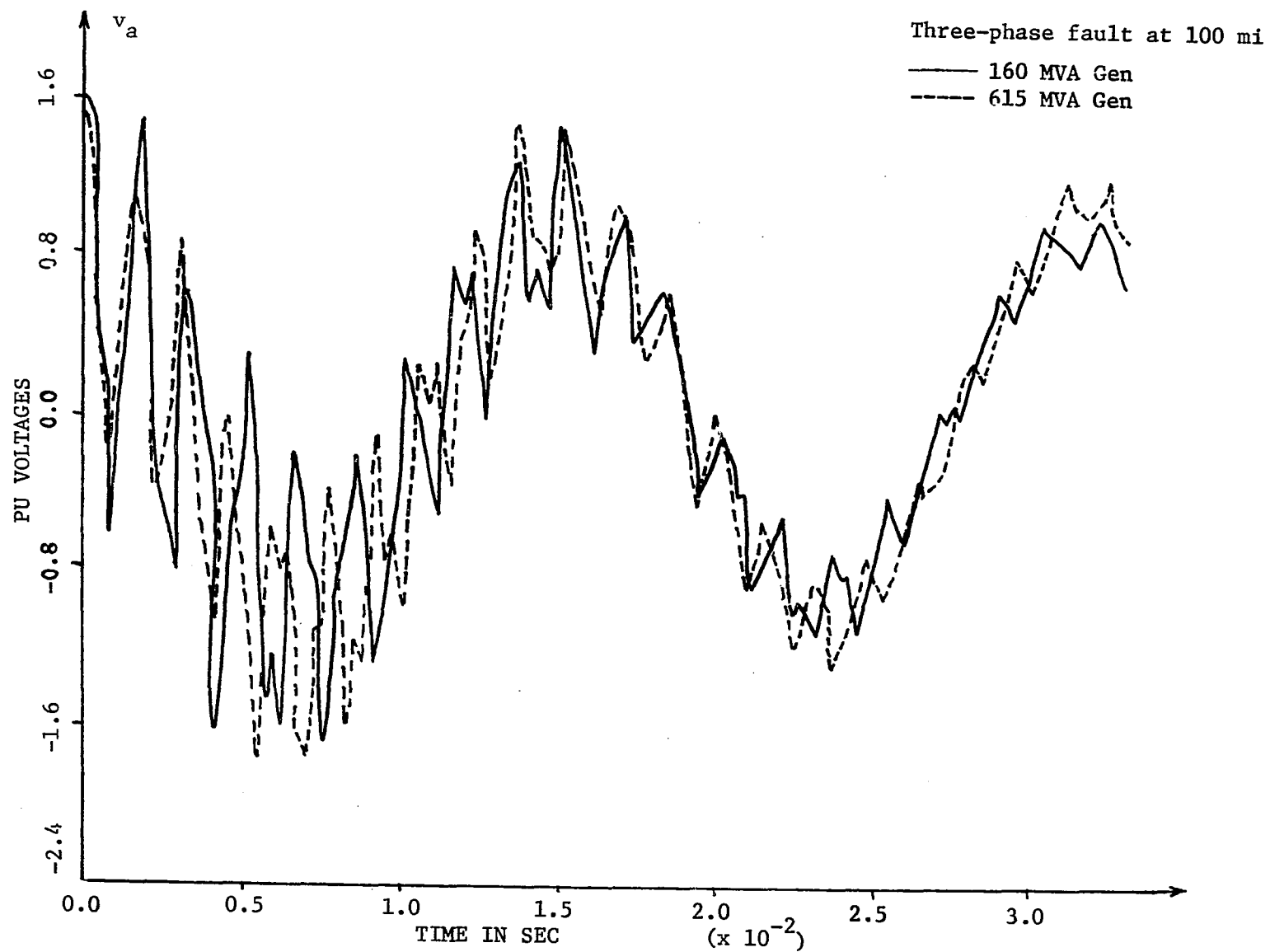


Figure 9.17a. Effect of the generator size on the S.E. voltage for 3LG fault (full machine model)

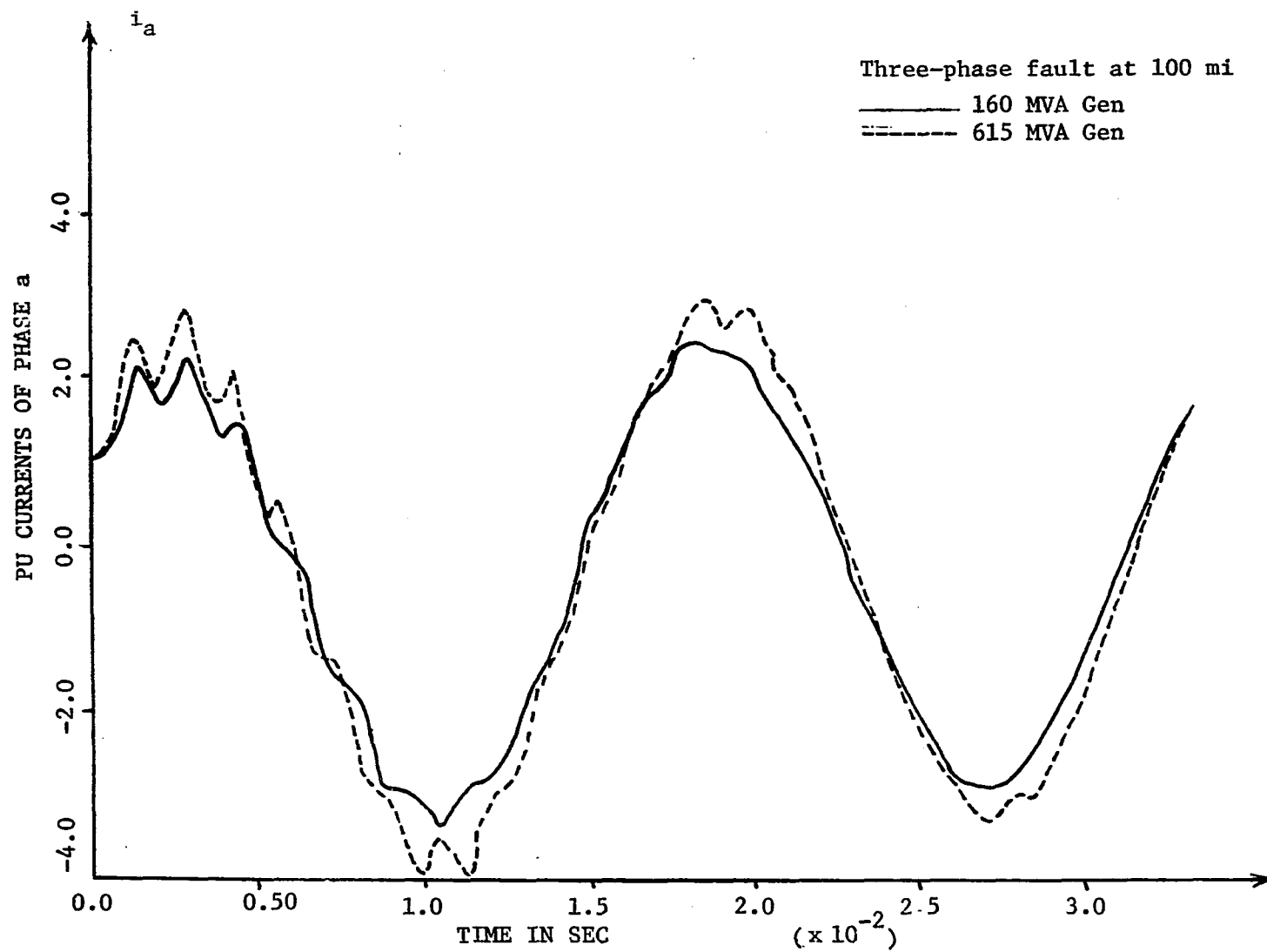


Figure 9.17b. Effect of the generator size on the S.E. current for 3LG fault (full machine model)

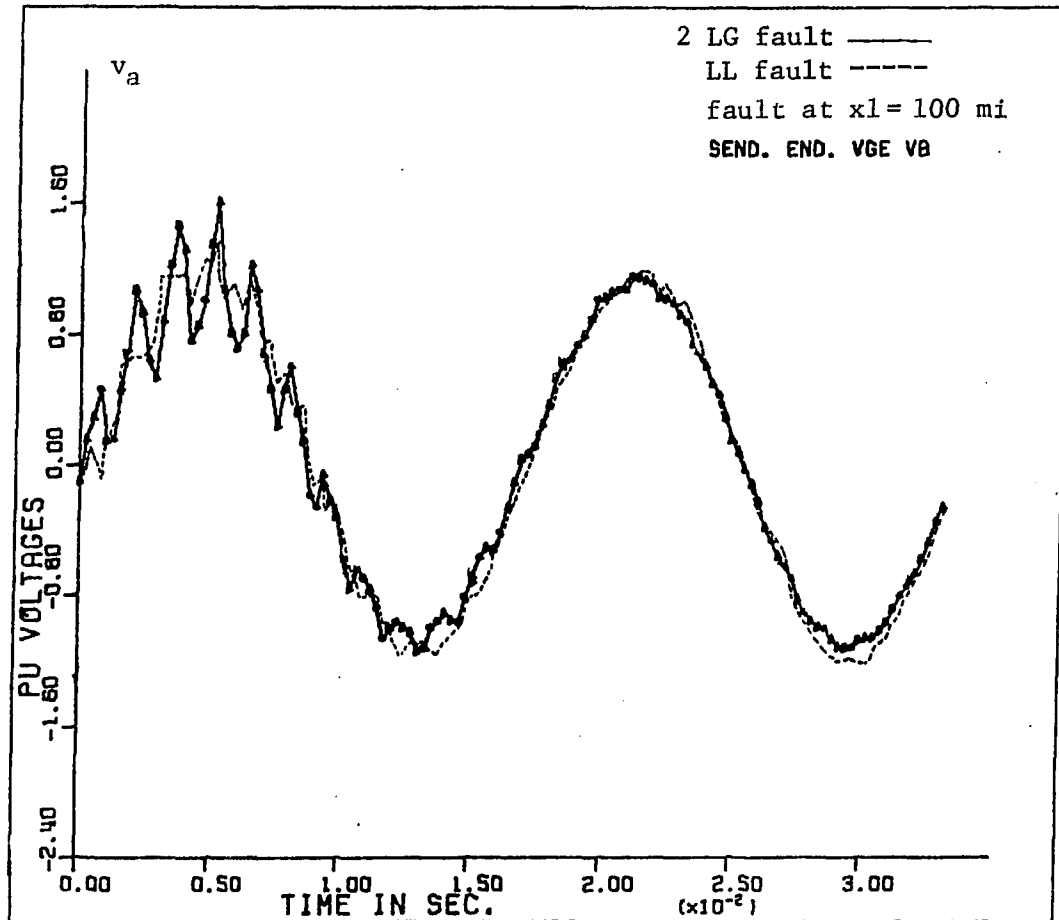


Figure 9.18. Effect of type of fault on S.E. voltage

X. REFERENCES

1. Bewley, L. V. I. Traveling Waves on Transmission System.
New York: John Wiley and Sons, 1951.
2. Bewley, L. V. II. Traveling Waves on Transmission System.
New York: John Wiley and Sons, 1963.
3. Frey, W. and Althammer, P. "The Calculation of Transients by Means of a Digital Computer." Brown Boveri Rev. 48 (1961):344-355.
4. Barthold, L. O. and Carter, G. K. "Digital Traveling Waves Solution for 1-Phase Single-Phase Equivalents." AIEE Trans 80 (December 1961):812-820.
5. McElroy, A. J. and Porter, R. M. "Digital Computer Calculation of Transients in Electric Networks." AIEE Trans. on PAS 86 (April 1963):88-96.
6. Uram, R. and Miller, R. W. "Mathematical Analysis and Solution of Transmission-Line Transients I-Theory." Trans. IEEE 83 (1964):1116.
7. Uram, R. and Ferro, W. E. "Mathematical Analysis and Solution of Transmission-Line Transients II-Applications." Trans. IEEE 83 (1964):1123.
8. Dommel, H. W. "Digital Computer Solution of Electromagnetic Transients in Single and Multiphase Networks." IEEE Trans. on PAS 88 (April 1969):388-399.
9. Meyer, W. S. and Liu, T. H. Electromagnetic Transients Program Rule Book. Portland, Oregon: Bonneville Power Administration, 1980.
10. Talukdar, Sarosh N. "METAP - A Modular and Expandable Program for Simulating Power System Transients." Trans. IEEE on PAS 95 (November/December 1976):1882-1891.
11. Thoren, H. B. and Carlsson, K. L. "A Digital Computer Program for the Calculation of Switching and Lightning Surges on Power Systems." IEEE Trans. on PAS 89, No. 2 (February 1970): 212-218.
12. Branin, F. H., Hogsett, G. R., Lunde, R. L., and Kugel, L. E. "ECAP-II, An Electronic Circuit Analysis Program." IEEE Spectrum 62 (June 1971):14-25.

13. Kalra, P. C. and Stanek, E. K. "An Indirect Technique Utilizing Lattice Approach and Superposition for Computing Switching Surge." IEEE Trans. PAS 92 (June 1973):916-925.
14. Dommel, H. W. and Meyer, W. S. "Computation of Electromagnetic Transients." IEEE 62, No. 7 (July 1974):983-993.
15. Wedepohl, M. "Application of Matrix Methods to the Solution of Traveling-Wave Phenomena in Polyphase Systems." IEE 110, No. 12 (December 1963):1200-1212.
16. Carroll, D. P. and Nozari, F. "An Efficient Computer Method for Simulating Transients on Transmission Line with Frequency Dependent Parameters." IEEE Trans. on PAS 94, No. 4 (July/August 1975):1167-1176.
17. Jones, A. T. and Aggarwal, R. K. "Digital Simulation of Faulted e.h.v. Transmission Lines with Particular Reference to Very High-Speed Protection." IEE 123, No. 4 (April 1976):353-359.
18. Triezenberg, D. M. "An Efficient State Variable Transmission-Line Model." IEEE PAS 98 (March/April 1979):484-492.
19. Ku, Y. H. Electric Energy Conversion. New York: The Ronald Press, 1959.
20. Greenwood, A. Electrical Transients in Power Systems. New York: John Wiley and Sons, 1971.
21. Subramaniam, P. and Malik, O. P. "Digital Simulation of a Synchronous Generator in Direct-Phase Quantities." IEE 118, No. 1 (January 1971):153-160.
22. Adkins, B. The General Theory of Electrical Machines. London, England: Chapman and Hall, 1962.
23. Anderson, P. M. Analysis of Faulted Power Systems. Ames, Iowa: Iowa State University Press, 1976.
24. Bergmann, R. G. and Pensioen, J. M. "Calculation of Electrical Transients in Power Systems." IEE 126, No. 8 (August 1979): 764-770.
25. Gross, C. H. Power System Analysis. New York: John Wiley and Sons, 1979.
26. Peskin, Edward. Transient and Steady-State Analysis of Electric Networks. New York: The Ronald Press Company, 1961.

27. Electric Research Council and Electric Power Research Institute.
Transmission Line Reference Book, New York, 1979.
28. Stevenson, W. D. Elements of Power System Analysis. 2nd ed.
New York: McGraw-Hill Book Company, 1933.
29. Anderson, P. M. And Fouad, A. A. Power System Control and
Stability. Ames, Iowa: Iowa State University Press, 1977.
30. Openheim, A. V. and Schafer, R. W. Digital Signal Processing.
Englewood Cliffs, New Jersey: Prentice-Hall, Inc., 1975.
31. Day, Sylvia J., Mullineux, N. and Reed, J. R. "Developments in
Obtaining Transient Response Using Fourier Transforms, Part II:
Use the Modified Fourier Transform." J. EE Educ. 4 (1966):
31-40.
32. Bickford, J. P., Mullineux, N., and Reed, J. R. "Computation of
Power System Transients." IEE Monograph Series 18, England,
1976.
33. Day, Sylvia J., Mullineux, N., and Reed, J. R. "Developments in
Obtaining Transient Response Using Fourier Transforms, Part I:
Gibb's Phenomena and Fourier Integrals. J. EE Educ. 3 (1965):
501-506.
34. Wilcox, D. J. "Numerical Laplace Transformation and Inversion."
J. EE Educ. 15 (1978):247-265.
35. Westinghouse Electric Corporation. Electrical Transmission and
Distribution Book. East Pittsburgh, Penn.: Westinghouse,
1950.

XI. ACKNOWLEDGMENTS

The author would like to express her thanks and appreciation to the members of her committee, Dr. E. C. Jones, Dr. G. G. Koerber, Dr. R. J. Lambert, G. M. Montag, Dr. J. D. Musil, and Dr. R. E. Post. A special thanks is given to her major professor, Dr. G. G. Koerber for his patience and guidance. Without his help this work would not be completed. A special thanks is extended to Dr. R. J. Lambert and G. M. Montag for their help and guidance. Also much appreciated is the advice received from Dr. K. C. Kruempel.

The Power Affiliates of Iowa State University also deserve thanks for their financial support.

A special thanks is given to J. O. Kopplin, Chairman of the Electrical Engineering Department at Iowa State University for his understanding and encouragement.

A special thanks is extended to Jeanne Gehm for her excellent typing in a short period of time.

The author would like to express her gratitude to her husband for his understanding, support, and useful discussion and to her son for his patience. Without their help this work would not have been possible.

XII. APPENDIX A: NUMERICAL EXAMPLE

A fault study of the general transmission system on the digital computer has been carried out using both the simple and the full model of the synchronous generator. The system parameters have been carefully selected to be of most practical value. The one-line diagram of the system to be studied is given in Figure 12.1. The system data are taken from references [27], [29], and [35].

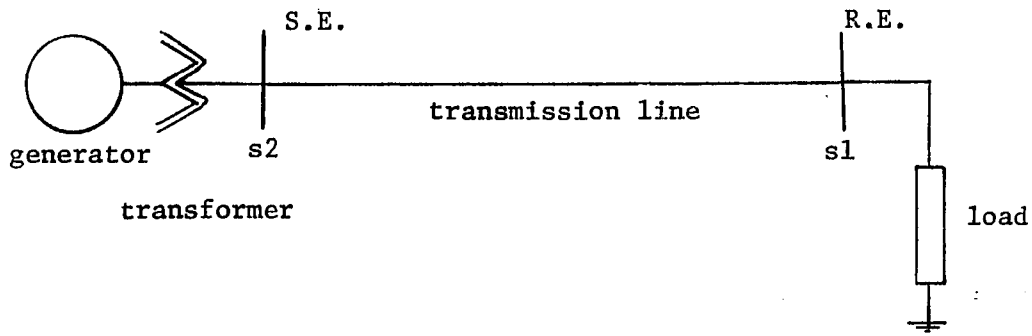


Figure 12.1. An illustrative transmission system

Transmission Line:

In this example, a three-phase transmission line with flat configuration and a ground wire is used as shown in Figure 12.2. The distances between conductors are shown in that figure in ft.

Conductors are AL, ACSR 26/7, KCmi/A1 636

Line length = 200 miles

Voltage = 220 KV

Conductor diameter = .99" = .0825 ft.

Conductor resistance at 50°C = .1618 ohm

GMR = .0335 ft.

Ground wire: steel, diameter = .001 ft., resistance = 4 ohm/mi.,
and GMR = .001 ft.

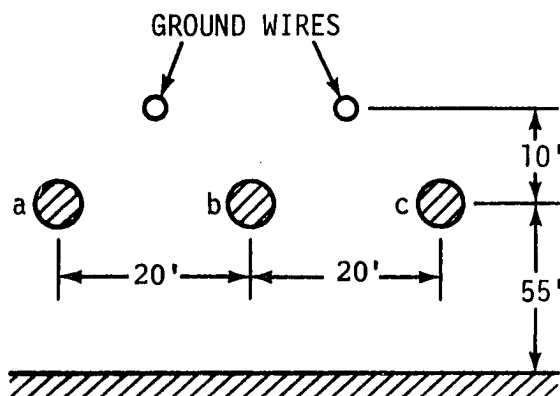


Figure 12.2. Transmission line configuration

Synchronous generator:

The following data are from reference [29] which is based on a 15 KV,
160 MVA system

Rated MVA = 160 MVA , .85 p.f.

Rated KV = 15 KV

$$r_f = .000742 \text{ pu}$$

$$T_d^{\sim} = .023 \text{ sec}$$

$$x_f = 1.651 \text{ pu}$$

$$T_d' = .98 \text{ sec}$$

$$x_d^{\sim} = .185 \text{ pu}$$

$$T_{do}^{\sim} = .033 \text{ sec}$$

$$x_d' = .245 \text{ pu}$$

$$T_{do}' = 5.9 \text{ sec}$$

$$x_d = 1.7 \text{ pu}$$

$$T_q^{\sim} = .023 \text{ sec}$$

$$x_q^{\sim} = .185 \text{ pu}$$

$$T_q' = .51 \text{ sec}$$

$$x_q' = .38 \text{ pu}$$

$$T_{qo}^{\sim} = .076 \text{ sec}$$

$$x_q = 1.64 \text{ pu}$$

$$T'_{qo} = .54 \text{ sec}$$

$$r_a = .0011 \text{ pu}$$

$$r_Q = .054 \text{ pu}$$

$$x_l = x_d = x_q = .15 \text{ pu}$$

$$x_Q = 1.526 \text{ pu}$$

$$r_2 = .016 \text{ pu}$$

$$r_D = .0131 \text{ pu}$$

$$x_2 = .115 \text{ pu}$$

$$x_D = 1.605 \text{ pu}$$

$$x_o = .1 \text{ pu}$$

$$x_{AD} = K M_D = K M_F = M_R = 1.7 - 1.5 = 1.55 \text{ pu}$$

$$x_{AQ} = K M_Q = 1.64 - .15 = 1.49 \text{ pu}$$

If Z_{new} represents the new impedance in the new set of data and Z_{old} represents the old impedance in the old set of data, in order to adapt the foregoing data to a 15 KV, 200 MVA system, the generator parameters must be changed in the following way:

$$Z_{\text{new pu}} = Z_{\text{old pu}} \left(\frac{KV_{\text{old}}}{KV_{\text{new}}} \right)^2 \left(\frac{MVA_{\text{new}}}{MVA_{\text{old}}} \right)$$

$$Z_{\text{base}} \text{ for the generator side} = \frac{(15)^2}{200} = 1.125 \text{ ohm}$$

$$L_{\text{base}} \text{ for the generator side} = Z_{\text{base}} / \omega_o = \frac{1.125}{377} = 2.9841 \times 10^{-3} \text{ H.}$$

$$x_d = 1.7 (200/160) = 2.125 \text{ pu} = 6.3412 \times 10^{-3} \text{ H.}$$

$$x_q = 1.64 (200/160) = 2.05 \text{ pu} = 6.1174 \times 10^{-3} \text{ H.}$$

$$r_a = .0011 \times 1.25 = .001375 \text{ pu} = .001547 \text{ ohm}$$

$$x_{RD} = K M_D = K M_F = M_R = 1.55 \times (200/160) = 1.9375 \text{ pu} = 5.7817 \times 10^{-3} \text{ H.}$$

$$X_{AQ} = K M_Q = 1.49 \times (200/160) = 1.8625 \text{ pu} = 5.5579 \times 10^{-3} \text{ H.}$$

$$x_o = .1 \times (200/160) = .125 \text{ pu} = .373 \times 10^{-3} \text{ H.}$$

$$v_F = .000742 \times (200/160) = .0009275 \text{ pu} = 1.0434 \times 10^{-3} \text{ ohm}$$

$$x_F = 1.651 \times (200/160) = 2.06375 \text{ pu} = 6.15844 \times 10^{-3} \text{ H.}$$

$$L_D = 1.605 \times (200/160) = 2.00625 \text{ pu} = 5.98685 \times 10^{-3} \text{ H.}$$

$$L_Q = 1.526 \times (200/160) = 1.9075 \text{ pu} = 5.6922 \times 10^{-3} \text{ H.}$$

$$r_D = .0131 \times (200/160) = .016375 \text{ pu} = .018422 \text{ ohm}$$

$$r_Q = .054 \times (200/160) = .0675 \text{ pu} = .07594 \text{ ohm}$$

Transformer:

Three-phase

15/220 KV

200 MVA

$$x_1 = x_2 = x_o = .1 \text{ pu}$$

$$r_1 = r_2 = r_o = .0015 \text{ pu}$$

Load:

Load power = 160 MW, unity power factor

Load bus voltage = 200 KV

Fault impedance:

$$r_f = 10 \text{ ohm}$$

$$L_f = .1 \text{ m.H.}$$

System base:

$$\text{Base KV} = 220 \text{ KV}$$

$$\text{Base MVA} = 200 \text{ MVA}$$

$$\text{Base synchronous speed} = 377 \text{ rad/s.}$$

$$\text{Base impedance} = (\text{KV})^2/\text{MVA} = (220)^2/200 = 242 \text{ ohm}$$

$$\text{Base current} = \frac{\text{KV}_L \times 10^3}{\sqrt{3} \times Z_{\text{base}}} = \frac{220 \times 10^3}{\sqrt{3} \times 242} = 524.86 \text{ Amp.}$$

For studying the effect of the generator size, another set of generator data was used. This set of data for a larger generator size is based on 15 KV and 615 MVA as in reference [29].

Generator rating = 615 MVA and 15 KV

$$\text{p.f.} = .975$$

$$x_d'' = .23 \text{ pu}$$

$$x_d' = .2993 \text{ pu}$$

$$x_d = .8979 \text{ pu}$$

$$x_q'' = .2847 \text{ pu}$$

$$x_q' = .646 \text{ pu}$$

$$x_q = .646 \text{ pu}$$

$$r_a = .001 \text{ pu}$$

$$x = .2396 \text{ pu}$$

$$r_2 = .004 \text{ pu}$$

$$x_2 = .298 \text{ pu}$$

$$x_0 = .12 \text{ pu}$$

$$x_F = .74 \text{ pu}$$

$$T_{do}' = 7.4 \text{ sec}$$

$$r_Q = .1 \text{ pu}$$

$$X_Q = .545 \text{ pu}$$

$$r_D = .072 \text{ pu}$$

$$x_D = .698 \text{ pu}$$

$$r_F = .1 \text{ pu}$$

$$X_{AD} = KM_D = KM_F = M_R = .8979 - .2396 = .6583 \text{ pu}$$

$$X_{AQ} = KM_Q = .646 - .2396 = .4064 \text{ pu}$$

By transforming the above data to be based on 15 KV and 200 MVA as

$$x_d = .8979 \times (200/615) = .292 \text{ pu} = .87145 \times 10^{-3} \text{ H.}$$

$$x_q = .646 \times (200/615) = .21 \text{ pu} = .627 \times 10^{-3} \text{ H.}$$

$$r_a = .001 \times (200/615) = .00033 \text{ pu} = .00037 \text{ ohm}$$

$$x_0 = .12 \times (200/615) = .039 \text{ pu} = .11638 \times 10^{-3} \text{ H.}$$

$$x_{AD} = KM_D = KM_F = M_R = .6583 \times (200/615) = .214 \text{ pu} = .6386 \times 10^{-3} \text{ H.}$$

$$x_{AQ} = KM_Q = .4064 \times (200/615) = .1322 \text{ pu} = .3945 \times 10^{-3} \text{ H.}$$

$$r_Q = .1 \times (200/615) = .0325 \text{ pu} = .03656 \text{ ohm}$$

$$x_Q = .545 \times (200/615) = .1772 \text{ pu} = .5288 \times 10^{-3} \text{ H.}$$

$$r_D = .072 \times (200/615) = .0234 \text{ pu} = .02633 \text{ ohm}$$

$$x_D = .698 \times (200/615) = .227 \text{ pu} = .6774 \times 10^{-3} \text{ H.}$$

$$r_F = .1 \times (200/615) = .03252 \text{ pu} = .0366 \text{ ohm}$$

$$x_F = .74 \times (200/615) = .24065 \text{ pu} = .71812 \times 10^{-3} \text{ H.}$$

XIII. APPENDIX B: FAULT TRANSIENT PROGRAM


```

C
C *****
C *
C * FAULT TRANSIENT PROGRAM FOR UNTRANSPOSED TRANSMISSION LINE *
C *
C *****
C
C THIS PROGRAM IS DESIGNED FOR COMPUTING FAULT TRANSIENT VOLTAGES AND
C CURRENTS AND IT'S WAVEFORMS AT THE FAULT LOCATION AND AT THE SEND.
C END OF THE TRANSMISSION LINE BY USING THE CLASSICAL MODEL OF THE
C GENERATOR FOR ALL TYPES OF FAULT.
C TYPES OF FAULTS :
C TYPE 1. LLL THREE PHASE FAULT.
C TYPE 2. LL LINE-TO-LINE FAULT ON PHASES B AND C.
C TYPE 3. LLG DOUBLE-LINE-TO-GROUND FAULT ON PHASES B AND C.
C TYPE 4. LGF SINGLE-LINE-TO-GROUND FAULT ON PHASE A.
C THE FOLLOWING ARE THE INPUT DATA TO BE READ IN
C
C *****
C *
C * READ(5,9)M,N,NI,NCASE,NFT
C * READ(5,10)RF,XLF,DW,DAA,DWW
C * READ(5,10)DAB,DAC,DBC,DS,DWS,RA
C * READ(5,10)HAA,HAB,HAC,HWW,HAW,HBW
C * READ(5,10)DW,DAW,DBW,DCW,XL,XI
C * READ(5,10)RO,GTXS,GTXM,RDP,RW,ZBASE
C * READ(5,10)(VS2(I),I=1,3)
C * READ(5,10)(CS2(I),I=1,3)
C * 9 FORMAT(5I10)
C * 10 FORMAT(6E13.6)
C *
C *****
C

```

```

C      NOTATION USED IN THE PROGRAM
C      *****
C
C      NCASE=NUMBER OF CASES TO BE STUDIED
C      NFT=TYPE OF FAULT NUMBER
C      RF=FAULT RESISTANCE IN PU.
C      XLF=FAULT INDUCTANCE IN H./BASE IMPEDANCE
C      DAA=OUTER DIAMETER OF THE CONDUCTOR IN FT.
C      DWW=OUTER DIAMETER OF THE GROUND WIRE IN FT.
C      DAB,DAC,&DBC ARE THE DISTANCES BETWEEN CONDUCTORS IN FT.
C      DS&DWS ARE THE SELF G.M.D. OF THE CONDUCTOR AND THE GROUND WIRE.
C      RA=RESISTANCE OF THE CONDUCTOR IN OHM PER MILE.
C      HAA,HAB,HAC,HWW,HAW&HBW ARE THE DISTANCES BETWEEN THE CONDUCTORS
C      A,B,C&W AND THEIR IMAGE.
C      RW=RESISTANCE OF THE GROUND WIRE IN OHM PER MILE.
C      DAW,DBW&DCW ARE THE DISTANCES BETWEEN THE GROUND WIRE AND THE
C      CONDUCTORS A,B&C IN FT.
C      XL=TRANSMISSION LINE LENGTH IN MILE.
C      X1=DISTANCE BETWEEN THE FAULT LOCATION AND THE SENDING END BUS.
C      RO=AVERAGE RESISTIVITY OF THE EARTH.
C      GTXS=SELF IMPEDANCE OF THE GENERATOR AND THE TRANSFORMER IN PU.
C      GTXM=MUTUAL IMPEDANCE OF THE GENERATOR AND THE TRANSFORMER IN PU.
C      ZBASE=BASE IMPEDANCE
C      ZBG=EASE IMPEDANCE IN THE GENERATOR SIDE.
C
C      THE SUBROUTINES USED IN THE MAIN PROGRAM
C      *****
C
C      1. SUBROUTINE (LEQ1C) TO FIND THE INVERSE OF A COMPLEX MATRIX.
C      2. SUBROUTINE (EIGCC) TO FIND THE EIGENVALUES AND THE EIGENVECTORS
C      OF A COMPLEX MATRIX.
C      3. SUBROUTINE (ABCD) TO FIND THE CONSTANTS A,B,C&D OF THE TRANSM.
C      LINE IN STEADY STATE CCNDITION.
C      4. SUBROUTINE (VRIR) TO FIND THE VOLTAGES AND THE CURRENTS AT ANY
C      POSITION OF THE TRANSMISSION LINE IN STEADY STATE CCNDITION.

```

C 5. SUBROUTINE (VFT) TO FIND THE PREFault VOLTAGE IN FREQ. DOMAIN.
 C 6. SUBROUTINE (LLLF) TO FIND THE VOLTAGE AT THE FAULT POSITION FOR
 C THREE PHASE FAULT.
 C 7. SUBROUTINE (LLF) TO FIND THE VOLTAGE AT THE FAULT POSITION FOR
 C LINE TO LINE FAULT.
 C 8. SUBROUTINE (LLGF) TO FIND THE VOLTAGE AT THE FAULT POSITION FOR
 C DOUBLE LINE TO GROUND FAULT.
 C 9. SUBROUTINE (LGF) TO FIND THE VOLTAGE AT THE FAULT POSITION FOR
 C SINGLE LINE TO GROUND FAULT.
 C 10. SUBROUTINE (AIFFT) TO FIND THE VOLTAGES AND THE CURRENTS IN THE
 C TIME DOMAIN BY USING THE INVERSE OF THE FAST FOURIER TRANSFORM.

C THE MAIN PROGRAM

C *****

C
 C COMPLEX Z(4,4),ZABC(3,3),YABC(3,3),A(3,3),S(3,3),QI(3,3),
 *GAMA(3),SI(3,3),Q(3,3),B1(3),A2(3),B2(3),A1QI(3,3),A2QI(3,3),
 *QB2QI(3,3),SA1SI(3,3),SA2SI(3,3),QA1QI(3,3),QA2QI(3,3),
 *A1SI(3,3),T11(3,3),T31(3,3),T1(3,3),T3(3,3),T41(3,3),T2(3,3)
 COMPLEX T4(3,3),TVRI(3,3),VR(3),CR(3),VS(3),CS(3),VSA1(1024),
 *CSA1(1024),CSB1(1024),CSC1(1024),VFA(1024),VFB(1024),VFC(1024),
 *T2I(3,3),T4I(3,3),T2IT1(3,3),T4IT3(3,3),ZT23(3,3),T2I43(3,3),
 *A2SI(3,3),QB1QI(3,3),VSC1(1024),T21(3,3),A1(3),GAMA(3)
 COMPLEX CFB(1024),CFC(1024),TVR(3,3),CFA(1024),VSB1(1024),
 *APL(3,3),BPL(3,3),CPL(3,3),AS(3,3),BS(3,3),AJFS,VS2(3),U1(3,3),
 *ZGTS(3,3),ZF(3,3),ZLD(3,3),YP(3,3),VSP(3),CSP(3),ZP(3,3),CS2(3),
 *CMPLX,CEXP,CSQRT,EV(3,3),ZN,CLMDA(3),C(3,3),TI(3,3),CFFA
 COMPLEX VRP(3),CRP(3),CSS(3,3),VF(3),DPL(3,3),DSS(3,3),ZABCW(4,4),
 *SIZ(3,3),GSIZ(3,3),ZO(3,3),ZOI(3,3),B1QI(3,3),B2QI(3,3),T22(3,3),
 *T42(3,3),QIZOI(3,3),B1QIZI(3,3),B2QIZI(3,3),T111(3,3),T311(3,3),
 *CFFB,CFFC,ZFT,CWK(129)
 DIMENSION IWK(8),ST(129),CT(129),FREQU(129),AMAG(129)
 DIMENSION WA(18),VRM(3),TIME(1024),WK(30),CCS1(1024),CA(3,3),
 *CRM(3),PHVR(3),PHCR(3),VSPM(3),PHVS(3),CSPM(3),PHCS(3),
 *CCF(1024),VAS1(1024),VBS1(1024),VCS1(1024),CAS1(1024),CBS1(1024),

```

*VAF(1024),VBF(1024),VCF(1024),CAF(1024),CBF(1024),P(4,4),PABC(3,3)
PI=3.1415927
WO=120.*PI
READ(5,9)M,N,NI,NCASE,NFT
READ(5,10)RF,XLF,DW,DIA,DWW,ZBG
READ(5,10) DAB,DAC,DBC,DS,DWS,RA
READ(5,10)HAA,HAB,HAC,HWW,HAW,HBW
READ(5,10) RW,DAW,DBW,DCW,XL,X1
READ(5,10) RD,GTXS,GTXM,RDP,RW,ZBASE
9  FORMAT(5I10)
10 FORMAT(6E13.6)
X2=XL-X1

C
C *****
C * STEADY STATE CONDITION *
C *****
C
C COMPUTE THE IMPEDANCE AND THE ADMITTANCE MATRICES.
RPA=RA+RDP
RPW=RW+RDP
WLAA=.12134*ALOG(2790/DS)
WLAB=.12134*ALOG(2790/DAB)
WLAC=.12134*ALOG(2790/DAC)
WLBC=.12134*ALOG(2790/DBC)
WLG=.12134*ALOG(2790/DWS)
WLAG=.12134*ALOG(2790/DAW)
WLBG=.12134*ALOG(2790/DBW)
WLCG=.12134*ALOG(2790/DCW)
ZABCW(1,1)=CMPLX(RPA,WLAA)/ZBASE
ZABCW(1,2)=CMPLX(RDP,WLAB)/ZBASE
ZABCW(1,3)=CMPLX(RDP,WLAC)/ZBASE
ZABCW(1,4)=CMPLX(RDP,WLAG)/ZBASE
ZABCW(2,2)=ZABCW(1,1)
ZABCW(2,3)=CMPLX(RDP,WLBC)/ZBASE
ZABCW(2,4)=CMPLX(RDP,WLBG)/ZBASE

```

```

ZABCW(3,3)=ZABCW(1,1)
ZABCW(3,4)=CMPLX(RDP,WLCG)/ZBASE
ZABCW(4,4)=CMPLX(RPW,WLG)/ZBASE
ZP(1,1)=ZABCW(1,1)-ZABCW(1,4)*ZABCW(1,4)/ZABCW(4,4)
ZP(1,2)=ZABCW(1,2)-ZABCW(1,4)*ZABCW(2,4)/ZABCW(4,4)
ZP(1,3)=ZABCW(1,3)-ZABCW(1,4)*ZABCW(3,4)/ZABCW(4,4)
ZP(2,2)=ZABCW(2,2)-ZABCW(2,4)*ZABCW(2,4)/ZABCW(4,4)
ZP(2,3)=ZABCW(2,3)-ZABCW(2,4)*ZABCW(3,4)/ZABCW(4,4)
ZP(3,3)=ZABCW(3,3)-ZABCW(3,4)*ZABCW(3,4)/ZABCW(4,4)
ZP(2,1)=ZP(1,2)
ZP(3,1)=ZP(1,3)
ZP(3,2)=ZP(2,3)
C  CALCULATION OF THE CAPICITANCE OF THE TRANSMISSION LINE.
C  CALCULATION OF MATRIX 'P' IN MI/MF
P(1,1)=11.185*ALOG(2*HAA/DAA)
P(1,2)=11.185*ALOG(HAB/DAB)
P(1,3)=11.185*ALOG(HAC/DAC)
P(1,4)=11.185*ALOG(HAW/DAW)
P(2,4)=11.185*ALOG(HBW/DBW)
P(2,2)=P(1,1)
P(2,3)=P(1,2)
P(3,3)=P(1,1)
P(3,4)=P(1,4)
P(4,4)=11.185*ALOG(2*HWW/DWW)
PABC(1,1)=P(1,1)-P(1,4)*P(1,4)/P(4,4)
PABC(1,2)=P(1,2)-P(1,4)*P(2,4)/P(4,4)
PABC(1,3)=P(1,3)-P(1,4)*P(3,4)/P(4,4)
PABC(2,2)=P(2,2)-P(2,4)*P(2,4)/P(4,4)
PABC(2,3)=P(2,3)-P(2,4)*P(3,4)/P(4,4)
PABC(3,3)=P(3,3)-P(3,4)*P(3,4)/P(4,4)
PABC(2,1)=PABC(1,2)
PABC(3,1)=PABC(1,3)
PABC(3,2)=PABC(2,3)
C  FIND THE INVERSE OF MATRIX 'P' AND THAT IS MATRIX 'C' IN MIC.F./MI
DO 401 I=1,3

```

```

      DO 402 J=1,3
      UI(I,J)=CMFLX(PABC(I,J),0.0)
402  C(I,J)=(0.0,0.0)
401  C(I,I)=(1.0,0.0)
      CALL LEQTIC(U1,3,3,C,3,3,0,WA,IER)
      IF(IER.NE.0)GO TO 1111
C    TO FIND 'C' IN FARAD AND 'YP' IN P.U.
      DO 403 I=1,3
      DO 403 J=1,3
      CA(I,J)=-CABS(C(I,J))*1.E-06
      CA(I,I)=CABS(C(I,I))*1.E-06
      YP(I,J)=CMPLX(0.0,CA(I,J)*WD)*ZBASE
403  CONTINUE
C    LOAD IMPEDANCE MATRIX AND CALL IT (ZLD)
      DO 211 I=1,3
      READ(5,10){ZLD(I,J),J=1,3}
211  CONTINUE
C    READ THE VOLTAGES AND CURRENTS AT THE R.E.OF THE TRANSMISSION LINE.
      READ(5,10){VS2(I),I=1,3}
      READ(5,10){CS2(I),I=1,3}
C    CALL SUBROUTINE TO FIND THE CONSTANTS A,B,C,&D AT THE SENDING END.
      CALL ABCD(XL,ZP,YP,APL,BPL,CPL,DPL)
C    CALL SUBROUTINE TO FIND THE CONSTANTS A,B,C,&D AT THE FAULT LOC.
      CALL ABCD(X2,ZP,YP,AS,BS,CSS,DSS)
C    CALL SUBROUTINE TO FIND VOLTAGES AND CURRENTS AT THE FAULT POSIT.
      CALL VRIR(VS2,CS2,AS,BS,CSS,DSS,VRP,CRP,VRM,CRM,PHVR,PHCR)
      WRITE(6,363)
363  FORMAT('0',10X,'PREFault VOLTAGES & CURRENTS AT X1',//,10X,'*****
*****',//,12X,'VRM',21X,'PHVR',20X,
*'CRM',21X,'PHCR')
      DO 367 I=1,3
367  WRITE(6,368) VRM(I),PHVR(I),CRM(I),PHCR(I)
368  FORMAT('0',10X,4(E13.6,11X))
C    CALL SUBROUTINE TO FIND VOLTAGES AND CURRENTS AT THE S.E.
      CALL VRIR(VS2,CS2,APL,BPL,CPL,DPL,VSP,CSP,VSPM,CSPM,PHVS,PHCS)

```

```

WRITE(6,361)
361  FORMAT('0',10X,'SENDING PREFault CONDITION',//,10X,'*****
*****',//,12X,'VSPM',20X,'PHVS',20X,'CSPM',20X,'PHCS')
DO 366 I=1,3
366  WRITE(6,368) VSPM(I),PHVS(I),CSPM(I),PHCS(I)
C
C      *****
C      * TRANSIENT CONDITION *
C      *****
C
DW=DW*PI
DWC11=DW*CA(1,1)
DWC12=DW*CA(1,2)
DWC13=DW*CA(1,3)
DWC22=DW*CA(2,2)
DWC23=DW*CA(2,3)
DWC33=DW*CA(3,3)
DO 1 IK=1,N
    IJ=2*IK-1
    AJ=FLOAT(IJ)/2.0
    W=DW*AJ
    FREQ=W/(2.0*PI)
C      GENERATOR AND TRANSFORMER IMPEDANCE MATRIX AND CALL IT (ZGTS)
    GTLS=GTXS/W0
    GTLM=GTXM/W0
    DO 5 I=1,3
    DO 7 J=1,3
7      ZGTS(I,J)=-CMPLX((DW*GTLM),(W*GTLM))
5      ZGTS(I,I)=CMPLX((DW*GTLS),(W*GTLS))
C      INPUT FAULT IMPEDANCE MATRIX
    DO 15 I=1,3
    DO 20 J=1,3
20      ZF(I,J)=(0.0,0.0)
15      ZF(I,I)=CMPLX((RF+DW*XLf),W*XLf)
C      COMPUTE THE IMPEDANCE AND ADMITTANCE MATRICES OF THE T.L.

```

```

C      COMPUTE THE RESISTANCE OF THE CONDUCTORS BY BESSEL FUNCTION.
C      (A) FOR THE THREE PHASE CONDUCTORS
      RMA=.0636*SQRT(FREQ/RA)
      BERM R=1.-(RMA)**4/64.
      BERM RP=- (RMA)**3/16.
      BEIM R=(RMA)**2/4.
      BEIM RP=(RMA)/2.
      RAA=RA*RMA/2.*((BERM R*BEIM RP-BEIM R*BERM RP)/(BERM RP**2+BEIM RP**2))
C      (B) THE RESISTANCE OF THE GROUND WIRE
      RMW=.0636*SQRT(FREQ/RW)
      BERM W=1-(RMW)**4/64.
      BERM WP=- (RMW)**3/16.
      BEIM W=(RMW)**2/4.
      BEIM WP=(RMW)/2.
      RWW=RW*RMW/2.*((BERM W*BEIM WP-BEIM W*BERM WP)/(BERM WP**2+BEIM WP**2))
      RD=1.588*.1E-02*FREQ
      R=RAA+RD
      DE=DW*.3219E-03*ALOG(2160.*SQRT(RD/FREQ))
      DWL=DE-.3219E-03*ALOG(DS)*DW
      DWLAB=DE-.3219E-03*ALOG(DAB)*DW
      DWLAC=DE-.3219E-03*ALOG(DAC)*DW
      DWLBC=DE-.3219E-03*ALOG(DBC)*DW
      DWLG=DE-.3219E-03*ALOG(DWS)*DW
      DWLAG=DE-.3219E-03*ALOG(DAW)*DW
      DWLBG=DE-.3219E-03*ALOG(DBW)*DW
      DWLCG=DE-.3219E-03*ALOG(DCW)*DW
      Z(1,1)=CMPLX((R+DWL),DWL*AJ)/ZBASE
      Z(1,2)=CMPLX((RD+DWLAB),DWLAB*AJ)/ZBASE
      Z(1,3)=CMPLX((RD+DWLAC),DWLAC*AJ)/ZBASE
      Z(1,4)=CMPLX((RD+DWLAG),DWLAG*AJ)/ZBASE
      Z(2,2)=Z(1,1)
      Z(2,3)=CMPLX((RD+DWLBC),DWLBC*AJ)/ZBASE
      Z(2,4)=CMPLX((RD+DWLBG),DWLBG*AJ)/ZBASE
      Z(3,3)=Z(1,1)
      Z(3,4)=CMPLX((RD+DWLCG),DWLCG*AJ)/ZBASE

```



```

Z(4,4)=CMPLX((RWW+RD+DWLG),DWLG*AJ)/ZBASE
ZABC(1,1)=Z(1,1)-Z(1,4)*Z(1,4)/Z(4,4)
ZABC(1,2)=Z(1,2)-Z(1,4)*Z(2,4)/Z(4,4)
ZABC(1,3)=Z(1,3)-Z(1,4)*Z(3,4)/Z(4,4)
ZABC(2,2)=Z(2,2)-Z(2,4)*Z(2,4)/Z(4,4)
ZABC(2,3)=Z(2,3)-Z(2,4)*Z(3,4)/Z(4,4)
ZABC(3,3)=Z(3,3)-Z(3,4)*Z(3,4)/Z(4,4)
ZABC(2,1)=ZABC(1,2)
ZABC(3,1)=ZABC(1,3)
ZABC(3,2)=ZABC(2,3)
YABC(1,1)=CMPLX(DWC11,DWC11*AJ)*ZBASE
YABC(1,2)=CMPLX(DWC12,DWC12*AJ)*ZBASE
YABC(1,3)=CMPLX(DWC13,DWC13*AJ)*ZBASE
YABC(2,2)=CMPLX(DWC22,DWC22*AJ)*ZBASE
YABC(2,3)=CMPLX(DWC23,DWC23*AJ)*ZBASE
YABC(3,3)=CMPLX(DWC33,DWC33*AJ)*ZBASE
YABC(2,1)=YABC(1,2)
YABC(3,1)=YABC(1,3)
YABC(3,2)=YABC(2,3)
C      MULTIPLY ZABC BY YABC AND CALL IT 'A'
      DO 40 II=1,3
      DO 40 JJ=1,3
      A(II,JJ)=(0.0,0.0)
      DO 40 KK=1,3
      A(II,JJ)=A(II,JJ)+ZABC(II,KK)*YABC(KK,JJ)
40     CONTINUE
C      CALL SUBROUTINE TO GET EIGENVALUES AND EIGENVECTORS
      CALL EIGCC(A,3,3,1,CLMDA,EV,3,WK,IER)
      IF(WK(1).GT.100.0)GO TO 3333
      DO 45 I=1,3
      DO 45 J=1,3
      ZN=EV(1,J)
      EV(I,J)=EV(I,J)/ZN
      S(I,J)=EV(I,J)
45     CONTINUE

```

```

DO 50 I=1,3
DO 50 J=1,3
50 QI(I,J)=S(J,I)
C TO GET THE MATRIX GAMA
DO 55 I=1,3
GAMA(I)=CSQRT(CLMDA(I))
GAMAI(I)=1.0/GAMA(I)
55 CONTINUE
C CALL THE SUBROUTINE TO GET THE THE INVERSE OF S AND CALL IT SI
DO 60 I=1,3
DO 65 J=1,3
U1(I,J)=S(I,J)
65 SI(I,J)=(0.0,0.0)
60 SI(I,I)=(1.0,0.0)
CALL LEQTIC(U1,3,3,SI,3,3,0,WA,IER)
IF(IER.NE.0)GO TO 1111
DO 70 I=1,3
DO 75 J=1,3
U1(I,J)=QI(I,J)
75 Q(I,J)=(0.0,0.0)
70 Q(I,I)=(1.0,0.0)
CALL LEQTIC(U1,3,3,Q,3,3,0,WA,IER)
IF(IER.NE.0)GO TO 1111
C FIND SI*ZABC AND CALL IT SIZ
DO 85 I=1,3
DO 85 J=1,3
SIZ(I,J)=(0.0,0.0)
DO 85 K=1,3
SIZ(I,J)=SIZ(I,J)+SI(I,K)*ZABC(K,J)
85 CONTINUE
C COMPUTE GAMA*SI*Z AND CALL IT GSIZ
DO 90 I=1,3
DO 90 J=1,3
90 GSIZ(I,J)=GAMAI(I)*SIZ(I,J)
C FIND ZO WHICH IS EQUAL TO (GAMAI*SI*Z*Q) AND CALL IT ZO

```

```

      DO 100 I=1,3
      DO 100 J=1,3
      ZO(I,J)=(0.0,0.0)
      DO 100 K=1,3
      ZO(I,J)=ZO(I,J)+S(I,K)*GSIZ(K,J)
100    CONTINUE
C      CALL SUBROUTINE TO GET THE INVERSE OF ZO AND CALL IT ZOI
      DO 105 I=1,3
      DO 110 J=1,3
      UI(I,J)=ZO(I,J)
110    ZOI(I,J)=(0.0,0.0)
105    ZOI(I,1)=(1.0,0.0)
      CALL LEQTIC(UI,3,3,ZOI,3,3,0,WA,IER)
      IF(IER.NE.0)GO TO 1111
C      CALCULATION OF THE TRANSMISSION LINE CONSTANTS
      DO 115 I=1,3
      A1(I)=.5*(CEXP(X1*GAMA(I))+CEXP(-X1*GAMA(I)))
      A2(I)=.5*(CEXP(X2*GAMA(I))+CEXP(-X2*GAMA(I)))
      B1(I)=.5*(CEXP(X1*GAMA(I))-CEXP(-X1*GAMA(I)))
      B2(I)=.5*(CEXP(X2*GAMA(I))-CEXP(-X2*GAMA(I)))
115    CONTINUE
      DO 120 I=1,3
      DO 120 J=1,3
      A1QI(I,J)=A1(I)*QI(I,J)
      A2QI(I,J)=A2(I)*QI(I,J)
      A1SI(I,J)=A1(I)*SI(I,J)
      A2SI(I,J)=A2(I)*SI(I,J)
      B1QI(I,J)=B1(I)*QI(I,J)
      B2QI(I,J)=B2(I)*QI(I,J)
120    CONTINUE
C      GET S*(COSH.GAMAX1)*QI AND CALL IT (SA1SI)
C      GET S*(COSH.GAMAX2)*QI AND CALL IT (SA2SI)
C      GET Q*(COSH.GAMX1)*QI AND CALL IT (QA1QI)
C      GET Q*(COSH.GAMX2)*QI AND CALL IT (QA2QI)
C      GET Q*(SINH.GAMAX1)*QI AND CALL IT (QB1QI)

```

```

C
GET Q*(SINH.GAMAX2)*QI AND CALL IT (QB2QI)
DO 130 I=1,3
DO 130 J=1,3
SA1SI(I,J)=(0.0,0.0)
SA2SI(I,J)=(0.0,0.0)
QA1QI(I,J)=(0.0,0.0)
QA2QI(I,J)=(0.0,0.0)
QB1QI(I,J)=(0.0,0.0)
QB2QI(I,J)=(0.0,0.0)
DO 130 K=1,3
QA1QI(I,J)=QA1QI(I,J)+Q(I,K)*A1QI(K,J)
QA2QI(I,J)=QA2QI(I,J)+Q(I,K)*A2QI(K,J)
SA1SI(I,J)=SA1SI(I,J)+S(I,K)*A1SI(K,J)
SA2SI(I,J)=SA2SI(I,J)+S(I,K)*A2SI(K,J)
QB1QI(I,J)=QB1QI(I,J)+Q(I,K)*B1QI(K,J)
QB2QI(I,J)=QB2QI(I,J)+Q(I,K)*B2QI(K,J)
CONTINUE
130
C
CALCULATION OF THE TS MATRICES (T1,T2,T3,T4)
T2=ZQ*(QB1QI)+(ZGTS)*(QA1QI)=T21+T22
T4=ZQ*(QB2QI)+(ZLD)*(QA2QI)=T41+T42
DO 140 I=1,3
DO 140 J=1,3
T21(I,J)=(0.0,0.0)
T22(I,J)=(0.0,0.0)
T41(I,J)=(0.0,0.0)
T42(I,J)=(0.0,0.0)
DO 140 K=1,3
T21(I,J)=T21(I,J)+ZQ(I,K)*QB1QI(K,J)
T22(I,J)=T22(I,J)+ZGTS(I,K)*QA1QI(K,J)
T41(I,J)=T41(I,J)+T22(I,J)
T41(I,J)=T41(I,J)+ZQ(I,K)*QB2QI(K,J)
T42(I,J)=T42(I,J)+ZLD(I,K)*QA2QI(K,J)
T4(I,J)=T42(I,J)+T41(I,J)
CONTINUE
140
C
GET QI*ZOI AND CALL IT (QIZOI)

```

```

DO 150 I=1,3
DO 150 J=1,3
QIZOI(I,J)=(0.0,0.0)
DO 150 K=1,3
QIZOI(I,J)=QIZOI(I,J)+QI(I,K)*ZOI(K,J)
150 CONTINUE
C COMPUTE SINH(GAMAX1)*(QI*ZOI) AND CALL IT (B1QIZI)
C COMPUTE SINH(GAMAX2)*(QI*ZOI) AND CALL IT (B2QIZI)
DO 155 I=1,3
DO 155 J=1,3
B1QIZI(I,J)=(0.0,0.0)
B2QIZI(I,J)=(0.0,0.0)
155 CONTINUE
DO 160 I=1,3
DO 160 J=1,3
B1QIZI(I,J)=B1QIZI(I,J)+B1(I)*QIZOI(I,J)
B2QIZI(I,J)=B2QIZI(I,J)+B2(I)*QIZOI(I,J)
160 CONTINUE
C COMPUTE T11=Q*(SINH.GAMAX1)*QI*ZOI
C COMPUTE T31=Q*(SINH.GAMAX2)*QI*ZOI
DO 170 I=1,3
DO 170 J=1,3
T11(I,J)=(0.0,0.0)
T31(I,J)=(0.0,0.0)
DO 170 K=1,3
T11(I,J)=T11(I,J)+Q(I,K)*B1QIZI(K,J)
T31(I,J)=T31(I,J)+Q(I,K)*B2QIZI(K,J)
170 CONTINUE
C COMPUTE T111 AND T311 WHERE: T111=ZGTS*T11 AND T311=ZLD*T31
DO 180 I=1,3
DO 180 J=1,3
T111(I,J)=(0.0,0.0)
T311(I,J)=(0.0,0.0)
DO 180 K=1,3
T111(I,J)=T111(I,J)+ZGTS(I,K)*T11(K,J)

```

```

      T311(I,J)=T311(I,J)+ZLD(I,K)*T31(K,J)
180  CONTINUE
      DO 185 I=1,3
      DO 185 J=1,3
      T1(I,J)=SA1SI(I,J)+T111(I,J)
      T3(I,J)=SA2SI(I,J)+T311(I,J)
185  CONTINUE
C    CALL SUBROUTINE TO GET THE INVERSE OF T2 & T4, THEN CALL IT T2I
C    AND T4I.
      DO 190 I=1,3
      DO 195 J=1,3
      U1(I,J)=T2(I,J)
195  T2I(I,J)=(0.0,0.0)
190  T2I(I,I)=(1.0,0.0)
      CALL LEQTIC(U1,3,3,T2I,3,3,0,WA,IER)
      IF(IER.NE.0)GO TO 1111
      DO 200 I=1,3
      DO 205 J=1,3
      U1(I,J)=T4(I,J)
205  T4I(I,J)=(0.0,0.0)
200  T4I(I,I)=(1.0,0.0)
      CALL LEQTIC(U1,3,3,T4I,3,3,0,WA,IER)
      IF(IER.NE.0)GO TO 1111
      DO 215 I=1,3
      DO 215 J=1,3
      T2IT1(I,J)=(0.0,0.0)
      T4IT3(I,J)=(0.0,0.0)
      DO 215 K=1,3
      T2IT1(I,J)=T2IT1(I,J)+T2I(I,K)*T1(K,J)
      T4IT3(I,J)=T4IT3(I,J)+T4I(I,K)*T3(K,J)
      T2143(I,J)=T2IT1(I,J)+T4IT3(I,J)
215  CONTINUE
C    MULTIPLY ZF*T2143 AND CA - IT ZT23
      DO 225 I=1,3
      DO 225 J=1,3

```

```

      ZT23(I,J)=(0.0,0.0)
      DO 225 K=1,3
      ZT23(I,J)=ZT23(I,J)+ZF(I,K)*T2143(K,J)
      IF(I.EQ.J)GO TO 230
      TVR(I,J)=ZT23(I,J)
      GO TO 225
230    TVR(I,J)=1.0+ZT23(I,J)
225    CONTINUE
C      CALL SUBROUTINE TO GET THE INVERSE OF TVR AND CALL IT TVRI
      DO 235 I=1,3
      DO 240 J=1,3
      U1(I,J)=TVR(I,J)
240    TVRI(I,J)=(0.0,0.0)
235    TVRI(I,I)=(1.0,0.0)
      CALL LEQTIC(U1,3,3,TVRI,3,3,0,WA,IER)
      IF(IER.NE.0)GO TO 1111
C      CALL SUBROUTINE TO FIND THE THREE PHASE VOLTAGES AT THE FAULT
C      LOCATION (VR).
      CALL VFT(VRM,W,W0,DW,PHVR,VF)
      IF(NFT.EQ.1)GO TO 1000
      IF(NFT.EQ.2)GO TO 2000
      IF(NFT.EQ.3)GO TO 3000
      IF(NFT.EQ.4)GO TO 4000
1000    CALL LLLF(TVRI,T2IT1,VF,VR)
      GO TO 5000
2000    CALL LLF(VF,TI,ZF,VR)
      GO TO 5000
3000    CALL LLGF(VF,TI,ZF,VR)
      GO TO 5000
4000    CALL LGF(VF,TI,ZF,VR)
5000    CONTINUE
C      FINDING THE THREE PHASE CURRENTS AT THE FAULT LOCATION (CR).
      DO 245 I=1,3
      CR(I)=(0.0,0.0)
245    CONTINUE

```

```

750      DO 750 I=1,3
750      DO 750 J=1,3
750      CR(I)=CR(I)-T2IT1(I,J)*VR(J)
750      FINDING THE THREE PHASE VOLTAGES AND CURRENTS AT THE S.E.
255      DO 255 I=1,3
255      VS(I)=(0.0,0.0)
255      CS(I)=(0.0,0.0)
255      CONTINUE
260      DO 260 I=1,3
260      DO 260 J=1,3
260      VS(I)=VS(I)+SA1SI(I,J)*VR(J)+T2I1(I,J)*CR(J)
260      CS(I)=CS(I)+T1I1(I,J)*VR(J)+QA1QI(I,J)*CR(J)
260      CONTINUE
260      FINDING THE VOLTAGE AND THE CURRENT COMPONENTS AT THE FAULT
260      LOCATION AND AT THE SENDING END IN FREQUENCY DOMAIN.
260      ARC=PI*AJ/FLOAT(N)
260      SIGMA=SIN(ARC)/ARC
260      VFA(IK)=VR(1)*SIGMA*DW
260      VFB(IK)=VR(2)*SIGMA*DW
260      VFC(IK)=VR(3)*SIGMA*DW
260      CFA(IK)=CR(1)*SIGMA*DW
260      CFB(IK)=CR(2)*SIGMA*DW
260      CFC(IK)=CR(3)*SIGMA*DW
260      VSA1(IK)=VS(1)*SIGMA*DW
260      VSB1(IK)=VS(2)*SIGMA*DW
260      VSC1(IK)=VS(3)*SIGMA*DW
260      CSA1(IK)=CS(1)*SIGMA*DW
260      CSB1(IK)=CS(2)*SIGMA*DW
260      CSC1(IK)=CS(3)*SIGMA*DW
1      CONTINUE
1      FINDING THE VOLTAGE AND THE CURRENT COMPONENTS AT THE FAULT
1      LOCATION AND AT THE SENDING END IN TIME DOMAIN.
1      CALL AIFFT(VSA1,M)
1      CALL AIFFT(VSB1,M)
1      CALL AIFFT(VSC1,M)

```



```

CALL AIFFT(CSA1,M)
CALL AIFFT(CSB1,M)
CALL AIFFT(CSC1,M)
CALL AIFFT(VFA,M)
CALL AIFFT(VFB,M)
CALL AIFFT(VFC,M)
CALL AIFFT(CFA,M)
CALL AIFFT(CFB,M)
CALL AIFFT(CFC,M)
DT=2.*PI/(DW*FLOAT(N))
N2=N/4
DO 265 I=1,N2
JJ=I-1
AJ=FLOAT(JJ)
WOT=WC*DT*AJ
ADT=DW*DT*AJ
ATN=EXP(ADT)/PI
AJFS=CMPLX(COS(PI*AJ/FLOAT(N)),SIN(PI*AJ/FLOAT(N)))
VFA(I)=VFA(I)*AJFS
VFB(I)=VFB(I)*AJFS
VFC(I)=VFC(I)*AJFS
CFA(I)=CFA(I)*AJFS
CFB(I)=CFB(I)*AJFS
CFC(I)=CFC(I)*AJFS
VSA1(I)=VSA1(I)*AJFS
VSB1(I)=VSB1(I)*AJFS
VSC1(I)=VSC1(I)*AJFS
CSA1(I)=CSA1(I)*AJFS
CSB1(I)=CSB1(I)*AJFS
CSC1(I)=CSC1(I)*AJFS
TIME(I)=DT*FLOAT(I-1)
VAF(I)=ATN*REAL(VFA(I))+VRM(1)*COS(WOT+PHVR(1))
VBF(I)=ATN*REAL(VFB(I))+VRM(2)*COS(WOT+PHVR(2))
VCF(I)=ATN*REAL(VFC(I))+VRM(3)*COS(WOT+PHVR(3))
CAF(I)=ATN*REAL(CFA(I))+CRM(1)*COS(WOT+PHCR(1))

```

```

      CBF(I)=ATN*REAL(CFB(I))+CRM(2)*CCS(WOT+PHCR(2))
      CCF(I)=ATN*REAL(CFC(I))+CRM(3)*CCS(WOT+PHCR(3))
      VAS1(I)=ATN*REAL(VSA1(I))+VSPM(1)*COS(WOT+PHVS(1))
      VBS1(I)=ATN*REAL(VSB1(I))+VSPM(2)*COS(WOT+PHVS(2))
      VCS1(I)=ATN*REAL(VSC1(I))+VSPM(3)*COS(WOT+PHVS(3))
      CAS1(I)=ATN*REAL(CSA1(I))+CSPM(1)*COS(WOT+PHCS(1))
      CBS1(I)=ATN*REAL(CSB1(I))+CSPM(2)*COS(WOT+PHCS(2))
      CCS1(I)=ATN*REAL(CSC1(I))+CSPM(3)*COS(WOT+PHCS(3))
265  CONTINUE
      WRITE(6,264) X1
264  FORMAT('1',10X,'CURRENTS & VOLTAGES AT FAULT LOCATION FOR 3 PHASE
*FAULT AT',E13.6,'MILES',//,10X,'*****'
*****',//,8X,'TIME',15X,'VAF'
*,15X,'CAF',15X,'VBF',15X,'CBF',15X,'VCF',15X,'CCF')
      DO 269 I=1,N2
269  WRITE(6,268) TIME(I),VAF(I),CAF(I),VBF(I),CBF(I),VCF(I),CCF(I)
268  FORMAT(4X,7(E13.6,5X))
      WRITE(6,266) X1
266  FORMAT('1',10X,'SENDING END CURRENTS & VOLTAGES FOR 3 PHASE FAULT
* AT',E13.6,'MILES',//,10X,'*****'
*****',//,8X,'TIME',15X,'VAS',15X,'CAS
*',15X,'VBS',15X,'CBS',15X,'VCS',15X,'CCF')
      DO 267 I=1,N2
267  WRITE(6,268) TIME(I),VAS1(I),CAS1(I),VBS1(I),CBS1(I),VCS1(I),
*CCS1(I)
C    FINDING THE MAGNITUDE OF THE SENDING END VOLTAGE OF PHASE A AT
C    DIFFERENT FREQUENCY COMPONENTS BY USING SUBROUTINE FFTSC.
      CALL FFTSC(VAS1,N2,ST,CT,IWK,WK,CWK)
      WRITE(6,460)
460  FORMAT('1',10X,'THE MAGNITUDE OF THE FREQUENCY COMP. OF THE VOLTAGE
*E OF PH. A (VSA1) AT THE S.E.',//,10X,'*****'
*****',//,20X,'FRE
*QUENCY',20X,'MAGNITUDE')
455  FORMAT(20X,2(E11.4,18X))
      DO 450 I=1,129

```



```

SUBROUTINE ABCD(X1,ZP,YP,AP,BP,CP,DP)
  COMPLEX AP(3,3),BP(3,3),CP(3,3),ZP(3,3),YP(3,3),
  *SZYP(3,3),ZYP(3,3),SZYP(3,3),ZPI(3,3),COSZYP(3,3),DP(3,3),
  *SINSZY(3,3),COSSZY(3,3),ZCI(3,3),TEMP(3,3)
  DIMENSION WA(18),U(3,3)
C    MULTIPLY ZP*YP AND CALL IT ZYP
      DO 275 I=1,3
      DO 275 J=1,3
275    ZYP(I,J)=(0.0,0.0)
      DO 280 I=1,3
      DO 280 J=1,3
      DO 280 K=1,3
280    ZYP(I,J)=ZYP(I,J)+ZP(I,K)*YP(K,J)
C    FIND THE SQRT OF ZYP AND CALL IT SZYP
      DO 285 I=1,3
      DO 285 J=1,3
285    SZYP(I,J)=CSQRT(ZYP(I,J))
C    FIND THE INVERSE OF SZYP AND CALL IT SZYPI
      DO 290 I=1,3
      DO 295 J=1,3
      TEMP(I,J)=SZYP(I,J)
295    SZYPI(I,J)=(0.0,0.0)
290    SZYPI(I,I)=(1.0,0.0)
      CALL LEQTIC(TEMP,3,3,SZYPI,3,3,0,WA,IER)
C    FIND THE SINSH AND COSH WHICH ARE EQUAL TO (EX1-EX2)/2. AND (EX1+EX2)/2.
      DO 300 I=1,3
      DO 305 J=1,3
305    U(I,J)=0.0
300    U(I,I)=1.0
      DO 310 I=1,3
      DO 310 J=1,3
310    SINSZY(I,J)=SZYP(I,J)*X1
      DO 315 I=1,3
      DO 315 J=1,3
315    COSSZY(I,J)=U(I,J)+.5*X1*X1*ZYP(I,J)

```

```

      DO 360 I=1,3
      DO 360 J=1,3
360   AP(I,J)=COSSZY(I,J)
C     MULTIPLY SINSZY * SZYPI * ZP WHICH IS EQUAL TO BP
      DO 301 I=1,3
      DO 301 J=1,3
      ZCI(I,J)=(0.0,0.0)
      DO 301 K=1,3
301   ZCI(I,J)=ZCI(I,J)+SINSZY(I,K)*SZYPI(K,J)
      DO 302 I=1,3
      DO 302 J=1,3
      BP(I,J)=(0.0,0.0)
      DO 302 K=1,3
302   BP(I,J)=BP(I,J)+ZCI(I,K)*ZP(K,J)
C     FIND THE INVERSE OF MATRIX ZP AND CALL IT ZPI
      DO 314 I=1,3
      DO 320 J=1,3
      TEMP(I,J)=ZP(I,J)
320   ZPI(I,J)=(0.0,0.0)
314   ZPI(I,I)=(1.0,0.0)
      CALL LEQT1C(TEMP,3,3,ZPI,3,3,0,WA,IER)
C     MULTIPLY ZPI * SZYP AND CALL IT ZYPI
      DO 330 I=1,3
      DO 330 J=1,3
      ZYPI(I,J)=(0.0,0.0)
      DO 330 K=1,3
330   ZYPI(I,J)=ZYPI(I,J)+ZPI(I,K)*SZYP(K,J)
C     MULTIPLY SZYP * SINSZY TO GET CP
      DO 335 I=1,3
      DO 335 J=1,3
      CP(I,J)=(0.0,0.0)
      DO 335 K=1,3
335   CP(I,J)=CP(I,J)+SZYP(I,K)*SINSZY(K,J)
C     MULTIPLY ZPI * COSSZY AND CALL IT COSZYP
      DO 340 I=1,3

```

```

      DO 340 J=1,3
      COSZYP(I,J)=(0.0,0.0)
      DO 340 K=1,3
340   COSZYP(I,J)=COSZYP(I,J)+ZPI(I,K)*COSSZY(K,J)
C     MULTIPLY COSZYP * ZP AND CALL IT DP
      DO 345 I=1,3
      DO 345 J=1,3
      DP(I,J)=(0.0,0.0)
      DO 345 K=1,3
345   DP(I,J)=DP(I,J)+COSZYP(I,K)*ZP(K,J)
      RETURN
      END

C
C     *****
C     * SUBROUTINE VRIR *
C     *****
C
      SUBROUTINE VRIR(VS22,CS22,APP,BPP,CPP,DPP,VV,CC,VM,CM,PHV,PHC)
      COMPLEX VS22(3),CS22(3),APP(3,3),BPP(3,3),CPP(3,3),VV(3),CC(3),
      *DPP(3,3)
      DIMENSION CM(3),VM(3),PHV(3),PHC(3)
      DO 365 I=1,3
      VV(I)=(0.0,0.0)
      CC(I)=(0.0,0.0)
365   CONTINUE
      DO 370 I=1,3
      DO 370 J=1,3
      VV(I)=VV(I)+APP(I,J)*VS22(J)+BPP(I,J)*CS22(J)
      CC(I)=CC(I)+DPP(I,J)*CS22(J)+CPP(I,J)*VS22(J)
370   CONTINUE
      DO 371 I=1,3
      VM(I)=CABS(VV(I))*SQRT(2.0)
      PHV(I)=ATAN2(AIMAG(VV(I)),REAL(VV(I)))
      CM(I)=CABS(CC(I))*SQRT(2.0)
      PHC(I)=ATAN2(AIMAG(CC(I)),REAL(CC(I)))

```

```

371  CONTINUE
      RETURN
      END

C
C
C      *****
C      * SUBROUTINE VFT *
C      *****
C
      SUBROUTINE VFT(VFM,W,WO,DW,PHF,VFP)
      COMPLEX VFP(3),EJPH(3),EJPHC(3),VF(3),CMPLX,EP1,EP2
      DIMENSION VFM(3),PHF(3)
      EP1=1.0/CMPLX(DW,(W-WO))
      EP2=1.0/CMPLX(DW,(W+WO))
      DO 3 I=1,3
      EJPH(I)=CMPLX(COS(PHF(I)),SIN(PHF(I)))
      EJPHC(I)=CONJG(EJPH(I))
      VFP(I)=-.5*(VFM(I))*(EP1*EJPH(I)+EP2*EJPHC(I))
3     CONTINUE
      RETURN
      END

C
C      *****
C      * SUBROUTINE LLLF *
C      *****
C
      SUBROUTINE LLLF(TVRI,T2IT1,VF,VRF)
      COMPLEX TVRI(3,3),T2IT1(3,3),VF(3),VRF(3)
      DO 245 I=1,3
245  VRF(I)=(0.0,0.0)
      DO 250 I=1,3
      DO 250 J=1,3
250  VRF(I)=VRF(I)+TVRI(I,J)*VF(J)
      RETURN
      END

```

```

      CFA=-VF(1)/(TI(1,1)+ZF(1,1))
      VRF(1)=-TI(1,1)*CFA
      VRF(2)=-TI(2,1)*CFA
      VRF(3)=-TI(3,1)*CFA
      RETURN
      END

C
C      *****
C      * SUBROUTINE AIFFT *
C      *****
C
      SUBROUTINE AIFFT(X,M)
      COMPLEX X(1024),U,W,T,CMLPX
      N=2**M
      NV2=N/2
      NM1=N-1
      J=1
C      BIT REVERSAL SECTION
      DO 30 I=1,NM1
      IF(I.GE.J) GO TO 10
      T=X(J)
      X(J)=X(I)
      X(I)=T
10  K=NV2
20  IF(K.GE.J) GO TO 30
      J=J-K
      K=K/2
      GO TO 20
30  J=J+K
      PI=3.14159265358979
C      CALCULATION OF THE COMPLEX MULTIPLYING
C      FACTORS; AND THE BASIC BUTTERFLY SECTION.
      DO 50 L=1,M
      LE=2**L
      LE1=LE/2

```



```

C
C      *****
C      * SUBROUTINE LLF *
C      *****
C
SUBROUTINE LLF(VF, TI, ZF, VRF)
COMPLEX VF(3), TI(3,3), ZF(3,3), VRF(3), CFB
CFB=(VF(2)-VF(3))/(TI(2,3)-TI(2,2)-TI(3,3)+TI(3,2)-ZF(1,1))
VRF(1)=(TI(1,3)-TI(1,2))*CFB
VRF(2)=(TI(2,3)-TI(2,2))*CFB
VRF(3)=(TI(3,3)-TI(3,2))*CFB
RETURN
END

```

```

C
C      *****
C      * SUBROUTINE LLGF *
C      *****
C
SUBROUTINE LLGF(VF, TI, ZF, VRF)
COMPLEX VF(3), TI(3,3), ZF(3,3), VRF(3), CFB, CFC, ZFT
ZFT=-(ZF(1,1)+TI(3,3))/TI(2,3)
CFB=-(ZFT*VF(2)+VF(3))/(ZFT*(ZF(1,1)+TI(2,2))+TI(3,2))
CFC=-((ZF(1,1)+TI(2,2))*CFB+VF(2))/TI(2,3)
VRF(1)=-TI(1,2)*CFB-TI(1,3)*CFC
VRF(2)=-TI(2,2)*CFB-TI(2,3)*CFC
VRF(3)=-TI(3,2)*CFB-TI(3,3)*CFC
RETURN
END

```

```

C
C      *****
C      * SUBROUTINE LGF *
C      *****
C
SUBROUTINE LGF(VF, TI, ZF, VRF)
COMPLEX VF(3), TI(3,3), ZF(3,3), CFA, VRF(3)

```

```

      U=(1.0,0.0)
      W=CMPLX(COS(PI/FLOAT(LE1)),SIN(PI/FLOAT(LE1)))
      DO 50 J=1,LE1
      DO 40 I=J,N,LE
      IP=I+LE1
      T=X(IP)*U
      X(IP)=X(I)-T
40    X(I)=X(I)+T
50    U=U*W
      RETURN
      END

```